Report No.: KS-14-17 ▪ FINAL REPORT ▪ April 2015

Calibrating the Mechanistic-Empirical Pavement Design Guide for Kansas

Xiaohui Sun
Jie Han, Ph.D., P.E.
Robert L. Parsons, Ph.D., P.E.
Anil Misra, Ph.D., P.E.
Jitendra K. Thakur

The University of Kansas

Kansas Department of Transportation

1 Report No. KS-14-17	**2 Government Accession No.**	**3 Recipient Catalog No.**
4 Title and Subtitle Calibrating the Mechanistic-Empirical Pavement Design Guide for Kansas		**5 Report Date** April 2015 **6 Performing Organization Code**
7 Author(s) Xiaohui Sun, Jie Han, Ph.D., P.E., Robert L. Parsons, Ph.D., P.E., Anil Misra, Ph.D., P.E., Jitendra K. Thakur		**7 Performing Organization Report No.**
9 Performing Organization Name and Address The University of Kansas Department of Civil, Environmental and Architectural Engineering 1530 West 15th St Lawrence, Kansas 66045-7609		**10 Work Unit No. (TRAIS)** **11 Contract or Grant No.** C1931
12 Sponsoring Agency Name and Address Kansas Department of Transportation Bureau of Research 2300 SW Van Buren Topeka, Kansas 66611-1195		**13 Type of Report and Period Covered** Final Report July 2012–September 2014 **14 Sponsoring Agency Code** RE-0610-01
15 Supplementary Notes For more information write to address in block 9.		

The Kansas Department of Transportation (KDOT) is moving toward the implementation of the new American Association of State Highway and Transportation Officials (AASHTO) *Mechanistic-Empirical Pavement Design Guide* (MEPDG) for pavement design. The MEPDG provides a rational pavement design framework based on mechanistic-empirical principles to characterize the effects of climate, traffic, and material properties on the pavement performance, as compared with the 1993 *AASHTO Guide for Design of Pavement Structures*. Before moving to the MEPDG, the nationally calibrated MEPDG distress prediction models need to be further validated and calibrated to the local condition.

The objective of this research was to improve the accuracy of the MEPDG to predict the pavement performance in Kansas. This objective was achieved by evaluating the MEPDG-predicted performance of Kansas projects, as compared with the pavement performance data from the pavement management system (PMS), and calibrating the MEPDG models based on the pavement performance data. In this study, 28 flexible pavement projects and 32 rigid pavement projects with different material properties, traffic volumes, and climate conditions were strategically selected throughout Kansas. The AASHTO ME Design software (Version 1.3) was used in this study.

The comparisons between the MEPDG-predicted pavement performance using the nationally calibrated models and the measured pavement performance indicated the need for the calibration of the MEPDG models to the Kansas conditions. For new flexible pavements, the MEPDG using the nationally calibrated models overestimated the rutting due to the overprediction of the deformation of the subgrade layer. Biases also existed between the predicted top-down cracking, thermal cracking, and International Roughness Index (IRI) and the measured data. The relationship between the measured and the predicted IRIs was more obvious than that for the cracking. Using the coefficients determined through local calibration in this study, the biases and the standard errors were minimized for all the models based on the statistical analysis.

For new rigid pavements, very low mean joint faulting was measured in actual projects as compared with the default threshold of the MEPDG. The type of base course had a minor effect on the pavement performance. The traditional splitting data method was adopted in the process of local calibration. After the local calibration, the biases between the predicted pavement performance (mean joint faulting and IRI) and the measured pavement performance were minimized, and the standard errors were reduced.

17 Key Words Mechanistic-Empirical Pavement Design Guide (MEPDG), Local Calibration, Pavement Performance		**18 Distribution Statement** No restrictions. This document is available to the public through the National Technical Information Service www.ntis.gov.	
19 Security Classification (of this report) Unclassified	**20 Security Classification (of this page)** Unclassified	**21 No. of pages** 235	**22 Price**

Form DOT F 1700.7 (8-72)

This page intentionally left blank.

Calibrating the Mechanistic-Empirical Pavement Design Guide for Kansas

Final Report

Prepared by

Xiaohui Sun, Graduate Research Assistant
Jie Han, Ph.D., P.E., Professor
Robert L. Parsons, Ph.D., P.E., Professor
Anil Misra, Ph.D., P.E., Professor
Jitendra K. Thakur, Formerly Graduate Research Assistant

The University of Kansas

A Report on Research Sponsored by

THE KANSAS DEPARTMENT OF TRANSPORTATION
TOPEKA, KANSAS

and

THE UNIVERSITY OF KANSAS
LAWRENCE, KANSAS

April 2015

NOTICE

The authors and the state of Kansas do not endorse products or manufacturers. Trade and manufacturers names appear herein solely because they are considered essential to the object of this report.

This information is available in alternative accessible formats. To obtain an alternative format, contact the Office of Public Affairs, Kansas Department of Transportation, 700 SW Harrison, 2nd Floor – West Wing, Topeka, Kansas 66603-3745 or phone (785) 296-3585 (Voice) (TDD).

DISCLAIMER

The contents of this report reflect the views of the authors who are responsible for the facts and accuracy of the data presented herein. The contents do not necessarily reflect the views or the policies of the state of Kansas. This report does not constitute a standard, specification or regulation.

Abstract

The Kansas Department of Transportation (KDOT) is moving toward the implementation of the new American Association of State Highway and Transportation Officials (AASHTO) *Mechanistic-Empirical Pavement Design Guide* (MEPDG) for pavement design. The MEPDG provides a rational pavement design framework based on mechanistic-empirical principles to characterize the effects of climate, traffic, and material properties on the pavement performance, as compared with the 1993 *AASHTO Guide for Design of Pavement Structures*. Before moving to the MEPDG, the nationally calibrated MEPDG distress prediction models need to be further validated and calibrated to the local condition.

The objective of this research was to improve the accuracy of the MEPDG to predict the pavement performance in Kansas. This objective was achieved by evaluating the MEPDG-predicted performance of Kansas projects, as compared with the pavement performance data from the pavement management system (PMS), and calibrating the MEPDG models based on the pavement performance data. In this study, 28 flexible pavement projects and 32 rigid pavement projects with different material properties, traffic volumes, and climate conditions were strategically selected throughout Kansas. The AASHTO ME Design software (Version 1.3) was used in this study.

The comparisons between the MEPDG-predicted pavement performance using the nationally calibrated models and the measured pavement performance indicated the need for the calibration of the MEPDG models to the Kansas conditions. For new flexible pavements, the MEPDG using the nationally calibrated models overestimated the rutting due to the overprediction of the deformation of the subgrade layer. Biases also existed between the predicted top-down cracking, thermal cracking, and International Roughness Index (IRI) and the measured data. The relationship between the measured and the predicted IRIs was more obvious than that for the cracking. Using the coefficients determined through local calibration in this study, the biases and the standard errors were minimized for all the models based on the statistical analysis.

For new rigid pavements, very low mean joint faulting was measured in actual projects as compared with the default threshold of the MEPDG. The type of base course had a minor effect on the pavement performance. The traditional splitting data method was adopted in the process of local calibration. After the local calibration, the biases between the predicted pavement performance (mean joint faulting and IRI) and the measured pavement performance were minimized, and the standard errors were reduced.

Acknowledgements

This research was financially sponsored by the Kansas Department of Transportation (KDOT). Mr. James J. Brennan, the Chief Geotechnical Engineer of KDOT, was the monitor for this project. During the data collection, we received great help from KDOT researchers and engineers including Mr. Rodney Montney, Mr. Rick Miller, Dr. Heather McLeod, Mr. Rick Kreider, Mr. Jonathan Marburger, and Mr. Nat Velasquez. The authors would like to express their appreciation to these individuals for their help and support.

Table of Contents

List of Figures

List of Tables

Chapter 1: Introduction

1.1 Background

The Kansas Department of Transportation (KDOT) has used the American Association of State Highway and Transportation Officials (AASHTO) *Guide for Design of Pavement Structures* (1993) to design flexible and rigid pavements for many years. The empirically based *AASHTO Guide for Design of Pavement Structures* originated from pavement design equations developed using the performance data of asphalt and portland cement concrete (PCC) pavements collected in a national research program in 1958, known as the AASHO Road Test (Kim, Jadoun, Hou, & Muthadi, 2011). The most recent version of the AASHTO empirically based pavement design guide was made available in 1993 and, since that time, it has served as the most widely used method for designing new and rehabilitated flexible and rigid pavements among state highway agencies in the United States. Although the 1993 *AASHTO Guide for Design of Pavement Structures* was improved over the years, there are multiple limitations, such as (1) the lack of sophisticated material and traffic loading characterization algorithms and (2) the absence of the pavement mechanical response, which leads to the development and accumulation of damage, distresses, and smoothness loss. Therefore, the AASHTO Joint Technical Committee on Pavements (JTCP) proposed a change from the empirically based to a mechanistically based pavement design (Mallela et al., 2013).

A mechanistic-empirical (ME) pavement design procedure was developed under the National Cooperative Highway Research Program (NCHRP) Project 1-37A, which was sponsored by the AASHTO Joint Task Force on Pavements, NCHRP, and the Federal Highway Administration (FHWA) in 2004. The 2004 version of the MEPDG has undergone several independent reviews and refinements since its initial completion. Design software has been developed to assist with the use of the MEPDG, and has been updated with the refinements. To the date of this report, the current version of the AASHTO MEPDG design software is Version 1.3 (Pierce & McGovern, 2014).

1.2 Overview of the MEPDG

Moving from the previous empirically-based design method to the ME-based design procedures provides several advantages, such as a broader range of vehicle loadings, material properties, climatic effects, and improved reliability of pavement performance predictions (Pierce & McGovern, 2014). Key principles in the new pavement design include (NCHRP, 2004):

- Characterizing material properties (asphalt concrete, portland cement concrete, chemically-stabilized unbound granular and soil materials) accurately and in real-time.
- Simulating temperature and moisture conditions and their interaction with pavement material properties.
- Simulating truck traffic loading and forecasting its growth.
- Mechanistically calculating pavement responses (i.e., stresses, strains, and deflections) due to traffic loadings under various environmental conditions.
- Empirically relating pavement responses to incremental and accumulating pavement damages, and then to distress developments (cracking, rutting, faulting, etc.).

The ME pavement design approach, which consists of three major stages, is shown in Figure 1.1.

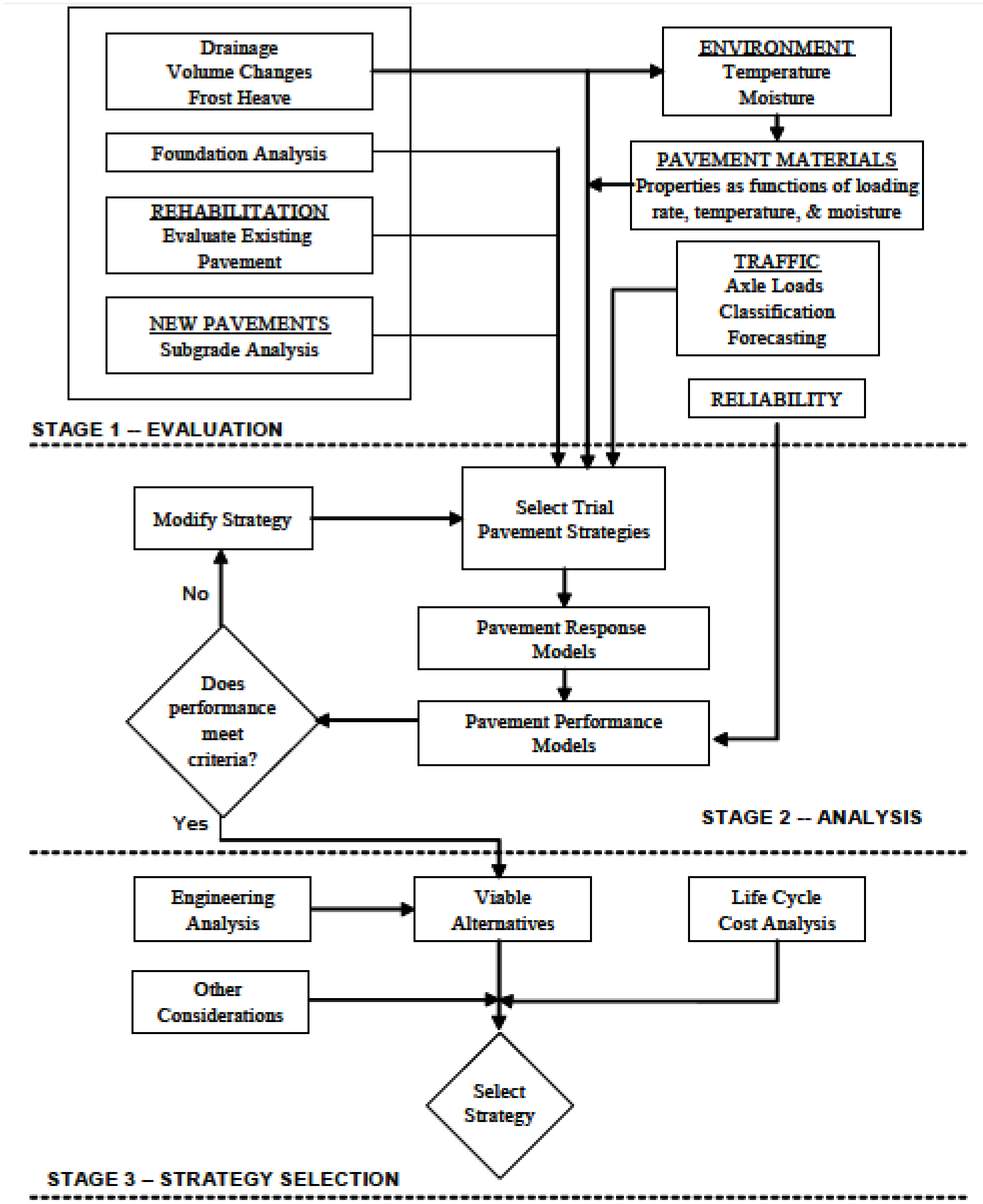

Figure 1.1: Pavement Mechanistic-Empirical (ME) Design Methodology
Source: AASHTO, 2008

As shown in Figure 1.1, Stage 1 consists of the development of input values (including material characterization, traffic, and climatic data) and establishment of performance criteria and design reliability levels for each criterion. Stage 2 is the structural/performance analysis. In this stage, an iterative approach begins with the selection of an initial trial design. If the trial design does not meet the performance criteria based on pavement response and distress models, modifications are made and the analysis is re-run until a satisfactory result is obtained. Stage 3 of the design process is to evaluate the structurally viable alternatives, including the engineering analysis and the life-cycle cost analysis of the design alternatives.

Compared with the 1993 *AASHTO Guide for Design of Pavement Structures*, which only evaluates one performance indicator (i.e., Pavement Service Index [PSI]), the MEPDG predicts multiple performance indicators (Wu & Yang, 2012).

1.3 Problem Statement

KDOT is in the process of implementing the MEPDG for the design of flexible and rigid pavements in Kansas. This design guide replaced the *AASHTO Guide for Design of Pavement Structures* (1993) commonly used in the past. The MEPDG software designs pavements based on desired performance, and thus is more theoretically sound. This design guide contains distress models which can predict the structural and functional performance of flexible and rigid pavements. However, these models were developed and calibrated with nation-wide data. To accurately predict pavement performance in Kansas, these models must be calibrated to local conditions. KDOT has unique knowledge and experience in pavement design and construction which have been proven successful in Kansas; for example, the use of lime stabilization of subgrade and full-depth flexible pavements. The successful KDOT pavement design and construction practice should be incorporated in future designs when the MEPDG is used.

1.4 Objectives

The objective of this research was to improve the accuracy of MEPDG predictions of pavement performance in Kansas through local calibration of the MEPDG performance prediction models, so that the calibrated MEPDG models can be used for future design of pavements in Kansas.

AASHTO published a guide for the local calibration of the MEPDG (AASHTO, 2010) which requires traffic, climate, material, and performance data. In this research, the traffic, climate, material, and performance data were collected from the pavement management system (PMS) database of KDOT. The distress models for flexible (e.g., rutting, fatigue, thermal cracking, roughness, etc.) and rigid (e.g., faulting, roughness, etc.) pavements were calibrated using the collected data. It is expected that the calibrated models will more accurately predict the performance of flexible and rigid pavements in Kansas.

1.5 Tasks of Study

The report documents the work done for this research project, which includes the following tasks:

- Task 1: Conducted a comprehensive literature review on the related research.
- Task 2: Collected the traffic, climate, material, and performance data for flexible and rigid pavements from KDOT.
- Task 3: Analyzed the collected data from KDOT, evaluated the quality and completeness of the data, selected pavement sections with sufficient information for calibration, grouped the data for input and different distress models, and determined the levels of calibration.
- Task 4: Performed the calibration of the distress models following the AASHTO guide (AASHTO, 2010) for the local calibration of the MEPDG. In this calibration, the predicted performance was first obtained using the MEPDG software with the input data provided by KDOT for the selected pavements with the performance data. The predicted performance was compared with the actual performance. Calibration factors were established for the relevant distress models by matching the predicted performance with the actual performance.
- Task 5: Prepared a final report to summarize the above tasks and the calibration factors and make recommendations for possible improvement of the locally calibrated models in the future.

1.6 Organization of Report

Chapter 1 provides the overview of this research project and report. Chapter 2 presents a detailed description of the distress models used in the MEPDG and a comprehensive literature review related to this research topic. Chapter 3 describes the framework used for the MEPDG nationally calibrated models, model validation, and local calibration for Kansas conditions, by following the guidelines presented in the AASHTO local calibration guide (AASHTO, 2010). Chapter 3 also includes the description of the project selection and development of the validation/calibration database. Chapter 4 presents the statistical analysis performed to validate and calibrate the MEPDG models for Kansas conditions and the validation of the newly calibrated models. Chapter 5 summarizes the work done in this project, including the locally calibrated coefficients and provides recommendations for possible improvement of the locally calibrated MEPDG prediction models in the future. Appendices summarize the comparisons of the measured and MEPDG-predicted performance for both flexible and rigid pavements, before and after the local calibration.

Chapter 2: Flexible/Rigid Pavement Performance Prediction Models and Literature Review

A description of the MEPDG performance prediction models and a literature review regarding the local calibration of the MEPDG are presented in this chapter. Detailed descriptions of these models and the entire design procedures have been published in the AASHTO MEPDG Manual of Practice and the MEPDG reports developed under the NCHRP Project 1-37A and the NCHRP Project 1-40D (AASHTO, 2008). All the models presented in this Chapter are from AASHTO (2008).

2.1 New Flexible Pavements

2.1.1 Load-Related Fatigue Cracking

Load-related fatigue cracking is the cracking in the asphalt course (AC) layer that is caused by repeated traffic loading. Two types of load-related fatigue cracking in flexible pavements are predicted in the MEPDG: bottom-up cracking (also referred to as alligator cracking) and top-down cracking (also referred to as longitudinal cracking). The prediction of these two types of cracking begins with the computation incrementally of hot mix asphalt (HMA) fatigue damage. An incremental damage index, ΔDI, is calculated by dividing the actual number of axle loads by the allowable number of axle loads within a specific time increment and an axle load interval for each axle type (Miner, 1945). The cumulative damage index for each critical location is determined by summing the incremental damage over time and traffic using Equation 2.1 (AASHTO, 2008):

$$DI = \sum(\Delta DI)_{j,m,l,p,T} = \sum(\frac{n}{N_{f-HMA}})_{j,m,l,p,T}$$ Equation 2.1

Where:

n = actual number of axle load applications within a specific time period,

j = axle load interval,

m = axle load type (single, tandem, tridem, quad, or special axle configuration),

l = truck type using the truck classification groups included in the MEPDG,

p = month,

T = median temperature for the five temperature intervals used to subdivide each month, °F, and

$N_{f\text{-HMA}}$ = allowable number of axle load applications for a flexible pavement and HMA overlays to fatigue cracking.

The allowable number of axle load applications needed for the incremental damage index computation is shown in Equation 2.2 (AASHTO, 2008).

$$N_{f-HMA} = k_{f1}(C)(C_H)\beta_{f1}(\varepsilon_t)^{k_{f2}\beta_{f2}}(E_{HMA})^{k_{f3}\beta_{f3}}$$ Equation 2.2

Where:

ε_t = tensile strain at critical locations and calculated by the structural response model, in./in.,

E_{HMA} = dynamic modulus of the HMA measured under compression, psi,

k_{f1}, k_{f2}, k_{f3} = global field calibration parameters (k_{f1} = 0.007566, k_{f2} = -3.9492, and k_{f3} = -1.281), and

β_{f1}, β_{f2}, β_{f3} = local or mixture specific field calibration constants; for the global calibration effort, these constants were set to 1.0.

$C = 10^M$ Equation 2.3

$M = 4.84\left(\frac{V_{be}}{V_a+V_{be}} - 0.69\right)$ Equation 2.4

Where:

V_{be} = effective asphalt content by volume, %,

V_a = percent air voids in the HMA mixture (in situ only, not mixture design), and

C_H = thickness correction term, depending on the type of cracking.

For bottom-up cracking:

$$C_H = \frac{1}{0.000398 + \frac{0.003602}{1+e^{(11.02-3.49H_{HMA})}}}$$ Equation 2.5

For top-down cracking:

$$C_H = \frac{1}{0.01 + \frac{12.00}{1+e^{(15.676-2.8186H_{HMA})}}}$$ Equation 2.6

H_{HMA} = total HMA thickness, in.

Bottom-up cracking initiates from the bottom of an HMA layer as a few short longitudinal or transverse cracks in the early stage, and eventually develops into interconnected cracks with an alligator pattern. The unit for bottom-up cracking in the MEPDG is the percentage of the total lane area. The transfer function for bottom-up cracking in the MEPDG is (AASHTO, 2008):

$$FC_{Bottom} = \left(\frac{1}{60}\right)\left(\frac{C_4}{1+e^{\left(C_1 C_1^* + C_2 C_2^* Log\left(DI_{Bottom} * 100\right)\right)}}\right)$$

Equation 2.7

Where:

FC_{Bottom} = area of alligator cracking that initiates at the bottom of the HMA layer, percent of total lane area,

DI_{Bottom} = cumulative damage index at the bottom of the HMA layer, and

$C_{1,2,4}$ = transfer function regression constants: C_4= 6,000, C_1=1.00, and C_2=1.00.

$$C_1^* = -2C_2^*$$

Equation 2.8

$$C_2^* = -2.40874 - 39.748(1 + H_{HMA})^{-2.856}$$

Equation 2.9

Equation 2.10 is the relationship used to predict the length of longitudinal fatigue cracks, FC_{Top} (AASHTO, 2008).

$$FC_{Top} = 10.56\left(\frac{C_4}{1+e^{\left(C_1 - C_2 Log\left(DI_{Top}\right)\right)}}\right)$$

Equation 2.10

Where:

FC_{Top} = length of longitudinal cracks that initiate at the top of the HMA layer, ft/mile,

DI_{Top} = cumulative damage index near the top of the HMA surface, and

$C_{1,2,4}$ = transfer function regression constants: C_4= 1,000, C_1=7.00, and C_2=3.5.

2.1.2 Low-Temperature Induced Transverse Cracking

Transverse cracking is non-load-related cracking, which is usually caused by low temperature or thermal cycling. The unit for transverse cracking in the MEPDG is feet per mile.

The amount of cracking induced by a given thermal cooling cycle is predicted using the Paris law of crack propagation in the MEPDG (AASHTO, 2008).

$$\Delta C = A\left(\Delta K\right)^{n} \qquad \text{Equation 2.11}$$

Where:

ΔC = change in the crack depth due to a cooling cycle,

ΔK = change in the stress intensity factor due to a cooling cycle, and

A, n = fracture parameters for the HMA mixture.

Experimental results indicate that reasonable estimates of A and n can be obtained from the indirect tensile creep-compliance and strength of the HMA in accordance with Equations 2.12 and 2.13:

$$A = 10^{k_t \beta_t \left(4.389 - 2.52 Log\left(E_{HMA} \sigma_m n\right)\right)} \qquad \text{Equation 2.12}$$

$$\eta = 0.8\left[1 + \frac{1}{m}\right] \qquad \text{Equation 2.13}$$

Where:

k_t = coefficient determined through global calibration for each input level (Level 1 = 5.0, Level 2 = 1.5, and Level 3 = 3.0),

E_{HMA} = HMA indirect tensile modulus, psi,

σ_m = mixture tensile strength, psi,

m = m-value derived from the indirect tensile creep compliance curve measured in the laboratory, and

β_t = local or mixture calibration factor.

The stress intensity factor, K, has been incorporated in the MEPDG through the use of a simplified equation developed from the finite element studies, as shown in Equation 2.14 (AASHTO, 2008).

$$K = \sigma_{tip}\left(0.45 + 1.99(C_o)^{0.56}\right) \qquad \text{Equation 2.14}$$

Where:

σ_{tip} = far-field stress from the pavement response model at a depth of crack tip, psi, and

C_o = current crack length, feet.

The thermal cracking is predicted by the MEPDG using an assumed relationship between the probability distribution of the log of the crack depth to HMA layer thickness ratio and the percent of cracking. Equation 2.15 shows the expression used to determine the extent of thermal cracking (AASHTO, 2008).

$$TC = \beta_{t1} N\left[\frac{1}{\sigma_d} Log\left(\frac{C_d}{H_{HMA}}\right)\right] \qquad \text{Equation 2.15}$$

Where:

TC = observed amount of thermal cracking, ft/mile,

β_{t1} = regression coefficient determined through global calibration (400),

$N[z]$ = standard normal distribution evaluated at [z],

σ_d = standard deviation of the log of the depth of cracks in the pavement (0.769), in.,

C_d = crack depth, in., and

H_{HMA} = thickness of the HMA layer, in.

2.1.3 Rut Depth

Rutting results from vertical plastic deformations in the HMA, unbound layers, and subgrade/foundation soil. Rut depth is defined as the maximum difference in elevations between the transverse profile of the HMA surface and a wire-line across the lane width (AASHTO, 2010). In the MEPDG, rut depth is obtained by calculating incremental distortion or rutting within each sublayer. The unit for rut depth in the MEPDG is inches.

The transfer function for the AC layer is (AASHTO, 2008):

$$\Delta_{p(HMA)} = \varepsilon_{p(HMA)} h_{HMA} = \beta_{1r} k_z \varepsilon_{r(HMA)} 10^{k_{1r}} n^{k_{2r}\beta_{2r}} T^{k_{3r}\beta_{3r}} \qquad \text{Equation 2.16}$$

Where:

$\Delta_{p(HMA)}$ = accumulated vertical permanent or plastic deformation in the HMA layer/sublayer, in.,

$\varepsilon_{p(HMA)}$ = accumulated permanent or plastic axial strain in the HMA layer/sublayer, in./in.,

$\varepsilon_{r(HMA)}$ = resilient or elastic strain calculated by the structural response model at the mid-depth of each HMA sublayer, in./in.,

$h_{(HMA)}$ = thickness of the HMA layer/sublayer, in.,

n = number of axle load repetitions,

T = mix or pavement temperature, °F,

k_z = depth confinement factor,

k_{1r}, k_{2r}, k_{3r} = global field calibration parameters (from the NCHRP 1-40D recalibration; k_{1r} = -3.35412, k_{2r} = 0.4791, k_{3r} = 1.5606), and

$\beta_{r1}, \beta_{2r}, \beta_{3r}$, = local or mixture field calibration constants; for the global calibration, these constants were all set to 1.0.

$$k_z = (C_1 + C_2 D)0.328196^D$$ Equation 2.17

$$C_1 = -0.1039(H_{HMA})^2 + 2.4868 H_{HMA} - 17.342$$ Equation 2.18

$$C_2 = 0.0172(H_{HMA})^2 - 1.7331 H_{HMA} + 27.428$$ Equation 2.19

Where:

D = depth below the surface, in., and

H_{HMA} = total HMA thickness, in.

The transfer function for rutting of all the unbound pavement sublayers and the foundation or embankment soil is (AASHTO, 2008):

$$\Delta_{p(soil)} = \beta_{s1} k_{s1} \varepsilon_v h_{soil} \left(\frac{\varepsilon_o}{\varepsilon_r} \right) e^{-\left(\frac{\rho}{n}\right)^{\beta}}$$ Equation 2.20

Where:

$\Delta_{p(Soil)}$ = permanent or plastic deformation of the layer/sublayer, in.,

n = number of axle load applications,

ε_o = intercept determined from laboratory repeated load permanent deformation tests, in./in.,

ε_r = resilient strain imposed in laboratory tests to obtain material properties ε_o, β, and ρ, in./in.,

ε_v = average vertical resilient or elastic strain in the layer/sublayer and calculated by the structural response model, in./in.,

h_{Soil} = thickness of the unbound layer/sublayer, in.,

k_{s1} = global calibration coefficients: k_{s1}=1.673 for granular materials and 1.35 for fine-grained materials, and

β_{s1} = local calibration constant for the rutting in the unbound layers: the local calibration constant was set to 1.0 for the global calibration effort.

$$Log\beta = -0.61119 - 0.017638(W_c)$$ Equation 2.21

$$\rho = 10^9 \left(\frac{0.0075}{\left(1 - \left(10^9\right)^{\beta}\right)} \right)^{\frac{1}{\beta}}$$ Equation 2.22

2.1.4 Smoothness

International Roughness Index (IRI) is used to define the pavement smoothness. The unit of IRI is inch/mile. The design premise included in the MEPDG for predicting smoothness degradation is that the occurrence of surface distress results in a reduction in the smoothness. The following equation can be used to predict the IRI of new HMA pavements and HMA overlays of flexible pavements (AASHTO, 2008):

$$IRI = IRI_o + 0.0150(SF) + 0.400(FC_{Total}) + 0.0080(TC) + 40.0(RD)$$ Equation 2.23

Where:

IRI_o = initial IRI after construction, in./mi,

SF = site factor, refer to Equation 2.24,

FC_{Total} = area of fatigue cracking (combined alligator, longitudinal, and reflection cracking in the wheel path), percent of total lane area. All load-related cracks are combined on an area basis (the length of a crack is multiplied by 1 foot to convert the length into an area basis),

TC = length of transverse cracking (including the reflection of transverse cracks in existing HMA pavements), ft./mi, and

RD = average rut depth, in.

The site factor (SF) is calculated in accordance with the following equation:

$$SF = Age\left(0.02003\left(PI+1\right)+0.007947\left(Precip+1\right)+0.000636\left(FI+1\right)\right) \quad \text{Equation 2.24}$$

Where:

Age= pavement age, years,

PI = percent plasticity index of the soil,

FI = average annual freezing index, degree F days, and

Precip = average annual precipitation or rainfall, in.

2.2 New Rigid Pavement

2.2.1 Mean Transverse Joint Faulting

In the MEPDG, the mean transverse joint faulting of the jointed plain concrete pavement (JPCP) is predicted using an incremental approach month by month. For each month, a faulting increment is determined and the current faulting level affects the magnitude of increment. The faulting at each month is determined as a sum of faulting increments from all previous months in the pavement life from the traffic opening date using the following equations (AASHTO, 2008):

$$Fault_m = \sum_{i=1}^{m} \Delta Fault_i \quad \text{Equation 2.25}$$

$$\Delta Fault_i = C_{34} * (FAULTMAX_{i-1} - Fault_{i-1})^2 * DE_i \quad \text{Equation 2.26}$$

$$FAULTMAX_i = FAULTMAX_0 + C_7 * \sum_{j=1}^{m} DE_j * Log(1 + C_5 * 5.0^{EROD})^{C_6} \quad \text{Equation 2.27}$$

$$FAULTMAX_0 = C_{12} * \delta_{\text{curling}} * \left[Log(1 + C_5 * 5.0^{EROD}) * Log(\frac{P_{200} * WetDays}{p_s}) \right]^{C_6}$$

Equation 2.28

Where:

$Fault_m$ = mean joint faulting at the end of month m, in.,

$\Delta Fault$ = incremental change (monthly) in mean transverse joint faulting during month i, in.,

$FAULTMAX_i$ = maximum mean transverse joint faulting for month i, in.,

$FAULTMAX_0$ = initial maximum mean transverse joint faulting, in.,

$EROD$ = base/subbase erodibility factor,

DE_i = differential density of energy of subgrade deformation accumulated during month I,

$\delta_{curling}$ = maximum mean monthly slab corner upward deflection PCC due to temperature curling and moisture warping,

P_S = overburden on subgrade, lb,

P_{200} = percent subgrade material passing #200 sieve,

$WetDays$ = average annual number of wet days (greater than 0.1 inch rainfall), and

$C_{1,2,3,4,5,6,7,12,24}$ = global calibration constants: C_1 = 1.29, C_2 = 1.1, C_3 = 0.001725, C_4 = 0.0008, C_5 = 250, C_6 = 0.4, C_7 = 1.2, and C_{12} and C_{34} are defined by Equations 2.29 and 2.30.

$$C_{12} = C_1 + C_2 * FR^{0.25}$$ Equation 2.29

$$C_{34} = C_3 + C_4 * FR^{0.25}$$ Equation 2.30

Where:

FR = base freezing index defined as percentage of time the top base temperature is below freezing (32 °F) temperature.

2.2.2 Smoothness

In the MEPDG, the following equation is the calibrated model for the smoothness of a JPCP:

$$IRI = IRI_I + C1*CRK + C2*SPALL + C3*TFAULT + C4*SF$$ Equation 2.31

Where:

IRI = predicted IRI, in./mi.,

IRI_I = initial smoothness measured as IRI, in./mi.,

CRK = percent slabs with transverse cracks (including all severities),

SPALL= percentage of joints with spalling (including medium and high severities),

TFAULT = total joint faulting cumulated per mile, in.,

C1 = 0. 8203,

C2 = 0.4417,

C3 = 0.4929,

C4 = 25.24, and

SF = site factor.

$SF = AGE\ (1+0.5556*FI)\ (1+P_{200})*10^{-6}$ Equation 2.32

Where:

AGE = pavement age, years,

FI = freezing index, °F-days, and

P_{200} = percent subgrade material passing No. 200 sieve.

The transverse joint spalling is determined in accordance with Equation 2.33, which was calibrated using Long Term Pavement Performance (LTPP) data:

$$SPALL = \left[\frac{AGE}{AGE + 0.01}\right]\left[\frac{100}{1 + 1.005^{(-12*AGE+SCF)}}\right]$$ Equation 2.33

Where:

SPALL = percentage joints spalled (including medium- and high-severities),

AGE = pavement age since construction, years, and

SCF = scaling factor, which is site-, design-, and climate-related.

$SCF = -1400 + 350\ AIR\%\ (0.5 + PREFORM) + 3.4\ f'c \times 0.4$

$-\ 0.2\ (FTCYC \times AGE) + 43\ h_{PCC} - 536\ WC\_Ratio$ Equation 2.34

Where:

AIR% = PCC air content, percent,

AGE = time since construction, years,

PREFORM = 1 if preformed sealant is present, 0 if not,

f'c = PCC compressive strength, psi,

FTCYC = average annual number of freeze-thaw cycles,

h_{PCC} = PCC slab thickness, in., and

WC_Ratio = PCC water/cement ratio.

2.3 Literature Review

The original version of the MEPDG was completed and released in 2004, and several national-level research studies supported by the NCHRP and FHWA were conducted after the release of the original version (NCHRP, 2004). Parallel to national-level studies, a large number of state agencies conducted or plan to undertake local calibrations of the MEPDG for their local implementation.

Two NCHRP research projects that are closely related to local calibrations of the MEPDG performance predictions are: (1) the NCHRP 9-30 project (NCHRP, 2003a; 2003b) and (2) the NCHRP 1-40B project. In order to quantify the bias and residual error of the flexible pavement distress models, a pre-implementation study involving verification and recalibration in the MEPDG models was conducted in the NCHRP 9-30 project (Muthadi, 2007). The NCHRP 1-40B project was focused on preparing a user manual for the MEPDG and its software, and a practical guide for local or regional calibration of the distress models. Due to lack of accuracy in the predictions, the longitudinal cracking and reflection cracking models were not considered in the local calibration guide during the NCHRP 1-40B study (Von Quintus & Moulthrop, 2007; Ceylan, Kim, Gopalakrishnan, & Ma, 2013). Moreover, one reason for the fatigue cracking prediction models to have relatively high errors is that none of the LTPP test sections included in the calibration effort confirmed whether the fatigue cracks started at the top or bottom of the HMA layers (AASHTO, 2008).

The FHWA studies (2006a, 2006b) evaluated the potential use of Pavement Management Information System (PMIS) for MEPDG local calibrations and concluded that it is feasible for Departments of Transportation (DOTs) to use PMIS data for MEPDG calibrations. It was also recommended that each DOT should develop a pavement management/pavement design database for each project designed by the MEPDG. An FHWA study entitled “Local Calibration of the MEPDG Using Pavement Management” (FHWA, 2010) was conducted to develop a framework for the use of PMS database to calibrate the MEPDG performance models.

Local-level MEPDG calibration studies have also been conducted parallel to the national-level studies. Most of the local-level MEPDG calibration studies were focused on flexible pavements while a few studies were conducted for JPCP. Table 2.1 summarizes the local calibration studies done by researchers.

Table 2.1: Summary of the Local Calibration Studies on the MEPDG

Flexible pavement	Location	Rigid pavement	Location
Galal and Chehab (2005)	Indiana	Li et al. (2006)	Washington
Von Quintus and Moulthrop (2007)	Montana	Schram and Abdelrahman (2006)	Nebraska
Kang et al. (2007)	Wisconsin	Darter et al. (2009)	Utah
Schram and Abdelrahman (2006)	Nebraska	Velasquez et al (2009)	Minnesota
Mehta et al.(2008)	New Jersey	Kim et al. (2010)	Iowa
Muthadi and Kim (2008)	North Carolina	Bustos et al. (2011)	Argentina
Corley-Lay et al. (2010)	North Carolina	Delgadillo et al (2011)	Chile
Jadoun (2011)	North Carolina	Ceylan et al. (2013)	Iowa
Li et al. (2009; 2010)	Washington	Mallela et al. (2013)	Colorado
Banerjee et al. (2009; 2010; and 2011)	Washington Texas		
Titus-Glover and Mallela (2009)	Ohio		
Darter et al. (2009)	Utah		
Souliman et al. (2010)	Arizona		
Mamlouk and Zapata (2010)	Arizona		
Kim et al. (2010)	Iowa		
Ceylan et al. (2013)	Iowa		
Khazanovich et al. (2008)	Minnesota		
Velasquez et al. (2009)	Minnesota		
Hoegh et al. (2010)	Minnesota		
Wu and Yang (2012)	Louisiana		
Hall et al. (2011)	Arkansas		
Caliendo (2012)	Italy		
Mallela et al. (2013)	Colorado		

A brief summary of the above studies:

Banerjee, Aguiar-Moya, and Prozzi (2009) conducted the calibration of the MEPDG for the new HMA and rehabilitated pavements in Texas using the LTPP database. In this study, the calibration factors for subgrade permanent deformations and the HMA mixture temperature dependency term were assumed by experts, and the coefficients of βr1 and βr3 were calibrated by minimizing the sum of squared error (SSE) between the measured and predicted results.

Bustos, Cordo, Girardi, and Pereyra (2011) conducted a calibration of the MEPDG distress models based on the local conditions in Argentina for the design of rigid pavements. The test sections of rigid pavements in the central region of the country were selected to cover a wide range of climatic conditions. The locally calibrated coefficients reduced the errors in distress predictions by more than one-half in all cases.

Caliendo (2012) reported the local calibration of the MEPDG for the design of flexible pavements in Italy. In this study, a comprehensive parametric analysis was performed, including load spectra, temperature, dynamic modulus of asphalt concrete (AC), and resilient modulus of subgrade. The MEPDG results were compared with those from a local mechanistic-empirical method. The difference between these two design methods was quantified. To verify the results obtained from the MEPDG, the *AASHTO Guide for Design of Pavement Structures* (1993) was used.

Darter, Titus-Glover, and Von Quintus (2009) conducted a local validation and calibration of the MEPDG in Utah using the data from the LTPP projects and the Utah Department of Transportation (UDOT) PMS. In this study, the nationally calibrated MEPDG models were evaluated. With the exception of the total rutting model for new HMA pavements, all other models were found reasonable. The rutting model was locally calibrated to improve the accuracy of prediction and minimize significant bias.

Galal and Chehab (2005) in Indiana compared the measured distress data of the existing HMA overlay over a rubblized PCC slab section with the predicted performance results using the *AASHTO Guide for Design of Pavement Structures* (1993) and the MEPDG (Version 0.7) with the same design inputs. The comparison indicated that the MEPDG provided good estimation of the measured distresses except for the top-down cracking. The authors noted that local calibration of performance prediction models is important.

Hall, Xiao, and Wang (2011) conducted a local calibration study for flexible pavements using 26 LTPP and PMS segments. When the sites had available vehicle class distribution data, the site-specific data was used. For other sites, the MEPDG default values were selected. In addition, the axle load spectra were adopted from a previous study and Level-3 materials inputs were used. This study indicated that the MEPDG overpredicted the subgrade rutting but under-predicted the AC rutting.

Hoegh, Khazanovich, and Jensen (2010) conducted a local calibration of the MEPDG rutting model using the data from the Minnesota Department of Transportation (MnDOT) fullscale pavement research facility, known as MnROAD. This study showed that the current MEPDG subgrade and base rutting models grossly overestimated the rutting for the MnROAD test sections. Velasquez et al. (2009) calibrated the MEPDG fatigue damage model in Minnesota and compared the results with those predicted by the MnPAVE, an ME design software of MnDOT. The comparison showed that the bottom-up cracking predicted by the MEPDG was much higher than that predicted by the MnPAVE.

Kang, Adams, and Bahia (2007) studied the Midwest implementation of the MEPDG by preparing a regional pavement performance database. The input data required by the MEPDG as well as the measured fatigue cracking data for flexible and rigid pavements were collected from the Michigan, Ohio, Iowa, and Wisconsin Departments of Transportation. Due to the low reliability in the collected pavement data, however, the calibration factors were evaluated based on the Wisconsin data, and the distresses predicted using the national calibration factors were compared to the field distresses. This study concluded that the nationally calibrated MEPDG could not predict the field distresses well in the Midwest.

Khazanovich, Yut, Husein, Turgeon, and Burnham (2008) compared the performance prediction of the MEPDG for the low-volume rigid pavement with the measured performance data in Minnesota. It was noted that the faulting model in the MEPDG produced acceptable predictions, whereas the cracking model in the MEPDG must be adjusted.

Li, Pierce, and Uhlmeyer (2009) presented the Washington State Department of Transportation's (WSDOT) efforts on the calibration of the MEPDG for the flexible pavements with the data from the Washington State PMS. The flexible pavement distress models were calibrated successfully. The locally calibrated factors for the WSDOT flexible pavements were different from the defaults. The software bug did not allow the calibration of the roughness model. After making a few improvements and resolving the software bugs, the MEPDG software can be used as an advanced tool to design flexible pavements and predict future pavement performance.

Mallela et al. (2013) performed an implementation study on the MEPDG for the Colorado Department of Transportation (CDOT). This study was accomplished using the data from LTPP projects located in Colorado and the CDOT PMS sections. The default key data inputs were developed for using the MEPDG in Colorado.

Mehta, Sauber, Owad, and Krause (2008) described the implementation of the MEPDG using Level-3 inputs for the state of New Jersey. The data were collected from the LTPP, PaveView, and Highway Pavement Management Application (HPMA) databases. The predicted and measured performance data for every section and each distress were compared case-by-case. This study found that the rutting predicted by using default truck distribution was greater than the measured rutting in the state of New Jersey. The predicted rate of increase in IRI was higher than the measured results as well. However, the fatigue and thermal cracking predictions compared well with the measured performance.

Muthadi and Kim (2008) conducted the calibration of the MEPDG for flexible pavements for North Carolina. Fifty-three pavement sections including 30 LTPP segments and 23 PMS segments were selected for the calibration and validation process. In this study, only the alligator cracking model and the rutting model were studied. Traffic inputs for each segment were collected from nearby weigh-in-motion (WIM) stations. The structure and material inputs were collected from the construction unit of the North Carolina Department of Transportation (NCDOT). This study concluded that the standard errors for the rutting model and the alligator cracking model were significantly lower after the calibration. The nationally calibrated MEPDG overpredicted the total rutting, but under-predicted the bottom-up cracking.

Schram and Abdelrahman (2006) calibrated two MEPDG IRI models for the JPCP and the HMA overlays on rigid pavements at the local level using the Nebraska Department of Roads (NDOR) pavement management data. This study demonstrated that the local-level calibration reduced the model prediction error by nearly half that of the national-level calibration.

Souliman, Mamlouk, El-Basyouny, and Zapata (2010) reported the calibration of the MEPDG prediction models for flexible pavements in Arizona with the data collected from 39 LTPP segments. This study adopted the Arizona default axle load spectra and the Level 3 material inputs. In addition, the subgrade moduli calculated using a local empirical correlation were compared with the MEPDG default values. The MEPDG with the nationally calibrated factors underpredicted the AC and subgrade rutting, but overpredicted the granular base rutting.

Mamlouk and Zapata (2010) examined the differences between the Arizona Department of Transportation (ADOT) PMS database and the LTPP database including the types of measuring equipment, the data processing methods, the units of measurements, the sampling methods, the unit length of the pavement section, the number of runs of measuring devices, and the survey manuals used.

Corley-Lay, Jadoun, Mastin, and Kim (2010) compared the the flexible pavement distresses monitored by NCDOT and long-term pavement performance program and found that the LTPP survey revealed a higher amount of distress than the NCDOT survey. Rut depths measured by LTPP were also found to be greater than those measured by NCDOT.

Von Quintus and Moulthrop (2007) conducted the local calibration study of the MEPDG for flexible pavements for the Montana Department of Transportation. A total of 89 LTPP and PMS segments from Montana and adjacent states were selected. This study created a calibration database and back-calculated the initial daily traffic volume from the measured traffic during the service life, while the MEPDG default or Montana default values were used for other traffic inputs. The results showed that the MEPDG overpredicted the bottom-up cracking for new flexible pavements, but under-predicted the bottom-up cracking for overlay pavements. Moreover, the MEPDG overpredicted the total rut depth, since the rutting in unbound layers and embankment soils was overpredicted. A poor correlation was found between the measured and predicted top-down cracking, although the bias was low. In addition, no consistent trend for the predicted top-down cracking could be identified to improve the accuracy of this prediction model.

Wu and Yang (2012) performed the local calibration of the MEPDG for flexible pavements for the Louisiana Department of Transportation and Development (LADOTD) based on the Louisiana PMS database. The comparison between predicted and measured performance indicated that the MEPDG rutting model overpredicted the total rutting of pavements. Further statistical analysis revealed that the MEPDG prediction errors for both the rutting and fatigue cracking models were greatly influenced by design factors, such as pavement type, traffic volume, subgrade modules, and project location.

Chapter 3: Framework for MEPDG Model Validation and Calibration

Based on the guidelines presented in the NCHRP Project 1-40B MEPDG local calibration guide (AASHTO, 2010), the framework for MEPDG model validation and local calibration for Kansas is outlined in this Chapter, which consists of 11 steps.

3.1 Step 1 - Selected Hierarchical Input Level

Hierarchical input levels in the AASHTO MEPDG Manual of Practice (the interim edition) can be described as follows (AASHTO, 2008):

- Level 1 inputs provide the highest level of accuracy and, thus, would have the lowest level of uncertainty or error. At Level 1, material inputs require laboratory or field testing, such as the dynamic modulus testing of asphalt concrete, binder G*, and site-specific traffic load spectra data.
- Level 2 inputs provide an intermediate level of accuracy, and would be closest to the typical procedures used with the earlier editions of the AASHTO Guide. Level 2 inputs are typically user-selected, possibly from an agency database, derived from a limited testing program, or estimated through correlations.
- Level 3 inputs provide the lowest level of accuracy. Inputs are user-selected typical values or typical averages for the region.

The goal of this first step was to determine the hierarchical input level which is appropriate for current and future data collection practices in Kansas. The selected inputs include traffic, materials, and climate.

3.1.1 Traffic

Below is a summary of the traffic inputs adopted in this study:

- The site-specific traffic inputs included the Average Annual Daily Truck Traffic (AADTT) data, the operational speed, the number of lanes, and the percentage of trucks in a design direction/lane. The details of the site-specific inputs are presented in Step 5.

- The KDOT suggested values, as presented in Tables 3.1 to 3.5, were selected for the inputs of the general information, the growth factor, the vehicle class distribution, the axle per truck, the monthly adjust factor, and the hourly distribution.
- The MEPDG default values were chosen for other inputs, such as the axle load spectra.

Since the KDOT suggested values and the MEPDG default values were mainly used, the MEPDG traffic inputs for this study can be considered as Level 3.

Table 3.1: KDOT Suggested Values for the General Information of Traffic

Parameters		Input value
Average Annual Daily Truck Traffic (AADTT)	Two-way AADTT	APD[a]
	Number of lanes	APD
	Percent trucks in design direction	50
	Percent trucks in design lane	95 or 100[b]
	Operational speed (mph)	APD
Axle Configuration	Average axle width (ft)	8.5
	Dual tire spacing (in.)	12
	Tire pressure (psi)	120
	Tandem axle spacing (in.)	51.6
	Tridem axle spacing (in.)	49.2
	Quad axle spacing (in.)	49.2
Lateral Wander	Mean wheel location (in.)	18
	Traffic wander standard deviation (in.)	10
	Design lane width (ft)	12
Wheelbase	Average spacing of short axles (ft)	12
	Average spacing of medium axles (ft)	15
	Average spacing of long axles (ft)	18
	Percent trucks with short axles	50
	Percent trucks with medium axles	25
	Percent trucks with long axles	25
Growth factor (%)		Use 3% in Johnson, Wyandotte, Sedgwick, Shawnee, Geary, and Riley Counties. Use 2% in the rest of the state.

[a]APD = actual project data
[b]Use 100 when the number of lanes is 2

Table 3.2: Vehicle Class Distribution

Vehicle class distribution (%)	Class 4	1.2
	Class 5	24.0
	Class 6	7.3
	Class 7	1.1
	Class 8	6.2
	Class 9	53.1
	Class 10	2.4
	Class 11	3.0
	Class 12	0.9
	Class 13	0.7

Table 3.3: Axles per Truck

Vehicle class	Single	Tandem	Tridem	Quad
Class 4	1.62	0.39	0	0
Class 5	2	0	0	0
Class 6	1.02	0.99	0	0
Class 7	1	0.26	0.83	0
Class 8	2.38	0.67	0	0
Class 9	1.13	1.93	0	0
Class 10	1.19	1.09	0.89	0
Class 11	4.29	0.26	0.06	0
Class 12	3.52	1.14	0.06	0
Class 13	2.15	2.13	0.35	0

Table 3.4: Monthly Adjusted Factor

January	1.164
February	1.152
March	1.034
April	1.034
May	0.973
June	0.948
July	0.93
August	0.956
September	1.012
October	1.022
November	1.011
December	1.048

Table 3.5: Hourly Truck Distribution (%)

Midnight	2.1
1:00 AM	2
2:00 AM	2.1
3:00 AM	1.7
4:00 AM	1.9
5:00 AM	2.3
6:00 AM	2.1
7:00 AM	3.4
8:00 AM	4.1
9:00 AM	4.8
10:00 AM	4.6
11:00 AM	5.7
Noon	5.5
1:00 PM	6.7
2:00 PM	6.1
3:00 PM	6.9
4:00 PM	6.4
5:00 PM	6
6:00 PM	5.6
7:00 PM	5.1
8:00 PM	4.3
9:00 PM	4.4
10:00 PM	3.5
11:00 PM	2.7

3.1.2 Materials

Below is a summary of the material inputs adopted in this study:

- The site-specific values for material inputs included the volumetric data of the asphalt concrete and the physical properties of the concrete pavement. The details of these values are presented in Step 5.
- The KDOT suggested values were selected for the inputs of the dynamic modulus, G* and the resilient modulus of subgrade, and the coefficient of thermal expansion for JPCP.
- Table 3.6 presents the G* values used in this study. For each binder, the G* values and the phase angles at two different temperatures were provided and input, even though the values at three different temperatures

are preferred in the Pavement ME design software. Table 3.7 provides the typical test results of the dynamic moduli for the samples at different PG grades. Figures 3.1 to 3.4 present the comparisons between the provided KDOT data and the MEPDG default values at Level 3, which show the reasonableness of the KDOT-provided dynamic modulus data. Tables 3.8 to 3.10 show all other input values suggested by KDOT.

- The MEPDG default values were used for the creep compliance, the indirect tensile strength, the thermal conductivity, the heat capacity, and the thermal contraction. Table 3.11 shows the MEPDG default values for the gradation and the engineering properties of the subgrade soil (A-7-6 was chosen in this study).

Therefore, the material inputs in this study can also be categorized as Level 3.

Table 3.6: G* Inputs

Grade	Temp 1 (°C)	G* (Pa)	Angle (°)	Temp 2 (°C)	G* (Pa)	Angle (°)
52-xx	52.0	3585	80	58.0	1660	82
58-xx	58.0	3400	80	64.0	1612	82
64-xx	64.0	3270	80	70.0	1575	82
70-xx	70.0	3075	60	76.0	1950	60

Table 3.7: Test Results of Dynamic Modulus for Asphalt Concrete at Different PG Grade

Performance grade	Temp (deg F)	Dynamic modulus (psi)					
		Frequency (Hz)					
		0.1	0.5	1	5	10	25
PG 58-28 (sample 1)	14	2286484	2531163	2617877	2780828	2836518	2898836
	40	1176386	1564576	1727181	2074215	2206498	2363555
	70	252267	446847	558000	875118	1031704	1249345
	100	42100	76745	100670	189653	247241	345754
	130	12822	18808	22840	38262	48978	69078
PG 58-28 (sample 2)	14	15694888	17373061	17967775	19085301	19467214	19894575
	40	8079073	10742695	11858273	14238899	15146261	16223509
	70	1734543	3071096	3834376	6011416	7086155	8579735
	100	289870	528171	692681	1304310	1700012	2376772
	130	88361	129582	157334	263463	337191	475441
PG 58-28 (sample 3)	14	15607285	17274508	17865305	18975426	19354794	19779300
	40	8038793	10686388	11795067	14160666	15062204	16132473
	70	1728292	3058452	3817825	5983040	7051660	8536496
	100	289292	526832	690756	1299944	1693917	2367534
	130	88279	129418	157106	262961	336473	474281
PG 58-28 (sample 4)	14	10312998	13005191	14090014	16336208	17170514	18146985
	40	3995890	6144670	7220011	9913223	11097223	12626948
	70	1003471	1716838	2160182	3587882	4387694	5609780
	100	330498	504992	619632	1034670	1303130	1770863
	130	174045	225101	257393	372167	447006	581368
PG 64-22 (sample 1)	14	2315049	2563306	2651300	2816671	2873193	2936444
	40	1189501	1582921	1747778	2099719	2233904	2393242
	70	254295	450955	563380	884351	1042932	1263425
	100	42287	77179	101294	191069	249219	348754
	130	12848	18862	22913	38424	49211	69453
PG 64-22 (sample 2)	14	2325320	2574865	2663320	2829563	2886384	2949971
	40	1194212	1589514	1755181	2108888	2243758	2403916
	70	255022	452429	565311	887666	1046965	1268484
	100	42354	77334	101517	191577	249928	349830
	130	12857	18881	22940	38482	49294	69588
PG 70-22	14	2332580	2583037	2671817	2838677	2895709	2959535
	40	1197541	1594173	1760413	2115370	2250724	2411462
	70	255535	453470	566675	890008	1049815	1272058
	100	42401	77443	101674	191935	250428	350589
	130	12864	18894	22958	38523	49352	69682
PG 70-28	14	2283486	2527790	2614370	2777067	2832670	2894890
	40	1175008	1562650	1725018	2071538	2203621	2360439
	70	252053	446415	557435	874148	1030525	1247866
	100	42080	76700	100605	189504	247033	345439
	130	12819	18803	22832	38245	48954	69038

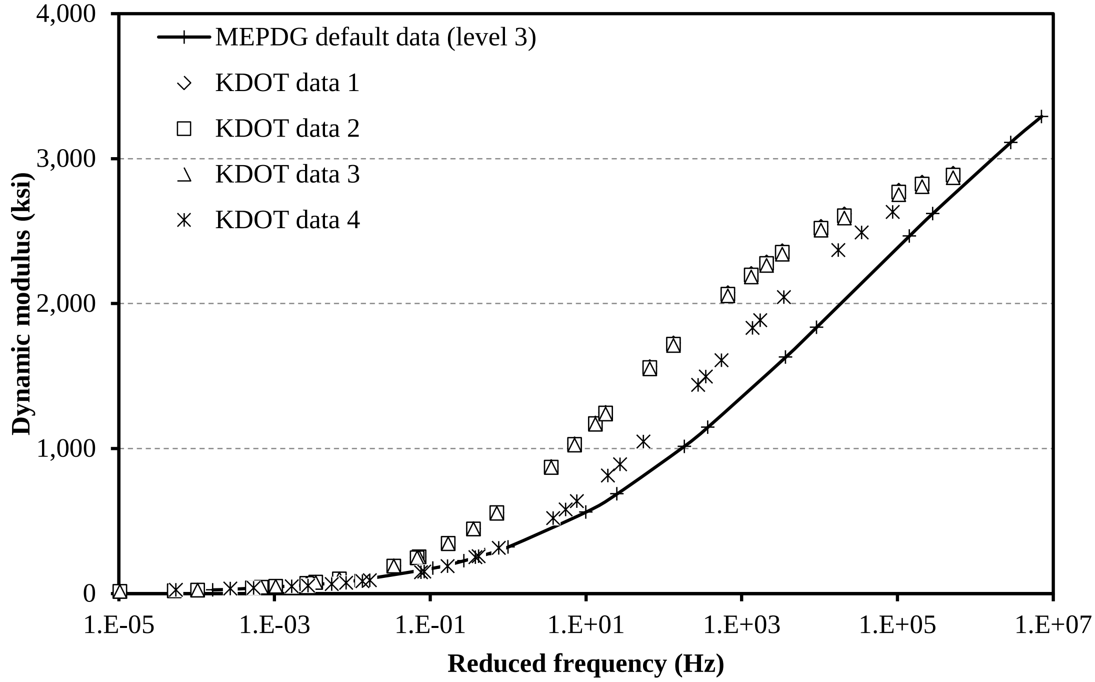

Figure 3.1: Comparison of the Dynamic Modulus between the KDOT Test Data and the MEPDG Default Data at Level 3 for the Samples with the PG 58-28 Binder

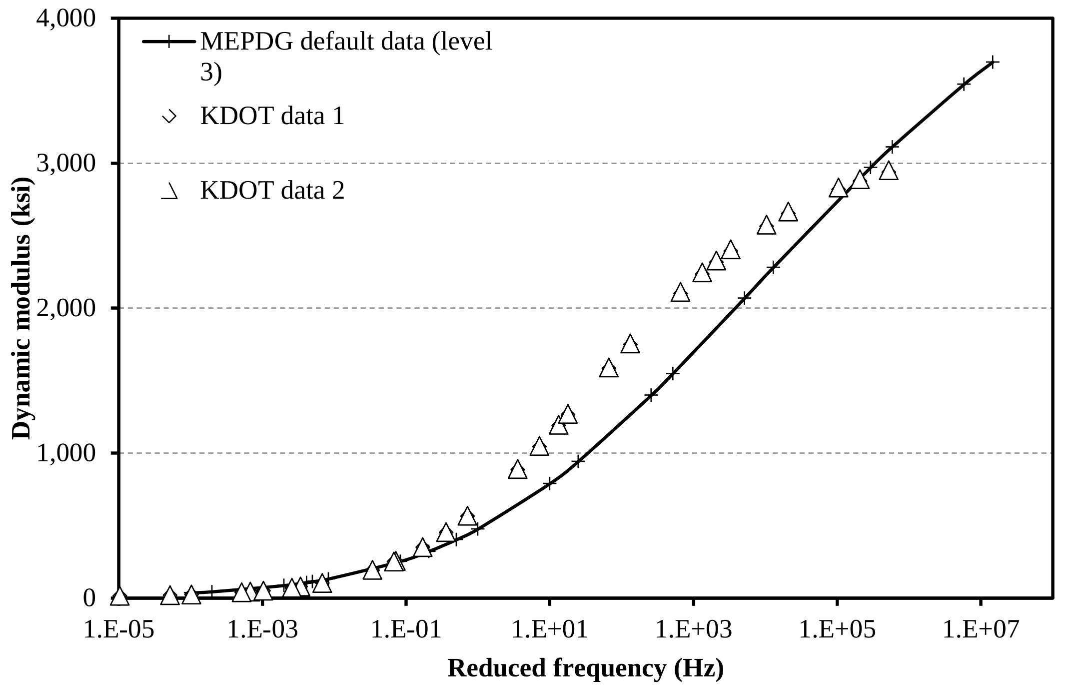

Figure 3.2: Comparison of the Dynamic Modulus between the KDOT Test Data and the MEPDG Default Data at Level 3 for the Samples with the PG 64-22 Binder

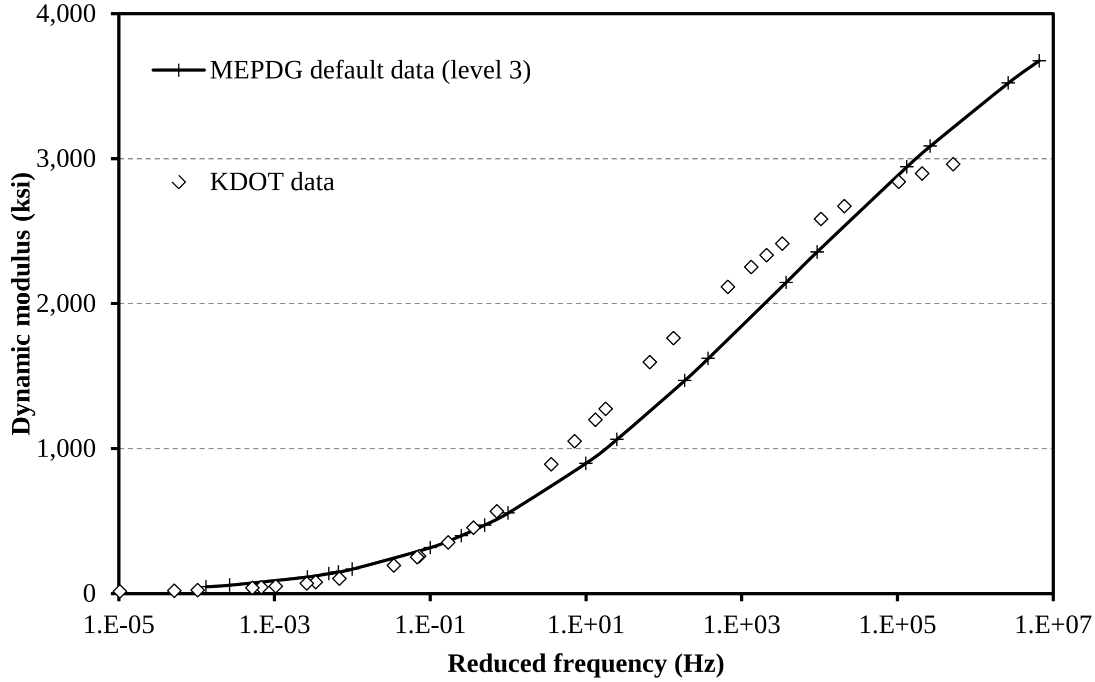

Figure 3.3: Comparison of the Dynamic Modulus between the KDOT Test Data and the MEPDG Default Data at Level 3 for the Samples with the PG 70-22 Binder

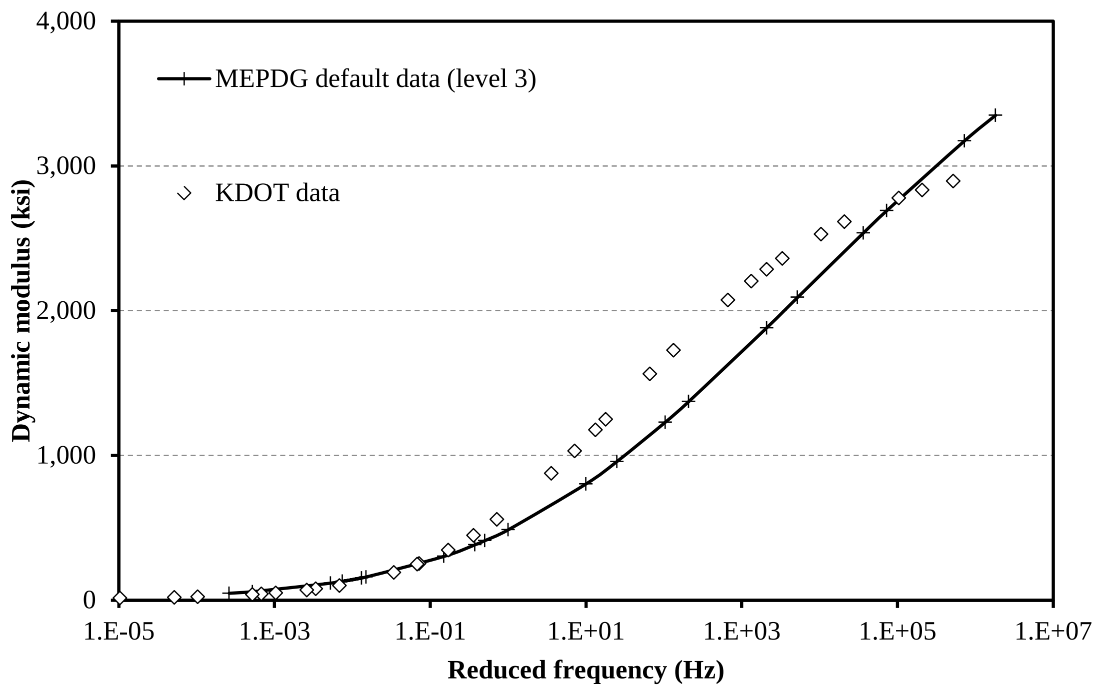

Figure 3.4: Comparison of the Dynamic Modulus between the KDOT Test Data and the MEPDG Default Data at Level 3 for the Samples with the PG 70-28 Binder

Table 3.8: KDOT Suggested Values for Inputs of AC Properties

Property		Input value
Mixture Volumetrics	Thickness (in.)	APD
	Unit weight (pcf)	140
	Poisson's ratio	0.35
	Air voids (%)	7%
	Effective binder content (%)	APD
Mechanical Properties	Dynamic modulus and Asphalt binder	Input E* and G* provided by KDOT
	Select HMA Estar predictive model	Use viscosity based model (nationally calibrated)
	Preference temperature (deg F)	70
	Indirect tensile strength at 14 deg F (psi)	National default value
	Creep compliance (1/psi)	National default value
Thermal	Thermal conductivity (BTU/hr-ft-deg F)	0.67
	Heat capacity (BTU/lb-deg F)	0.23
	Thermal contraction	1.30E-05
AC Layer Properties	AC surface shortwave absorptivity	0.85
	Is endurance limit applied?	FALSE
	Endurance limit (Microstrain)	100
	Layer interface	Full friction interface

APD = actual project data

Table 3.9: KDOT Suggested Values for Inputs of JPCP Properties

Property		KDOT suggested values for calibration	Notes
Thickness		APD	
Unit Weight		APD	If APD N/A, use 141 lbs/ft^3
Poisson's Ratio		0.2	National default value
Coeff. of Thermal Expansion	Limestone	$6.3x10^{-6}$	in/in/deg F; adjusted value to reflect the "old" test method used in the MEPDG software. Update when the software is updated.
	Non-Limestone	6.8×10^{-6}	in/in/deg F; adjusted value to reflect the “old” test method used in the MEPDG software. Update when the software is updated.
Thermal Conductivity		1.25	BTU/hr-ft-deg F; National default value
PCC Heat Capacity		0.28	BTU/lb-deg F; National default value
Cement Type		APD	If APD N/A, use Type II
Cementitious Content		APD	If APD N/A, use 602 lbs/yd^3 for CF mixes and 620 lbs/yd^3 for MA mixes
Water to Cement Ratio		APD	If APD N/A, use 0.42
Aggregate Type		APD	Geographic West: gravel containing granite and sandstone. East: limestone or granite in KC, Topeka, and Lawrence.
Reversible Shrinkage		35	Less than 50%
50% of Ultimate Shrink		35	National default value
Curing Method		APD	If APD N/A, use curing compound
Compressive Strength		APD	If APD N/A, use 4500 psi
Surface Shortwave Abs		0.85	National default value
Joint Spacing		APD	If APD N/A, use 15 ft
Sealant Type		APD	If APD N/A, use Preformed
Dowel Spacing		APD	If APD N/A, use 1 ft
Dowel Diameter		APD	If APD N/A, use thickness/8 (inches)
Widened Slab		APD	If APD N/A, use No or 12-ft wide lanes with 24-ft wide slab
Tied Shoulders		APD	If APD N/A, use Yes
Erodibility Index		2	

APD = actual project data

Table 3.10: KDOT Suggested Values for Inputs of Base Course and Subgrade

Base course/subgrade type	Property	KDOT suggested value for calibration
Chemically Stabilized Base CTB/ATB	Thickness (in.)	APD
	Poisson's Ratio	0.2
	Unit Weight (lb/ft^3)	APD
	Elastic/Resilient Modulus (psi)	125000
	Heat Capacity (BTU/lb-deg F)	0.28
	Thermal Conductivity (BTU/hr-ft-deg F)	1.25
Non-Stabilized Base GSB	Thickness (in.)	APD
	Poisson's Ratio	0.35
	Coefficients of Lateral Earth Pressure	0.5
	Elastic/Resilient Modulus (psi)	38000
	Gradation/Engineering Properties	APD
Subgrade	Thickness (in.)	APD
	Poisson's Ratio	0.35
	Coefficients of Lateral Earth Pressure	0.5
	Elastic/Resilient Modulus (psi)	APD
	Gradation/Engineering Properties	National default value
Lime Treated Subgrade	Thickness (in.)	APD
	Poisson's Ratio	0.35
	Coefficients of Lateral Earth Pressure	0.5
	Elastic/Resilient Modulus (psi)	LTSG M_r = (2.03 × untreated subgrade M_r) + 225
	Gradation/Engineering Properties	National default value

APD = actual project data
M_r = resilient modulus

Table 3.11: MEPDG Default Values for Inputs of Subgrade Soil (A-7-6)

Liquid limit		51.0
Plasticity index		30.0
Is layer compacted?		True
Maximum dry unit weight (pcf)		98.6
Saturated hydraulic conductivity (ft/hr)		8.849×10^{-6}
Specific gravity of solids		2.7
Optimum gravimetric water content (%)		22.2
Sieve size, % passing	#200	79.1
	#80	84.9
	#40	88.8
	#10	93.0
	#4	94.9
	3/8-in.	96.9
	1/2-in.	97.5
	3/4-in.	98.3
	1-in.	98.8
	1 1/2-in.	99.3
	2-in.	99.6
	3 1/2-in.	99.9

3.1.3 Climate

A summary of the climate inputs adopted in this study:

- The coordinates and elevations for all the segments were input as site-specific values. The details of these values are shown in Step 5.
- The groundwater table for all the segments was set as 50 ft, since this value would not have any effect on the performance predicted by the MEPDG.
- The climate stations used in this study were chosen from the MEPDG software, as shown in Table 3.12 and Figure 3.5.

Therefore, the climatic inputs are also categorized as Level 3.

Table 3.12: Climate Stations Used in this Study

Climate station	Latitude	Longitude
Chanute, KS	37.67	-95.484
Concordia, KS	39.549	-97.652
Dodge City, KS	37.773	-99.97
Emporia, KS	38.331	-96.19
Garden City, KS	37.927	-100.725
Goodland, KS	39.368	-101.693
Guymon, OK	36.682	-101.505
Hill City, KS	39.376	-99.83
Joplin, MO	37.149	-94.498
Kansas City, MO	39.299	-94.718
Lawrence, KS	39.008	-95.212
Manhattan, KS	39.134	-96.679
Olathe, KS	38.831	-94.89
Parsons, KS	37.328	-95.504
Russell, KS	38.872	-98.828
Salina, KS	38.813	-97.661
St. Joseph, MO	39.774	-94.907
Topeka, KS	38.95	-95.664
Wichita, KS	37.647	-97.429
Wichita, KS	37.75	-97.219
Winfield/Arkansas City, KS	37.168	-97.037

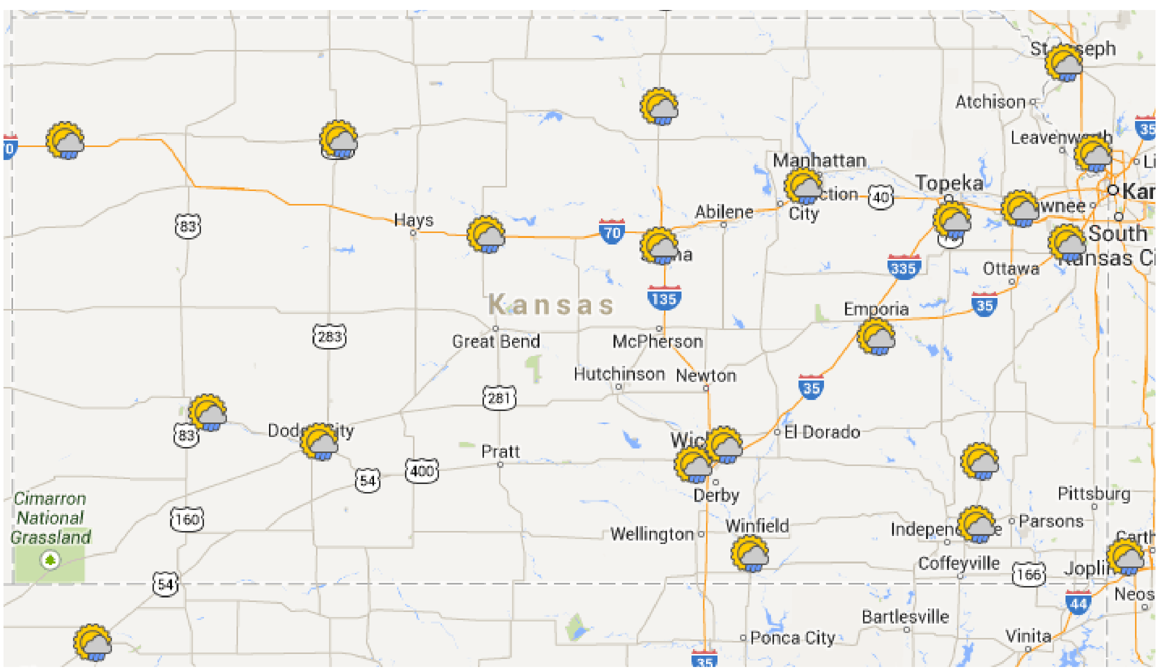

Figure 3.5: Locations of the Climate Stations on the Kansas Map

3.2 Step 2 - Experimental Factorial and Matrix or Sampling Template

The goal of this step is to create a sampling template for selecting projects which reflect the current and future KDOT pavement design features. Tables 3.13 and 3.14 show the sampling matrix created for the validation and local calibration of the MEPDG models in Kansas.

Table 3.13: Simplified Sampling Template for the Local Calibration of New HMA Pavements

HMA thickness (in)	With/without base course	Base and subgrade type							
		Subgrade resilient modulus (2700 psi)				Subgrade resilient modulus (more than 2700 psi)			
4 to 8									
$\geqslant$8									

Table 3.14: Simplified Sampling Template for the Local Calibration of New JPCPs

PCC Thickness (in)	Dowel diameter, (in)	Edge support	Joint spacing, (ft)	Base and subgrade type					
				Subgrade resilient modulus (2700 psi)			Subgrade resilient modulus (more than 2700 psi)		
$\leqslant$10		None	<15						
		Tied PCC	$\geqslant$15						
$\geqslant$10		None	<15						
		Tied PCC	$\geqslant$15						

3.3 Step 3 - Minimum Sample Size Required for Validation and Local Calibration of Distress Prediction Model

The minimum sample size or the minimum number of pavement projects is needed for validation and local calibration of distress prediction models in the MEPDG and depends on the model error (i.e., standard error of the estimate [SEE]), the confidence level for statistical analysis, and the threshold value of performance indicators at an agency's design reliability level. Table 3.15 presents the required number of pavement projects for the validation and local calibration of the MEPDG models for different pavement types recommended by AASHTO (2008). Overall, the required minimum number of HMA pavement and JPCP projects should be followed, except for the required number for the validation and local calibration of IRI. This is because the accuracy of the IRI models depends on the accuracy of other pavement distress predictions. In other words, it is not necessary to sample a large number of projects to validate the IRI model if other distress prediction models are judged to be accurate and reasonable.

Table 3.15: Estimated Number of Pavement Projects Required for the Validation and Local Calibration

Pavement Type	Performance Indicator	Performance Indicator Threshold (at 90% Reliability)	Standard Error of the Estimate (SEE)	Minimum Number of Projects Required for Validation & Local Calibration	Minimum Number of Projects Required for Each Pavement Type (n)*
New HMA	Alligator cracking	20 percent lane area	5.01 percent	16	18
	Transverse thermal cracking	Crack spacing > 100 ft of 630 ft/mi	N/A	18	
	Rutting	0.4 in.	0.107 in.	14	
	IRI	169 in./mi	18.9 in./mi	80	
New JPCP	Faulting	< 0.15 in.	0.033 in.	21	21
	Transverse cracking	< 10 percent slabs	4.52 percent	5	
	IRI	169 in./mi	17.1 in./mi	98	

Source: AASHTO, 2010

*n = $\left(\frac{Z_{\alpha/2}\sigma}{E}\right)^2$, where $Z_{\alpha/2}$= 1.601 (for a 90 percent confidence level), σ = performance indicator threshold (design criteria), and E = tolerable bias at 90 percent reliability (1.601*SEE).

3.4 Step 4 - Selection of Projects

The possible projects to be used in this study were selected from the PMS database of KDOT. To identify as many projects as possible to ensure the accuracy of the validation and local calibration, the following project selection criteria were applied:

For new JPCP pavements:

- projects were constructed after 1990;
- segments were longer than 1 mile;
- no D-cracking existed;
- dowel spacing was 15 ft; and
- material properties and distress data were available.

For new flexible pavements:

- projects were constructed after 1999;
- segments were longer than 1 mile;
- the Superpave mixes were used; and
- volumetric data and distress data were available.

As a result, the number of projects was selected as follows:

- new flexible pavements: 28 projects.
- new JPCPs: 32 projects.

The above number of selected projects met the requirement for local calibration as recommended in Table 3.15.

The locations of the selected projects are shown on the maps in Figures 3.6 and 3.7. The general descriptions of both the flexible pavement projects and the rigid pavement projects are provided in Tables 3.16 to 3.19.

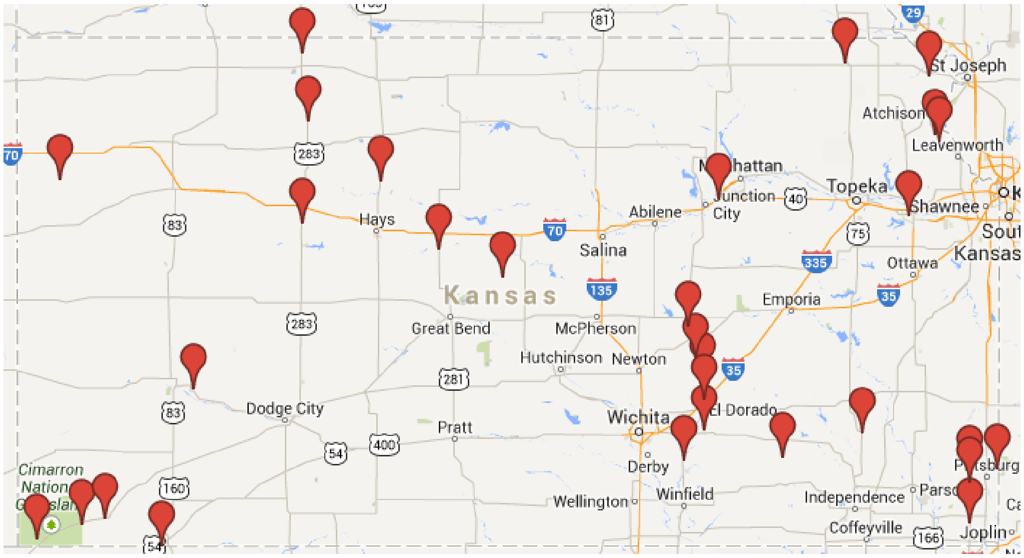

Figure 3.6: Locations of the Selected New Flexible Pavement Projects in Kansas

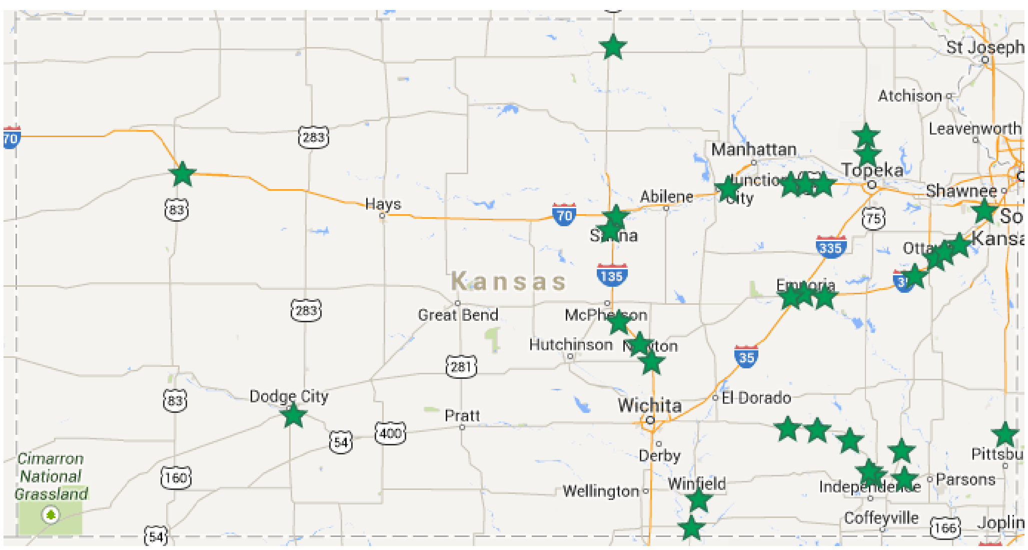

Figure 3.7: Locations of the Selected New JPCP Projects in Kansas

Table 3.16: General Descriptions of the Selected Flexible Pavement Projects

No.	Project name	Begin milepost	End milepost	Length (mile)	Construction date	Project ID
1	003U0007300-NB	0	4.14	4.14	31-Dec-02	K-5761-01
2	007U0007500-NB	13.05	19.68	6.63	18-Nov-05	K-5766-01
3	008U0005400-EB	17.47	25.69	8.22	4-Dec-05	K-6811-01
4	008U0007700-NB-1	0	12.71	12.71	2-Dec-04	K-5767-01
5	008U0007700-NB-2	33.88	43.44	9.56	8-Aug-06	K-6384-01
6	008U0007700-NB-3	43.44	50.67	7.23	1-Dec-04	K-7347-01
7	011U0006900-NB	8.45	11.44	2.99	27-Jul-09	K-6799-01
8	019K0000700-NB-1	0	4.97	4.97	15-May-06	K-7404-01
9	019K0000700-NB-2	4.97	10.99	6.02	7-Nov-08	K-7405-01
10	019U0016000-EB	9.69	14.54	4.85	1-Dec-04	K-6405-01
11	022K0000700-NB	5.92	11.71	5.79	11-May-06	K-6393-01
12	023U0004000-EB	11.24	12.44	1.20	1-Dec-05	K-6880-01
13	025K0009900-NB	12.92	21.72	8.80	30-Jul-07	K-7418-01
14	027K0015600-EB	5.63	18.40	12.77	21-Nov-07	K-6802-01
15	028U0005000-EB	19.88	29.37	9.48	1-Dec-05	K-6374-01
16	031K0001800-WB	15.55	17.55	2.00	29-Sep-07	K-6795-01
17	033U0028300-NB	16.96	30.36	13.40	1-Dec-04	K-5770-01
18	052U0007300-NB	18.45	20.92	2.47	31-Dec-02	K-5762-01
19	065K0002700-NB	0.00	2.67	2.67	31-Dec-02	K-4438-01
20	065U0005600-EB	19.76	21.87	2.12	1-Dec-04	K-6399-01
21	069U0028300-NB	21.55	32.05	10.50	1-Dec-02	K-5752-01
22	082U0018300-NB	0	5.92	5.92	31-Oct-06	K-6377-01
23	084U0028100-NB	4.77	6.11	1.34	1-Dec-04	K-7337-01
24	088U0005400-WB	0	3.87	3.87	12-Dec-07	K-7283-01
25	091K0002700-NB	0	4.19	4.19	13-Sep-07	K-6809-01
26	095U0005600-EB	8.57	11.12	2.55	22-Aug-06	K-6400-01
27	098U0028300-NB	10.03	21.49	11.46	31-Oct-06	K-6804-01
28	103K0003900-NB	14.47	16.43	1.96	1-Dec-04	K-5748-01

Table 3.17: Latitudes, Longitudes, and Elevations of the Selected Flexible Pavement Projects and Depths of the Groundwater Table Used in this Study

Project name	Latitude (deg)	Longitude (deg)	Elevation (ft)	Depth to groundwater table (ft)
003U0007300-NB-1	39.4441	-95.095	1071	50
007U0007500-NB	39.8607	-95.777	1251	50
008U0005400-EB	37.6994	-96.845	1341	50
008U0007700-NB-1	37.5187	-96.998	1223	50
008U0007700-NB-2	37.8878	-96.849	1392	50
008U0007700-NB-3	38.0155	-96.859	1392	50
011U0006900-NB	37.1438	-94.832	919	50
019K0000700-NB-1	37.4693	-94.627	974	50
019K0000700-NB-2	37.3835	-94.833	948	50
019U0016000-EB	37.4567	-94.836	935	50
022K0000700-NB	39.7824	-95.143	1119	50
023U0004000-EB	38.9714	-95.3	1011	50
025K0009900-NB	37.5376	-96.253	1078	50
027K0015600-EB	38.6108	-98.371	1825	50
028U0005000-EB	37.9465	-100.71	2903	50
031K0001800-WB	39.0668	-96.732	1096	50
033U0028300-NB	39.5184	-99.845	2446	50
052U0007300-NB	39.4015	-95.067	1097	50
065K0002700-NB	37.1346	-101.56	3521	50
065U0005600-EB	37.0502	-101.9	3272	50
069U0028300-NB	39.914	-99.889	2428	50
082U0018300-NB	39.1763	-99.299	2133	50
084U0028100-NB	38.7682	-98.855	1751	50
088U0005400-WB	37.0055	-100.95	2865	50
091K0002700-NB	39.1771	-101.72	3624	50
095U0005600-EB	37.1701	-101.38	3124	50
098U0028300-NB	38.9279	-99.891	2413	50
103K0003900-NB	37.6873	-95.652	992	50

Table 3.18: General Descriptions of the Selected Rigid Pavement Projects

No.	Project name	Begin milepost	End milepost	Length (mile)	Construction date	Project ID
1	018K0036000-EB	0.00	2.95	2.95	1-Jan-96	K-4432-02
2	018U0007700-NB	4.62	8.51	3.89	1-Jan-99	K-7711-01
3	019U0006900-NB	15.71	23.90	8.19	1-Jan-98	K-3276-01
4	029U0005600-EB	12.17	15.60	3.43	1-Jan-96	K-4422-01
5	030I0003500-NB-1	3.25	9.05	5.80	1-Jan-96	K-3596-02
6	030I0003500-NB-2	14.20	17.40	3.20	31-Dec-02	K-5641-01
7	030I0003500-NB-3	19.87	26.85	6.97	31-Dec-02	K-5642-01
8	031I0007000	11.04	13.47	2.43	1-Jan-98	K-5086-01
9	031I0007000-EB	18.82	26.53	7.71	1-Jan-99	K-5090-01
10	037U0040000-EB-1	0.00	21.45	21.45	1-Jan-97	K-3293-04
11	037U0040000-EB-2	21.45	31.55	10.11	1-Jan-98	K-3293-04
12	040I0013500-NB-1	7.47	13.39	5.92	1-Dec-01	K-5634-01
13	040I0013500-NB-2	13.39	20.83	7.44	1-Dec-03	K-6392-01
14	043U0007500-NB-1	0.00	8.02	8.02	1-Jan-93	K-3250-01
15	043U0007500-NB-2	8.02	17.33	9.32	1-Jan-96	K-3251-01
16	046K0000700-SB	12.47	15.14	2.67	1-Jan-95	K-3382-01
17	055U0004000-WB	35.69	38.65	2.96	31-Dec-02	K-5742-01
18	056I0003500-SB-1	11.51	16.60	5.09	1-Jan-94	K-2633-01
19	056I0003500-SB-2	17.23	26.88	9.65	31-Dec-02	K-5088-01
20	056U0005000-EB-1	0.00	4.89	4.89	1-Jan-93	K-2853-01
21	059I0013500-NB	6.29	14.30	8.01	1-Jan-96	K-4689-01
22	061I0003500-NB	0.00	2.56	2.56	31-Dec-03	K-6356-01
23	063U0040000-EB	2.06	11.86	9.80	1-Jan-98	K-4892-02
24	067U0016900-NB	7.14	13.31	6.18	1-Dec-03	K-6376-01
25	079U0008100-NB	13.29	17.46	4.17	31-Dec-01	K-5022-02
26	085I0007000-EB	14.72	24.02	9.30	1-Dec-03	K-6778-01
27	085I0013500	11.15	18.80	7.64	1-Jan-99	K-5263-01
28	099I0007000-EB-1	0.00	5.19	5.19	1-Jan-01	K-5643-01
29	099I0007000-EB-2	5.19	8.02	2.83	1-Jan-99	K-5628-01
30	099I0007000-EB-3	16.03	18.09	2.07	1-Jan-99	K-5633-01
31	103U0007500-SB	0.00	1.97	1.97	1-Jan-99	K-3295-02
32	103U0040000-EB	3.56	11.75	8.19	1-Jan-98	K-3294-02

Table 3.19: Latitudes, Longitudes, and Elevations of the Selected Rigid Pavement Projects and Depths of the Groundwater Table used in this Study

Project name	Latitude (deg)	Longitude (deg)	Elevation (ft)	Depth to water table (ft)
018K0036000-EB	37.225067	-96.9781722	1117	50
018U0007700-NB	37.0564185	-97.0260268	1065	50
019U0006900-NB	37.6021277	-94.7045524	967	50
029U0005600-EB	37.7215386	-99.9819858	2490	50
030I0003500-NB-1	38.5322076	-95.3700381	1097	50
030I0003500-NB-2	38.6315674	-95.2168846	915	50
030I0003500-NB-3	38.6642283	-95.1548503	902	50
031I0007000	39.0365711	-96.7610068	1150	50
031I0007000-EB	39.0365711	-96.7610068	1392	50
037U0040000-EB-1	37.6362535	-96.3129775	1093	50
037U0040000-EB-2	37.6278466	-96.0994595	1489	50
040I0013500-NB-1	38.028131	-97.3226205	1489	50
040I0013500-NB-2	38.1309759	-97.4140485	1104	50
043U0007500-NB-1	39.2310673	-95.7197116	1146	50
043U0007500-NB-2	39.3448548	-95.7351634	960	50
046K0000700-SB	38.9054788	-94.8526591	894	50
055U0004000-WB	39.1193691	-100.8122137	1140	50
056I0003500-SB-1	38.4258742	-96.1946377	1148	50
056I0003500-SB-2	38.4109124	-96.0431732	1127	50
056U0005000-EB-1	38.406537	-96.2994248	1127	50
059I0013500-NB	38.2666037	-97.5738161	1489	50
061I0003500-NB	38.7112102	-95.0425239	990	50
063U0040000-EB	37.3587593	-95.685267	781	50
067U0016900-NB	37.509554	-95.4712541	1016	50
079U0008100-NB	39.8509181	-97.6153008	1552	50
085I0007000-EB	38.8765163	-97.5968604	1219	50
085I0013500	38.7967886	-97.6330247	1242	50
099I0007000-EB-1	39.0658049	-96.2978393	1246	50
099I0007000-EB-2	39.0657726	-96.1863126	1050	50
099I0007000-EB-3	39.059005	-96.0585087	1126	50
103U0007500-SB	37.384951	-95.710667	1155	50
103U0040000-EB	37.5711968	-95.8515186	1127	50

3.5 Step 5 - Extraction and Evaluation of Distress and Project Data

The following four tasks were completed in this step following the MEPDG local calibration guide (AASHTO, 2010):

1. Extraction and review of the distress/IRI data for each selected project. The distress/IRI data of each selected project was reviewed at this step. The data before any rehabilitation work was extracted and used as a new pavement for calibration.
2. Comparison of the performance indicator values to the design threshold values. The rut depths of the flexible pavements and the IRI of the flexible/rigid pavements were within the ranges of the design thresholds. However, the top-down cracking and the maximum values of the thermal cracking of flexible pavements were much higher than the MEPDG threshold values. Moreover, the measured mean joint faulting values of the rigid pavements were much lower than the MEPDG threshold value.
3. Evaluation of the distress data to identify anomalies and outliers. The selected projects in this study were not considered as anomalies and outliers; therefore, all the available distress data were used in the local calibration.
4. Determination of the MEPDG inputs. In addition to the KDOT suggested input values and the MEPDG default values for some parameters, the site-specific values for other parameters were determined. In Appendix A, Table A.1 presents the subgrade resilient modulus for each project in terms of the county in which the project is located. In Appendix B, Tables B.1 and B.2 provide the site-specific traffic inputs for the new flexible and rigid pavements, respectively. Tables B.3 and B.4 present the structure information for the flexible and rigid pavement projects. Tables B.5, B.6, and B.7 summarize the site-specific material properties for these two types of pavement projects. Additionally, Tables B.8 and B.9 show the climate inputs for the flexible and rigid pavement projects.

3.6 Step 6 - Field and Forensic Investigations

The inputs obtained from various databases, along with the default MEPDG and KDOT inputs, were considered sufficient for the local calibration, and no field or forensic investigation was conducted in this study. However, field or forensic investigation will further improve the reliability of the calibrated models.

3.7 Step 7 - Assessment of Local Bias from Global Calibration Factors

The MEPDG software, AASHTOWare Pavement ME design Version 1.3, was executed using the global calibration factors to predict the performance indicators for each selected roadway segment. Appendices C and D provide the comparisons of the measured and predicted distresses and IRI based on the nationally calibrated models for the flexible and rigid pavements, respectively. A reliability of 50% was used in this study to predict the average pavement performance.

The flexible pavement projects were divided into two groups in terms of their subgrade resilient moduli, which had an important influence on the distresses and IRI based on the review of the measured performance data. The rigid pavement projects were separated into three groups according to the base course type. Tables 3.20 and 3.21 list the grouped flexible and rigid pavement projects, respectively.

Table 3.20: Grouped Flexible Pavement Projects

Subgrade resilient modulus (2700 psi)	Subgrade resilient modulus (higher than 2700 psi)	
003U0007300-NB	008U0005400-EB	031K0001800-WB
007U0007500-NB	008U0007700-NB-1	033U0028300-NB
022K0000700-NB	008U0007700-NB-2	065K0002700-NB
052U0007300-NB	008U0007700-NB-3	065U0005600-EB
	011U0006900-NB	069U0028300-NB
	019K0000700-NB-1	082U0018300-NB
	019K0000700-NB-2	084U0028100-NB
	019U0016000-EB	088U0005400-WB
	023U0004000-EB	091K0002700-NB
	025K0009900-NB	095U0005600-EB
	027K0015600-EB	098U0028300-NB
	028U0005000-EB	103K0003900-NB

Table 3.21: Grouped Rigid Pavement Projects

PCCDCB[1]	CEMBAS[2]	DBWED[3]
018U0007700-NB	018K0036000-EB	019U0006900-NB
043U0007500-NB-2	031I0007000-EB	029U0005600-EB
056I0003500-SB	040I0013500-NB-1	030I0003500-2
063U0040000-EB	040I0013500-NB-2	030I0003500-3
103U0040000-EB	043U0007500-NB	031I0007000-2
	046K0000700-SB	037U0040000-EB
	055U0004000-EB	037U0040000-EB2
	056U0005000-EB	030I0003500-1
	059I0013500-NB	056I0003500-SB-2
	061I0003500-NB	085I0013501
	067U0016900-NB	099I0007000-EB-1
	079U0008100-NB	099I0007000-EB-2
	085I0007000-EB	099I0007000-EB-3
		103U0007500-SB

[1]PCCDCB: Drainable cement treated base under PCC
[2]CEMBAS: Cement treated base
[3]DBWED: Drainage base with edge drains (asphalt)

The null hypothesis, as shown in Equation 3.1, was checked for the entire sampling matrix. In this equation, the average residual error ($e_r = y_{measured} - x_{predicted}$) or bias is zero for a specified confidence level (95%).

$$H_0:\ \sum_{i=1}^{n}(y_{measured} - x_{predicted})_i = 0 \qquad \text{Equation 3.1}$$

It is helpful to assess the predicted performance through a comparison between the predicted ($x_{predicted}$) and the measured values ($y_{measured}$) and a comparison between the residual errors (e_r) and the predicted values ($x_{predicted}$) for each performance indicator.

When the calculated p-value is less than 0.05, the null hypothesis will be rejected, which implies a significant bias existing between the predicted and measured values.

Two other model parameters can also be used to evaluate the model bias, i.e., the intercept (b_0) and the slope (m) of a linear regression line between the measured ($y_{measured}$) and predicted ($x_{predicted}$) values as follows:

$$y_{measured} = b_0 + m(x_{predicted}) \qquad \text{Equation 3.2}$$

The intercept (b_0) and slope (m) can not only provide the accuracy of each prediction, but also identify the dependent factors. The rejection of the hypothesis means that the intercept (b_0)

is significantly different from 0 and the slope (m) is significantly different from 1. This statistical analysis will be presented in Chapter 4.

3.8 Step 8 - Elimination of Local Bias

If the null hypothesis in Equation 3.1 is rejected in Step 7, it means that a significant bias exists. If this situation happens, the cause for the bias should be identified and the bias should be removed. If possible, the analysis using the adjusted calibration coefficients should be re-run. The features to be considered in removing the bias include the traffic conditions, the climate, and the material characteristics. The details on the elimination of the bias will be presented in Chapter 4. Appendices E and F show the comparison between the measured and MEPDG predicted distresses and IRI after the local calibration.

3.9 Step 9 - Assessment of Standard Error of the Estimate

In this step, the standard error of the estimate (SEE) for the locally calibrated models is compared with the SEE of the nationally calibrated MEPDG models and checked for reasonableness. Table 3.15 provided the reasonable SEE values of nationally calibrated models. At different standard errors for the locally calibrated and nationally calibrated (i.e., MEPDG) models, the following courses of action may be taken (Pierce & McGovern, 2014):

- When their errors are not statistically significantly different, the locally calibrated performance prediction model coefficients should be used (proceed to Step 11).
- When their errors are statistically significantly different and the SEE of the locally calibrated performance prediction model is smaller than that of the nationally calibrated MEPDG model, the locally calibrated performance prediction model coefficients should be used (proceed to Step 11).
- When their errors are statistically significantly different and the SEE of the locally calibrated MEPDG model is larger than that of the nationally calibrated MEPDG model, the locally calibrated performance prediction

model should be recalibrated to lower the standard error. Alternatively, the locally calibrated performance prediction model could be accepted knowing it has a larger standard error than the nationally calibrated MEPDG model.

The analysis of the standard error of the estimate will be presented in Chapter 4.

3.10 Step 10 - Reduction of Standard Error of the Estimate

If the standard error for local calibration cannot be reduced, proceed to Step 11. If the standard error for local calibration can be reduced, determine if the standard error of each cell of the experimental matrix is dependent on other factors and adjust the local calibration coefficients to reduce the standard error.

3.11 Step 11 - Interpretation of the Results

The predicted distresses and IRI with the locally calibrated models should be compared with the measured distresses and IRI to ensure that acceptable results have been obtained.

Chapter 4: Validation and Recalibration of Selected MEPDG Models

This chapter presents the validation and local calibration of the nationally calibrated MEPDG models for Kansas. The statistical analysis presented in this chapter was done by the EXCEL statistical toolbox. In the statistical analysis, the hypothesis tests mentioned in Step 7 were performed. When the p-values (the probability of obtaining a predicted value equal to the measured value) were larger than 0.05, the hypotheses were accepted.

4.1 Flexible Pavements

The subgrade resilient modulus was found to have an important influence on the predicted rutting. Figure 4.1 shows that the predicted rutting by the nationally calibrated MEPDG model for the projects with a subgrade resilient modulus, M_r, of 2700 psi was much larger than that for the projects with a subgrade M_r equal to or higher than 4000 psi.

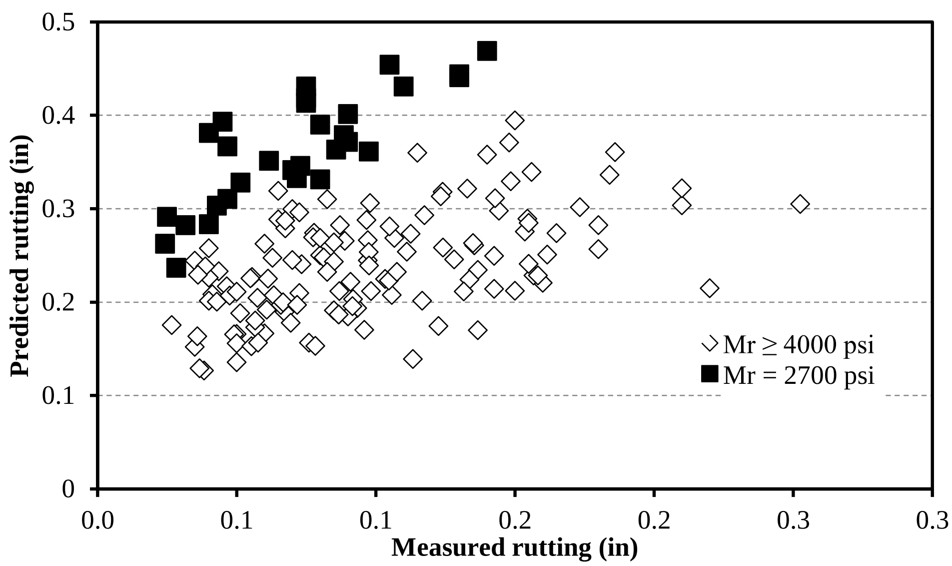

Figure 4.1: The Influence of Subgrade Resilient Modulus to the Predicted Rutting by the Nationally Calibrated MEPDG

In the following validation and local calibration, the flexible pavement projects in Kansas were divided into two groups, one with the subgrade M_r equal to 2700 psi and the other with the subgrade M_r equal to or higher than 4000 psi. There was no project with a subgrade resilient modulus between 2700 and 4000 psi, based on the county charts of subgrade resilient modulus of Kansas, as shown in Table A.1.

4.1.1 Bottom-Up Cracking

The KDOT PMS database shows that the measured bottom-up cracks were zero; therefore, it is not necessary to have a local calibration for the bottom-up cracking.

4.1.2 Top-Down Cracking

Figure 4.2 and Table 4.1 show the comparisons of measured and predicted top-down cracking by the nationally calibrated MEPDG for the projects with a subgrade M_r of 2700 psi. Figure 4.3 and Table 4.2 show similar comparisons for other projects with a subgrade M_r equal to or higher than 4000 psi.

It is found that a significant bias existed, and the MEPDG underestimated the top-down cracking. In addition, there was a poor correlation between the measured and predicted top-down cracking by the nationally calibrated MEPDG. Considering the biased prediction and the poor correlation, local calibration of the MEPDG top-down cracking model is needed to improve its prediction accuracy.

The top-down cracking model was locally calibrated by adjusting the calibration coefficients to minimize the bias and improve the correlation. Figures 4.4 and 4.5 and Tables 4.3 and 4.4 show that the bias was minimized after the local calibration; however, the hypotheses of the intercept and slope were still rejected. The SEEs were relatively high after local calibration due to the varibility of the measured top-down cracking.

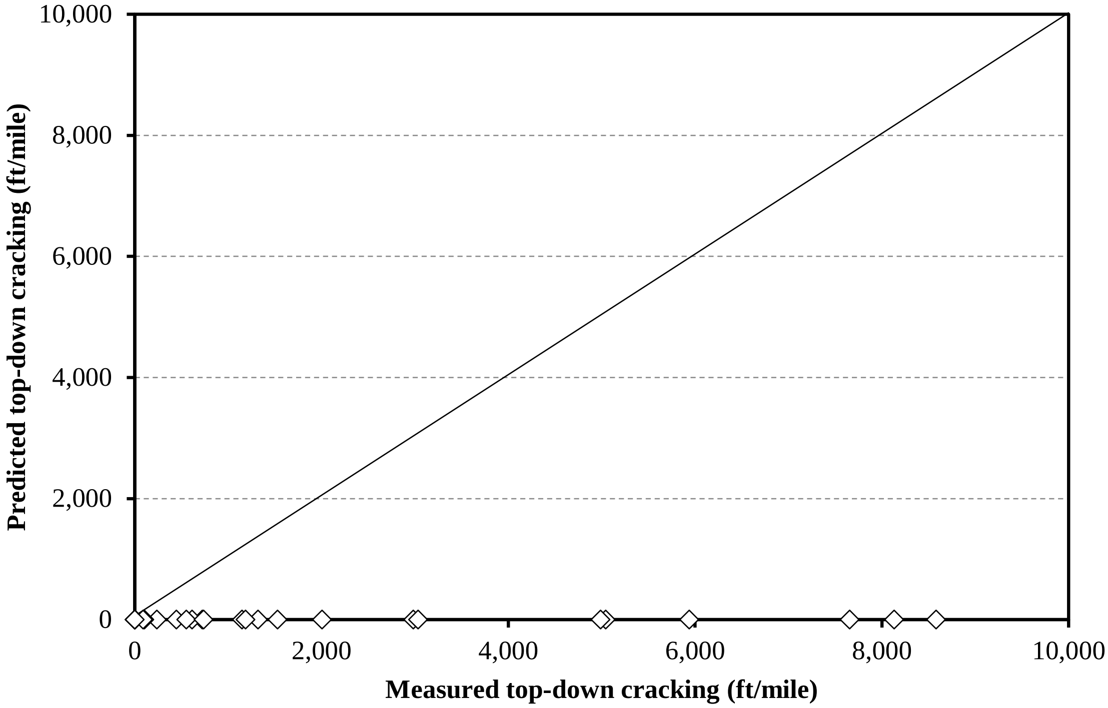

Figure 4.2: Measured versus Predicted Top-Down Cracking by the Nationally Calibrated MEPDG for the Projects with a Subgrade M_r = 2700 psi

Table 4.1: Statistical Analysis of Measured and Predicted Top-Down Cracking by the Nationally Calibrated MEPDG for the Projects with a Subgrade M_r = 2700 psi

Goodness of fit						
N = 29 R^2 = 0.72 SEE = 4.80E-05 ft/mile						
Hypothesis testing						
Hypothesis	Degree of freedom	Parameter estimate	Standard error	t-value	p-value	Reject/ accept
(1) H_0: Intercept = 0	1	7.44E-06	1.11E-05	0.67	0.51	Accept
(2) H_0: Slope = 1	1	2.28E-08	2.76E-09	3.57E+08	less than 0.0001	Reject
(3) H_0: Measured rutting - MEPDG predicted rutting = 0	29	-	-	3.92	5.16E-04	Reject

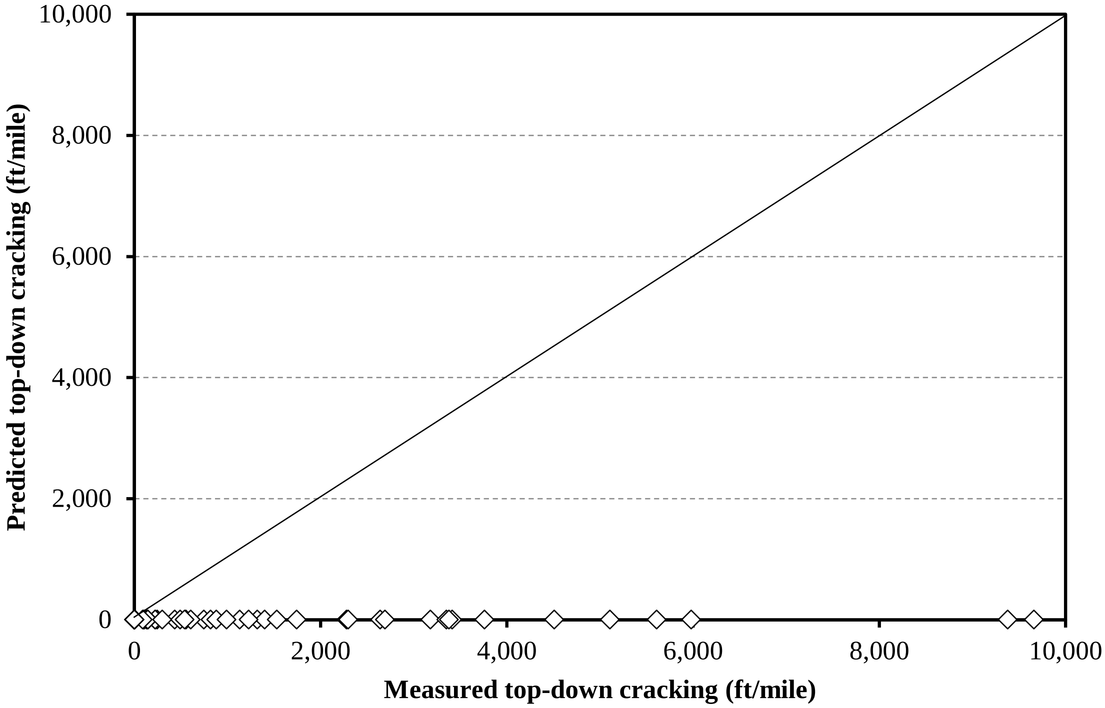

Figure 4.3: Measured versus Predicted Top-Down Cracking by the Nationally Calibrated MEPDG for the Projects with a Subgrade $M_r \geq 4000$ psi

Table 4.2: Statistical Analysis of Measured and Predicted Top-Down Cracking by the Nationally Calibrated MEPDG for the Projects with a Subgrade $M_r \geq 4000$ psi

Goodness of fit						
N = 132 R^2 = 1.34E-04 SEE = 4.76E-03 ft/mile						
Hypothesis testing						
Hypothesis	Degree of freedom	Parameter estimate	Standard error	t-value	p-value	Reject/ accept
(1) H_0: Intercept = 0	1	1.73E-03	4.44E-04	3.89	1.60E-04	Reject
(2) H_0: Slope = 1	1	2.37E-08	1.79E-07	5577244	less than 0.0001	Reject
(3) H_0: Measured rutting - MEPDG predicted rutting = 0	132	-	-	4.44	1.86E-05	Reject

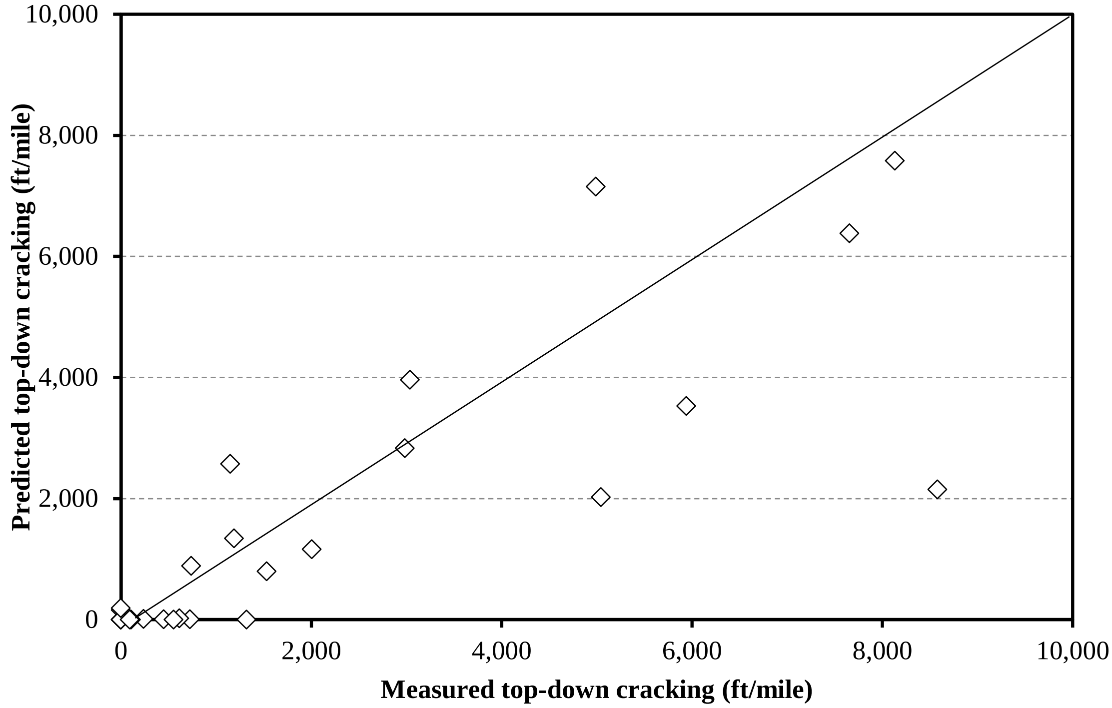

Figure 4.4: Measured versus Predicted Top-Down Cracking by the MEPDG after Local Calibration for the Projects with a Subgrade M_r = 2700 psi

Table 4.3: Statistical Analysis of Measured and Predicted Top-Down Cracking by the MEPDG after Local Calibration for the Projects with a Subgrade M_r = 2700 psi

Goodness of fit						
N = 29 R^2 = 0.72 SEE = 1317 ft/mile						
Hypothesis testing						
Hypothesis	Degree of freedom	Parameter estimate	Standard error	t-value	p-value	Reject/ accept
(1) H_0: Intercept = 0	1	199.89	304.54	0.66	0.52	Accept
(2) H_0: Slope = 1	1	0.63	0.08	4.9008	less than 0.0001	Reject
(3) H_0: Measured rutting - MEPDG predicted rutting = 0	29	-	-	2.09	0.05	Accept

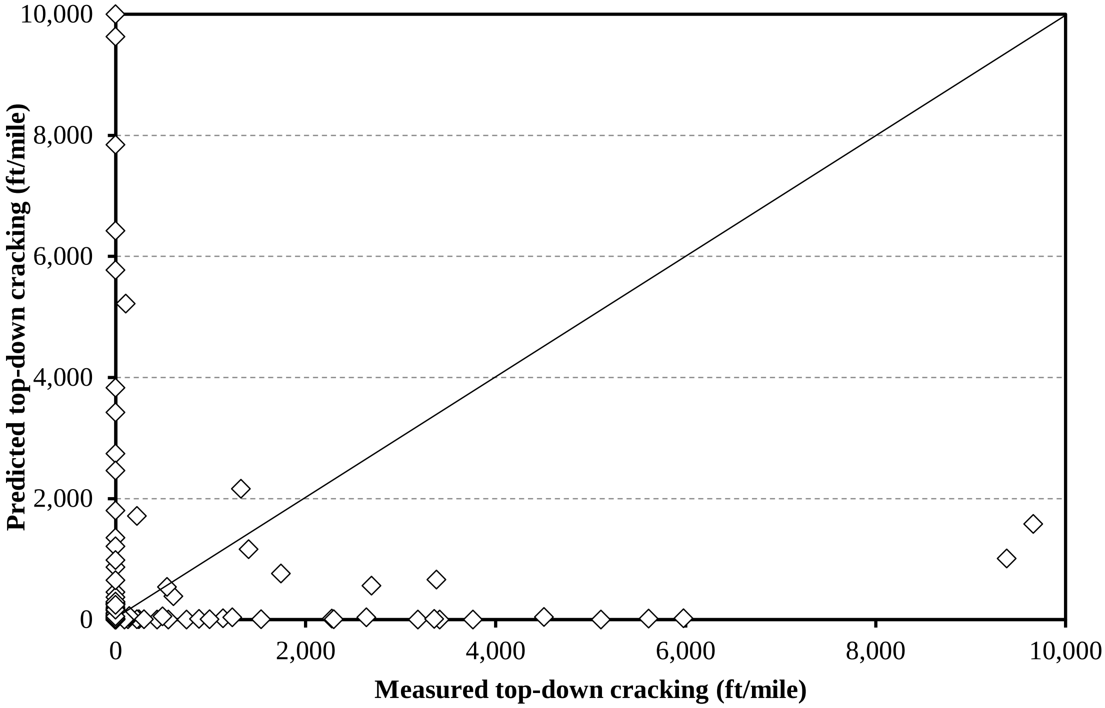

Figure 4.5: Measured versus Predicted Top-Down Cracking by the MEPDG after Local Calibration for the Projects with a Subgrade $M_r \geq 4000$ psi

Table 4.4: Statistical Analysis of Measured and Predicted Top-Down Cracking after Local Calibration for the Projects with a Subgrade $M_r \geq 4000$ psi

Goodness of fit						
N = 132 R^2 = 1.34E-04 SEE = 2227 ft/mile						
Hypothesis testing						
Hypothesis	Degree of freedom	Parameter estimate	Standard error	t-value	p-value	Reject/ accept
(1) H_0: Intercept = 0	1	814.19	207.95	3.92	0.0001	Reject
(2) H_0: Slope = 1	1	0.01	0.08	11.76	less than 0.0001	Reject
(3) H_0: Measured rutting - MEPDG predicted rutting = 0	132	-	-	0.25	0.7991	Accept

4.1.3 Thermal Cracking

Figure 4.6 shows the comparisons of the measured and predicted thermal cracking by the nationally calibrated MEPDG for the projects with subgrade resilient modulus of 2700 psi. Figure 4.7 shows similar comparisons for other projects with a subgrade resilient modulus of higher than 4000 psi. The predicted thermal cracks by the nationally calibrated MEPDG were zero for all the projects; therefore, the statistical analysis could not be performed.

The above comparisons show that a significant bias existed, and the nationally calibrated MEPDG highly underestimated the thermal cracking. There is a poor correlation between the measured and predicted thermal cracking by the nationally calibrated MEPDG.

The MEPDG was locally calibrated by adjusting the calibration coefficients to minimize the bias. Figures 4.8 and 4.9 and Tables 4.5 and 4.6 show that the bias was minimized after local calibration; however, the hypotheses of the intercept and the slope were rejected.

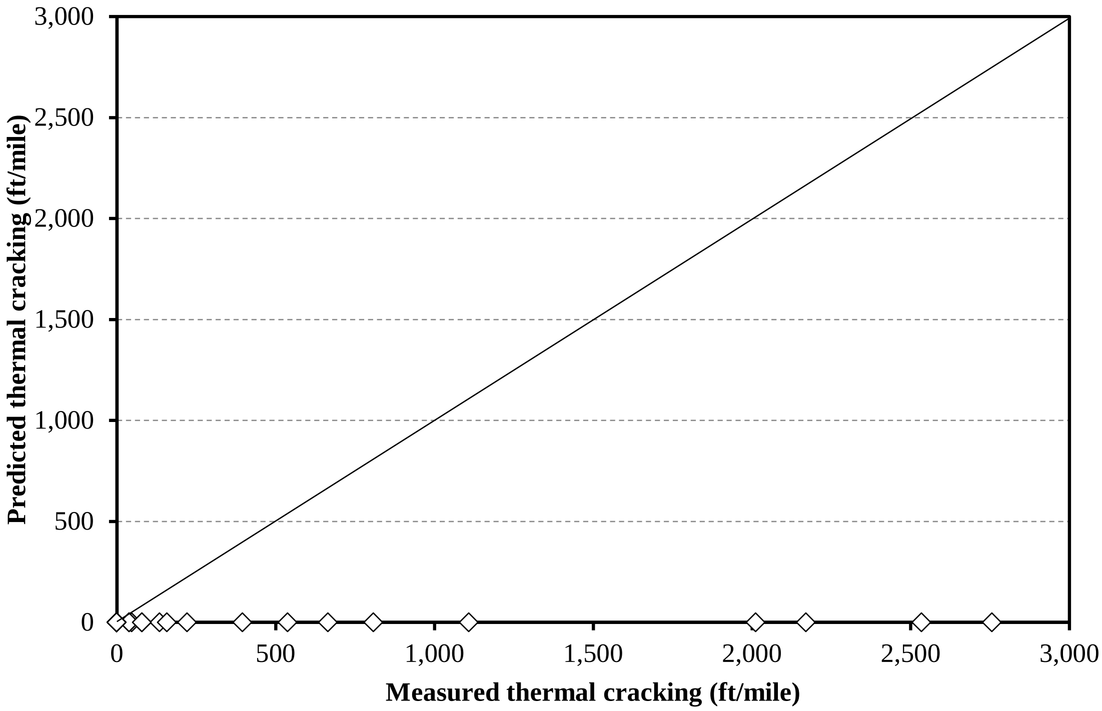

Figure 4.6: Measured versus Predicted Thermal Cracking by the Nationally Calibrated MEPDG for the Projects with a Subgrade M_r = 2700 psi

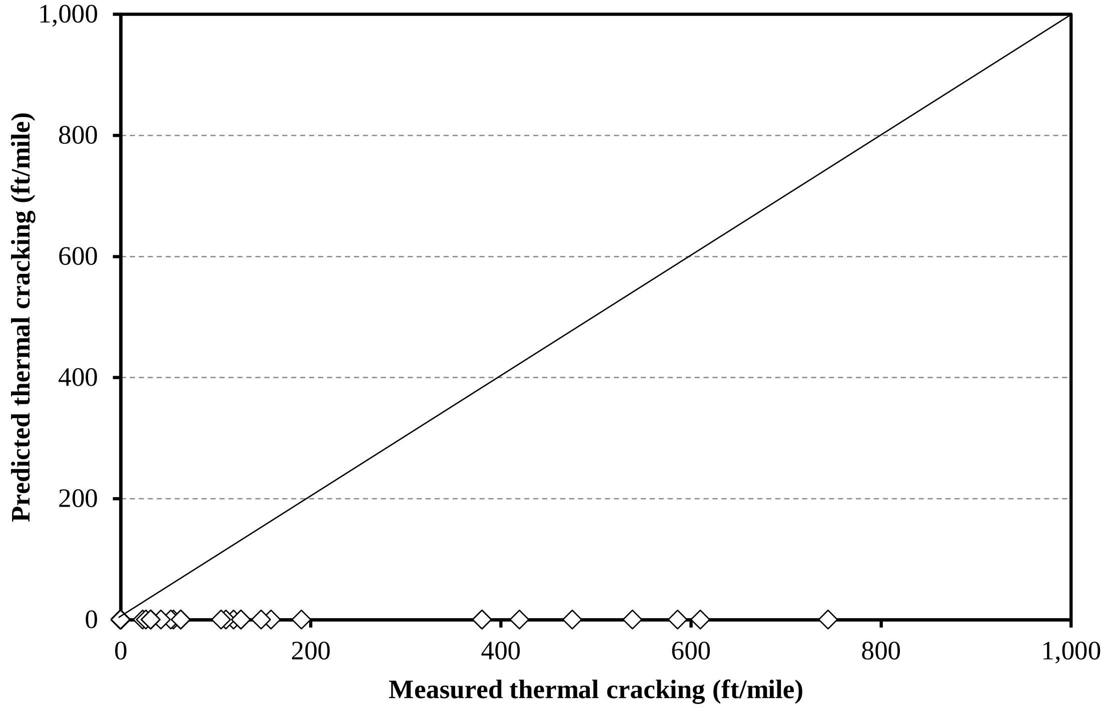

Figure 4.7: Measured versus Predicted Thermal Cracking by the Nationally Calibrated MEPDG for the Projects with a Subgrade M_r ≥ 4000 psi

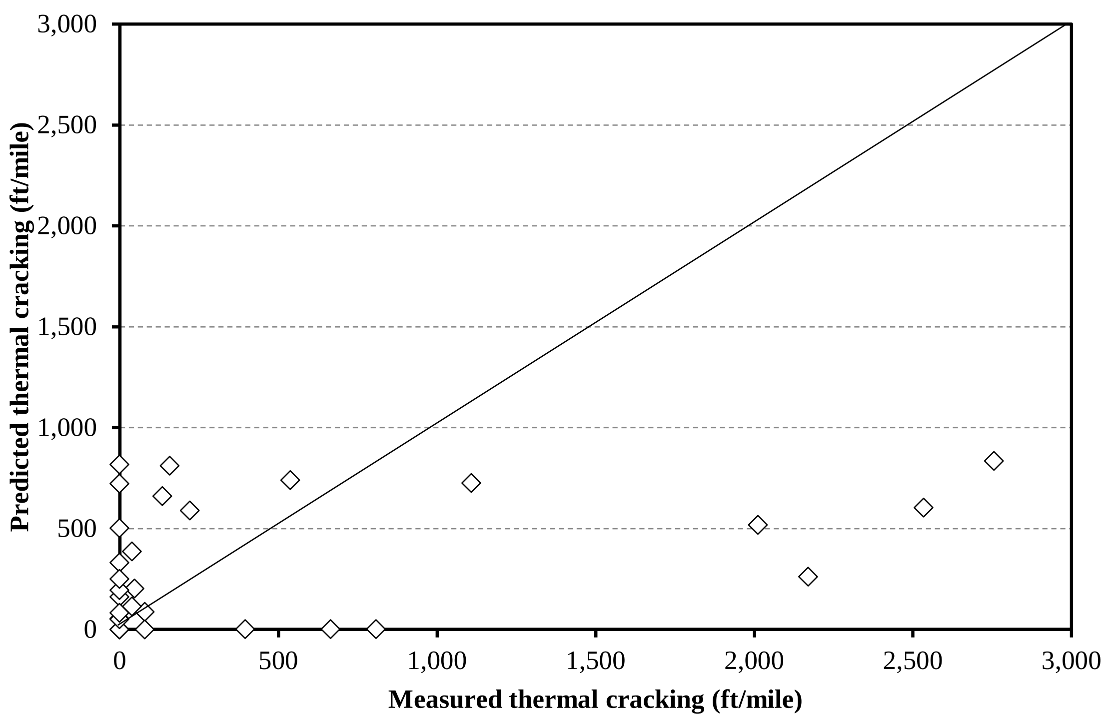

Figure 4.8: Measured versus Predicted Thermal Cracking by the MEPDG after Local Calibration for the Projects with a Subgrade M_r = 2700 psi

Table 4.5: Statistical Analysis of the Measured and Predicted Thermal Cracking by the MEPDG after Local Calibration for the Projects with a Subgrade M_r = 2700 psi

Goodness of fit						
N = 29 R^2 = 0.12 SEE = 289 ft/mile						
Hypothesis testing						
Hypothesis	Degree of freedom	Parameter estimate	Standard error	t-value	p-value	Reject/ accept
(1) H_0: Intercept = 0	1	274	62.28	4.41	0.0002	Reject
(2) H_0: Slope = 1	1	0.13	0.07	13.20	less than 0.0001	Reject
(3) H_0: Measured rutting - MEPDG predicted rutting = 0	29			0.98	0.3357	Accept

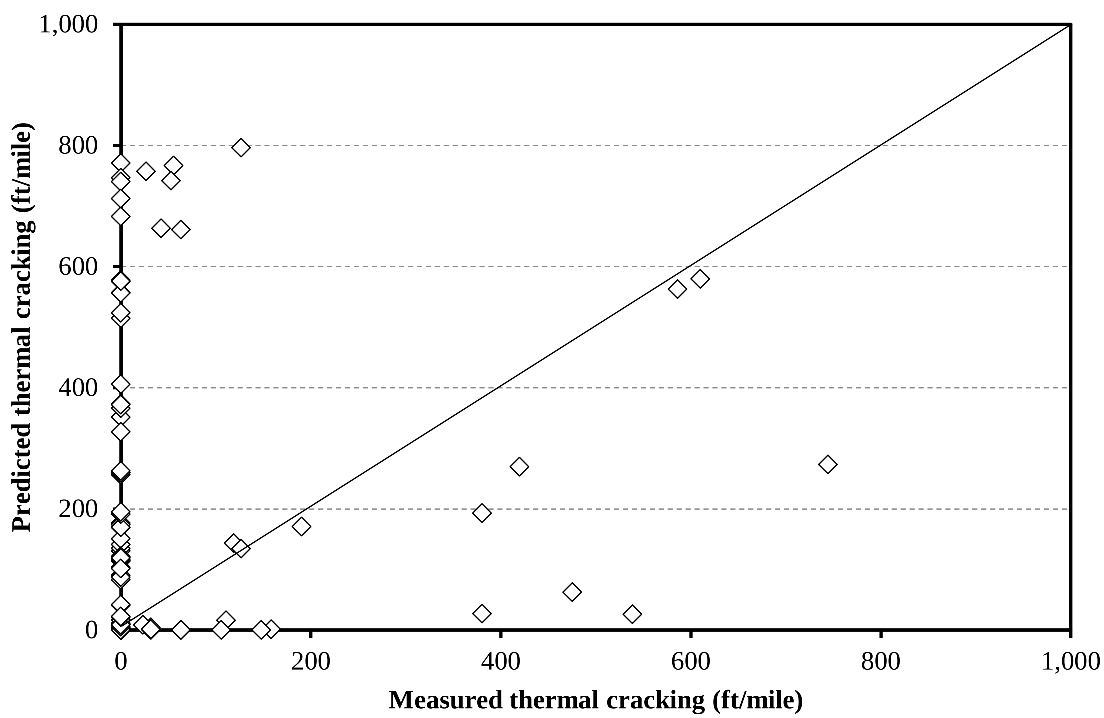

Figure 4.9: Measured versus Predicted Thermal Cracking by the MEPDG after Local Calibration for the Projects with a Subgrade Mr ≥ 4000 psi

Table 4.6: Statistical Analysis of Measured and Predicted Thermal Cracking by the MEPDG after Local Calibration for the Projects with a Subgrade $M_r \geq 4000$ psi

Goodness of fit						
N = 132 R^2 = 0.02 SEE = 97.8 ft/mile						
Hypothesis testing						
Hypothesis	Degree of freedom	Parameter estimate	Standard error	t-value	p-value	Reject/ accept
(1) H_0: Intercept = 0	1	60.9	8.99	6.77	3.98E-10	Reject
(2) H_0: Slope =1	1	0.11	0.07	13.44	less than 0.0001	Reject
(3) H_0: Measured rutting - MEPDG predicted rutting = 0	132			1.68	0.0961	Accept

4.1.4 Rutting

The validation and local calibration of the rutting of flexible pavements were focused on the projects without an unbound base course layer, since there were only 3 selected projects with an unbound base course layer. Figure 4.10 and Table 4.7 show the comparisons of the measured and predicted rutting by the nationally calibrated MEPDG for the projects with a subgrade resilient modulus of 2700 psi. Figure 4.11 and Table 4.8 show similar comparisons for other projects with a subgrade M_r equal to or higher than 4000 psi.

The above comparisons show that the bias existed and the nationally calibrated MEPDG highly overestimated the rutting of flexible pavements in Kansas. In addition, the subgrade condition influenced the predicted rutting significantly. Therefore, local calibration of the MEPDG is needed based on the subgrade condition.

The MEPDG was locally calibrated by adjusting the calibration coefficients to minimize the bias. Figures 4.12 and 4.13 show that the bias was minimized after local calibration. Tables 4.9 and 4.10 present the statistical analysis of the locally calibrated MEPDG. It is found that the hypotheses of the slope and the intercept were rejected, but the p-values were improved as compared with those for the nationally calibrated models. In addition, the SEE after local calibration decreased and was much lower than that for the nationally calibrated model as shown in Table 3.15.

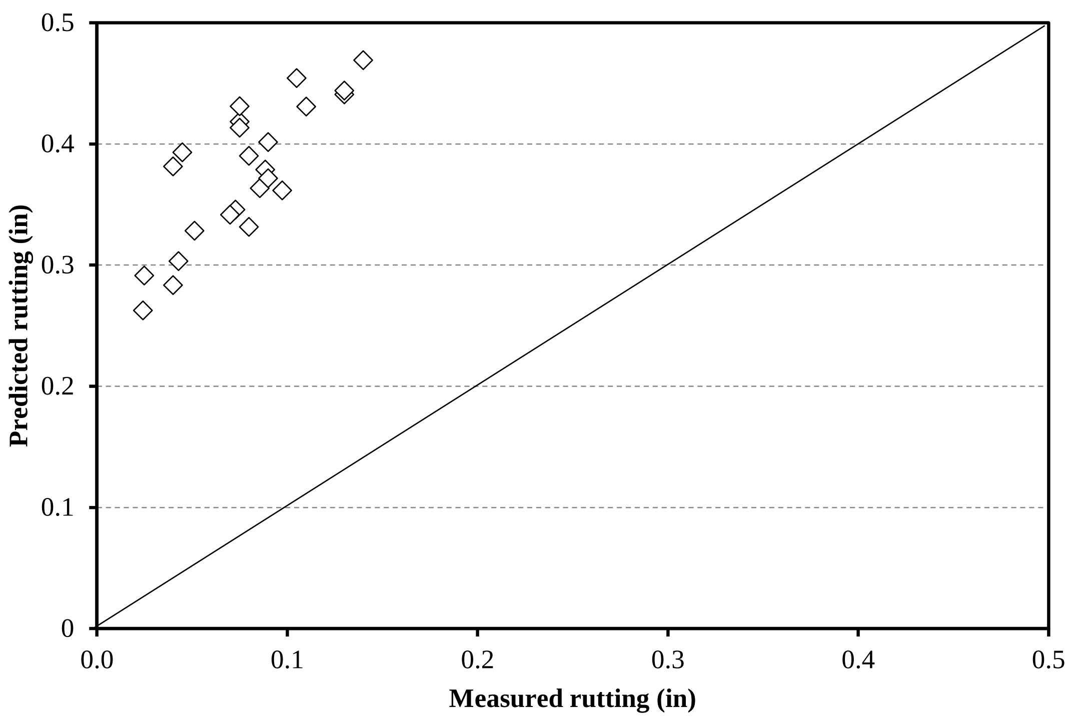

Figure 4.10: Measured versus Predicted Rutting by the Nationally Calibrated MEPDG for the Projects with a Subgrade Mr = 2700 psi

Table 4.7: Statistical Analysis of Measured and Predicted Rutting by the Nationally Calibrated MEPDG for the Projects with a Subgrade Mr = 2700 psi

Goodness of fit						
N = 24 R^2 = 0.64 SEE = 0.03 in.						
Hypothesis testing						
Hypothesis	Degree of freedom	Parameter estimate	Standard error	t-value	p-value	Reject/ accept
(1) H_0: Intercept = 0	1	0.27	0.02	13.94	2.13E-12	Reject
(2) H_0: Slope = 1	1	1.42	0.23	1.86	0.0756	Accept
(3) H0: Measured rutting - MEPDG predicted rutting = 0	24			-39.77	1.04E-22	Reject

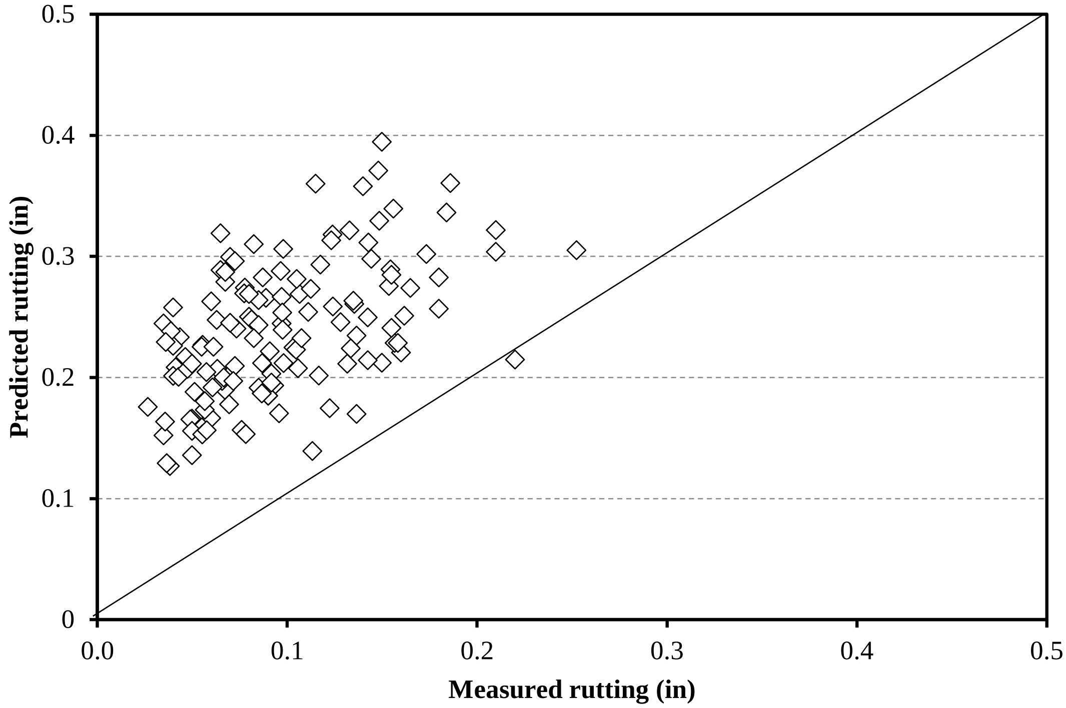

Figure 4.11: Measured versus Predicted Rutting by the Nationally Calibrated MEPDG for the Projects with a Subgrade M_r ≥ 4000 psi

Table 4.8: Statistical Analysis of Measured and Predicted Rutting by the Nationally Calibrated MEPDG for the Projects with a Subgrade M_r ≥ 4000 psi

Goodness of fit						
N = 132 R^2 = 0.28 SEE = 0.05 in.						
Hypothesis testing						
Hypothesis	Degree of freedom	Parameter estimate	Standard error	t-value	p-value	Reject/ accept
(1) H_0: Intercept = 0	1	0.18	0.01	17.92	6.34E-37	Reject
(2) H_0: Slope = 1	1	0.64	0.09	3.96	0.0001	Reject
(3) H_0: Measured rutting - MEPDG predicted rutting = 0	132	-	-	32.16	4.90E-64	Reject

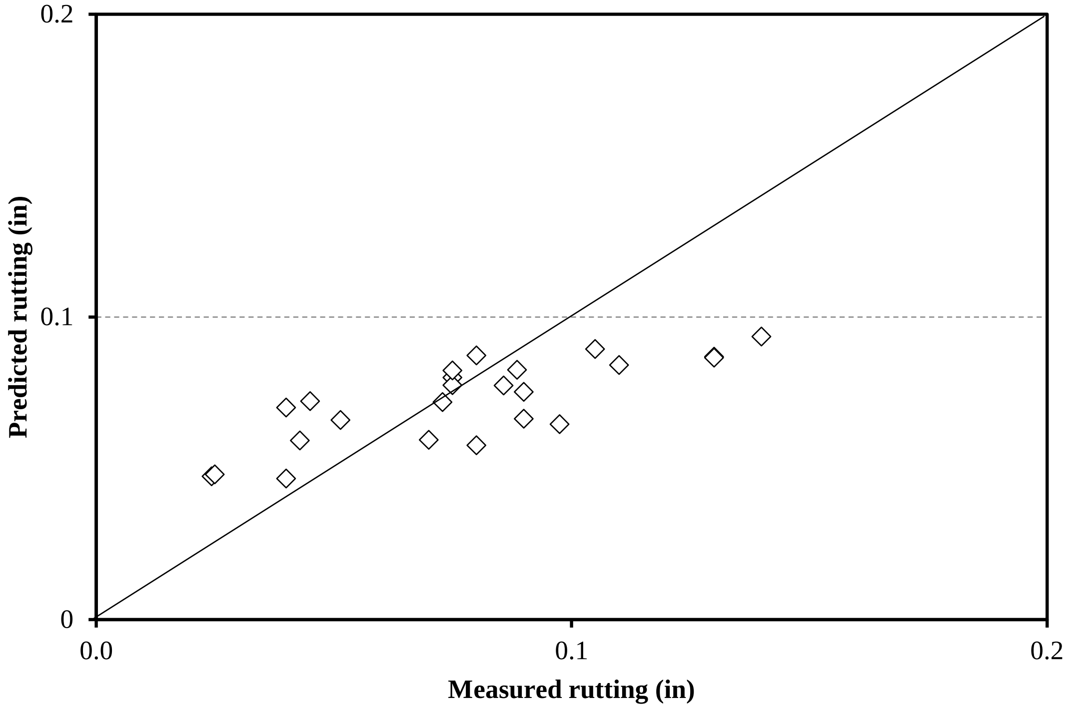

Figure 4.12: Measured versus Predicted Rutting by the MEPDG after Local Calibration for the Projects with a Subgrade M_r = 2700 psi

Table 4.9: Statistical Analysis of Measured and Predicted Rutting by the MEPDG after Local Calibration for the Projects with a Subgrade M_r = 2700 psi

<table>
<tr><td colspan="7">Goodness of fit</td></tr>
<tr><td colspan="7">N = 24
R^2 = 0.61
SEE = 0.02 in.</td></tr>
<tr><td colspan="7">Hypothesis testing</td></tr>
<tr><td>Hypothesis</td><td>Degree of freedom</td><td>Parameter estimate</td><td>Standard error</td><td>t-value</td><td>p-value</td><td>Reject/ accept</td></tr>
<tr><td>(1) H_0: Intercept = 0</td><td>1</td><td>-0.05</td><td>0.02</td><td>-2.33</td><td>0.03</td><td>Reject</td></tr>
<tr><td>(2) H_0: Slope = 1</td><td>1</td><td>1.81</td><td>0.31</td><td>2.63</td><td>0.02</td><td>Reject</td></tr>
<tr><td>(3) H_0: Measured rutting - MEPDG predicted rutting = 0</td><td>29</td><td>-</td><td>-</td><td>-1.18</td><td>0.25</td><td>Accept</td></tr>
</table>

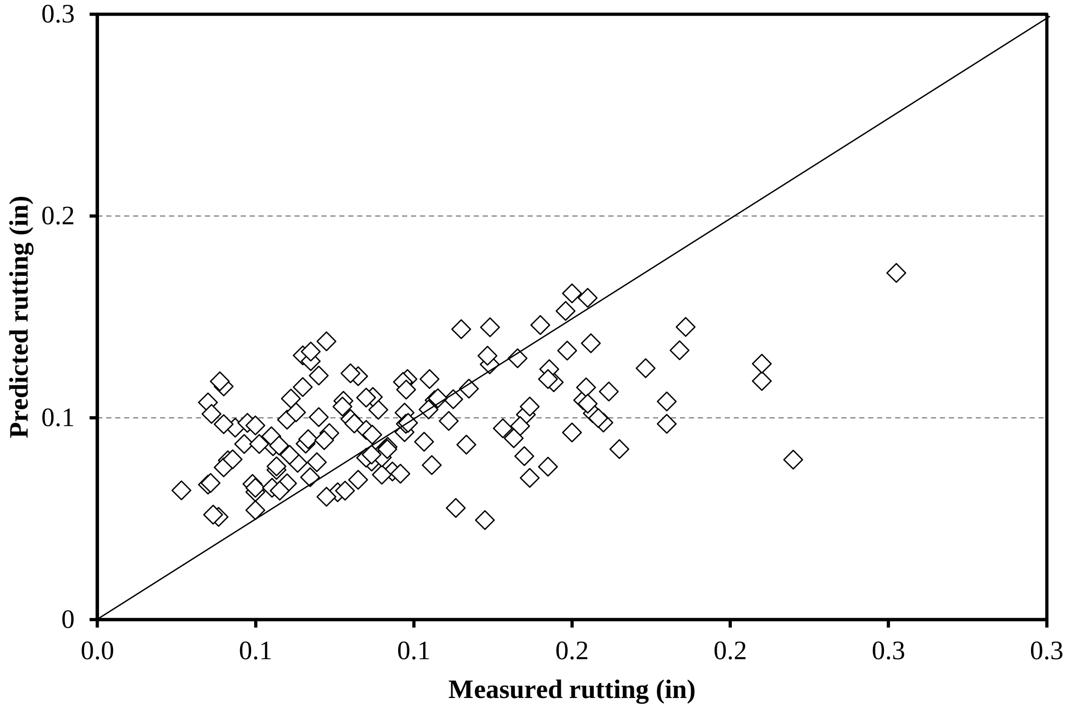

Figure 4.13: Measured versus Predicted Rutting by the MEPDG after Local Calibration for the Projects with a Subgrade $M_r \geq 4000$ psi

Table 4.10: Statistical Analysis of Measured and Predicted Rutting by the MEPDG after Local Calibration for the Projects with a Subgrade $M_r \geq 4000$ psi

Goodness of fit						
N = 132 R^2 = 0.24 SEE = 0.02 in.						
Hypothesis testing						
Hypothesis	Degree of freedom	Parameter estimate	Standard error	t-value	p-value	Reject/ accept
(1) H_0: Intercept = 0	1	0.07	0.00	15.84	3.77E-32	Reject
(2) H_0: Slope = 1	1	0.27	0.04	17.43	less than 0.0001	Reject
(3) H_0: Measured rutting - MEPDG predicted rutting = 0	132	-	-	0.06	0.96	Accept

4.1.5 Roughness

Figure 4.14 and Table 4.11 present the comparisons of the measured and predicted IRI values by the nationally calibrated MEPDG for the projects with a subgrade resilient modulus of 2700 psi. Figure 4.15 and Table 4.12 show similar comparisons for other projects with a subgrade resilient modulus of higher than 2700 psi.

The above comparisons show that the measured and predicted IRI by the nationally calibrated MEPDG matched well for projects with a subgrade resilient modulus of 2700 psi. But bias existed in projects with a subgrade resilient modulus equal to or higher than 4000 psi, and the nationally calibrated MEPDG slightly overestimated the IRI of flexible pavements in Kansas. In addition, the IRI model is dependent on other distress performances which were recalibrated. Therefore, the local calibration of the IRI model is needed.

The MEPDG was locally calibrated by adjusting the calibration coefficients to minimize the bias. Figures 4.16 and 4.17 show that the bias was minimized after local calibration. Tables 4.13 and 4.14 present the statistical analysis of the locally calibrated MEPDG. It is found that the hypotheses of the slope and the intercept were rejected, but the p-values were improved as compared with those from the nationally calibrated models. In addition, the SEE after local calibration was much lower than that for the nationally calibrated model as shown in Table 3.15.

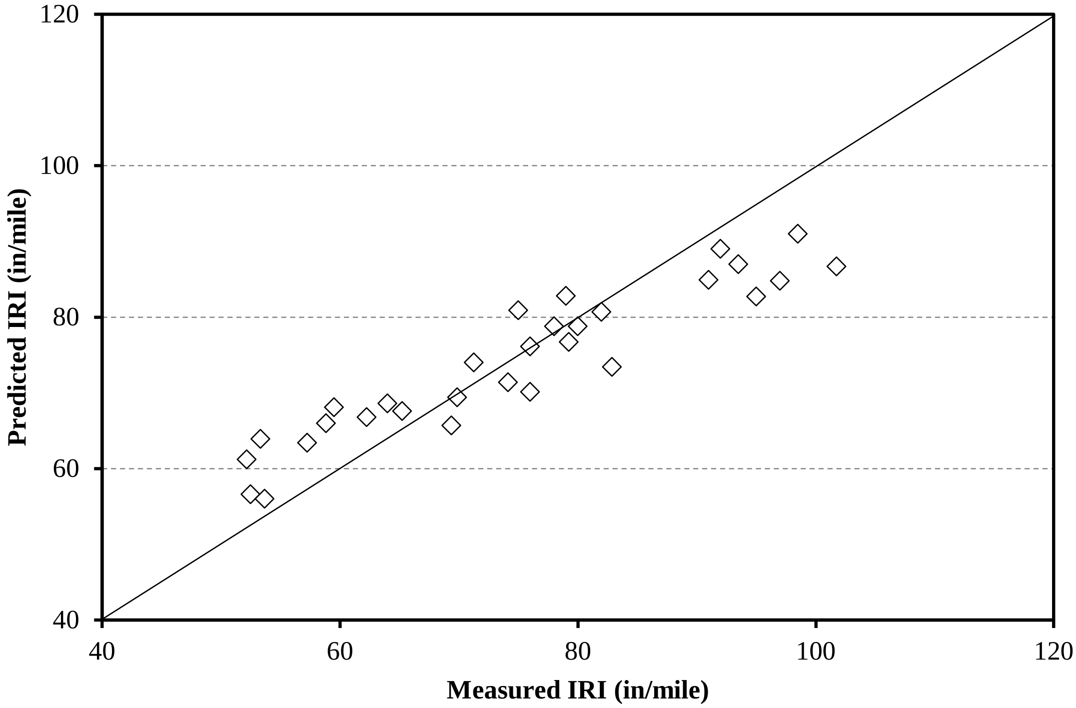

Figure 4.14: Measured versus Predicted IRI by the Nationally Calibrated MEPDG for the Projects with a Subgrade M_r = 2700 psi

Table 4.11: Statistical Analysis of Measured and Predicted Rutting by the Nationally Calibrated MEPDG for the Projects with a Subgrade M_r = 2700 psi

Goodness of fit						
N = 30 R^2 = 0.88 SEE = 3.4 in./mile						
Hypothesis testing						
Hypothesis	Degree of freedom	Parameter estimate	Standard error	t-value	p-value	Reject/ accept
(1) H_0: Intercept = 0	1	28.53	3.22	8.85	1.31E-09	Reject
(2) H_0: Slope = 1	1	0.61	0.04	9.20	less than 0.0001	Reject
(3) H_0: Measured rutting - MEPDG predicted rutting = 0	30	-	-	0.47	0.64	Accept

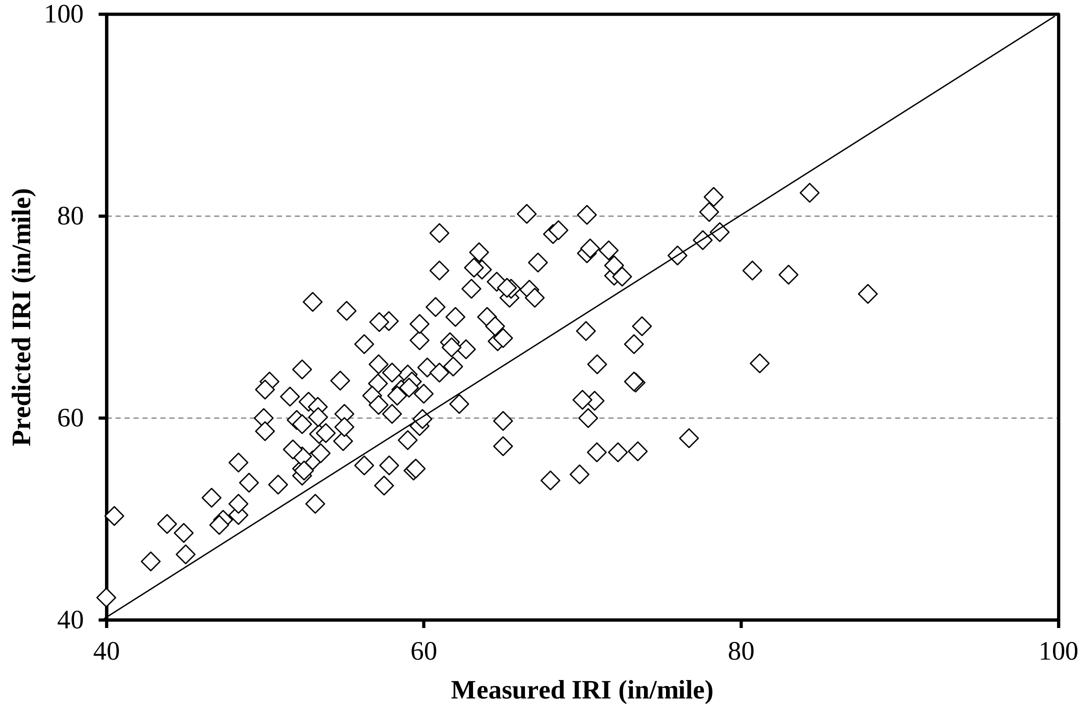

Figure 4.15: Measured versus Predicted IRI by the Nationally Calibrated MEPDG for the Projects with a Subgrade M_r ≥ 4000 psi

Table 4.12: Statistical Analysis of Measured and Predicted Rutting by the Nationally Calibrated MEPDG for the Projects with a Subgrade M_r ≥ 4000 psi

Goodness of fit						
N = 129 R^2 = 0.47 SEE = 6.53 in./mile						
Hypothesis testing						
Hypothesis	Degree of freedom	Parameter estimate	Standard error	t-value	p-value	Reject/ accept
(1) H_0: Intercept = 0	1	26.02	3.63	7.16	5.69E-11	Reject
(2) H_0: Slope = 1	1	0.62	0.06	6	less than 0.0001	Reject
(3) H_0: Measured rutting - MEPDG predicted rutting=0	129	-	-	4.43	2.04E-05	Reject

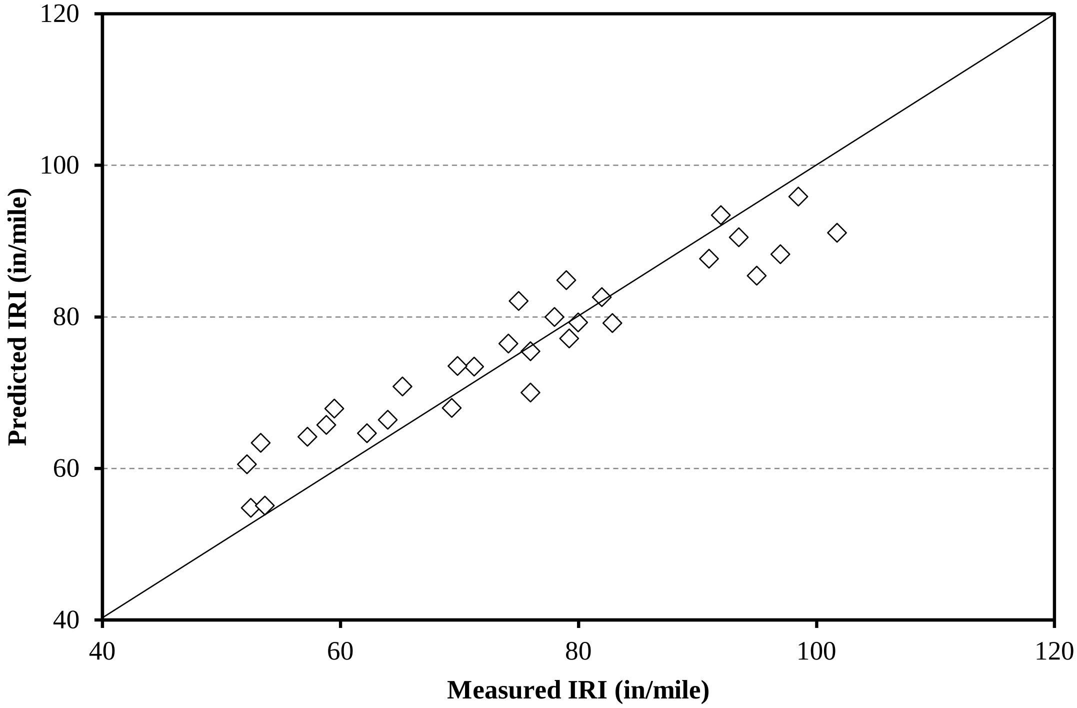

Figure 4.16: Measured versus Predicted IRI by the MEPDG after Local Calibration for the Projects with Subgrade M_r = 2700 psi

Table 4.13: Statistical Analysis of Measured and Predicted Rutting by the MEPDG after Local Calibration for the Projects with Subgrade M_r = 2700 psi

Goodness of fit						
N = 30 R^2 = 0.61 SEE = 0.02 in./mile						
Hypothesis testing						
Hypothesis	Degree of freedom	Parameter estimate	Standard error	t-value	p-value	Reject/ accept
(1) H_0: Intercept = 0	1	-0.05	0.02	2.33	0.03	Reject
(2) H_0: Slope = 1	1	1.81	0.31	2.63	0.02	Reject
(3) H_0: Measured rutting - MEPDG predicted rutting = 0	30	-	-	1.18	0.25	Accept

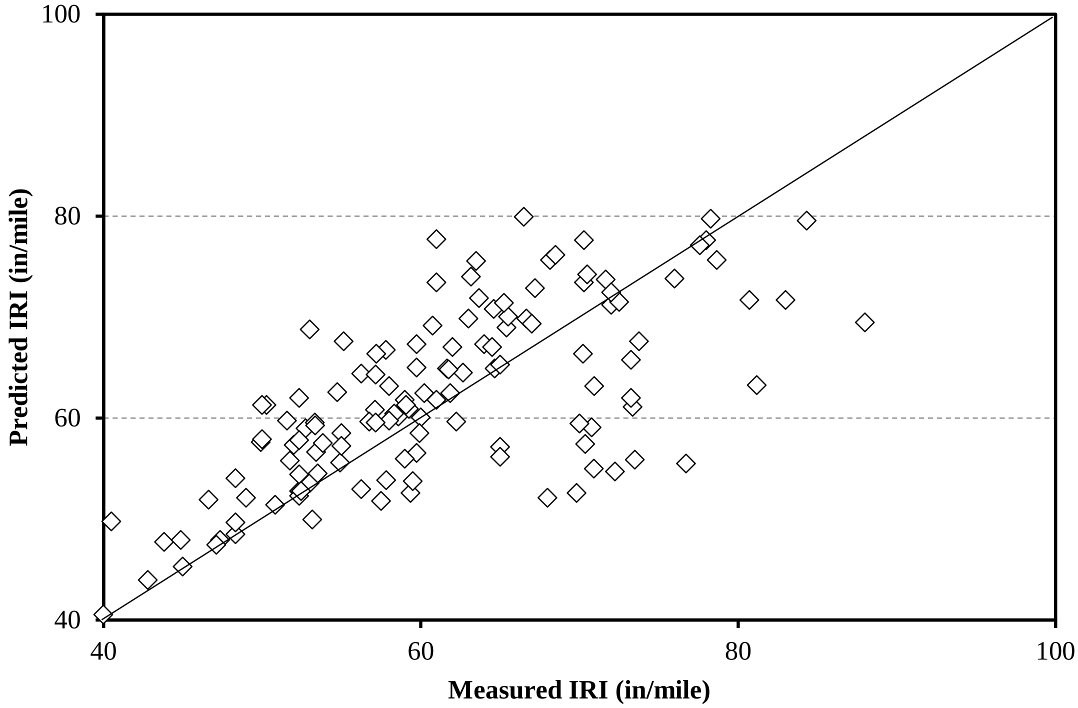

Figure 4.17: Measured versus Predicted IRI by the MEPDG after Local Calibration for the Projects with a Subgrade $M_r \geq 4000$ psi

Table 4.14: Statistical Analysis of Measured and Predicted Rutting by the MEPDG after Local Calibration for the Projects with a Subgrade $M_r \geq 4000$ psi

Goodness of fit						
N = 129 R^2 = 0.46 SEE = 7.29 in./mile						
Hypothesis testing						
Hypothesis	Degree of freedom	Parameter estimate	Standard error	t-value	p-value	Reject/ accept
(1) H_0: Intercept = 0	1	13.61	4.62	2.95	0.0038	Reject
(2) H_0: Slope = 1	1	0.77	0.07	3.17	0.0019	Reject
(3) H_0: Measured rutting - MEPDG predicted rutting = 0	129	-	-	1.32	0.1891	Accept

4.1.6 Summary of Locally Calibrated Coefficients for Flexible Pavements in Kansas

The locally calibrated coefficients for flexible pavements in Kansas considering all the distress models and the IRI model are summarized in Table 4.15. These coefficients are compared with those for other states cited from Pierce and McGovern (2014). The greyed numbers in Table 4.15 are the locally calibrated coefficients.

As discussed earlier, local calibration minimized the bias. However, the intercept and the slope of the correlation between the measured and MEPDG-predicted values still existed, even though the p-values were improved.

The reliability of the locally calibrated coefficients based on the projects with a subgrade resilient modulus of 2700 psi in Kansas is strongly suggested to be further validated, due to the limited number of the projects for this calibration. In addition, due to the measured top-down cracking varying in a wide range (lots of data was greater than the MEPDG design threshold), the SEE of the locally calibrated top-down cracking was relatively high. Except the top-down cracking model, the locally calibrated coefficients based on the projects with a subgrade resilient modulus equal to or higher than 4000 psi in Kansas can be considered as reliable, since the number of the projects used in the calibration was larger than the required number in Table 3.15 and the SEEs of locally calibrated MEPDG models were lower than those presented in the Table 3.15. Appendix E shows the comparisons of the measured and predicted distresses and IRI by the locally calibrated MEPDG for the flexible pavement projects.

Table 4.15: Summary of the Locally Calibrated Coefficients for Flexible Pavements in Kansas as Compared to Those in Other States

Calibration factors	National	Arizona	Colorado	Missouri	Oregon	Kansas	
						Subgrade resilient modulus (2700 psi)	Subgrade resilient modulus (≥4000 psi)
Cracking							
C1 Bottom	1.0	1.0	0.07	1.0	0.56	1.0	1.0
C1 Top	7.0	7.0	7.0	7.0	1.453	0.438	4.5
C2 Bottom	1.0	4.5	2.35	1.0	0.225	1.0	1.0
C2 Top	3.5	3.5	3.5	3.5	0.097	3.5	3.5
C3 Bottom	6000	6000	6000	6000	6000	6000	6000
C3 Top	0	0	0	0	0	0	0
C4 Top	1000	1000	1000	1000	1000	36000	36000
Fatigue							
BF1	1	249.00872	130.3674	1	1	0.01	0.01
BF2	1	1	1	1	1	1	1
BF3	1	1.23341	1.2178	1	1	1	1
Thermal Fracture							
Level 1	1.5	1.5	7.5	0.625	1.5	1.5	1.5
Level 2	0.5	0.5	0.5	0.5	0.5	0.5	0.5
Level 3	1.5	1.5	1.5	1.5	1.5	120	3.6
Rutting (asphalt)							
BR1	1.0	0.69	1.34		1.48	0.9	0.9
BR2	1.0	1.0	1.0		1.0	1.0	1.0
BR3	1.0	1.0	1.0		0.9	1.0	1.0
Rutting (subgrade)							
BS1 (fine)	1.0	0.37	0.84	0.4375	1.0	0.1281	0.3251
BS1 (granular)	1.0	0.14	0.4	0.01	1.0	1.0	1.0
IRI							
C1	40	1.2281	35	17.7	40	270	95
C2	0.4	0.1175	0.3	0.975	0.4	0.04	0.04
C3	0.008	0.008	0.02	0.008	0.008	0.001	0.001
C4	0.015	0.028	0.019	0.01	0.015	0.015	0.015

Source: Pierce & McGovern, 2014
Note: the locally calibrated coefficients for other states were cited from Pierce & McGovern, 2014

4.2: Rigid Pavements

For new rigid pavements in Kansas, the mean transverse joint faulting (referred to as faulting in the following paragraphs) and IRI were validated and recalibrated. In general, there are three types of chemically stabilized base courses in all the selected projects. The validation of the nationally calibrated MEPDG was performed for each type of project separately. In addition, the overall validation and local calibration were conducted as well. In the process of local calibration, the traditional splitting data method was used to verify the reliability of the identified local calibration coefficients. To perform this method, the projects with base courses of the PCCDCB and CEMBAS were selected to carry out the local calibration, and those with a base course of the DBWED were used to validate the locally calibrated models. Table 3.21 presents the grouped projects in terms of the three types of chemically stabilized base courses, the DBWED, the CEMBAS, and the PCCDCB.

4.2.1 Mean Transverse Joint Faulting

As compared with the MEPDG default threshold, the faulting measurements for Kansas were relatively low. Figures 4.18, 4.19, and 4.20 present the comparisons of the measured and predicted faultings by the nationally calibrated MEPDG for the rigid pavements with a base course of the PCCDCB, the CEMBAS, and the DBWED, respectively. Tables 4.16, 4.17, and 4.18 show the corresponding statistical analysis for each group of projects. In addition, Figure 4.21 and Table 4.19 show the comparison of the measured and predicted faultings by the nationally calibrated MEPDG for all the projects of rigid pavements.

The above comparisons show that significant bias existed in all the three groups of projects with different chemically stabilized base courses. Therefore, the local calibration of the MEPDG is needed to minimize the bias.

By adjusting the local calibration coefficients, the MEPDG was calibrated to minimize the bias using the traditional splitting data method. Figure 4.22 shows that the bias was minimized after the local calibration of projects with base courses of the DBWED and the CEMBAS. Table 4.20 presents the corresponding statistical analysis. Figure 4.23 and Table 4.21 present the comparisons of the measured and predicted faulting for projects with a base course of the PCCDCB by the locally calibrated MEPDG with calibration coefficients obtained before. It is found that the bias of projects with base courses of the CEMBAS and the DBWED was minimized. The hypotheses of the intercept and the slope were rejected, but the SEE was much lower than that for the nationally calibrated model, as shown in Table 3.15. The bias of projects with a base course of the PCCDCB was minimized as well by applying the obtained local calibration coefficients, which indicates that the identified local calibration coefficients were reliable and the types of base courses did not have much influence on the faulting.

To obtain a set of more accurate calibration coefficients, the local calibration was performed on all the projects. Figure 4.24 and Table 4.22 show the comparisons of the measured and predicted faulting by the locally calibrated MEPDG based on all the projects. The identified local calibration coefficients were summarized in Table 4.30.

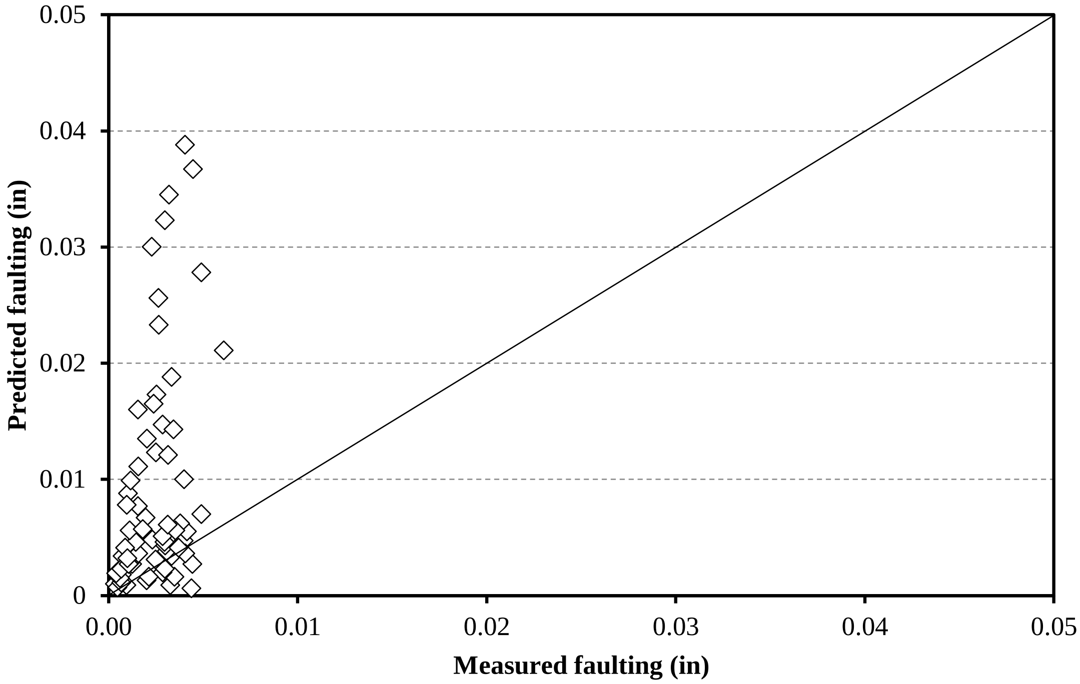

Figure 4.18: Measured versus Predicted Faulting by the Nationally Calibrated MEPDG for the Projects with a Base Course of the PCCDCB

Table 4.16: Statistical Analysis of Measured and Predicted Faulting by the Nationally Calibrated MEPDG for the Projects with a Base Course of the PCCDCB

Goodness of fit						
N = 66 R^2 = 0.16 SEE = 1.21E-03 in.						
Hypothesis testing						
Hypothesis	Degree of freedom	Parameter estimate	Standard error	t-value	p-value	Reject/ accept
(1) H_0: Intercept = 0	1	0.0019	0.0002	9.30	1.70E-13	Reject
(2) H_0: Slope = 1	1	0.05	0.02	3.55	1.00E-04	Reject
(3) H_0: Measured rutting - MEPDG predicted rutting = 0	66	-	-	5.82	1.97E-07	Reject

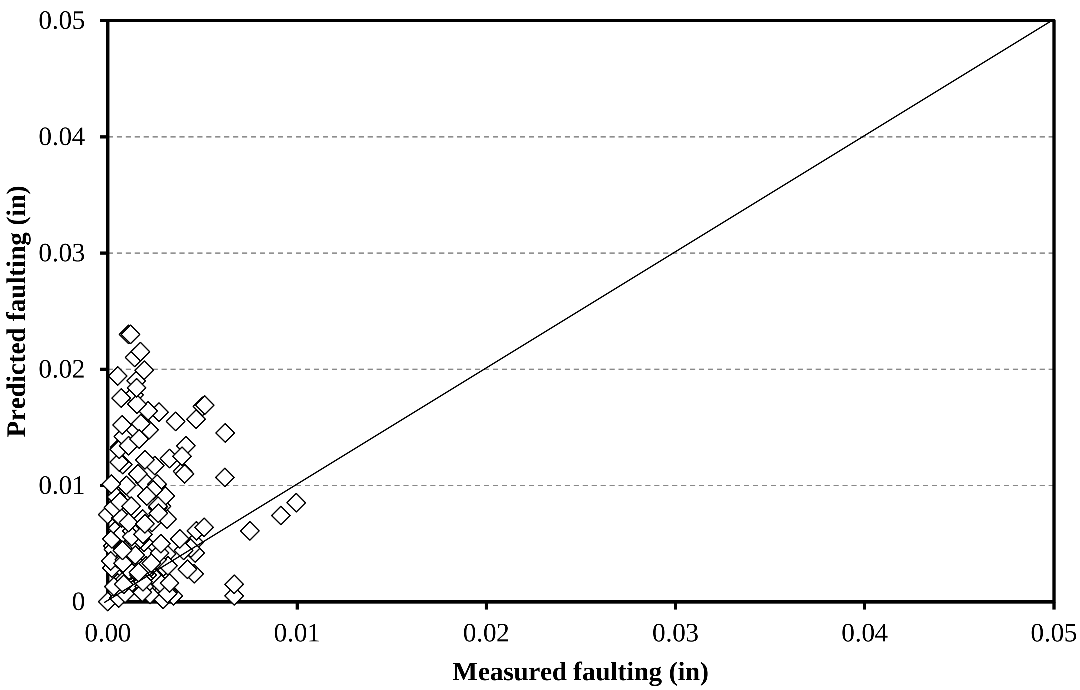

Figure 4.19: Measured versus Predicted Faulting by the Nationally Calibrated MEPDG for the Projects with a Base Course of the CEMBAS

Table 4.17: Statistical Analysis of Measured and Predicted Faulting by the Nationally Calibrated MEPDG for the Projects with a Base Course of the CEMBAS

Goodness of fit						
N = 155 $R^2 = 0.00$ SEE = 1.75E-03in.						
Hypothesis testing						
Hypothesis	Degree of freedom	Parameter estimate	Standard error	t-value	p-value	Reject/ accept
(1) H_0: Intercept = 0	1	0.0022	0.0002	9.81	6.12E-18	Reject
(2) H_0: Slope = 1	1	0.00	0.02	0.13	0.0001	Reject
(3) H_0: Measured rutting - MEPDG predicted rutting = 0	155	-	-	9.98	2.06E-18	Reject

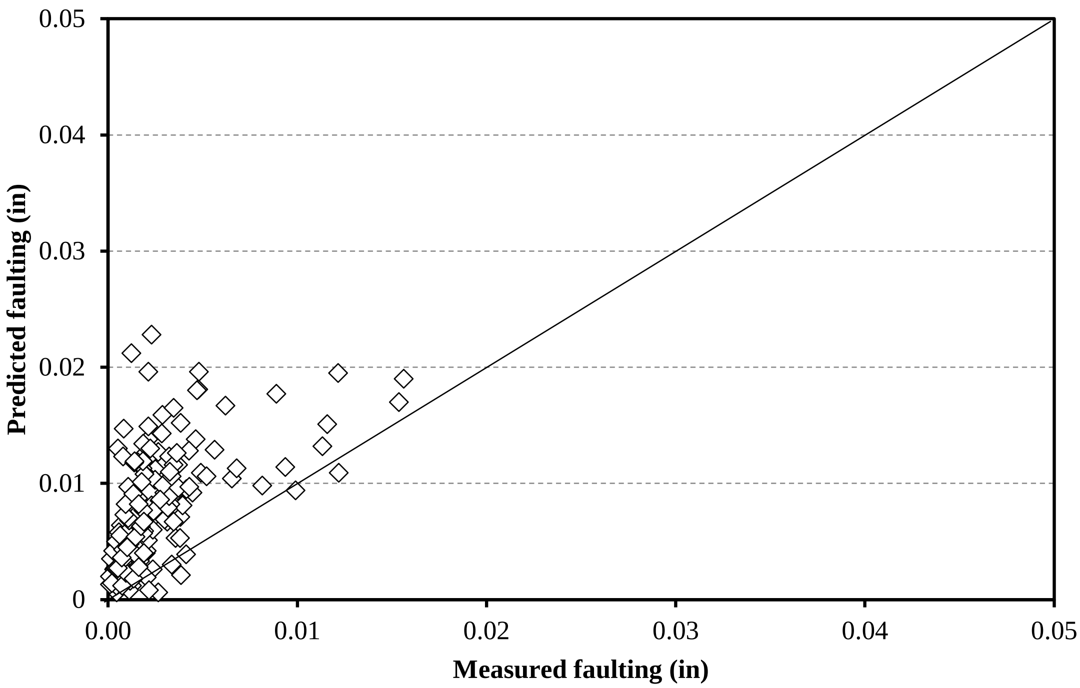

Figure 4.20: Measured versus Predicted Faulting by the Nationally Calibrated MEPDG for the Projects with a Base Course of the DBWED

Table 4.18: Statistical Analysis of Measured and Predicted Faulting by the Nationally Calibrated MEPDG for the Projects with a Base Course of the DBWED

Goodness of fit						
N = 182 R^2 = 0.15 SEE = 2.94E-03 in.						
Hypothesis testing						
Hypothesis	Degree of freedom	Parameter estimate	Standard error	t-value	p-value	Reject/ accept
(1) H_0: Intercept = 0	1	0.0009	0.0004	2.17	3.14E-02	Reject
(2) H_0: Slope = 1	1	0.24	0.04	5.57	1.00E-04	Reject
(3) H_0: Measured rutting - MEPDG predicted rutting = 0	182	-	-	13.60	1.77E-29	Reject

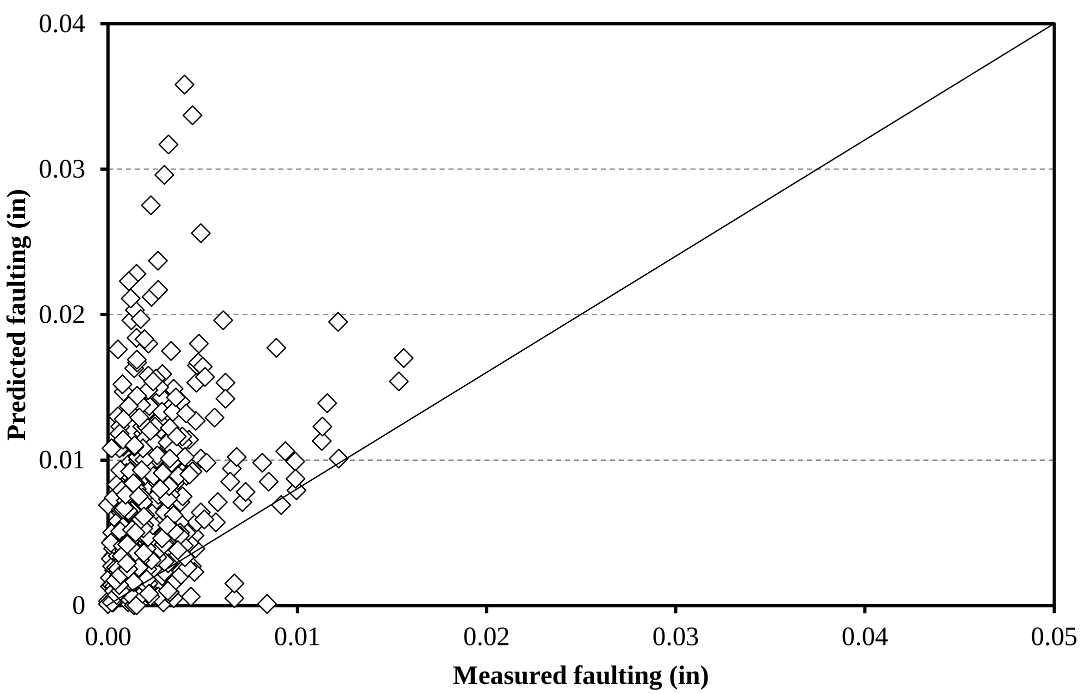

Figure 4.21: Measured versus Predicted Faulting by the Nationally Calibrated MEPDG for All the Projects of Rigid Pavements

Table 4.19: Statistical Analysis of Measured and Predicted Faulting by the Nationally Calibrated MEPDG for All the Projects

Goodness of fit						
N = 403 R^2 = 0.06 SEE = 2.39E-03 in.						
Hypothesis testing						
Hypothesis	Degree of freedom	Parameter estimate	Standard error	t-value	p-value	Reject/ accept
(1) H_0: Intercept = 0	1	0.0018	0.0002	9.45	2.89E-19	Reject
(2) H_0: Slope = 1	1	0.09	0.02	48.15	less than 0.0001	Reject
(3) H_0: Measured rutting - MEPDG predicted rutting = 0	403	-	-	16.56	2.50E-47	Reject

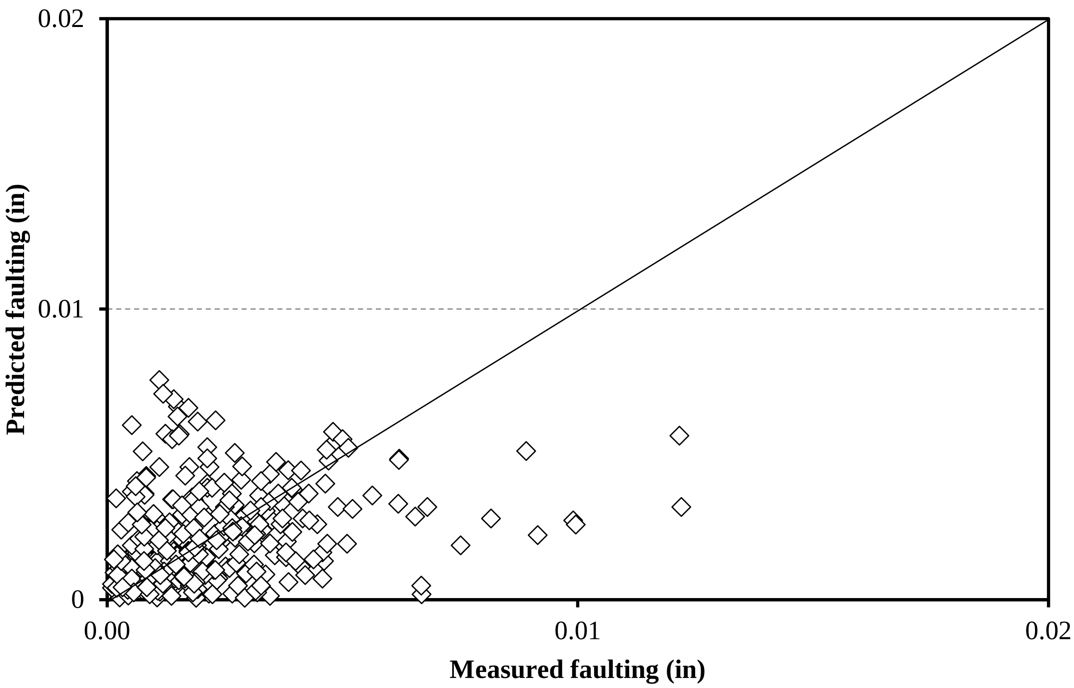

Figure 4.22: Measured versus Predicted Faulting by the MEPDG after Local Calibration for the Projects with Base Course of the CEMBAS and DBWED

Table 4.20: Statistical Analysis of Measured and Predicted Faulting by the MEPDG after Local Calibration for the Projects with Base Course of the CEMBAS and DBWED

Goodness of fit						
N = 337 R^2 = 0.734 SEE = 1.77E-03in.						
Hypothesis testing						
Hypothesis	Degree of freedom	Parameter estimate	Standard error	t-value	p-value	Reject/ accept
(1) H_0: Intercept = 0	1	0.0016	0.0002	9.22	4.22E-18	Reject
(2) H_0: Slope = 1	1	0.32	0.06	10.89	less than 0.0001	Reject
(3) H_0: Measured rutting - MEPDG predicted rutting = 0	322	-	-	0.04	0.96	Accept

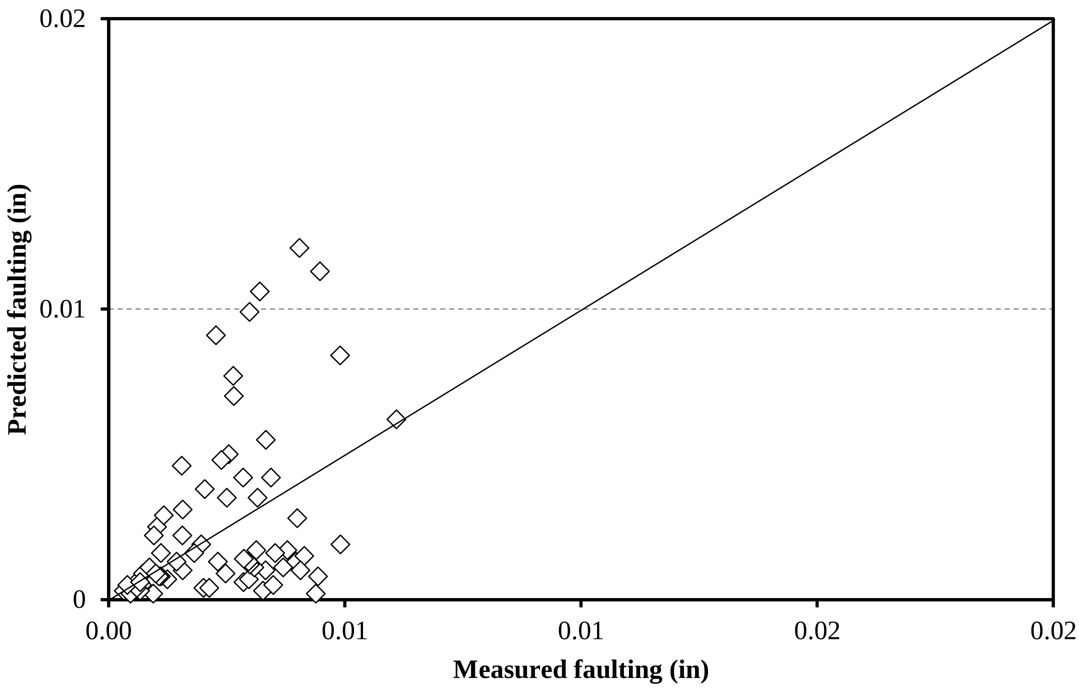

Figure 4.23: Measured versus Predicted Faulting by the MEPDG after Local Calibration for the Projects with a Base Course of the PCCDCB

Table 4.21: Statistical Analysis of Measured and Predicted Faulting by the MEPDG after Local Calibration for the Projects with a Base Course of the PCCDCB

Goodness of fit						
N = 66 R^2 = 0.16 SEE = 1.21E-03 in.						
Hypothesis testing						
Hypothesis	Degree of freedom	Parameter estimate	Standard error	t-value	p-value	Reject/ accept
(1) H_0: Intercept = 0	1	0.0019	0.0002	9.59	5.34E-14	Reject
(2) H_0: Slope = 1	1	0.18	0.05	16.26	less than 0.0001	Reject
(3) H_0: Measured rutting - MEPDG predicted rutting = 0	66	-	-	-0.76	0.45	Accept

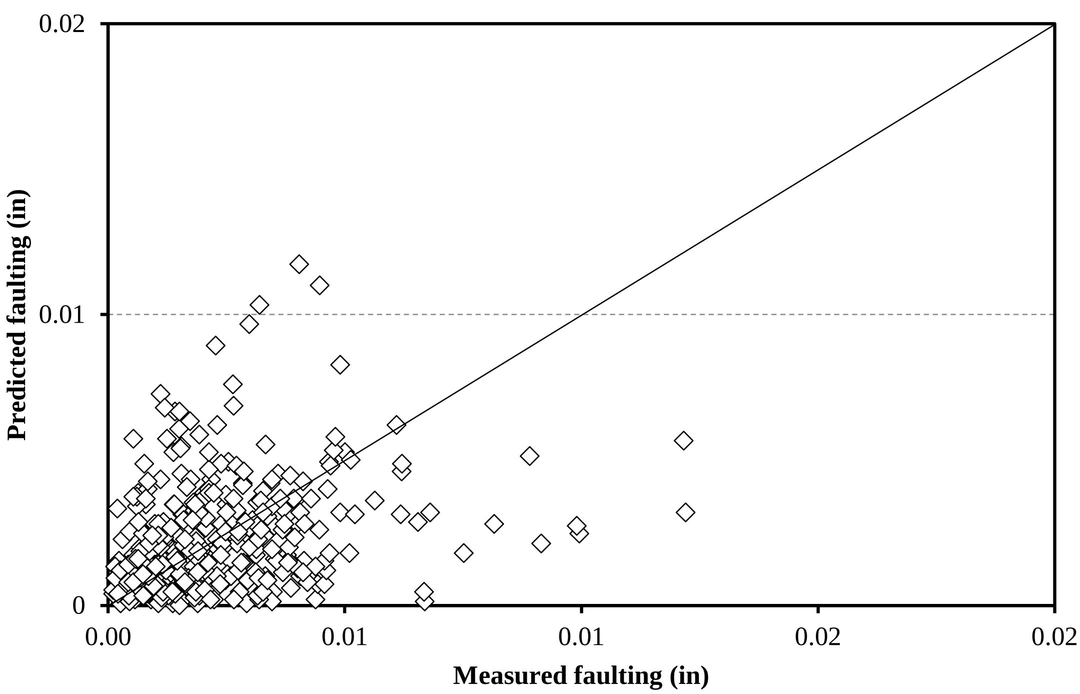

Figure 4.24: Measured versus Predicted Faulting by the MEPDG after Local Calibration for All the Projects of Rigid Pavements

Table 4.22: Statistical Analysis of Measured and Predicted Faulting by the MEPDG after Local Calibration for All the Projects of Rigid Pavements

Goodness of fit						
N = 403 R^2 = 0.08 SEE = 2.67E-03 in.						
Hypothesis testing						
Hypothesis	Degree of freedom	Parameter estimate	Standard error	t-value	p-value	Reject/ accept
(1) H_0: Intercept = 0	1	0.0023	0.0002	10.36	2.31E-22	Reject
(2) H_0: Slope = 1	1	0.46	0.08	7.08	less than 0.0001	Reject
(3) H_0: Measured rutting - MEPDG predicted rutting = 0	403	-	-	0.66	0.51	Accept

4.2.2 Roughness

Figures 4.25, 4.26, and 4.27 show the comparisons of the measured and predicted IRI by the nationally calibrated MEPDG for the rigid pavements with a base course of the PCCDCB, the CEMBAS, and the DBWED, respectively. Tables 4.23, 4.24, and 4.25 present the corresponding statistical analysis for each group of projects. Figure 4.28 and Table 4.26 show the comparison of the measured and predicted faultings by the nationally calibrated MEPDG for all the projects. The above comparisons show that bias existed in all the three groups of projects with different chemically stabilized base courses. Therefore, the local calibration of the MEPDG is needed to minimize the bias.

The traditional splitting data method was applied in the local calibration. Figure 4.29 shows that the bias was minimized after the local calibration of projects with base courses of the DBWED and the CEMBAS. Table 4.27 presents the corresponding statistical analysis. Figure 4.30 and Table 4.28 present the comparisons of the measured and predicted IRI for projects with a base course of the PCCDCB by the locally calibrated MEPDG with calibration coefficients obtained before.

It is found that the bias of projects with base courses of the CEMBAS and the DBWED was minimized after the local calibration. The hypotheses of the intercept and the slope were rejected, but the SEE was much lower than that for the nationally calibrated model, as shown in Table 3.15. Similarly to the faulting, the bias of the IRI for projects with a base course of the PCCDCB was minimized as well by applying the obtained local calibration coefficients, which means the validation of the identified local calibration coefficients. The local calibration was performed on all the projects as well. Figure 4.31 and Table 4.29 show the comparisons of the measured and predicted faulting by the locally calibrated MEPDG based on all the projects. The identified local calibration coefficients were summarized in Table 4.30.

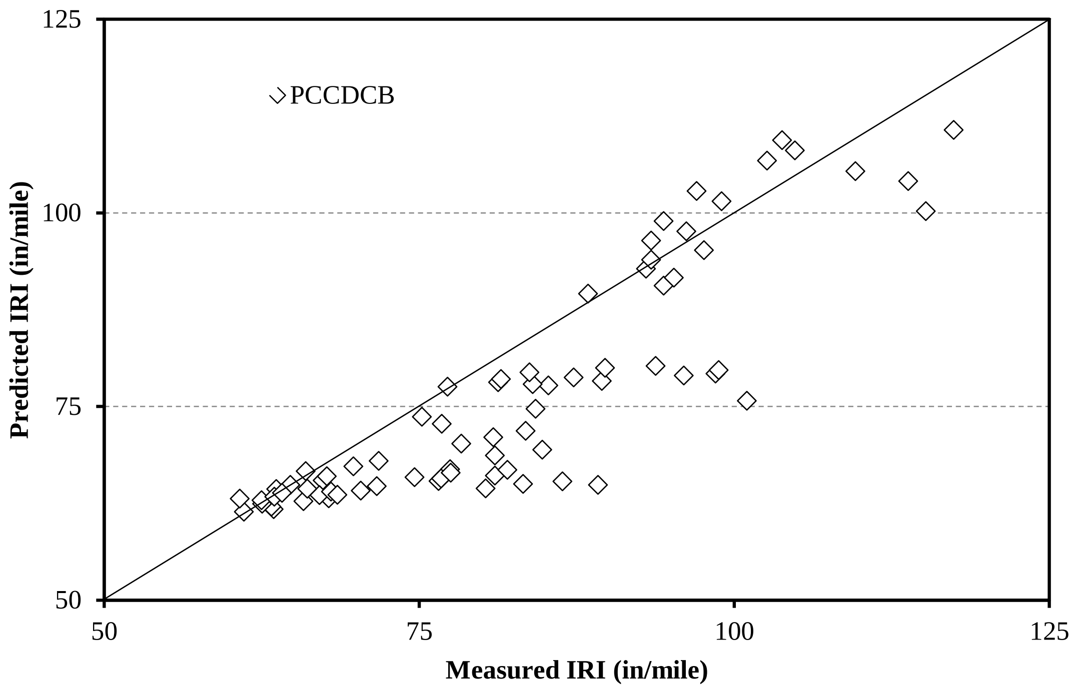

Figure 4.25: Measured versus Predicted IRI by the Nationally Calibrated MEPDG for the Projects with a Base Course of the PCCDCB

Table 4.23: Statistical Analysis of Measured and Predicted IRI by the Nationally Calibrated MEPDG for the Projects with a Base Course of the PCCDCB

Goodness of fit						
N = 71 R^2 = 0.77 SEE = 7.15 in./mile						
Hypothesis testing						
Hypothesis	Degree of freedom	Parameter estimate	Standard error	t-value	p-value	Reject/ accept
(1) H_0: Intercept = 0	1	15.76	4.52	3.49	8.55E-04	Reject
(2) H_0: Slope = 1	1	0.87	0.06	2.25	0.03	Reject
(3) H_0: Measured rutting - MEPDG predicted rutting = 0	71	-	-	6.60	6.52E-09	Reject

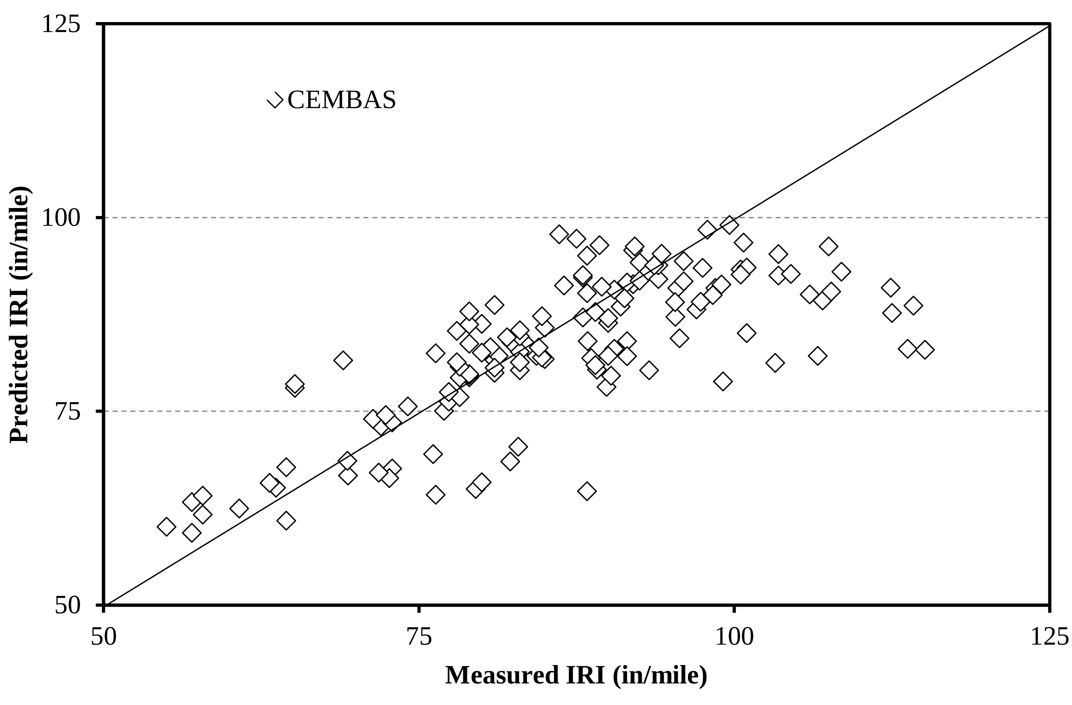

Figure 4.26: Measured versus Predicted IRI by the Nationally Calibrated MEPDG for the Projects with a Base Course of the CEMBAS

Table 4.24: Statistical Analysis of Measured and Predicted IRI by the Nationally Calibrated MEPDG for the Projects with a Base Course of the CEMBAS

Goodness of fit						
N = 165 R^2 = 0.48 SEE = 9.33 in./mile						
Hypothesis testing						
Hypothesis	Degree of freedom	Parameter estimate	Standard error	t-value	p-value	Reject/ Accept
(1) H_0: Intercept = 0	1	14.84	5.89	2.52	0.01	Reject
(2) H_0: Slope = 1	1	0.88	0.07	1.68	0.09	Accept
(3) H_0: Measured rutting - MEPDG predicted rutting = 0	165	-	-	6.87	1.27E-10	Reject

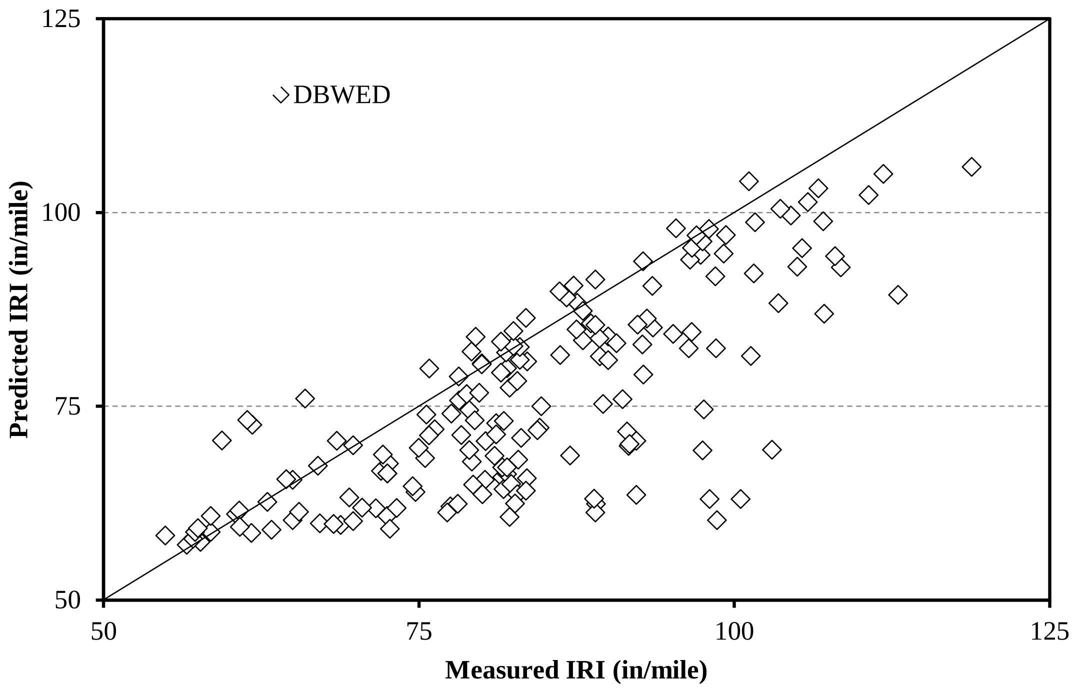

Figure 4.27: Measured versus Predicted IRI by the Nationally Calibrated MEPDG for the Projects with a Base Course of the DBWED

Table 4.25: Statistical Analysis of Measured and Predicted IRI by the Nationally Calibrated MEPDG for the Projects with a Base Course of the DBWED

Goodness of fit						
N = 191 R^2 = 0.62 SEE = 9.04 in.						
Hypothesis testing						
Hypothesis	Degree of freedom	Parameter estimate	Standard error	t-value	p-value	Reject/ accept
(1) H_0: Intercept = 0	1	20.03	3.61	5.55	9.74E-08	Reject
(2) H_0: Slope = 1	1	0.83	0.05	3.49	0.0006	Reject
(3) H_0: Measured rutting - MEPDG predicted rutting = 0	191	-	-	11.36	3.88E-23	Reject

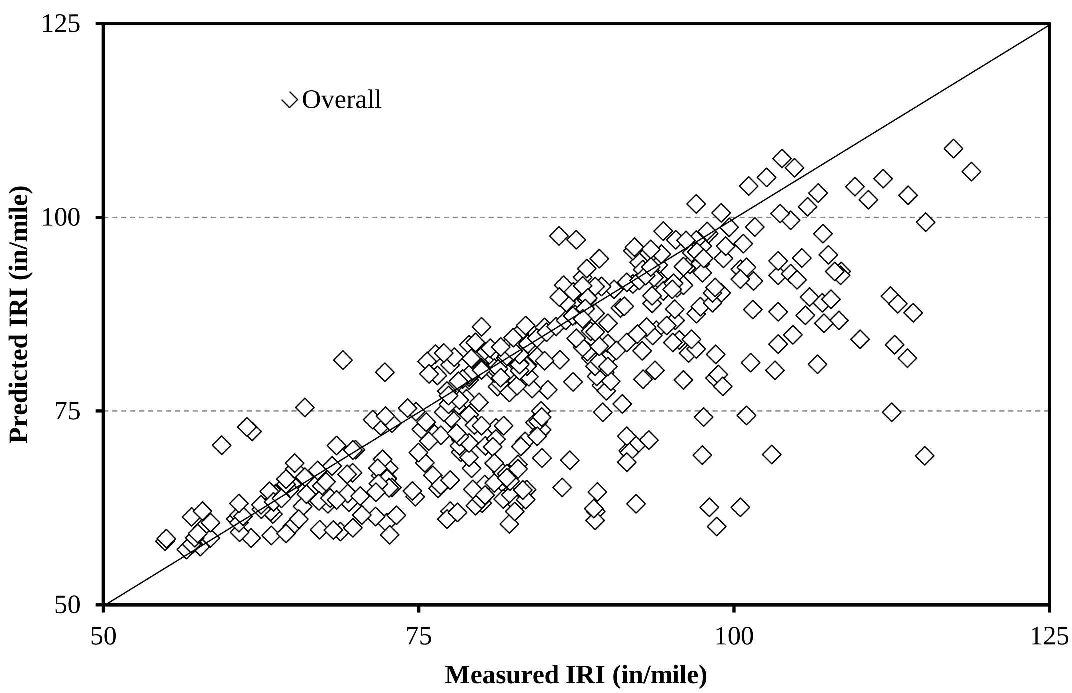

Figure 4.28: Measured versus Predicted IRI by the Nationally Calibrated MEPDG for All the Projects of Rigid Pavements

Table 4.26: Statistical Analysis of Measured and Predicted IRI by the Nationally Calibrated MEPDG for All the Projects of Rigid Pavements

Goodness of fit						
N = 427 R^2 = 0.61 SEE = 8.87 in./mile						
Hypothesis testing						
Hypothesis	Degree of freedom	Parameter estimate	Standard error	t-value	p-value	Reject/ accept
(1) H_0: Intercept = 0	1	18.74	2.59	7.24	2.14E-12	Reject
(2) H_0: Slope = 1	1	0.84	0.03	4.87	less than 0.0001	Reject
(3) H_0: Measured rutting - MEPDG predicted rutting = 0	427	-	-	14.34	2.5E-38	Reject

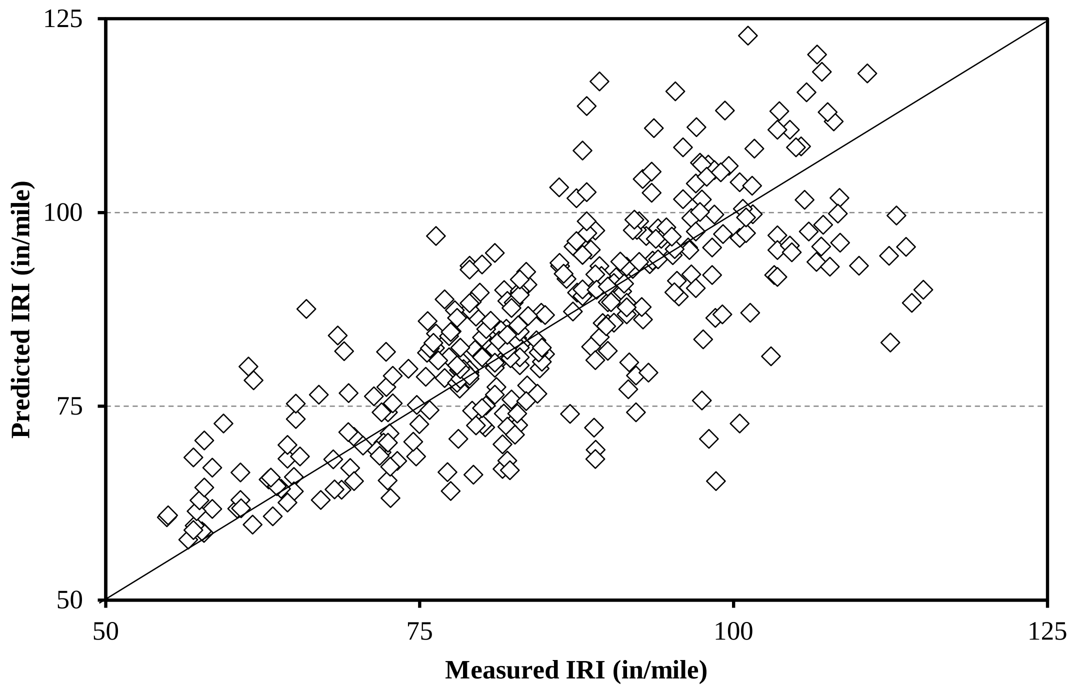

Figure 4.29: Measured versus MEPDG Predicted IRI by the MEPDG after Local Calibration for the Projects with the Base Course of the CEMBAS and DBWED

Table 4.27: Statistical Analysis of Measured and Predicted IRI by the MEPDG after Local Calibration for the Projects with the Base Course of the CEMBAS and DBWED

Goodness of fit						
N = 356 R^2 = 0.81 SEE = 8.68 in./mile						
Hypothesis testing						
Hypothesis	Degree of freedom	Parameter estimate	Standard error	t-value	p-value	Reject/ accept
(1) H_0: Intercept = 0	1	7.36	2.03	3.63	3.30E-04	Reject
(2) H_0: Slope = 1	1	0.92	0.02	3.50	5.00E-04	Reject
(3) H_0: Measured rutting - MEPDG predicted rutting = 0	356	-	-	-0.93	0.36	Accept

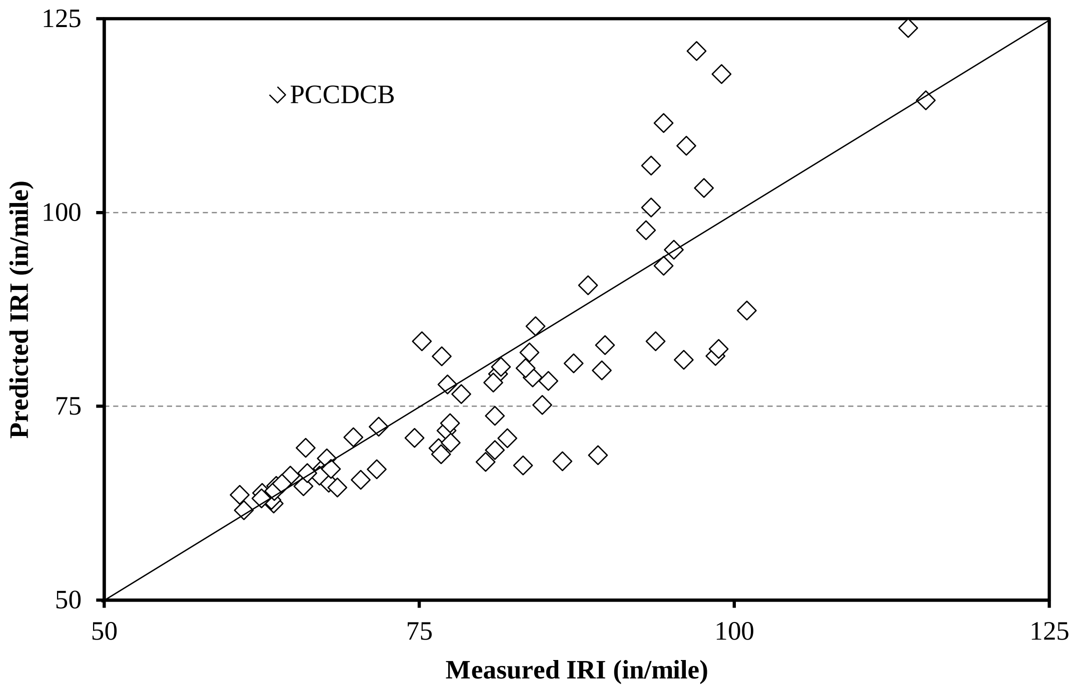

Figure 4.30: Measured versus Predicted IRI by the MEPDG after Local Calibration for the Projects with a Base Course of the PCCDCB

Table 4.28: Statistical Analysis of Measured and Predicted IRI by the MEPDG after Local Calibration for the Projects with a Base Course of the PCCDCB

Goodness of fit						
N = 71 R^2 = 0.75 SEE = 10.55 in./mile						
Hypothesis testing						
Hypothesis	Degree of freedom	Parameter estimate	Standard error	t-value	p-value	Reject/ accept
(1) H_0: Intercept = 0	1	-18.21	7.20	2.53	0.01	Reject
(2) H_0: Slope = 1	1	1.22	0.09	2.58	0.01	Reject
(3) H_0: Measured rutting - MEPDG predicted rutting = 0	71	-	-	1.24	0.16	Accept

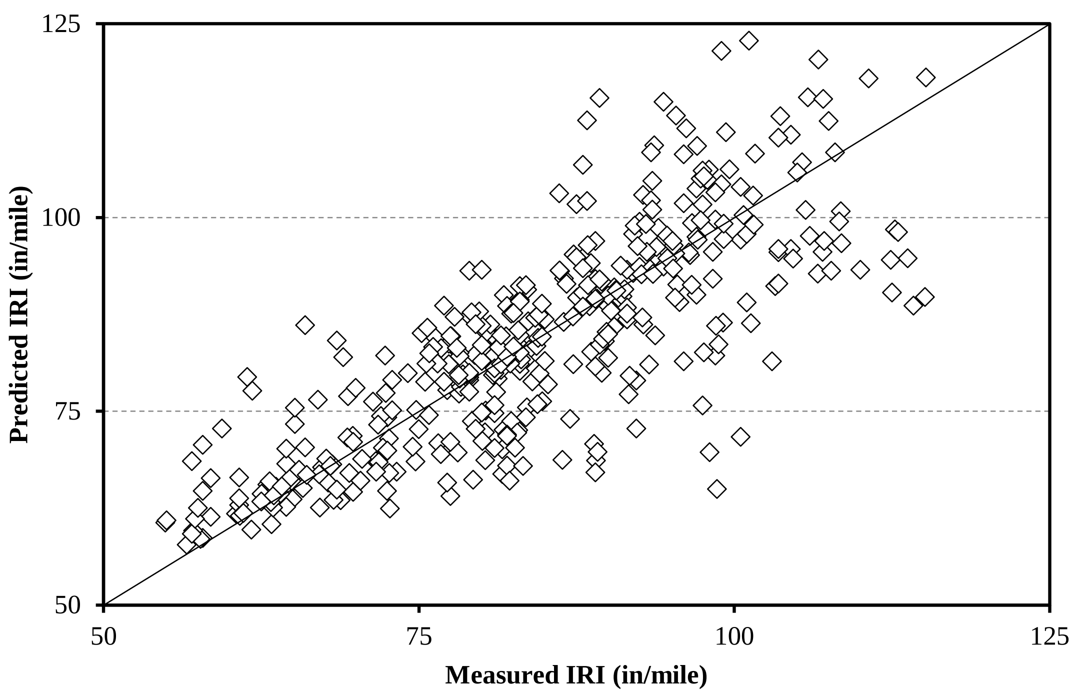

Figure 4.31: Measured versus MEPDG Predicted IRI by the MEPDG after Local Calibration for All the Projects of Rigid Pavements

Table 4.29: Statistical Analysis of Measured and Predicted IRI by the MEPDG after Local Calibration for All the Projects of Rigid Pavements

<table>
<tr><td colspan="7">Goodness of fit</td></tr>
<tr><td colspan="7">N = 427
R^2 = 0.62
SEE = 9.68 in./mile</td></tr>
<tr><td colspan="7">Hypothesis testing</td></tr>
<tr><td>Hypothesis</td><td>Degree of freedom</td><td>Parameter estimate</td><td>Standard error</td><td>t-value</td><td>p-value</td><td>Reject/ accept</td></tr>
<tr><td>(1) H_0: Intercept = 0</td><td>1</td><td>7.24</td><td>2.99</td><td>2.42</td><td>0.02</td><td>Reject</td></tr>
<tr><td>(2) H_0: Slope = 1</td><td>1</td><td>0.91</td><td>0.03</td><td>2.45</td><td>0.01</td><td>Reject</td></tr>
<tr><td>(3) H_0: Measured rutting - MEPDG predicted rutting = 0</td><td>427</td><td>-</td><td>-</td><td>0.08</td><td>0.94</td><td>Accept</td></tr>
</table>

Table 4.30: Summary of Local Calibrated Coefficients in the Traditional Splitting Data Method

<table>
<tr><td colspan="5">Mean Transverse joint faulting (in.)</td><td colspan="4">Roughness (in./mile)</td></tr>
<tr><td colspan="2"></td><td>C3</td><td>C6</td><td>C7</td><td colspan="2"></td><td>J3</td><td>J4</td></tr>
<tr><td>Calibration</td><td>CEMBAS and DBWED</td><td rowspan="2">0.0017</td><td rowspan="2">0.15</td><td rowspan="2">0.01</td><td>Calibration</td><td>CEMBAS and DBWED</td><td rowspan="2">9.2</td><td rowspan="2">70</td></tr>
<tr><td>Validation</td><td>PCCDCB</td><td>Validation</td><td>PCCDCB</td></tr>
<tr><td colspan="2">Overall</td><td>0.00164</td><td>0.15</td><td>0.01</td><td colspan="2">Overall</td><td>9.38</td><td>70</td></tr>
</table>

4.2.3 *Summary of the Locally Calibrated Coefficients for Rigid Pavements in Kansas*

Table 4.31 summarizes the locally calibrated coefficients of the faulting and roughness models for rigid pavements in Kansas, which are compared with those from other states (Pierce & McGovern, 2014). The greyed numbers in Table 4.15 are the locally calibrated coefficients. As compared with the coefficients from other states, the locally calibrated coefficients for rigid pavements in Kansas are in a reasonable range.

In general, the SEE of the nationally calibrated and locally calibrated models did not change much after their biases were minimized. However, the hypotheses of the intercept and the slope were still rejected after the local calibration, even though the p-values were improved significantly. Appendix F shows the comparisons of the measured and predicted faulting and IRI by the locally calibrated MEPDG for rigid pavements in Kansas.

Table 4.31: Summary of Coefficients of Local Calibration of Rigid Pavement for Kansas and Comparison of Coefficients of Different States

Calibration factors	National	Arizona	Colorado	Florida	Missouri	Kansas
Faulting						
C1	1.0184	0.0355	0.5104	4.0472	1.0184	1.0184
C2	0.91656	0.1147	0.00838	0.91656	0.91656	0.91656
C3	0.002848	0.00436	0.00147	0.002848	0.0028	0.00164
C4	0.000883739	1.10E-07	0.008345	0.000883739	0.000883739	0.000883739
C5	250	20000	5999	250	250	250
C6	0.4	2.309	0.8404	0.079	0.4	0.15
C7	1.8331	0.189	5.9293	1.8331	1.8331	0.01
C8	400	400	400	400	400	400
IRI						
J1	0.8203	0.6	0.8203	0.8203	0.82	0.8203
J2	0.4417	3.48	0.4417	0.4417	1.17	0.4417
J3	1.4929	1.22	1.4929	2.2555	1.43	9.38
J4	25.24	45.2	25.24	25.24	66.8	70

Source: Pierce & McGovern, 2014
Note: the locally calibrated coefficients for other states were cited from Pierce & McGovern, 2014

Chapter 5: Conclusions and Recommendations

This study aimed to improve the accuracy of the MEPDG predictions of pavement performance in Kansas through local calibration of the prediction models. A total of 28 new flexible pavement projects and 32 new rigid pavement projects were selected from the KDOT PMS database. The required MEPDG inputs for the selected projects were mainly from the Kansas pavement structure details (blackbook), the material testing records, the KDOT suggested inputs, and the MEPDG national default inputs. A database of the historical performance data for the selected projects was prepared from the KDOT PMS database.

The accuracies of the nationally calibrated MEPDG models were compared with the measured data and evaluated by statistical analysis. The locally calibrated coefficients were determined using the linear optimization approach. The statistical analysis was conducted to evaluate the effects of the local calibration on the improved accuracies of the prediction models. In addition, the traditional splitting data method was applied in the process of determining the locally calibrated coefficients for the rigid pavements in Kansas. The locally calibrated coefficients from this study are summarized in Table 4.15 for new flexible pavements, and in Table 4.31 for new rigid pavements.

The selected flexible pavement projects were divided into two groups: (1) the projects with a subgrade resilient modulus of 2700 psi and (2) the projects with a subgrade resilient modulus equal to or higher than 4000 psi. Local calibration was conducted on these two groups of projects. However, the reliability of the local calibration for the group with a subgrade resilient modulus of 2700 psi was relatively low due to the limited number of the projects. The following conclusions can be made about the local calibration of the MEPDG models for new flexible pavements in Kansas:

- The locally calibrated rutting model provided better predictions than the nationally calibrated model. The nationally calibrated model overestimated the rutting greatly, due to the overestimation of the rutting of the subgrade layer.

- Little or no bottom-up (alligator) cracking was predicted by the nationally calibrated MEPDG and measured in the field based on the PMS database; therefore, the local calibration work on the bottom-up cracking model was not conducted.
- The top-down cracking model was locally calibrated and the bias was minimized. Due to the significant varibility of the measured top-down cracking, the standard error of the estimate (SEE) of the locally calibrated top-down model was relatively high.
- A large bias existed in the nationally calibrated thermal cracking model as compared with the measured, since no thermal cracking was predicted by this model. After the local calibration, the bias was minimized.
- A small bias existed in the nationally calibrated IRI model as compared with the measured data. This IRI model was improved after local calibration.

Three types of chemically stabilized base courses were considered in the local calibration of the MEPDG models for new rigid pavements in Kansas. The following conclusions can be made:

- As compared with the default threshold of the MEPDG, very low faulting was measured according to the PMS database. After local calibration, the bias between the prediction and the measured data was minimized.
- The nationally calibrated IRI model underestimated the IRI as compared with the measured results. Local calibration minimized the bias successfully.
- The base course type did not influence the locally calibrated coefficients of the prediction models.

The following recommendations can be made for possible improvement of the locally calibrated prediction models in the future:

- The subgrade resilient moduli used in this local calibration were based on the county map provided by KDOT, which may not accurately represent the actual subgrade conditions. Accurate determination of the actual subgrade moduli will improve the reliability of the local calibration of the prediction models.
- More reliable distress models and data are needed for fatigue and thermal cracking of flexible pavements and joint faulting of rigid pavements.
- More reliable material inputs, such as the dynamic modulus of a asphalt mix and the G* value of asphalt binder, are needed for future calibration.

References

American Association of State Highway and Transportation Officials (AASHTO). (1993). *AASHTO Guide for design of pavement structures*. Washington, DC: Author.

American Association of State Highway and Transportation Officials (AASHTO). (2008). *Mechanistic-empirical pavement design guide: A manual of practice.* (Interim ed.). Washington, DC: Author.

American Association of State Highway and Transportation Officials (AASHTO). (2010). *Guide for the local calibration of the* Mechanistic-empirical pavement design guide. Washington, DC: Author.

Banerjee, A., Aguiar-Moya, J. P., & Prozzi, J. A. (2009). Calibration of *Mechanistic-empirical pavement design guide* permanent deformation models. *Transportation Research Record: Journal of the Transportation Research Board, 2094,* 12-20.

Banerjee, A., Prozzi, J. A., & Aguiar-Moya, J. P. (2010, January). Calibrating the MEPDG permanent deformation performance model for different maintenance and rehabilitation strategies. Presented at the 89th Annual Meeting of the Transportation Research Board, Washington, DC.

Banerjee, A., Prozzi, J. A., & Freiman, A. (2011). Regional calibration of permanent deformation performance models for rehabilitated flexible pavements. Presented at the 90th Annual Meeting of the Transportation Research Board, Washington, DC.

Bustos, M., Cordo, O., Girardi, P., & Pereyra, M. (2011). Calibration of distress models from the *Mechanistic-empirical pavement design guide* for rigid pavement design in Argentina. *Transportation Research Record: Journal of the Transportation Research Board, 2226*, 3-12.

Caliendo, C. (2012). Local calibration and implementation of the *Mechanistic-empirical pavement design guide* for flexible pavement design. *Journal of Transportation Engineering*, *138*(3), 348-360.

Ceylan, H., Kim, S., Gopalakrishnan, K., & Ma, D. (2013). *Iowa calibration of MEPDG performance prediction models* (InTrans Project 11-401). Ames, IA: Iowa State University.

Corley-Lay, J., Jadoun, F. M., Mastin, J. N., & Kim, Y. R. (2010). Comparison of flexible pavement distresses monitored by North Carolina Department of Transportation and Long-Term Pavement Performance program. *Transportation Research Record: Journal of the Transportation Research Board, 2153,* 91-96.

Darter, M. I., Titus-Glover, L., & Von Quintus, H. L. (2009). *Implementation of the* Mechanistic-empirical pavement design guide *in Utah: validation, calibration, and development of the UDOT MEPDG user's guide* (Report No. UT-09.11). Salt Lake City, UT: Utah Department of Transportation.

Delgadillo, R., Wahr, C., & Alarcón, J. P. (2011). Toward implementation of the *Mechanistic-empirical pavement design guide* in Latin America: Preliminary work in Chile. *Transportation Research Record: Journal of the Transportation Research Board, 2226,* 142-148.

Federal Highway Administration (FHWA). (2006a). *Using pavement management data to calibrate and validate the new MEPDG: An eight state study: Final report, volume I* (FHWA Contract No. DTFH 61-05-C-00011). Washington, DC: Author.

Federal Highway Administration (FHWA). (2006b.) *Using pavement management data to calibrate and validate the new MEPDG: An eight state study: Final report, volume II* (FHWA Contract No. DTFH 61-05-C-00011). Washington, DC: Author.

Federal Highway Administration (FHWA). (2010). *Local calibration of the MEPDG using pavement management systems* (Publication No. HIF-11-026). Washington, DC: Author.

Galal, K. A., & Chehab, G. R. (2005). Implementing the mechanistic-empirical design guide procedure for a hot-mix asphalt-rehabilitated pavement in Indiana. *Transportation Research Record: Journal of the Transportation Research Board, 1919,* 121-133.

Hall, K. D., Xiao, D. X., & Wang, K. C. P. (2011). Calibration of the *Mechanistic-empirical pavement design guide* for flexible pavement design in Arkansas. *Transportation Research Record: Journal of the Transportation Research Board, 2226,* 135-141.

Hoegh, K., Khazanovich, L., & Jensen, M. (2010). Local calibration of *Mechanistic-empirical pavement design guide* rutting model: Minnesota Road Research Project test sections. *Transportation Research Record: Journal of the Transportation Research Board, 2180,* 130-141.

Jadoun, F. M. (2011). *Calibration of the flexible pavement distress prediction models in the* Mechanistic empirical pavement design guide (MEPDG) *for North Carolina* (Doctoral dissertation). Raleigh, NC: North Carolina State University.

Kang, M., Adams, T. M., & Bahia, H. (2007). *Development of a regional pavement performance database for the AASHTO* Mechanistic-empirical pavement design guide*: Part 2: Validations and local calibration* (Report No. MRUTC 07-01). Madison, WI: University of Wisconsin.

Khazanovich, L., Yut, I., Husein, S., Turgeon, C., & Burnham, T. (2008). Adaptation of *Mechanistic-empirical pavement design guide* for design of Minnesota low-volume portland cement concrete pavements. *Transportation Research Record: Journal of the Transportation Research Board, 2087,* 57-67.

Kim, S., Ceylan, H., Gopalakrishnan, K., & Smadi, O. (2010). Use of pavement management information system for verification of *Mechanistic-empirical pavement design guide* performance predictions. *Transportation Research Record: Journal of the Transportation Research Board, 2153,* 30-39.

Kim, Y. R., Jadoun, F. M., Hou, T., & Muthadi, N. (2011). *Local calibration of the MEPDG for flexible pavement design* (Report No. FHWA/NC/2007-07). Raleigh, NC: North Carolina Department of Transportation.

Li, J., Luhr, D. R., & Uhlmeyer, J. S. (2010). Pavement performance modeling using piecewise approximation. *Transportation Research Record: Journal of the Transportation Research Board, 2153,* 24-29.

Li, J., Muench, S. T., Mahoney, J. P., Sivaneswaran, N., & Pierce, L. M. (2006). Calibration of NCHRP 1-37A software for the Washington State Department of Transportation: Rigid pavement portion. *Transportation Research Record: Journal of the Transportation Research Board, 1949,* 43-53.

Li, J., Pierce, L. M., & Uhlmeyer, J. (2009). Calibration of flexible pavement in *Mechanistic-empirical pavement design guide* for Washington state. *Transportation Research Record: Journal of the Transportation Research Board, 2095,* 73-83.

Mallela, J., Titus-Glover, L., Sadasivam, S., Bhattacharya, B., Darter, M., & Von Quintus, H. (2013). *Implementation of the AASHTO* Mechanistic-empirical pavement design guide *for Colorado* (Report no. CDOT-2013-4). Denver, CO: Colorado Department of Transportation.

Mamlouk, M., & Zapata, C. E. (2010). Necessary assessment of use of state pavement management system data in *Mechanistic-empirical pavement design guide* calibration process. *Transportation Research Record: Journal of the Transportation Research Board, 2153*, 58-66.

Mehta, Y. A., Sauber, R. W., Owad, J., & Krause, J. (2008, January). Lessons learned during implementation of *Mechanistic-empirical pavement design guide*. Presented at the 87th Annual Meeting of the Transportation Research Board, Washington, DC.

Miner, M. A. (1945). Cumulative damage in fatigue. *Journal of Applied Mechanics*, *12*(3), 159-164.

Muthadi, N. R. (2007). *Local calibration of the MEPDG for flexible pavement design* (Master's thesis). Raleigh, NC: North Carolina State University.

Muthadi, N. R., & Kim, Y. R. (2008). Local calibration of *Mechanistic-empirical pavement design guide* for flexible pavement design. *Transportation Research Record: Journal of the Transportation Research Board, 2087*, 131-141.

NCHRP. (2003a). *Jackknife testing—An experimental approach to refine model calibration and validation* (NCHRP Research Results Digest No. 283). Washington, DC: Transportation Research Board.

NCHRP. (2003b). *Refining the calibration and validation of hot mix asphalt performance models: An experimental plan and database* (NCHRP Research Results Digest No. 284). Washington, DC: Transportation Research Board.

NCHRP. (2004). *Guide for mechanistic-empirical design of new and rehabilitated pavement structures: Final report* (NCHRP Project 1-37A), Washington, DC: Transportation Research Board.

NCHRP Project 1-40D. (n.d.). *Technical assistance to NCHRP and NCHRP project 1-40A: Versions 0.9 and 1.0 of the M-E Pavement Design software*. Washington, DC: Transportation Research Board. Retrieved from http://apps.trb.org/cmsfeed/TRBNetProjectDisplay.asp?ProjectID=224 and http://apps.trb.org/cmsfeed/TRBNetProjectDisplay.asp?ProjectID=225.

Pierce, L. M., & McGovern, G. (2014). *Implementation of the AASHTO* Mechanistic-empirical pavement design guide *and software* (NCHRP Synthesis 457). Washington, DC: Transportation Research Board.

Schram, S., & Abdelrahman, M. (2006). Improving prediction accuracy in *Mechanistic-empirical pavement design guide. Transportation Research Record: Journal of the Transportation Research Board, 1947,* 59-68.

Souliman, M. I., Mamlouk, M. S., El-Basyouny, M. M., & Zapata, C. E. (2010, January). Calibration of the AASHTO MEPDG for flexible pavement for Arizona conditions. Presented at the 89th Annual Meeting of the Transportation Research Board, Washington, DC.

Titus-Glover, L., & Mallela, J. (2009). *Guidelines for implementing NCHRP 1-37A M-E design procedures in Ohio: Volume 4 -- MEPDG models validation & recalibration* (Report No. FHWA/OH-2009/9D). Columbus, OH: Ohio Department of Transportation.

Velasquez, R., Hoegh, K., Yut, I., Funk, N., Cochran, G., Marasteanu, M., & Khazanovich, L. (2009). *Implementation of the MEPDG for new and rehabilitated pavement structures for design of concrete and asphalt pavements in Minnesota* (Report No. MN/RC 2009-06). St. Paul, MN: Minnesota Department of Transportation.

Von Quintus, H. L., & Moulthrop, J. S. (2007). Mechanistic-empirical pavement design guide *flexible pavement performance prediction models for Montana: Volume I: Executive research summary* (Report No. FHWA/MT-07-008/8158-1). Helena, MT: Montana Department of Transportation.

Wu, Z., & Yang, X. (2012). *Evaluation of current Louisiana flexible pavement structures using PMS data and new* Mechanistic-empirical pavement design guide (Report No. FHWA/LA.11/482). Baton Rouge, LA: Louisiana Transportation Research Center.

Appendix A: Resilient Moduli Of Subgrade In Kansas Counties

Table A.1: Subgrade Resilient Moduli in Kansas Counties

COUNTY	CONAME	COSNAME	DIST	Resilient modulus (psi)
1	Allen	AL	4	4000
2	Anderson	AN	4	4000
3	Atchison	AT	1	2700
4	Barber	BA	5	7000
5	Barton	BT	5	5100
6	Bourbon	BB	4	4000
7	Brown	BR	1	2700
8	Butler	BU	5	4320
9	Chase	CS	2	4000
10	Chautauqua	CQ	4	4000
11	Cherokee	CK	4	4000
12	Cheyenne	CN	3	7000
13	Clark	CA	6	7000
14	Clay	CY	2	5100
15	Cloud	CD	2	5100
16	Coffey	CF	4	4000
17	Comanche	CM	5	7000
18	Cowley	CL	5	4320
19	Crawford	CR	4	4000
20	Decatur	DC	3	7000
21	Dickinson	DK	2	5100
22	Doniphan	DP	1	2700
23	Douglas	DG	1	4000
24	Edwards	ED	5	6900
25	Elk	EK	4	4000
26	Ellis	EL	3	5100
27	Ellsworth	EW	2	5100
28	Finney	FI	6	7000
29	Ford	FO	6	6500
30	Franklin	FR	4	4000
31	Geary	GE	2	4000
32	Gove	GO	3	7000
33	Graham	GH	3	7000
34	Grant	GT	6	7000
35	Gray	GY	6	7000

Table A.1: Subgrade Resilient Moduli in Kansas Counties (continued)

COUNTY	CONAME	COSNAME	DIST	Resilient modulus (psi)
36	Greeley	GL	6	7000
37	Greenwood	GW	4	4000
38	Hamilton	HM	6	7000
39	Harper	HP	5	7000
40	Harvey	HV	5	5100
41	Haskell	HS	6	7000
42	Hodgeman	HG	6	6200
43	Jackson	JA	1	2700
44	Jefferson	JF	1	2700
45	Jewell	JW	2	6500
46	Johnson	JO	1	4000
47	Kearny	KE	6	7000
48	Kingman	KM	5	7000
49	Kiowa	KW	5	7000
50	Labette	LB	4	4000
51	Lane	LE	6	7000
52	Leavenworth	LV	1	2700
53	Lincoln	LC	2	5100
54	Linn	LN	4	4000
55	Logan	LG	3	7000
56	Lyon	LY	1	4000
57	Marion	MN	2	5100
58	Marshall	MS	1	5100
59	McPherson	MP	2	5100
60	Meade	ME	6	7000
61	Miami	MI	4	4000
62	Mitchell	MC	2	5100
63	Montgomery	MG	4	4000
64	Morris	MR	2	4450
65	Morton	MT	6	7000
66	Nemaha	NM	1	2700
67	Neosho	NO	4	4000
68	Ness	NS	6	5100
69	Norton	NT	3	7000
70	Osage	OS	1	4000
71	Osborne	OB	3	5100
72	Ottawa	OT	2	5100

Table A.1: Subgrade Resilient Moduli in Kansas Counties (continued)

COUNTY	CONAME	COSNAME	DIST	Resilient modulus (psi)
73	Pawnee	PN	5	6900
74	Phillips	PL	3	7000
75	Pottawatomie	PT	1	4000
76	Pratt	PR	5	7000
77	Rawlins	RA	3	7000
78	Reno	RN	5	7000
79	Republic	RP	2	6500
80	Rice	RC	5	5100
81	Riley	RL	1	4320
82	Rooks	RO	3	6500
83	Rush	RH	5	5100
84	Russell	RS	3	5100
85	Saline	SA	2	5100
86	Scott	SC	6	7000
87	Sedgwick	SG	5	5100
88	Seward	SW	6	7000
89	Shawnee	SN	1	3300
90	Sheridan	SD	3	7000
91	Sherman	SH	3	7000
92	Smith	SM	3	7000
93	Stafford	SF	5	7000
94	Stanton	ST	6	7000
95	Stevens	SV	6	7000
96	Sumner	SU	5	5100
97	Thomas	TH	3	7000
98	Trego	TR	3	6500
99	Wabaunsee	WB	1	4000
100	Wallace	WA	3	7000
101	Washington	WS	2	5100
102	Wichita	WH	6	7000
103	Wilson	WL	4	4000
104	Woodson	WO	4	4000
105	Wyandotte	WY	1	2700

Appendix B: Site Specific Inputs For Both Flexible And Rigid Pavements in this Study

Table B.1: Site-Specific Traffic Inputs for Flexible Pavement Projects Selected in this Study

Project name	Two-way AADTT	Number of lane	Percent of truck in design direction	Percent of truck in design lane	Operational speed (mph)	AADTT growth rate (%)
003U0007300-NB	165	1	50	100	65	2
007U0007500-NB	1000	1	50	100	65	2
008U0005400-EB	235	1	50	100	65	2
008U0007700-NB-1	315	1	50	100	65	2
008U0007700-NB-2	345	1	50	100	65	2
008U0007700-NB-3	315	1	50	100	65	2
011U0006900-NB	540	1	50	100	65	2
019K0000700-NB-1	275	1	50	100	65	2
019K0000700-NB-2	275	1	50	100	65	2
019U0016000-EB	115	1	50	100	65	2
022K0000700-NB	130	1	50	100	65	2
023U0004000-EB	300	1	50	100	65	2
025K0009900-NB	250	1	50	100	65	2
027K0015600-EB	575	2	50	95	75	2
028U0005000-EB	1170	2	50	100	75	2
031K0001800-WB	600	2	50	100	75	3
033U0028300-NB	340	1	50	100	65	2
052U0007300-NB	180	1	50	100	65	2
065K0002700-NB	275	1	50	100	65	2
065U0005600-EB	345	1	50	100	65	2
069U0028300-NB	310	1	50	100	65	2
082U0018300-NB	485	1	50	100	65	2
084U0028100-NB	340	1	50	100	65	2
088U0005400-WB	1450	2	50	95	75	2
091K0002700-NB	330	1	50	100	65	2
095U0005600-EB	500	1	50	100	65	2
098U0028300-NB	335	1	50	100	65	2
103K0003900-NB	180	1	50	100	65	2

Table B.2: Site-Specific Traffic Inputs for Rigid Pavement Projects Selected in this Study

Project name	Two-way AADTT	Number of lane	Percent of truck in design direction	Percent of truck in design lane	Operational speed (mph)	AADTT Growth rate (%)
018K0036000-EB	220	1	50	100	65	2
018U0007700-NB	426	1	50	100	65	2
019U0006900-NB	775	1	50	100	65	2
029U0005600-EB	620	1	50	100	65	2
030I0003500-NB-1	3105	3	50	95	75	2
030I0003500-NB-2	4200	2	50	95	75	2
030I0003500-NB-3	4350	2	50	95	75	2
031I0007000	3100	2	50	95	75	3
031I0007000-EB	2860	2	50	95	75	3
037U0040000-EB-1	860	1	50	100	65	2
037U0040000-EB-2	850	1	50	100	65	2
040I0013500-NB-1	2600	2	50	100	65	2
040I0013500-NB-2	2750	2	50	95	75	2
043U0007500-NB-1	784	2	50	95	75	2
043U0007500-NB-2	1055	2	50	95	75	2
046K0000700-SB	900	2	50	95	75	3
055U0004000-WB	390	2	50	95	75	2
056I0003500-SB-1	3260	2	50	95	75	2
056I0003500-SB-2	4150	2	50	95	75	2
056U0005000-EB-1	1365	1	50	100	65	2
059I0013500-NB	2440	2	50	95	70	2
061I0003500-NB	4800	2	50	95	70	2
063U0040000-EB	675	1	50	100	65	2
067U0016900-NB	950	1	50	100	65	2
079U0008100-NB	1150	2	50	95	75	2
085I0007000-EB	4050	2	50	95	75	2
085I0013500	2530	2	50	95	75	2
099I0007000-EB-1	3600	2	50	95	75	2
099I0007000-EB-2	3030	2	50	95	75	2
099I0007000-EB-3	3070	2	50	95	75	2
103U0007500-SB	1136	2	50	95	75	2
103U0040000-EB	470	1	50	100	65	2

Table B.3: Summary of the Structural Information on New Flexible Pavements

Project name	Layer No.	Layer type	Material type	Thickness (in)
003U0007300-NB	1	Flexible	SM95T	0.8
	2	Flexible	SM190A	2.4
	3	Flexible	SM190A	6.5
	4	Subgrade	LIMSUB	6.0
	5	Subgrade	A-7-6	Semi-infinite
007U0007500-NB	1	Flexible	SM95A	1.6
	2	Flexible	SM190A	2.4
	3	Flexible	SM190A	11.8
	4	Subgrade	LIMSUB	5.9
	5	Subgrade	A-7-6	Semi-infinite
008U0005400-EB	1	Flexible	SM95T	1.6
	2	Flexible	SM190A	2.4
	3	Flexible	SM190A	8.7
	4	Subgrade	LIMSUB	5.9
	5	Subgrade	A-7-6	Semi-infinite
008U0007700-NB-1	1	Flexible	SM95T	1.6
	2	Flexible	SM190A	2.4
	3	Flexible	SM190A	3.9
	4	Non-stabilized	AB3	11.0
	5	Subgrade	LIMSUB	5.9
	6	Subgrade	A-7-6	Semi-infinite
008U0007700-NB-2	1	Flexible	SM95A	1.6
	2	Flexible	SM190A	2.4
	3	Flexible	SM190A	8.7
	4	Subgrade	LIMSUB	5.9
	5	Subgrade	A-7-6	Semi-infinite
008U0007700-NB-3	1	Flexible	SM95A	1.6
	2	Flexible	SM190A	2.4
	3	Flexible	SM190A	7.9
	4	Subgrade	LIMSUB	5.9
	5	Subgrade	A-7-6	Semi-infinite
011U0006900-NB	1	Flexible	SM95T	1.6
	2	Flexible	SM190A	2.4
	3	Flexible	SM190A	3.0
	4	Flexible	SM190A	3.3
	5	Subgrade	LIMSUB	5.9
	6	Subgrade	A-7-6	Semi-infinite

Table B.3: Summary of the Structural Information on New Flexible Pavements (continued)

Project name	Layer No.	Layer type	Material type	Thickness (in)
019K0000700-NB-1	1	Flexible	SM95A	1.6
	2	Flexible	SM190A	2.4
	3	Flexible	SM190A	7.9
	4	Subgrade	LIMSUB	5.9
	5	Subgrade	A-7-6	Semi-infinite
019K0000700-NB-2	1	Flexible	SM95A	1.6
	2	Flexible	SM190A	2.4
	3	Flexible	SM190A	6.3
	4	Subgrade	LIMSUB	5.9
	5	Subgrade	A-7-6	Semi-infinite
019U0016000-EB	1	Flexible	SM95T	1.6
	2	Flexible	SM190A	2.4
	3	Flexible	SM190A	7.1
	4	Non-stabilized	AB3	5.9
	5	Subgrade	A-7-6	Semi-infinite
022K0000700-NB	1	Flexible	SM95T	1.5
	2	Flexible	SM190A	2.4
	3	Flexible	SM190A	4.7
	4	Non-stabilized	AB3	11.0
	5	Subgrade	FLYSUB	5.9
	6	Subgrade	A-7-6	Semi-infinite
023U0004000-EB	1	Flexible	SM95T	1.6
	2	Flexible	SM190A	2.4
	3	Flexible	SM190A	8.7
	4	Subgrade	LIMSUB	5.9
	5	Subgrade	A-7-6	Semi-infinite
025K0009900-NB	1	Flexible	SM95A	1.6
	2	Flexible	SM190A	2.4
	3	Flexible	SM190A	7.1
	4	Subgrade	LIMSUB	5.9
	5	Subgrade	A-7-6	Semi-infinite
027K0015600-EB	1	Flexible	SM95A	1.6
	2	Flexible	SM190A	2.4
	3	Flexible	SM190A	10.2
	4	Subgrade	A-7-6	Semi-infinite

Table B.3: Summary of the Structural Information on New Flexible Pavements (continued)

Project name	Layer No.	Layer type	Material type	Thickness (in)
028U0005000-EB	1	Flexible	SM95T	1.6
	2	Flexible	SM190A	2.4
	3	Flexible	SM190A	11.0
	4	Subgrade	LIMSUB	5.9
	5	Subgrade	A-7-6	Semi-infinite
031K0001800-WB	1	Flexible	SM95T	1.6
	2	Flexible	SM190A	2.4
	3	Flexible	SM190A	10.2
	4	Subgrade	A-7-6	Semi-infinite
033U0028300-NB	1	Flexible	SM95A	1.6
	2	Flexible	SM190A	3.5
	3	Flexible	SM190A	7.1
	4	Subgrade	SUBMOD	5.9
	5	Subgrade	A-7-6	Semi-infinite
052U0007300-NB	1	Flexible	SM95T	0.8
	2	Flexible	SM190A	2.4
	3	Subgrade	SM190A	6.5
	4	Subgrade	A-7-6	Semi-infinite
065K0002700-NB	1	Flexible	SM95T	1.6
	2	Flexible	SM190A	2.4
	3	Flexible	SM190A	7.0
	4	Subgrade	SUBMOD	6.0
	5	Subgrade	A-7-6	Semi-infinite
065U0005600-EB	1	Flexible	SM95T	1.6
	2	Flexible	SM190B	2.4
	3	Flexible	SM190A	9.4
	4	Subgrade	SUBMOD	5.9
	5	Subgrade	A-7-6	Semi-infinite
069U0028300-NB	1	Flexible	SM95T	1.5
	2	Flexible	SM190A	2.4
	3	Flexible	SM190A	7.9
	4	Subgrade	SUBMOD	5.9
	5	Subgrade	A-7-6	Semi-infinite
082U0018300-NB	1	Flexible	SM95T	1.6
	2	Flexible	SM190A	2.4
	3	Flexible	SM190A	9.4
	4	Subgrade	FLYSUB	5.9
	5	Subgrade	A-7-6	Semi-infinite

Table B.3: Summary of the Structural Information on New Flexible Pavements (continued)

Project name	Layer No.	Layer type	Material type	Thickness (in)
084U0028100-NB	1	Flexible	SM95T	1.6
	2	Flexible	SM190A	2.4
	3	Flexible	SM190A	7.9
	4	Subgrade	A-7-6	Semi-infinite
088U0005400-WB	1	Flexible	SM95T	1.6
	2	Flexible	SM190A	2.4
	3	Flexible	SM190A	13.4
	4	Subgrade	FLYSUB	5.9
	5	Subgrade	A-7-6	Semi-infinite
091K0002700-NB	1	Flexible	SM95A	1.6
	2	Flexible	SM190A	2.4
	3	Flexible	SM190A	8.7
	4	Subgrade	SUBMOD	5.9
	5	Subgrade	A-7-6	Semi-infinite
095U0005600-EB	1	Flexible	SM95A	1.6
	2	Flexible	SM190A	2.4
	3	Flexible	SM190A	9.4
	4	Subgrade	FLYSUB	5.9
	5	Subgrade	A-7-6	Semi-infinite
098U0028300-NB	1	Flexible	SM95A	1.6
	2	Flexible	SM190A	2.4
	3	Flexible	SM190A	8.7
	4	Subgrade	LIMSUB	5.9
	5	Subgrade	A-7-6	Semi-infinite
103K0003900-NB	1	Flexible	SM95T	1.6
	2	Flexible	SR190A	2.4
	3	Flexible	SR190A	5.5
	4	Subgrade	SUBMOD	5.9

Table B.4: Summary of the Structural Information on New Rigid Pavements

Project name	Layer No.	Layer type	Material type	Thickness (in.)
018K0036000-EB	1	JPCP	PCCPDJ	8.0
	2	Chemically stabilized	CEMBAS	4.0
	3	Subgrade	LIMSUB	6.0
	4	Subgrade	A-7-6	Semi-infinite
018U0007700-NB	1	JPCP	PCCPDJ	9.5
	2	Chemically stabilized	PCCDCB	4.0
	3	Subgrade	A-7-6	Semi-infinite
019U0006900-NB	1	JPCP	PCCPDJ	9.0
	2	Chemically stabilized	DBWED	4.0
	3	Non-stabilized	AB3	6.0
	4	Subgrade	A-7-6	Semi-infinite
029U0005600-EB	1	JPCP	PCCPDJ	9.0
	2	Chemically stabilized	DBWED	4.0
	3	Subgrade	A-7-6	Semi-infinite
030I0003500-NB-1	1	JPCP	PCCPDJ	11.5
	2	Subgrade	LIMSUB	6.0
	3	Subgrade	A-7-6	Semi-infinite
030I0003500-NB-2	1	JPCP	PCCPDJ	12.0
	2	Chemically stabilized	DBWED	4.0
	3	Subgrade	LIMSUB	6.0
	4	Subgrade	A-7-6	Semi-infinite
030I0003500-NB-3	1	JPCP	PCCPDJ	12.0
	2	Chemically stabilized	DBWED	4.0
	3	Subgrade	LIMSUB	6.0
	4	Subgrade	A-7-6	Semi-infinite
031I0007000-EB	1	JPCP	PCCPDJ	11.5
	2	Chemically stabilized	CEMBAS	4.0
	3	Subgrade	LIMSUB	6.0
	4	Subgrade	A-7-6	Semi-infinite
031I0007000	1	JPCP	PCCPDJ	11.0
	2	Chemically stabilized	CEMBAS	4.0
	3	Subgrade	LIMSUB	6.0
	4	Subgrade	A-7-6	Semi-infinite

Table B.4: Summary of the Structural Information on New Rigid Pavements (continued)

Project name	Layer No.	Layer type	Material type	Thickness (in)
037U0040000-EB	1	JPCP	PCCPDJ	9.0
	2	Chemically stabilized	DBWED	4.0
	3	Subgrade	LIMSUB	6.0
	4	Subgrade	A-7-6	Semi-infinite
037U0040000-EB	1	JPCP	PCCPDJ	9.0
	2	Chemically stabilized	DBWED	4.0
	3	Subgrade	LIMSUB	6.0
	4	Subgrade	A-7-6	Semi-infinite
040I0013500-NB-1	1	JPCP	PCCPDJ	12.6
	2	Chemically stabilized	CEMBAS	3.9
	3	Subgrade	LIMSUB	5.9
	4	Subgrade	A-7-6	Semi-infinite
040I0013500-NB-2	1	JPCP	PCCPDJ	11.8
	2	Chemically stabilized	CEMBAS	3.9
	3	Subgrade	LIMSUB	5.9
	4	Subgrade	A-7-6	Semi-infinite
043U0007500-NB-1	1	JPCP	PCCPAV	9.0
	2	Chemically stabilized	CEMBAS	4.0
	3	Subgrade	LIMSUB	6.0
	4	Subgrade	A-7-6	Semi-infinite
043U0007500-NB-2	1	JPCP	PCCPDJ	9.0
	2	Chemically stabilized	PCCDCB	4.0
	3	Subgrade	LIMSUB	6.0
	4	Subgrade	A-7-6	Semi-infinite
046K0000700-SB	1	JPCP	PCCPDJ	9.0
	2	Chemically stabilized	CEMBAS	4.0
	3	Subgrade	LIMSUB	6.0
	4	Subgrade	A-7-6	Semi-infinite
055U0004000-WB	1	JPCP	PCCPDJ	9.0
	2	Chemically stabilized	CEMBAS	3.9
	3	Subgrade	LIMSUB	5.9
	4	Subgrade	A-7-6	Semi-infinite

Table B.4: Summary of the Structural Information on New Rigid Pavements (continued)

Project name	Layer No.	Layer type	Material type	Thickness (in)
056I0003500-SB-1	1	JPCP	PCCPDJ	1Semi-infinite
	2	Chemically stabilized	PCCDCB	4.0
	3	Subgrade	LIMSUB	6.0
	4	Subgrade	A-7-6	Semi-infinite
056I0003500-SB-2	1	JPCP	PCCPDJ	12.0
	2	Chemically stabilized	DBWED	4.0
	3	Subgrade	LIMSUB	6.0
	4	Subgrade	A-7-6	Semi-infinite
056U0005000-EB-1	1	JPCP	PCCPDJ	1Semi-infinite
	2	Chemically stabilized	CEMBAS	4.0
	3	Subgrade	LIMSUB	6.0
	4	Subgrade	A-7-6	Semi-infinite
056U0005000-EB-2	1	JPCP	PCCPDJ	1Semi-infinite
	2	Chemically stabilized	CEMBAS	4.0
	3	Subgrade	LIMSUB	6.0
	4	Subgrade	A-7-6	Semi-infinite
059I0013500-NB	1	JPCP	PCCPDJ	11.0
	2	Chemically stabilized	CEMBAS	4.0
	3	Subgrade	LIMSUB	6.0
	4	Subgrade	A-7-6	Semi-infinite
061I0003500-NB	1	JPCP	PCCPDJ	12.5
	2	Chemically stabilized	CEMBAS	4.0
	3	Subgrade	LIMSUB	6.0
	4	Subgrade	A-7-6	Semi-infinite
063U0040000-EB	1	JPCP	PCCPDJ	9.0
	2	Chemically stabilized	PCCDCB	4.0
	3	Subgrade	LIMSUB	6.0
	4	Subgrade	A-7-6	Semi-infinite
067U0016900-NB	1	JPCP	PCCPDJ	9.4
	2	Chemically stabilized	CEMBAS	3.9
	3	Subgrade	LIMSUB	5.9
	4	Subgrade	A-7-6	Semi-infinite
079U0008100-NB	1	JPCP	PCCPDJ	9.5
	2	Chemically stabilized	CEMBAS	4.0
	3	Subgrade	LIMSUB	6.0
	4	Subgrade	A-7-6	Semi-infinite

Table B.4: Summary of the Structural Information on New Rigid Pavements (continued)

Project name	Layer No.	Layer type	Material typetype	Thickness (in)
085I0007000-EB	1	JPCP	PCCPDJ	13.4
	2	Chemically stabilized	CEMBAS	3.9
	3	Subgrade	LIMSUB	5.9
	4	Subgrade	A-7-6	Semi-infinite
085I0013500	1	JPCP	PCCPDJ	11.0
	2	Chemically stabilized	DBWED	4.0
	3	Subgrade	LIMSUB	6.0
	4	Subgrade	A-7-6	Semi-infinite
099I0007000-EB-1	1	JPCP	PCCPDJ	12.0
	2	Chemically stabilized	DBWED	4.0
	3	Subgrade	LIMSUB	6.0
	4	Subgrade	A-7-6	Semi-infinite
099I0007000-EB-2	1	JPCP	PCCPDJ	12.5
	2	Chemically stabilized	CEMBAS	4.0
	3	Subgrade	LIMSUB	6.0
	4	Subgrade	A-7-6	Semi-infinite
099I0007000-EB-3	1	JPCP	PCCPDJ	12.6
	2	Chemically stabilized	DBWED	4.0
	3	Subgrade	LIMSUB	6.0
	4	Subgrade	A-7-6	Semi-infinite
103U0007500-SB	1	JPCP	PCCPDJ	9.0
	2	Chemically stabilized	DBWED	4.0
	3	Subgrade	LIMSUB	6.0
	4	Subgrade	A-7-6	Semi-infinite
103U0040000-EB	1	JPCP	PCCPDJ	9.0
	2	Chemically stabilized	PCCDCB	4.0
	3	Subgrade	LIMSUB	6.0
	4	Subgrade	A-7-6	Semi-infinite

Table B.5: Site-Specific Material Properties (Air Voids and Binder Content) for New Flexible Pavements

Project name	Layer No.	Mix type	Binder grade	Binder content by weight (%)	Air voids as designed (%)	Air voids as placed (%)	Binder content by volume (%)	Input average binder content (%)
003U0007300-NB	1	SM-9.5A	-	-	-	7	11.5	11.5
	2	SM-19A	-	-	-	7	9.7	9.5
	3	SM-19A	-	-	-	7	9.3	
007U0007500-NB	1	SM-9.5A	PG 70-28	6.2	3.44	7	10.4	10.4
	2	SM-19A	PG 64-22	5.7	4.02	7	9.6	9.4
	3	SM-19A	PG 70-22	5.5	4.15	7	9.2	
008U0005400-EB	1	SM-9.5T	PG 64-28	6.0	4.36	7	11.1	11.1
	2	SM-19A	PG 64-28	5.6	3.46	7	10.0	9.7
	3	SM-19A	PG 64-22	5.4	3.06	7	9.4	
008U0007700-NB-1	1	SM-9.5T	PG 64-28	6.2	3.53	7	11.8	11.8
	2	SM-19A	PG 64-28	5.4	3.84	7	9.1	9.1
	3	SM-19A	PG 64-28	5.4	3.84	7	9.1	
008U0007700-NB 2	1	SM-9.5T	PG 64-28	6.2	3.53	7	11.8	11.8
	2	SM-19A	PG 64-28	5.5	3.84	7	9.5	9.6
	3	SM-19A	PG 64-22	5.3	4.94	7	9.8	
008U0007700-NB 3	1	SM-9.5A	PG 64-28	6.1	3.32	7	11.1	11.1
	2	SM-19A	PG 64-28	5.5	3.51	7	10.3	9.4
	3	SM-19A	PG 64-22	5.2	4.37	7	8.5	
011U0006900-NB	1	SM-9.5T	PG 64-28	6.5	4.27	7	11.4	11.4
	2	SM-19A	PG 64-28	5.8	3.74	7	10.7	10.8
	3	SM-19A	PG 64-22	5.8	3.74	7	10.8	
019K0000700-NB-1	1	SM-9.5A	PG 64-28	6.0	4.97	7	8.8	8.8
	2	SM-19A	PG 64-28	5.5	3.68	7	9.4	9.6
	3	SM-19A	PG 64-22	5.5	3.68	7	9.7	
019K0000700-NB 2	1	SM-9.5A	PG 64-28	6.5	4.36	7	11.7	11.7
	3	SM-19A	PG 64-28	6.3	3.78	7	11.5	10.7
	2	SM-19A	PG 64-28	5.8	4.43	7	9.9	
019K0016000-EB	1	SM-9.5T	PG 64-22	6.3	2.76	7	10.8	10.8
	2	SM-19A	-	-	-	7	9.7	9.5
	3	SM-19A	-	-	-	7	9.3	

Table B.5: Site-Specific Material Properties (Air Voids and Binder Content) for New Flexible Pavements (continued)

Project name	Layer No.	Mix type	Binder grade	Binder content by weight of mix (%)	Air voids as designed (%)	Air voids as placed (%)	Binder content by volume (%)	Input average binder content (%)
022K0000700-NB	1	SM-9.5A	PG 64 -28	6.4	3.38	7	11.3	11.3
	2	SM-19A	PG 64 -28	5.7	3.01	7	9.8	9.6
	3	SM-19A	PG 64 -22	5.7	3.57	7	9.5	
023U0004000-EB	1	SM-9.5T	PG 76-28	6.3	3.78	7	11.5	11.5
	2	SM-19A	PG 76-28	5.8	6.33	7	8.6	8.5
	3	SM-19A	PG 64 -22	5.8	6.33	7	8.5	
025k0009900-NB	1	SM-9.5A	PG 64 -28	6.8	3.01	7	13.6	13.6
	2	SM-19A	PG 64 -28	5.5	3.05	7	10.0	9.9
	3	SM-19A	PG 64 -28	5.5	2.89	7	9.8	
027K0015600-EB	1	SM-9.5A	PG 70-28	5.8	4.20	7	11.6	11.6
	2	SM-19A	PG 70-28	5.1	4.24	7	10.3	9.9
	3	SM-19A	PG 64-22	4.8	4.47	7	9.5	
028U0005000-EB	1	SM-9.5T	PG 70 28	5.8	5.12	7	11.3	11.3
	2	SM-19A	PG 64-22	4.7	3.82	7	9.5	9.5
	3	SM-19A	PG 64-22	4.7	3.85	7	9.4	
031K0001800-WB	1	SM-9.5T	PG 70-28	6.2	4.18	7	11.4	11.4
	2	SM-19A	PG 70-28	5.4	5.13	7	9.2	9.3
	3	SM-19A	PG 64-22	5.4	3.18	7	9.4	
033U0028300-NB	1	SM-9.5A	PG 64-28	5.8	3.40	7	11.2	11.2
	2	SM-19A	PG 64-22	4.8	3.41	7	9.6	9.5
	3	SM-19A	-	-	-	7	9.3	
052U0007300-NB	1	SM-9.5T	PG 76-22	6.6	2.80	7	11.3	11.3
	2	SM-19A	-	-	-	7	9.7	9.5
	3	SM-19A	-	-	-	7	9.4	
065U0005600-EB	1	SM-9.5T	PG 70-28	5.8	3.57	7	11.4	11.4
	2	SM-19A	PG 64-22	4.6	3.41	7	9.6	9.4
	3	SM-19A	PG 64-22	5.8	3.29	7	9.2	
065U0002700-NB	1	SM-9.5T	PG 64-28	6.3	2.80	7	11.9	11.9
	2	SM-19A	PG 64-28	5.1	3.70	7	8.9	9.0
	3	SM-19A	PG 64-28*	5.1	3.10	7	9.0	

Table B.5: Site-Specific Material Properties (Air Voids and Binder Content) for New Flexible Pavements (continued)

Project name	Layer No.	Mix type	Binder grade	Binder content by weight of mix (%)	Air voids as designed (%)	Air voids as placed (%)	Converted binder content by volume, (%)	Input average binder content (%)
069U0028300-NB	1	SM-9.5A	PG 64-28	5.9	4.02	7	11.4	11.4
	2	SM-19A	PG 64-28	4.8	2.83	7	9.1	8.7
	3	SM-19A	PG 64-28	5.0	3.66	7	8.2	
082U0018300-NB	1	SM-9.5A	PG 64-22	5.1	4.62	7	9.9	9.9
	2	SM-19A	-	-	-	7	9.7	9.5
	3	SM-19A	-	-	-	7	9.3	
088U0005400-WB	1	SM-9.5T	PG 70-28	5.5	4.42	7	10.7	10.7
	2	SM-19A	PG 70-28	4.7	4.52	7	8.7	8.7
	3	SM-19A	PG 64-22	4.7	3.91	7	8.6	
091U0002700-WB	1	SM-9.5T	PG 64-28	5.7	4.59	7	11.5	11.5
	2	SM-19A	PG 64-28	5.1	4.55	7	9.8	9.9
	3	SM-19A	PG 64-22	5.2	4.09	7	9.9	
095U0005600-EB	1	SM-9.5A	PG 70-28	6.2	6.17	7	12.4	12.4
	2	SM-19A	PG 64-22	5.2	4.00	7	10.4	9.9
	3	SM-19A	PG 70-28	4.7	4.14	7	9.3	
098U00028300-EB	1	SM-9.5A	PG 64-28	6.0	3.57	7	12.2	12.2
	2	SM-19A	PG 64-28	5.0	3.04	7	10.0	9.9
	3	SM-19A	PG 64-22	5.0	4.02	7	9.8	
103K0003900-NB	1	SM-9.5A	-	-	-	7	11.5	11.5
	2	SM-19A	-	-	-	7	9.7	9.5
	3	SM-19A	-	-	-	7	9.3	
Average	1	SM-9.5A	PG 64-22	-	-	7	11.4	11.4
	2	SM-19A	PG 64-22	-	-	7	9.7	9.5
	3	SM-19A	PG 64-22	-	-	7	9.4	

Table B.6: Site-Specific Joint Properties for New Rigid Pavements

Project name	Joint orientation	joint spacing, (ft)	Dowel diameter (in).	Dowel Spacing (in.)
018K0036000-EB	Perpendicular	15	1.000	12
018U0007700-NB	Perpendicular	15	1.125	12
019U0006900-NB	Perpendicular	15	1.125	12
029U0005600-EB	Perpendicular	15	1.125	12
030I0003500-NB-1	Perpendicular	15	1.375	12
030I0003500-NB-2	Perpendicular	15	1.500	12
030I0003500-NB-3	Perpendicular	15	1.500	12
031I0007000	Perpendicular	15	1.375	12
031I0007000-EB	Perpendicular	15	1.375	12
037U0040000-EB-1	Perpendicular	15	1.125	12
037U0040000-EB-2	Perpendicular	15	1.125	12
040I0013500-NB-1	Perpendicular	15	1.500	12
040I0013500-NB-2	Perpendicular	15	1.375	12
043U0007500-NB-1	Perpendicular	15	1.125	12
043U0007500-NB-2	Perpendicular	15	1.125	12
046K0000700-SB	Perpendicular	15	1.125	12
055U0004000-WB	Perpendicular	15	1.125	12
056I0003500-SB-1	Perpendicular	15	1.250	12
056I0003500-SB-2	Perpendicular	15	1.500	12
056U0005000-EB-1	Perpendicular	15	1.250	12
059I0013500-NB	Perpendicular	15	1.375	12
061I0003500-NB	Perpendicular	15	1.500	12
063U0040000-EB	Perpendicular	15	1.125	12
067U0016900-NB	Perpendicular	15	1.125	12
079U0008100-NB	Perpendicular	15	1.125	12
085I0007000-EB	Perpendicular	15	1.625	12
085I0013500	Perpendicular	15	1.375	12
099I0007000-EB-1	Perpendicular	15	1.500	12
099I0007000-EB-2	Perpendicular	30	1.5	12
099I0007000-EB-3	Perpendicular	15	1.575	12
103U0007500-SB	Perpendicular	15	1.125	12
103U0040000-EB	Perpendicular	15	1.125	12

Table B.7: Site-Specific Concrete Properties for New Rigid Pavements

Project name	Aggregate type	Cement content (lb/yd^3)	w/c	cement type	Unit weight (pcf)	Average 28-day strength(psi)
018K0036000-EB	Limestone	620	0.4	Type I/II	141.56	7080
018U0007700-NB	Limestone	564	0.44	Type I/II	140.44	7030
019U0006900-NB	Limestone	580	0.44	Type IP	139.58	5360
029U0005600-EB	Granite	620	0.45	Type I/II	139.47	4765
030I0003500-NB-1	Limestone	602	0.45	Type II	141.05	5360
030I0003500-NB-2	Limestone	565	0.45	Type II	139.42	5256
030I0003500-NB-3	Limestone	565	0.45	Type I/II	139.42	5342
031I0007000	Limestone	520	0.45	Type II	140.37	5358
031I0007000-EB	Limestone	620	0.43	Type I/II	139.44	5087
037U0040000-EB-1	Limestone	520	0.45	Type I/II	143.22	5520
037U0040000-EB-2	Limestone	520	0.45	Type I/II	143.22	5520
040I0013500-NB-1	Limestone	521	0.47	Type I/II	141.20	-
040I0013500-NB-2	Limestone	521	0.49	Type I/II	135.71	5180
043U0007500-NB-1	Limestone	-	-	Type I/II	-	4540
043U0007500-NB-2	Limestone	564	0.43	Type I/II	143.30	4540
046K0000700-SB	Limestone	620	0.49	Type II	138.93	4910
055U0004000-WB	Granite	521	0.43	Type I/II	142.89	5000
056I0003500-SB-1	Limestone	-	-	Type I/II	-	5210
056I0003500-SB-2	Limestone	539	0.44	Type II	141.40	4897
056U0005000-EB-1	Limestone	-	-	Type I/II	-	4580
059I0013500-NB	Granite	564	0.45	Type I/II	140.16	5463
061I0003500-NB	Limestone	539	0.44	Type I/II	138.43	5366
063U0040000-EB	Limestone	564	0.45	Type II	139.73	5570
067U0016900-NB	Limestone	521	0.45	Type I/II	140.63	4844
079U0008100-NB	Limestone	540	0.45	Type I/II	141.94	5223
085I0007000-EB	Limestone	548	0.45	Type I/II	139.92	6428
085I0013500	Limestone	565	0.45	Type I/II	141.62	5305
099I0007000-EB-1	Limestone	526	0.44	Type I/II	142.40	5040
099I0007000-EB-2	Limestone	526	0.44	Type I/II	142.40	5040
099I0007000-EB-3	Limestone	539	0.47	Type II	142.47	5595
103U0007500-SB	Limestone	564	0.45	Type I/II	141.63	4330
103U0040000-EB	Limestone	564	0.45	Type II	141.61	-

Table B.8: Site-Specific Climate Inputs for Flexible Pavement Projects

Project name	Climate Station	Latitude (deg)	Longitude (deg)	Elevation (ft)
003U0007300-NB	KANSAS CITY, MO	39.299	-94.718	976
007U0007500-NB	ST. JOSEPH, MO	39.774	-94.907	810
008U0005400-EB	WICHITA, KS	37.75	-97.219	1412
008U0007700-NB-1	WICHITA, KS	37.75	-97.219	1412
008U0007700-NB-2	WICHITA, KS	37.75	-97.219	1412
008U0007700-NB-3	WICHITA, KS	37.75	-97.219	1412
011U0006900-NB	JOPLIN, MO	37.149	-94.498	972
019K0000700-NB-1	JOPLIN, MO	37.149	-94.498	972
019K0000700-NB-2	JOPLIN, MO	37.149	-94.498	972
019U0016000-EB	JOPLIN, MO	37.149	-94.498	972
022K0000700-NB	ST. JOSEPH, MO	39.774	-94.907	810
023U0004000-EB	LAWRENCE, KS	39.008	-95.212	827
025K0009900-NB	CHANUTE, KS	37.67	-95.484	985
027K0015600-EB	RUSSELL, KS	38.872	-98.828	1864
028U0005000-EB	GARDEN CITY, KS	37.927	-100.725	2878
031K0001800-WB	MANHATTAN, KS	39.134	-96.679	1048
033U0028300-NB	HILL CITY, KS	39.376	-99.83	2194
052U0007300-NB	KANSAS CITY, MO	39.299	-94.718	976
065K0002700-NB	GUYMON, OK	36.682	-101.505	3112
065U0005600-EB	GUYMON, OK	36.682	-101.505	3112
069U0028300-NB	HILL CITY, KS	39.376	-99.83	2194
082U0018300-NB	HILL CITY, KS	39.376	-99.83	2194
084U0028100-NB	RUSSELL, KS	38.872	-98.828	1864
088U0005400-WB	GUYMON, OK	36.682	-101.505	3112
091K0002700-NB	GOODLAND, KS	39.368	-101.693	3647
095U0005600-EB	GUYMON, OK	36.682	-101.505	3112
098U0028300-NB	HILL CITY, KS	39.376	-99.83	2194
103K0003900-NB	CHANUTE, KS	37.67	-95.484	985

Table B.9: Site-Specific Climate Inputs for Rigid Pavement Projects

Project name	Climate station	Latitude (deg)	Longitude (deg)	Elevation (ft)
018K0036000-EB	WINFIELD/ARKANSAS CITY, KS	37.168	-97.037	1156
018U0007700-NB	WINFIELD/ARKANSAS CITY, KS	37.168	-97.037	1156
019U0006900-NB	JOPLIN, MO	37.149	-94.498	972
029U0005600-EB	DODGE CITY, KS	37.773	-99.97	2576
030I0003500-NB-1	TOPEKA, KS	38.95	-95.664	1033
030I0003500-NB-2	OLATHE, KS	38.831	-94.89	1066
030I0003500-NB-3	OLATHE, KS	38.831	-94.89	1066
031I0007000	TOPEKA, KS	38.95	-95.664	1033
031I0007000-EB	MANHATTAN, KS	39.134	-96.679	1048
037U0040000-EB-1	PARSONS, KS	37.328	-95.504	869
037U0040000-EB-2	PARSONS, KS	37.328	-95.504	869
040I0013500-NB-1	WICHITA, KS	37.647	-97.429	1320
040I0013500-NB-2	WICHITA, KS	37.647	-97.429	1320
043U0007500-NB-1	TOPEKA, KS	38.95	-95.664	1033
043U0007500-NB-2	TOPEKA, KS	38.95	-95.664	1033
046K0000700-SB	OLATHE, KS	38.831	-94.89	1066
055U0004000-WB	GOODLAND, KS	39.368	-101.693	3647
056I0003500-SB-1	EMPORIA, KS	38.331	-96.19	1205
056I0003500-SB-2	EMPORIA, KS	38.331	-96.19	1205
056U0005000-EB-1	EMPORIA, KS	38.331	-96.19	1205
059I0013500-NB	MANHATTAN, KS	39.134	-96.679	1048
061I0003500-NB	OLATHE, KS	38.831	-94.89	1066
063U0040000-EB	PARSONS, KS	37.328	-95.504	869
067U0016900-NB	CHANUTE, KS	37.67	-95.484	985
079U0008100-NB	CONCORDIA, KS	39.549	-97.652	1469
085I0007000-EB	SALINA, KS	38.813	-97.661	1269
085I0013500	SALINA, KS	38.813	-97.661	1269
099I0007000-EB-1	MANHATTAN, KS	39.134	-96.679	1048
099I0007000-EB-2	MANHATTAN, KS	39.134	-96.679	1048
099I0007000-EB-3	TOPEKA, KS	38.95	-95.664	1033
103U0007500-SB	PARSONS, KS	37.328	-95.504	869
103U0040000-EB	CHANUTE, KS	37.67	-95.484	985

Appendix C: Measured And Predicted Performance Data For New Flexible Pavements (Nationally Calibrated)

This page intentionally left blank.

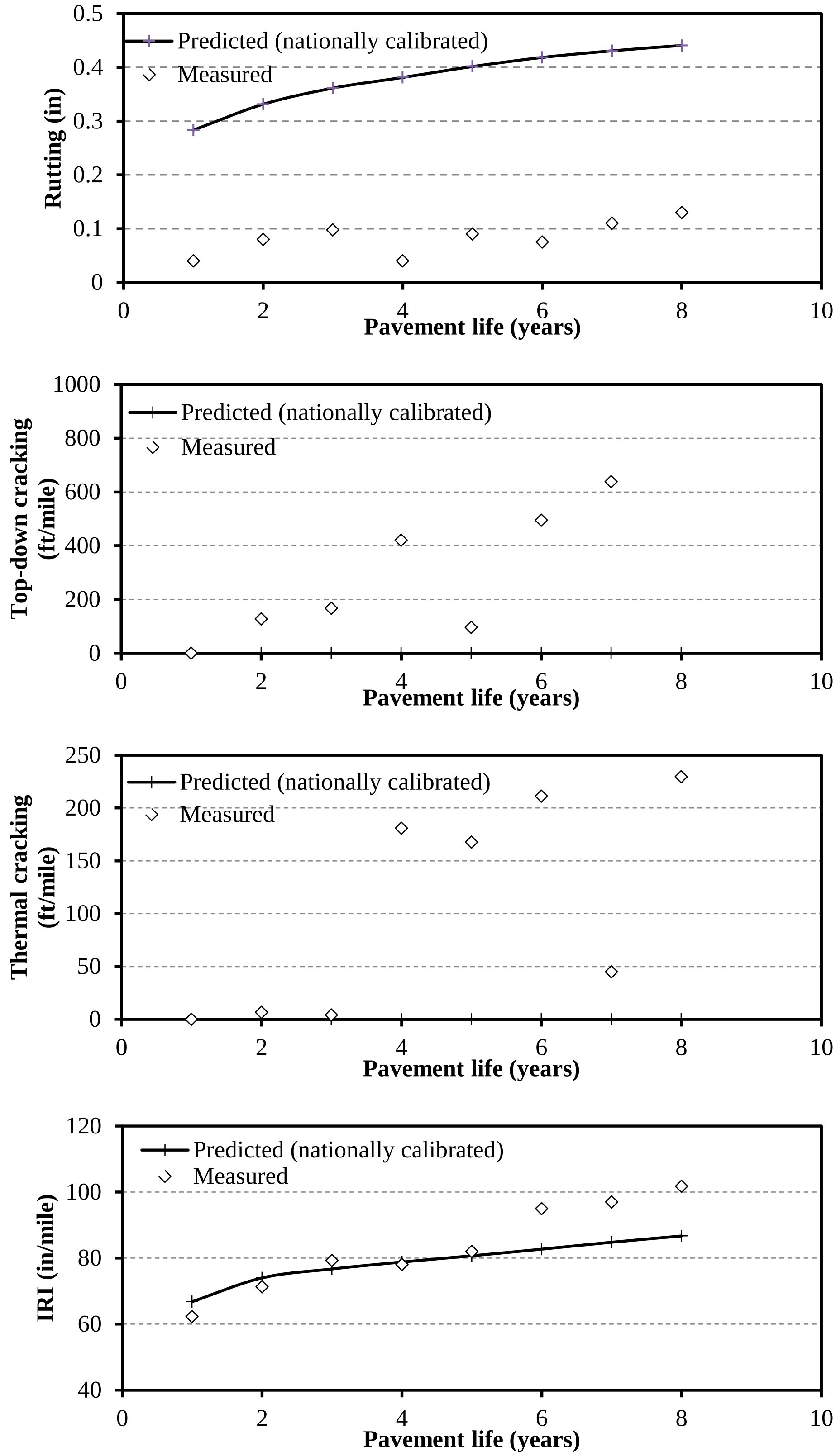

Figure C.1: Measured and Predicted Performance Data by the Nationally Calibrated MEPDG for Project 003U0007300-NB

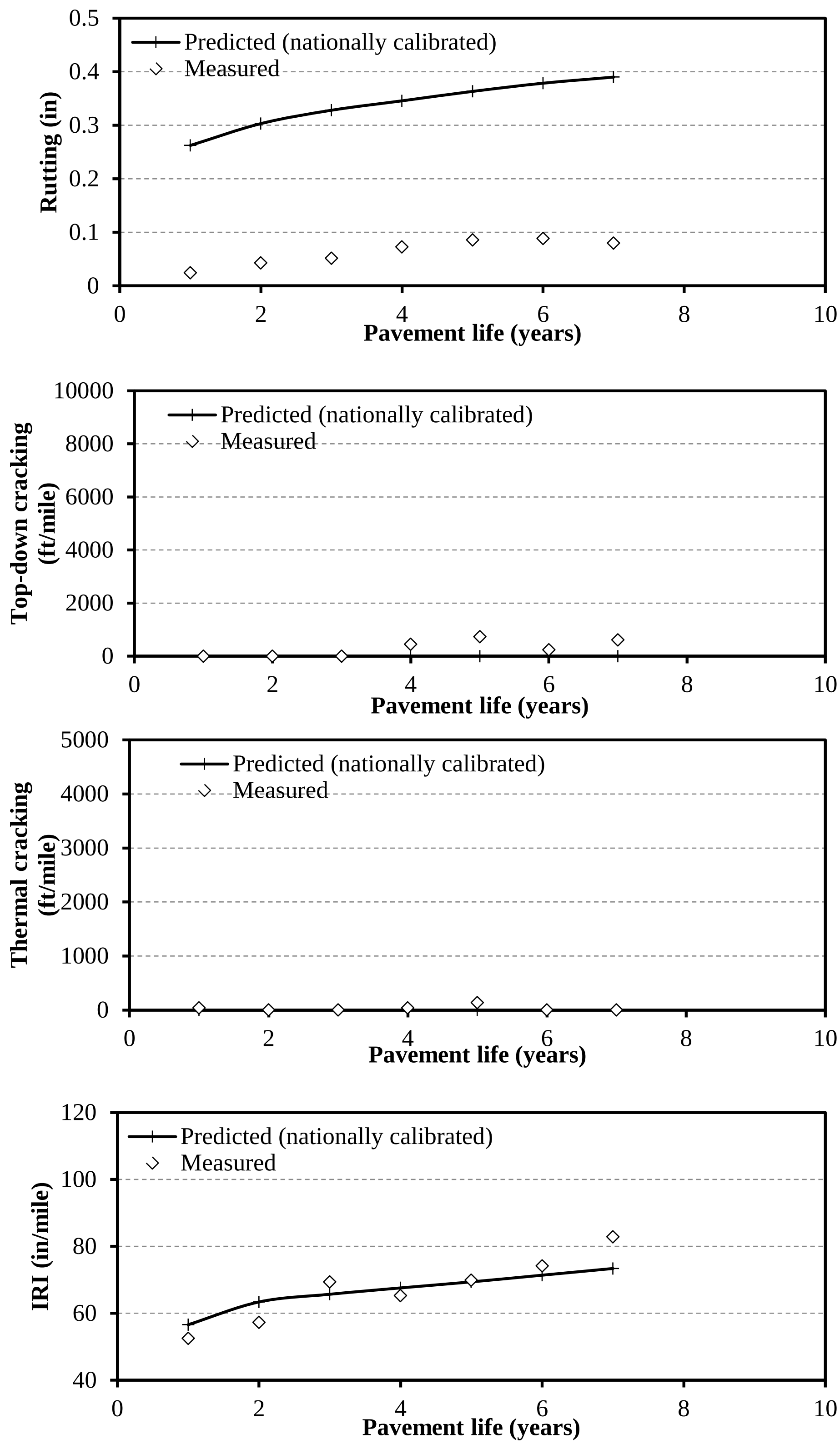

Figure C.2: Measured and Predicted Performance Data by the Nationally Calibrated MEPDG for Project 007U0007500-NB

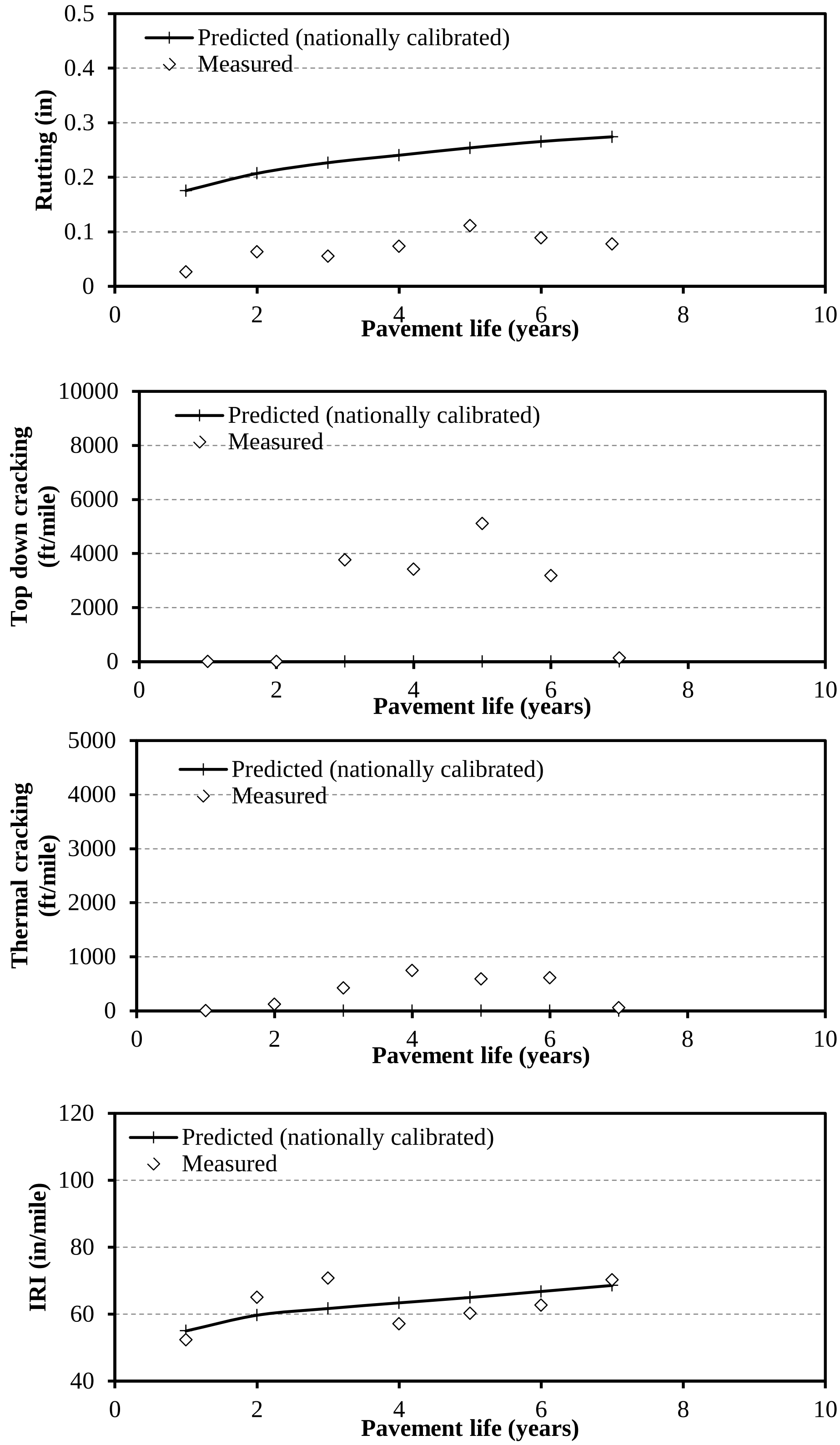

Figure C.3: Measured and Predicted Performance Data by the Nationally Calibrated MEPDG for Project 008U0005400-EB

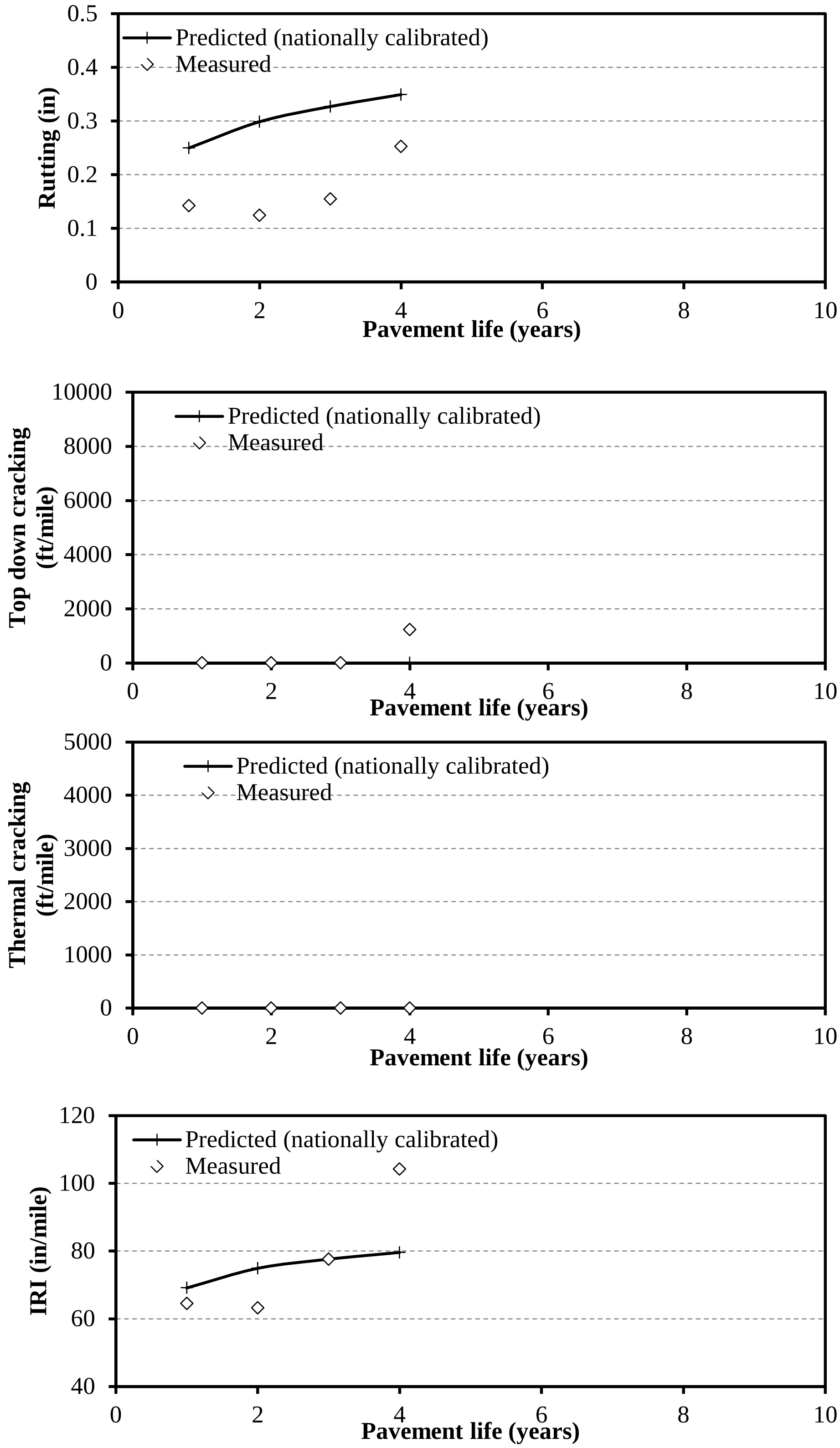

Figure C.4: Measured and Predicted Performance Data by the Nationally Calibrated MEPDG for Project 008U0007700-NB-1 under National Calibration

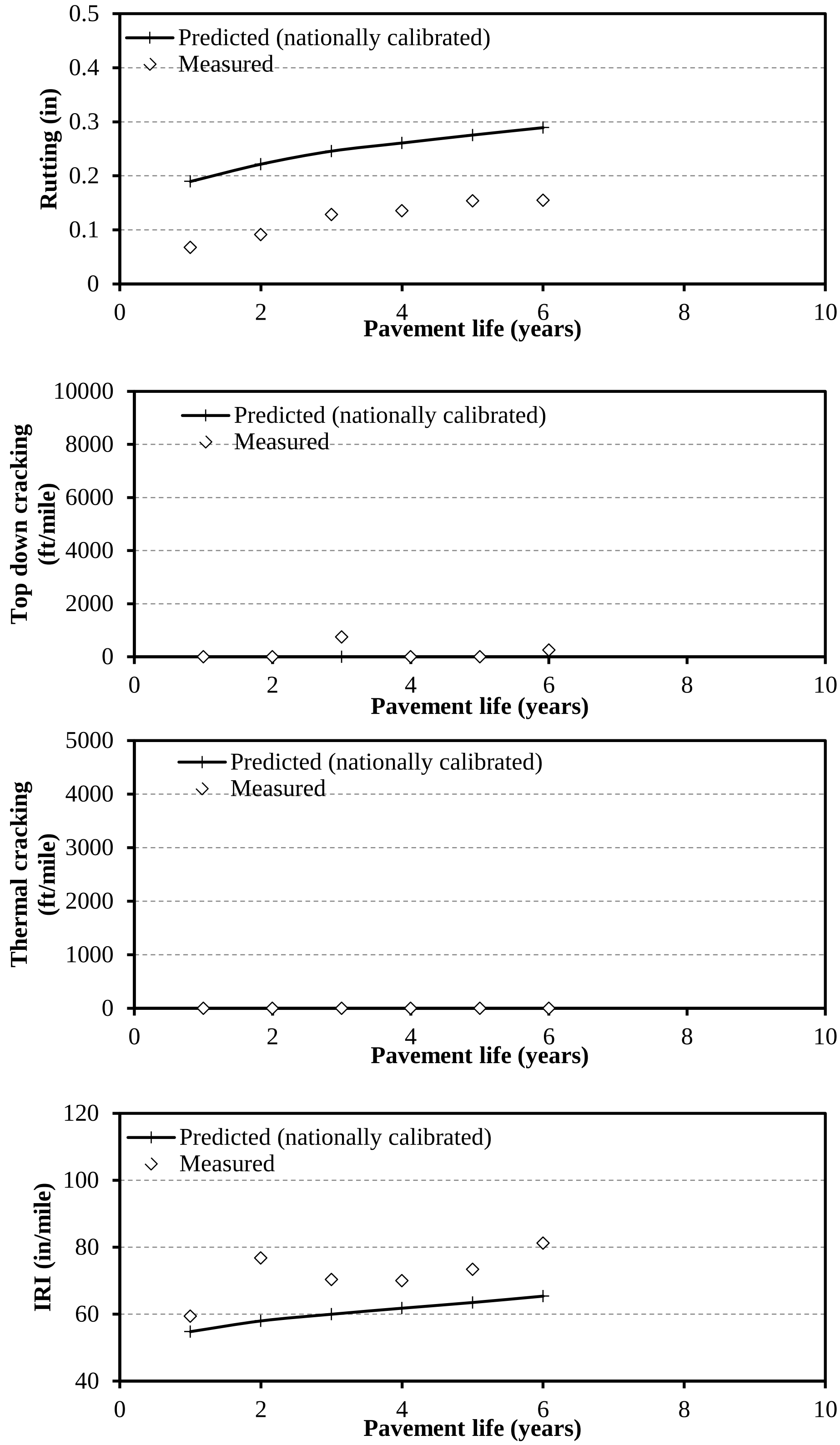

Figure C.5: Measured and Predicted Performance Data by the Nationally Calibrated MEPDG for Project 008U0007700-NB-2

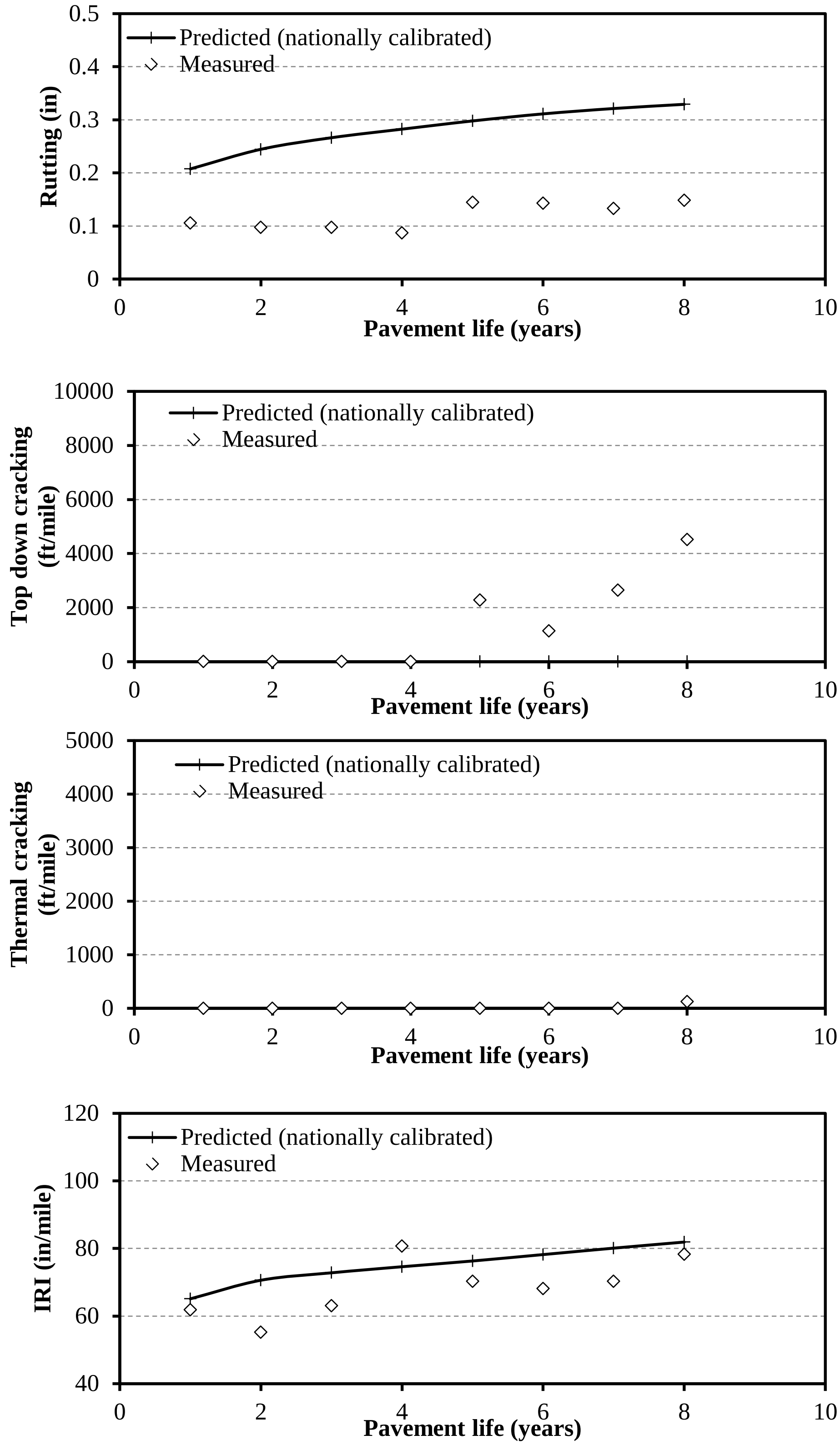

Figure C.6: Measured and Predicted Performance Data by the Nationally Calibrated MEPDG for Project 008U0007700-NB-3

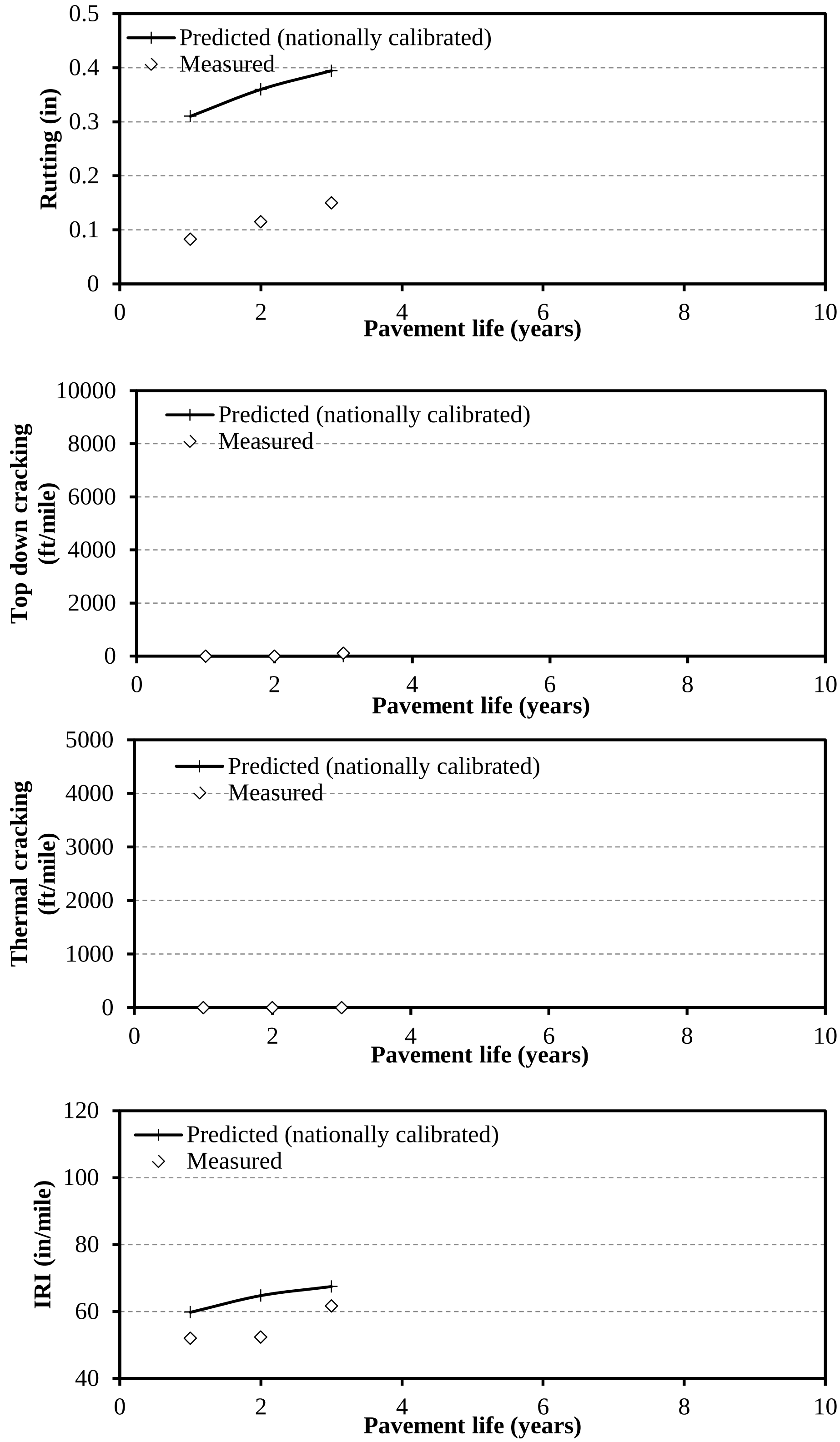

Figure C.7: Measured and Predicted Performance Data by the Nationally Calibrated MEPDG for Project 011U0006900-NB

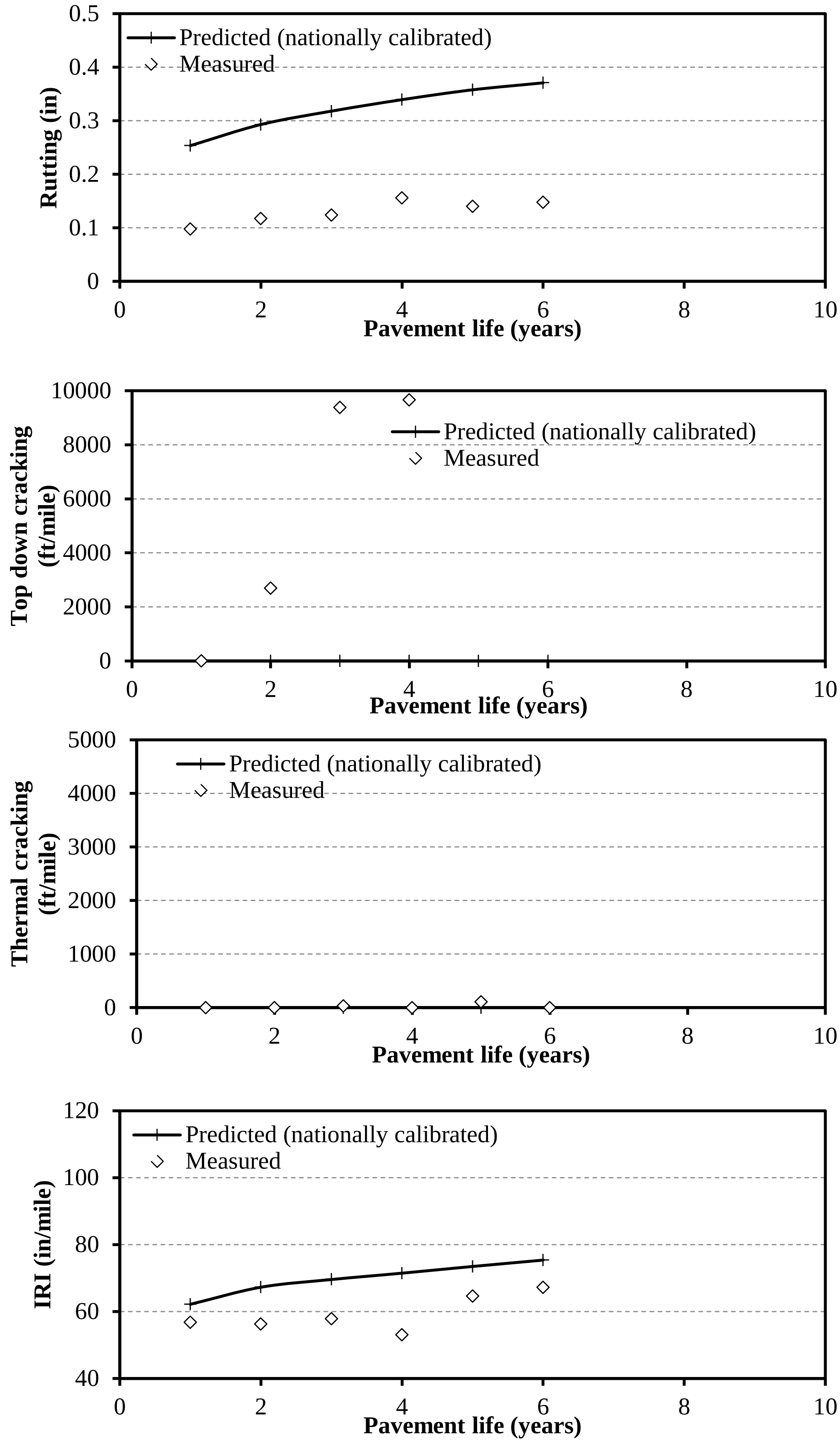

Figure C.8: Measured and Predicted Performance Data by the Nationally Calibrated MEPDG for Project 019K0000700-NB-1

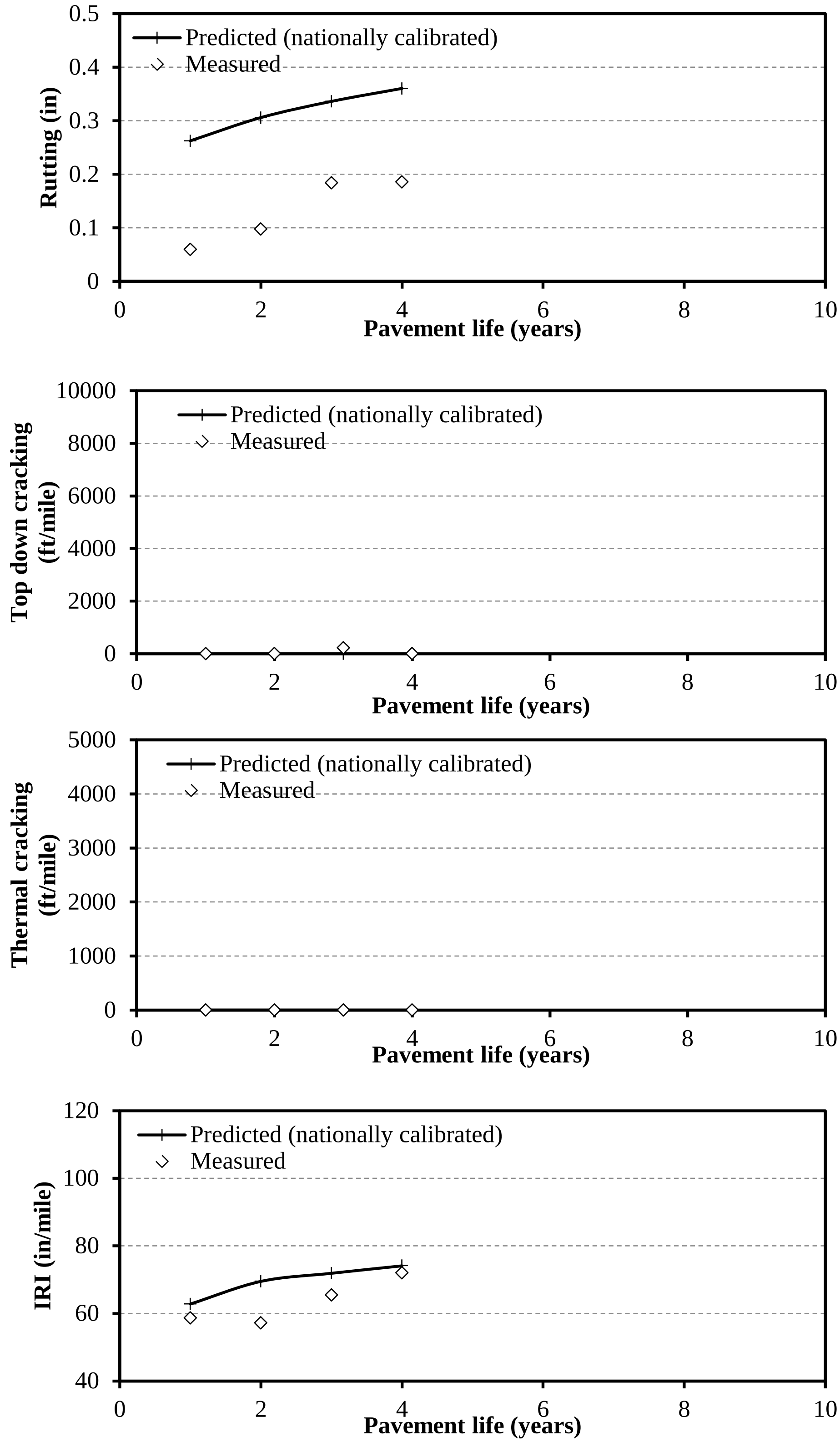

Figure C.9: Measured and Predicted Performance Data by the Nationally Calibrated MEPDG for Project 019K0000700-NB-2

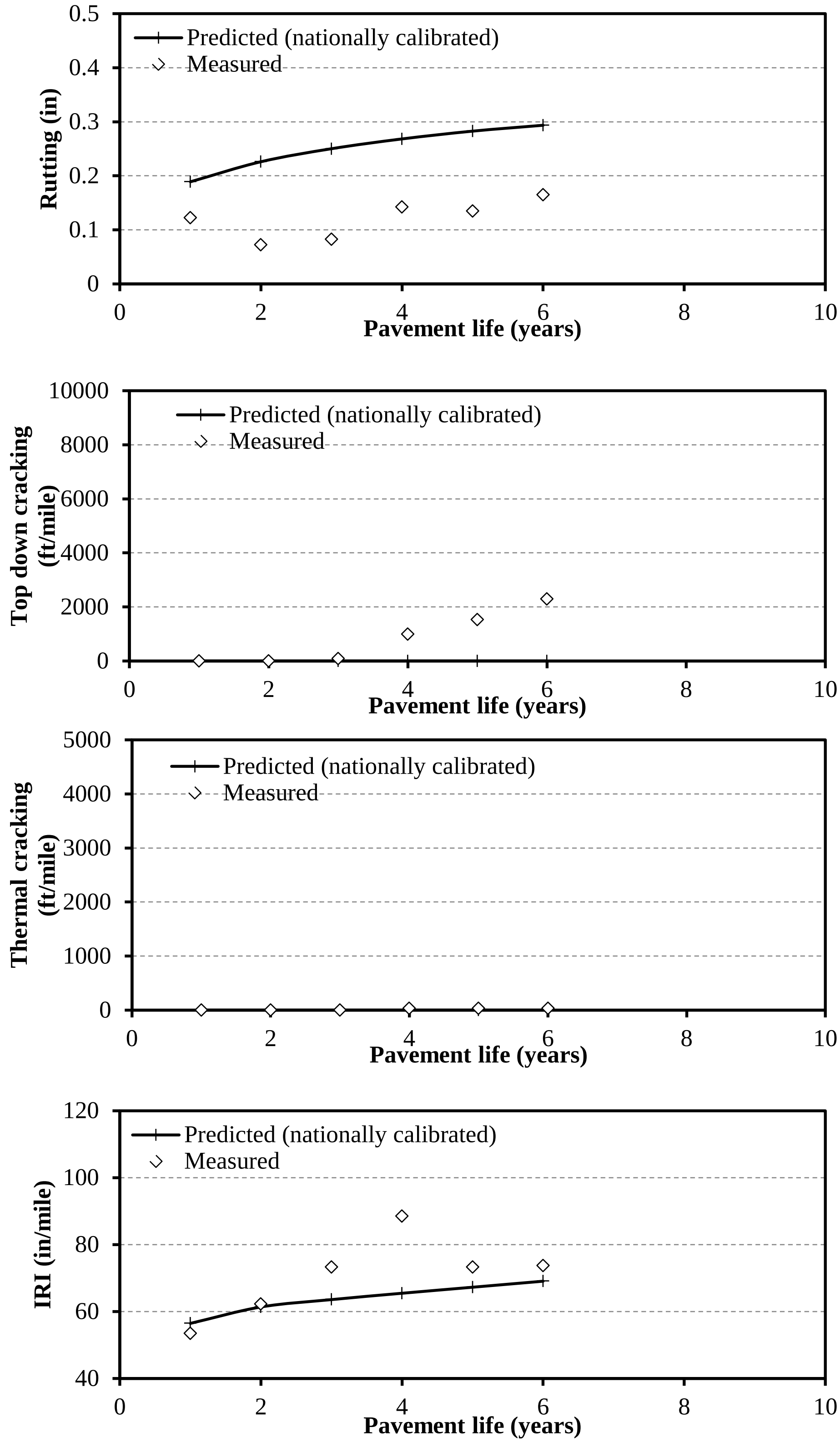

Figure C.10: Measured and Predicted Performance Data by the Nationally Calibrated MEPDG for Project 019U0016000-EB

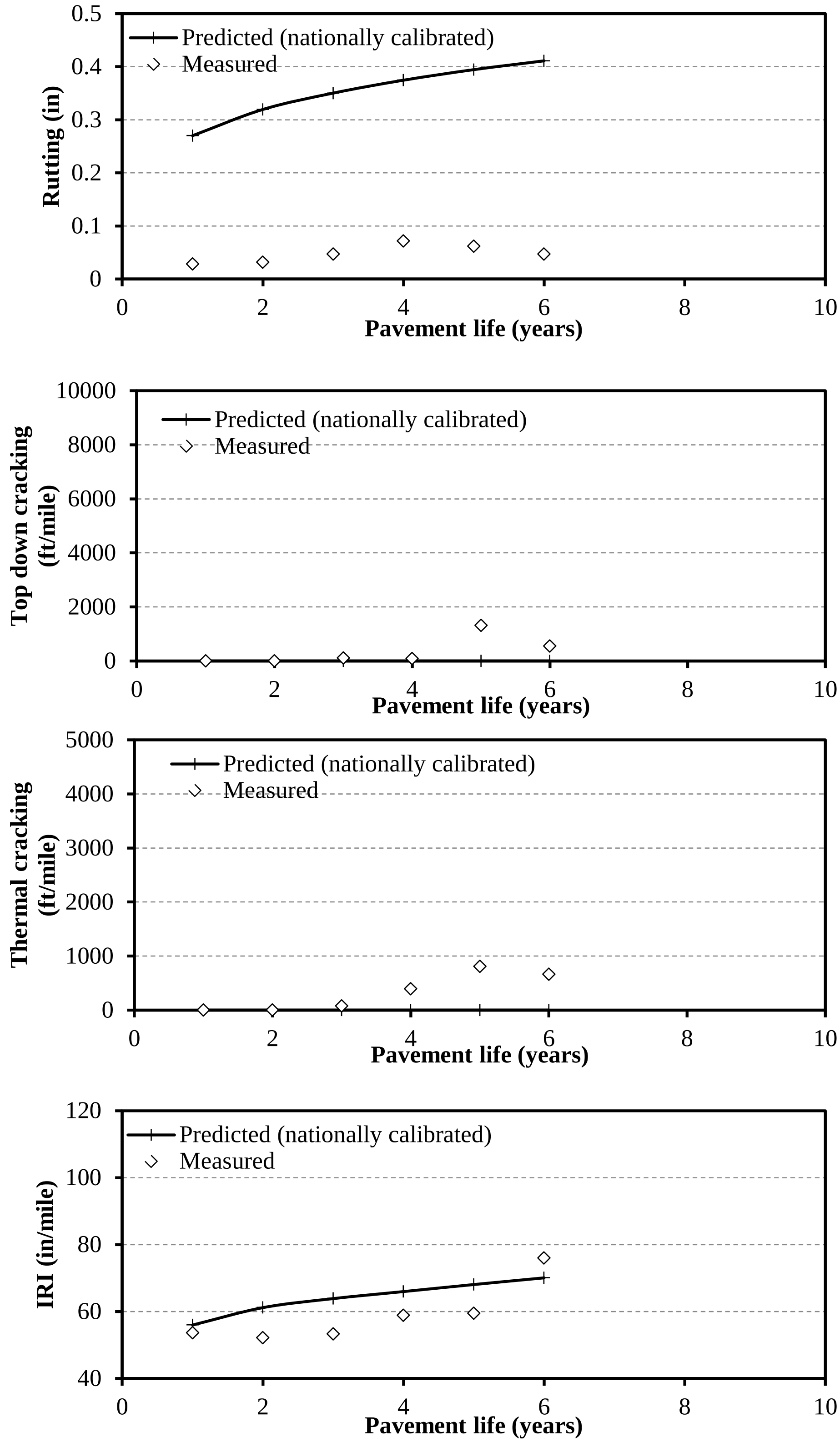

Figure C.11: Measured and Predicted Performance Data by the Nationally Calibrated MEPDG for Project 022K0000700-NB

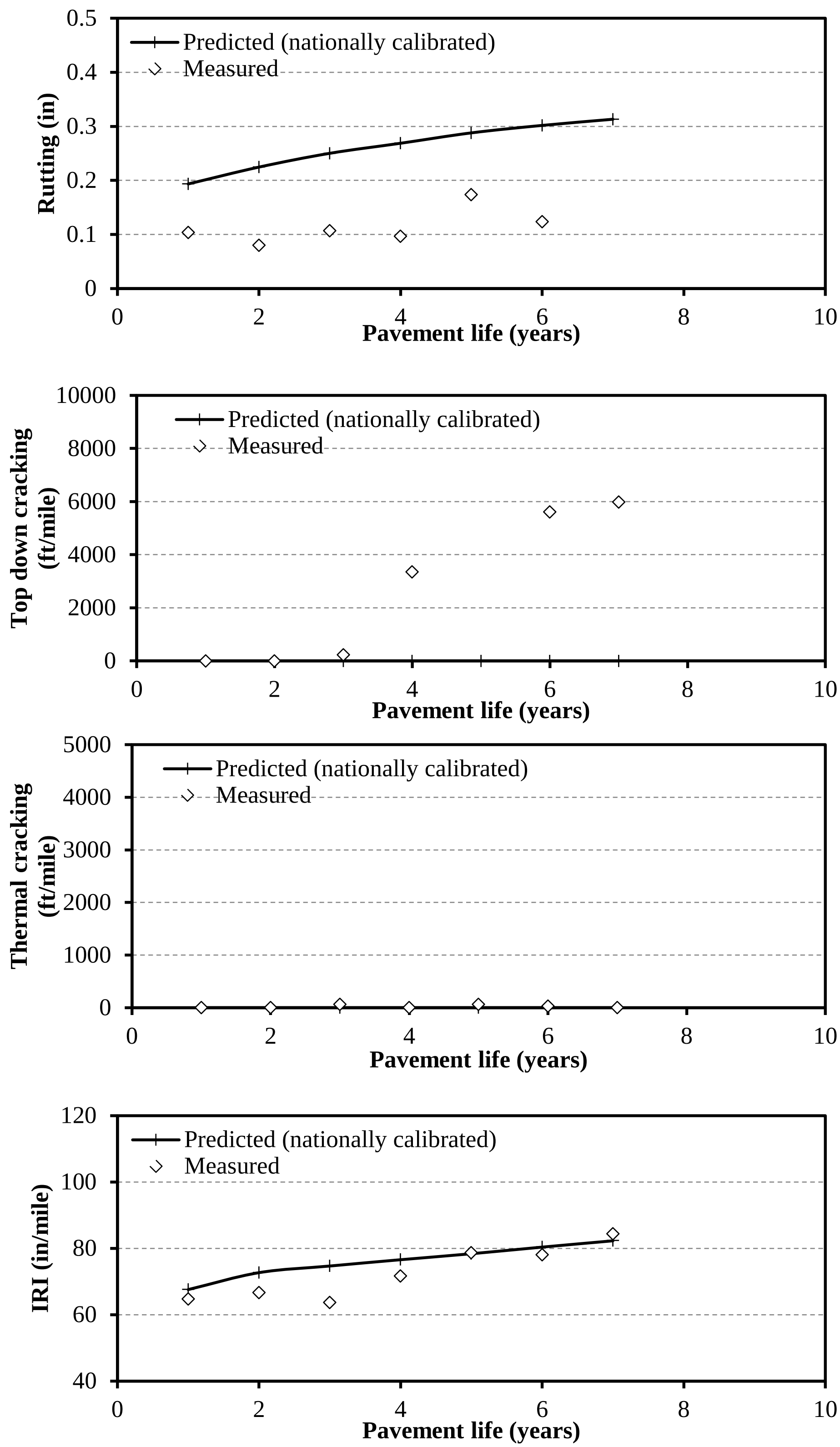

Figure C.12: Measured and Predicted Performance Data by the Nationally Calibrated MEPDG for Project 023U0004000-EB

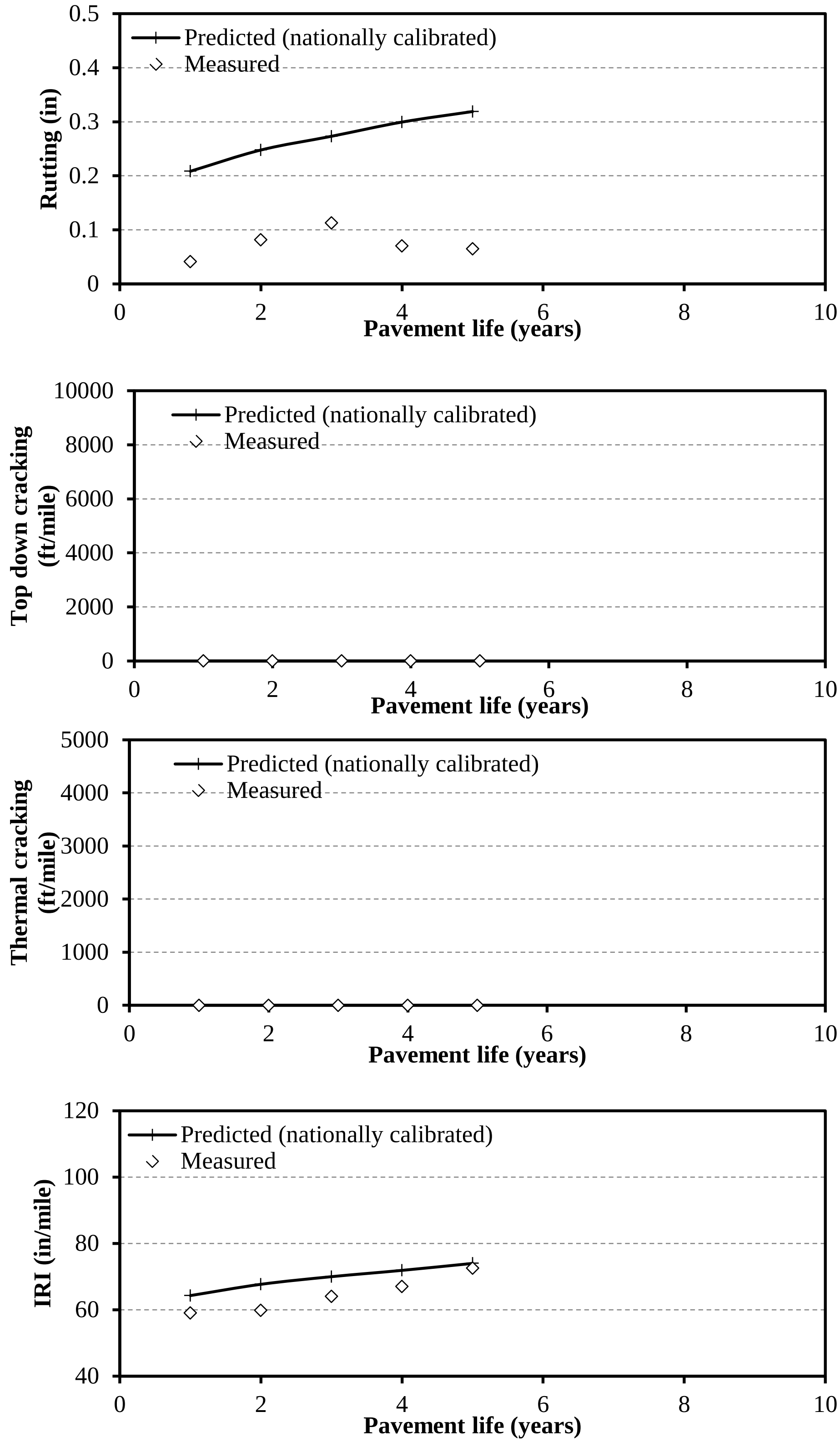

Figure C.13: Measured and Predicted Performance Data by the Nationally Calibrated MEPDG for Project 025K0009900-NB

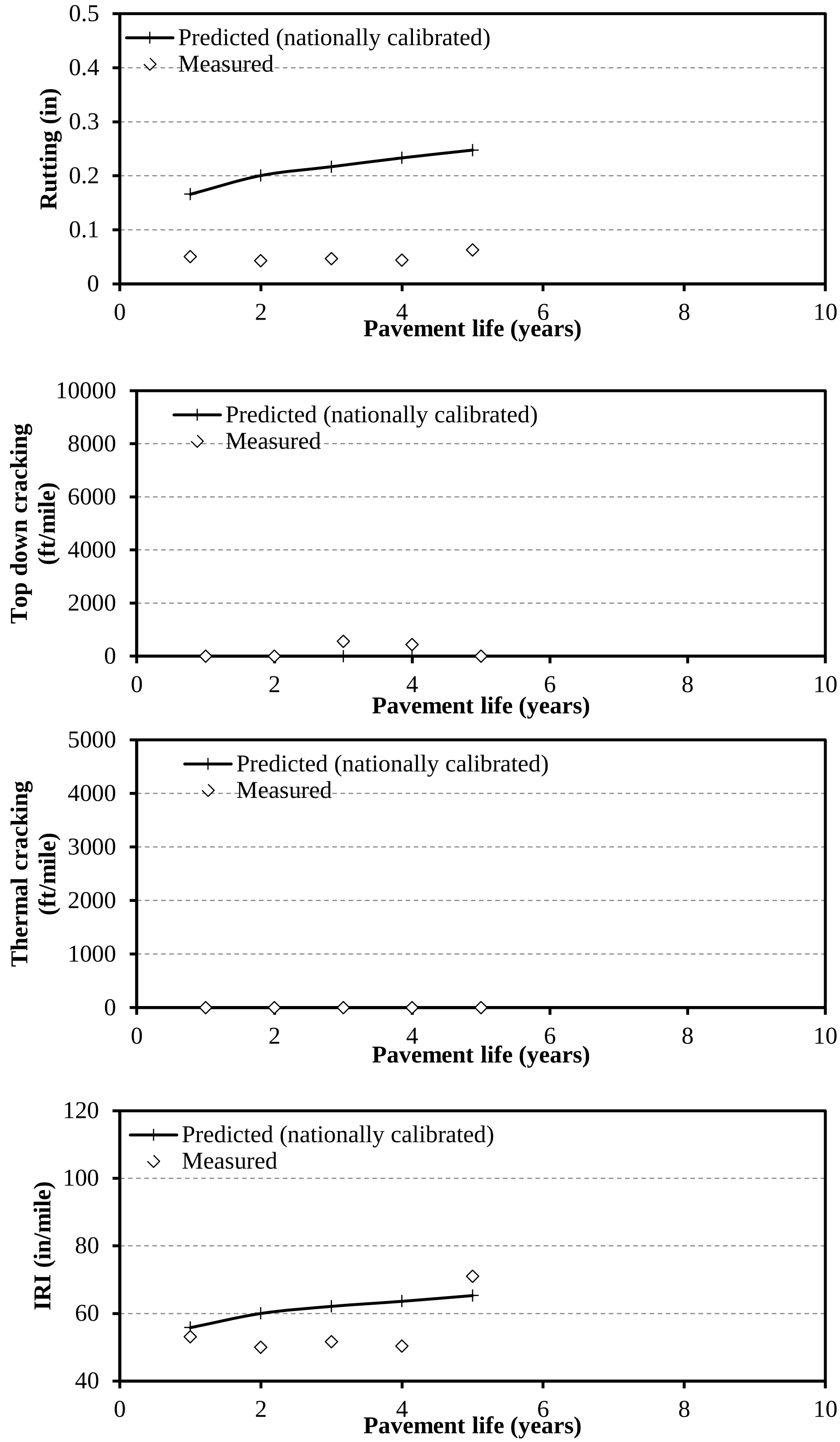

Figure C.14: Measured and Predicted Performance Data by the Nationally Calibrated MEPDG for Project 027K0015600-EB

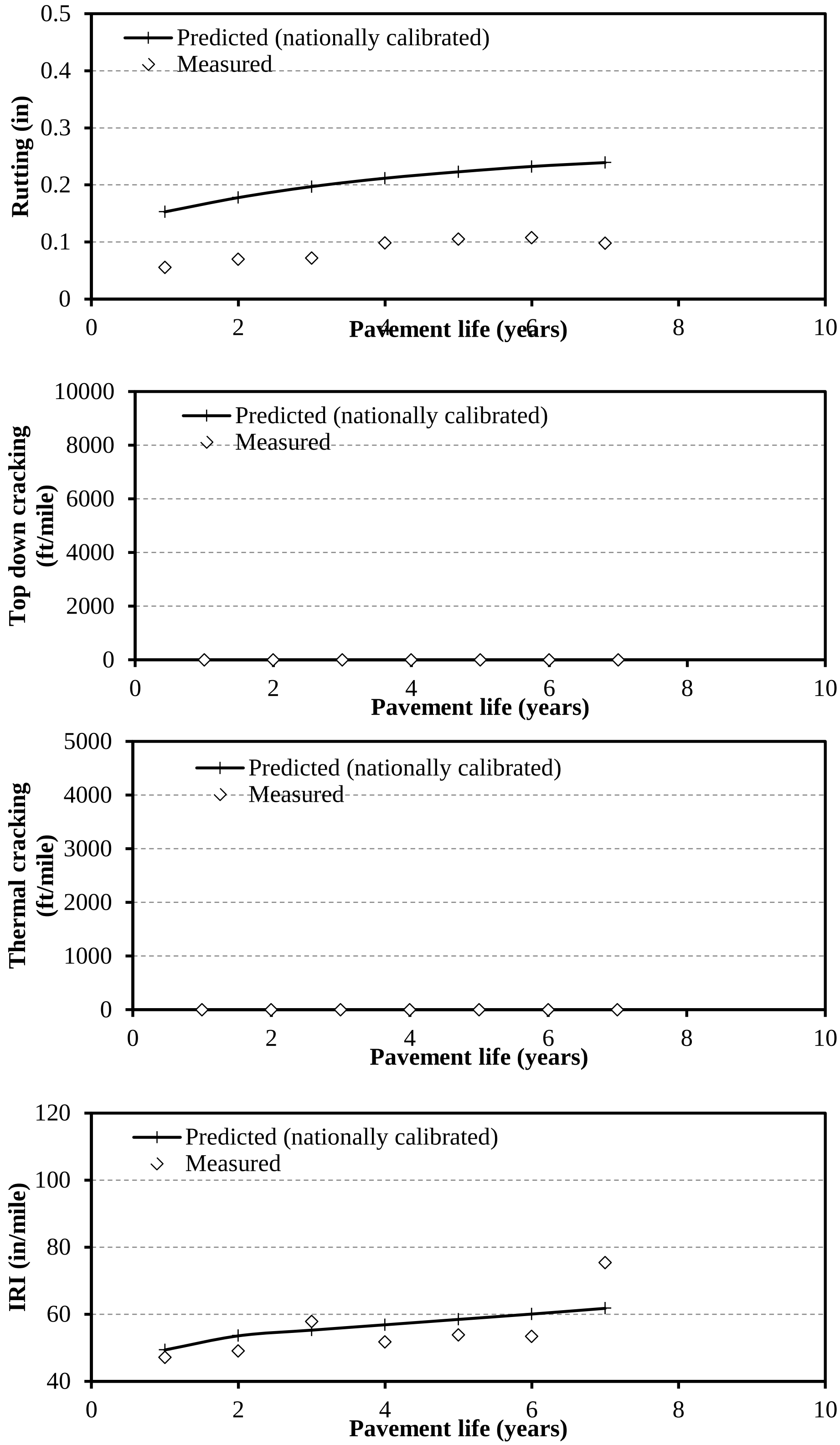

Figure C.15: Measured and Predicted Performance Data by the Nationally Calibrated MEPDG for Project 028U0005000-EB

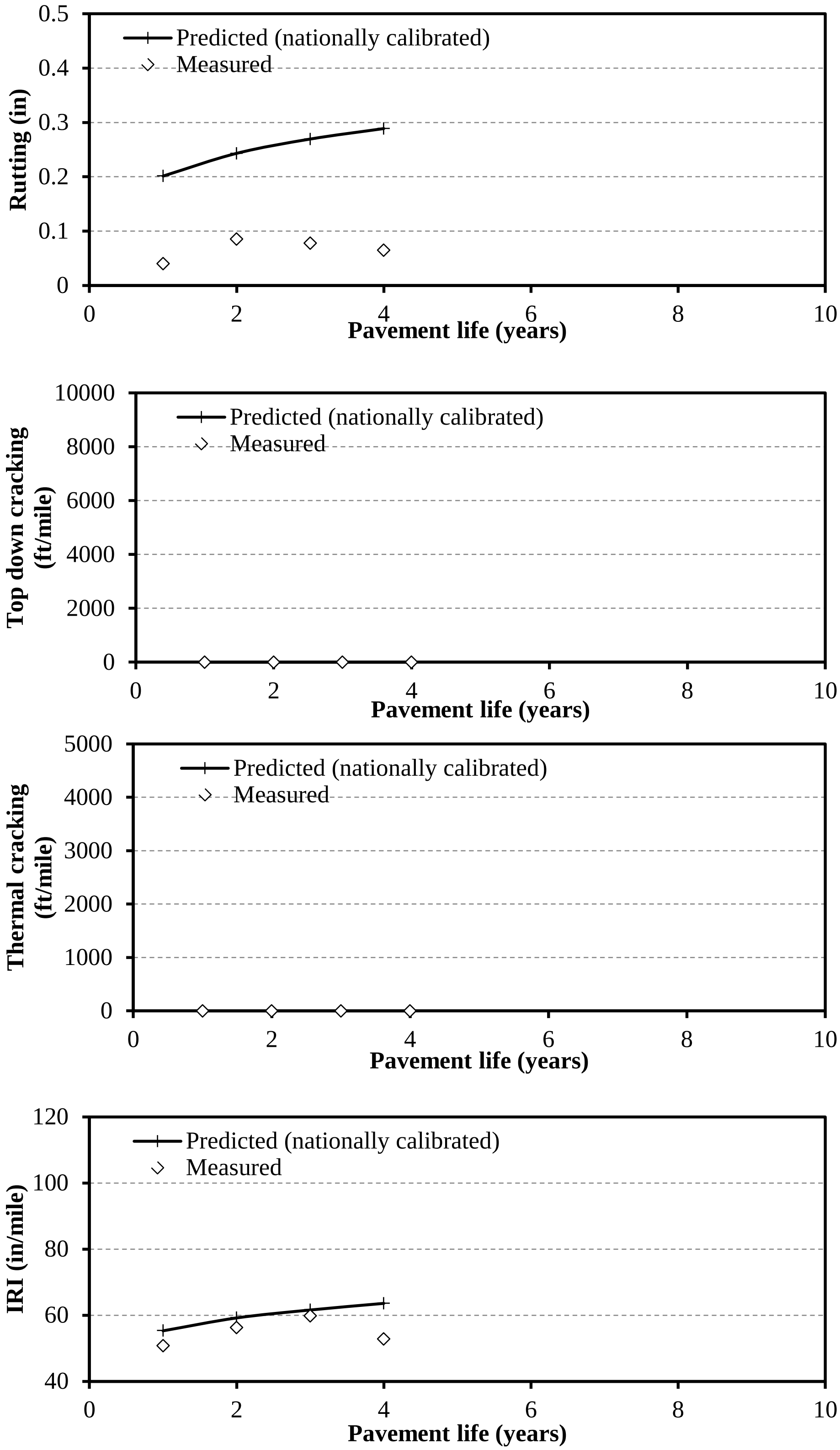

Figure C.16: Measured and Predicted Performance Data by the Nationally Calibrated MEPDG for Project 031K0001800-WB

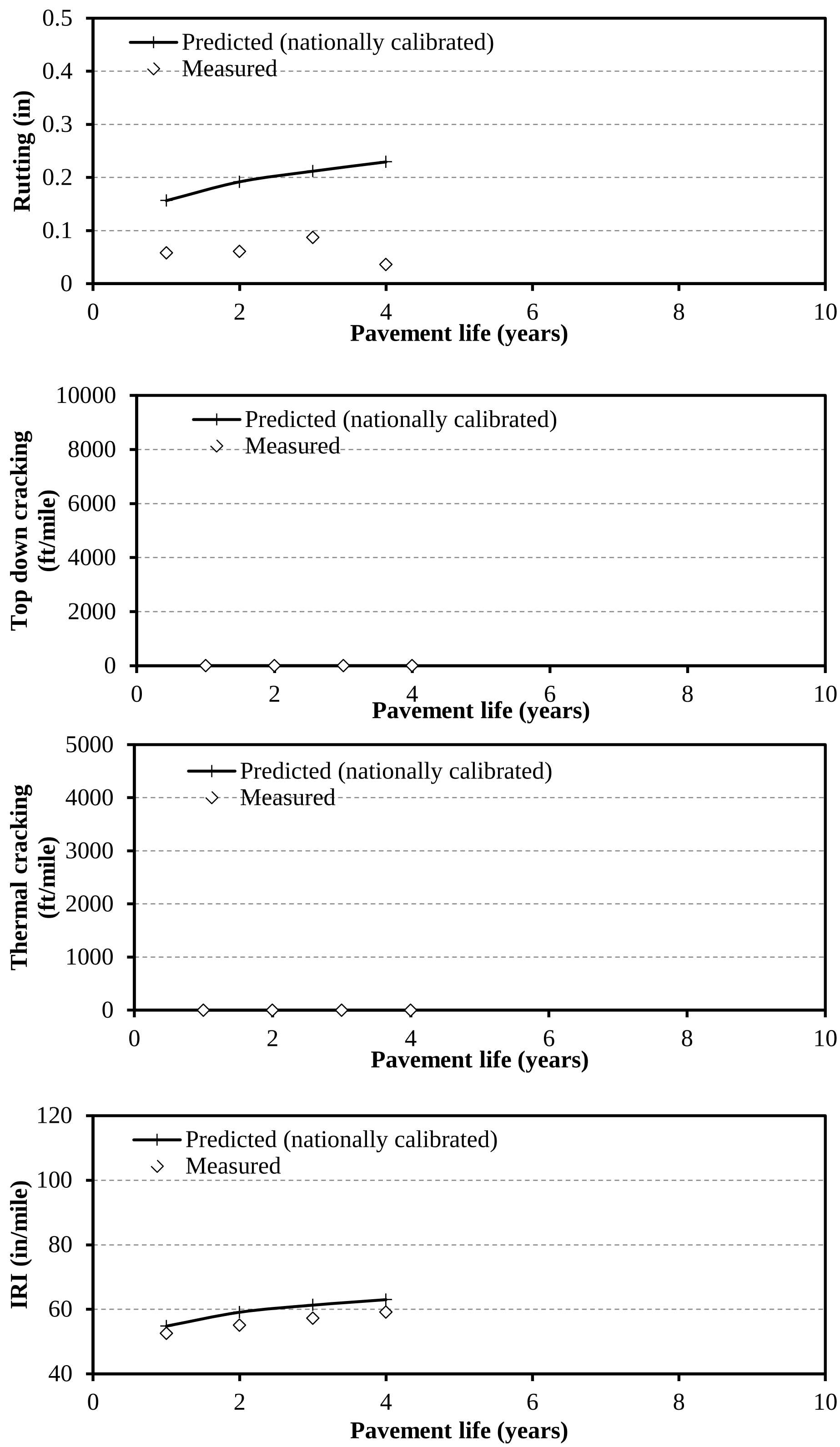

Figure C.17: Measured and Predicted Performance Data by the Nationally Calibrated MEPDG for Project 033U0028300-NB

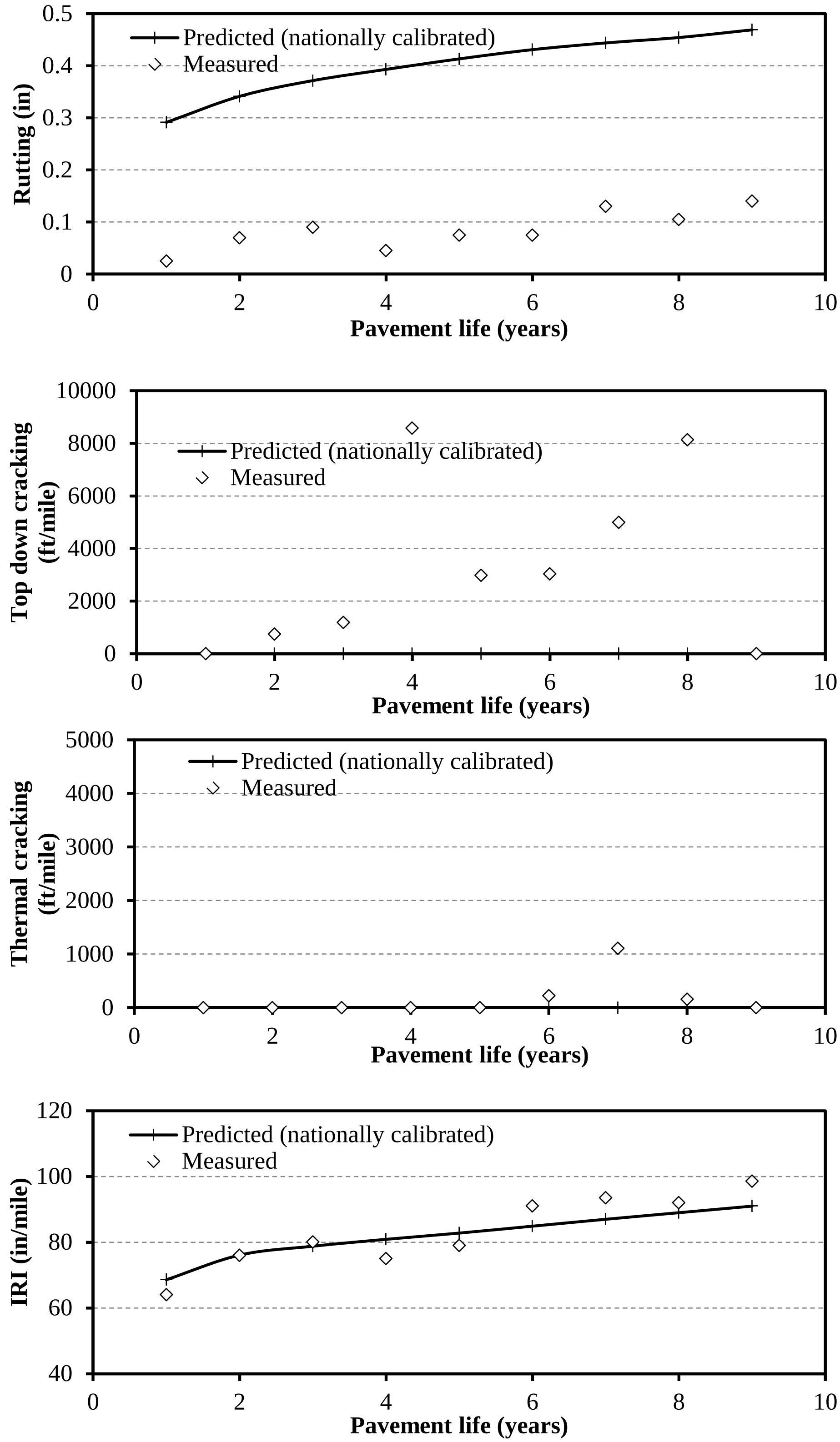

Figure C.18: Measured and Predicted Performance Data by the Nationally Calibrated MEPDG for Project 052U0007300-NB

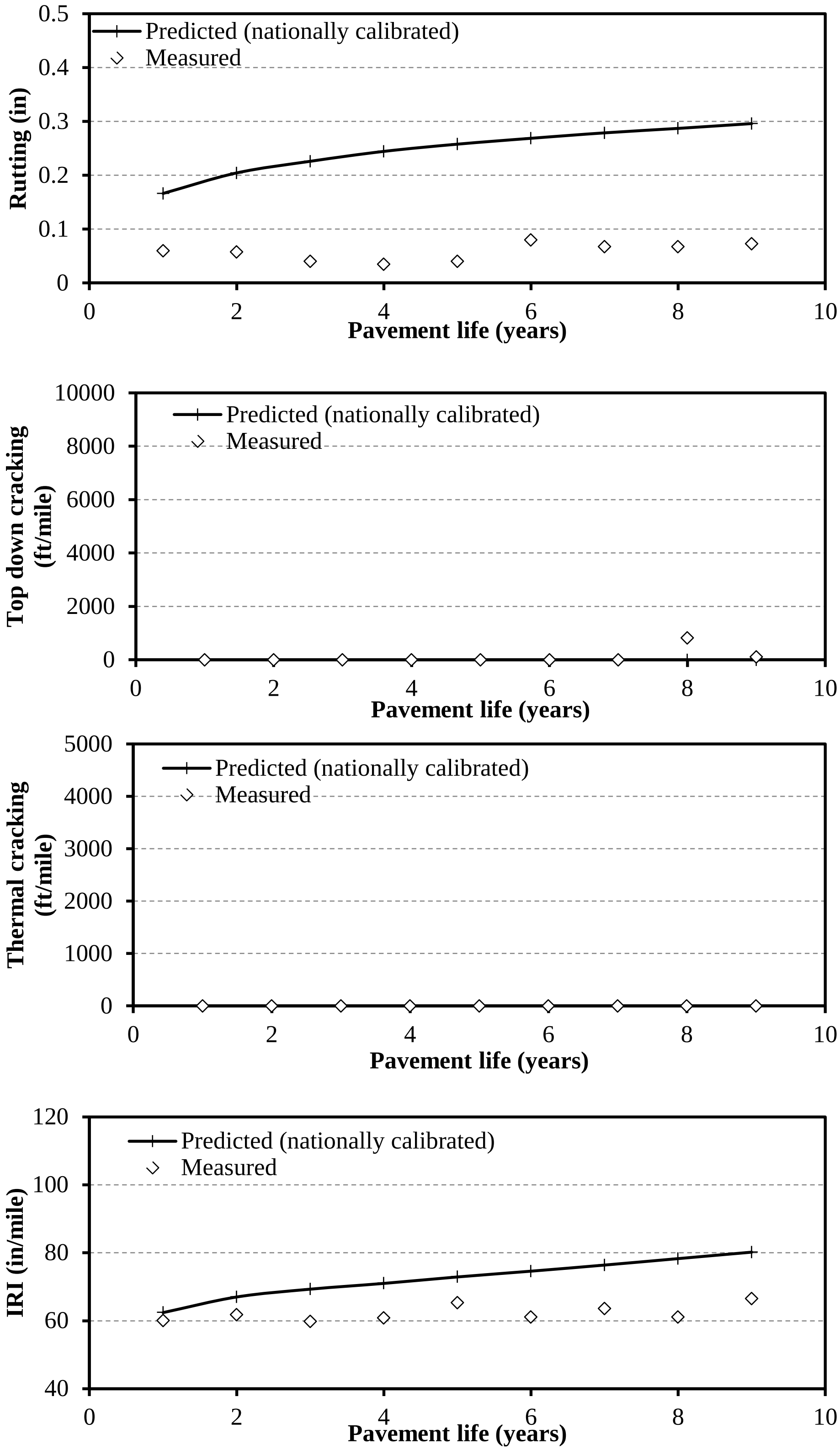

Figure C.19: Measured and Predicted Performance Data by the Nationally Calibrated MEPDG for Project 065K0002700-NB

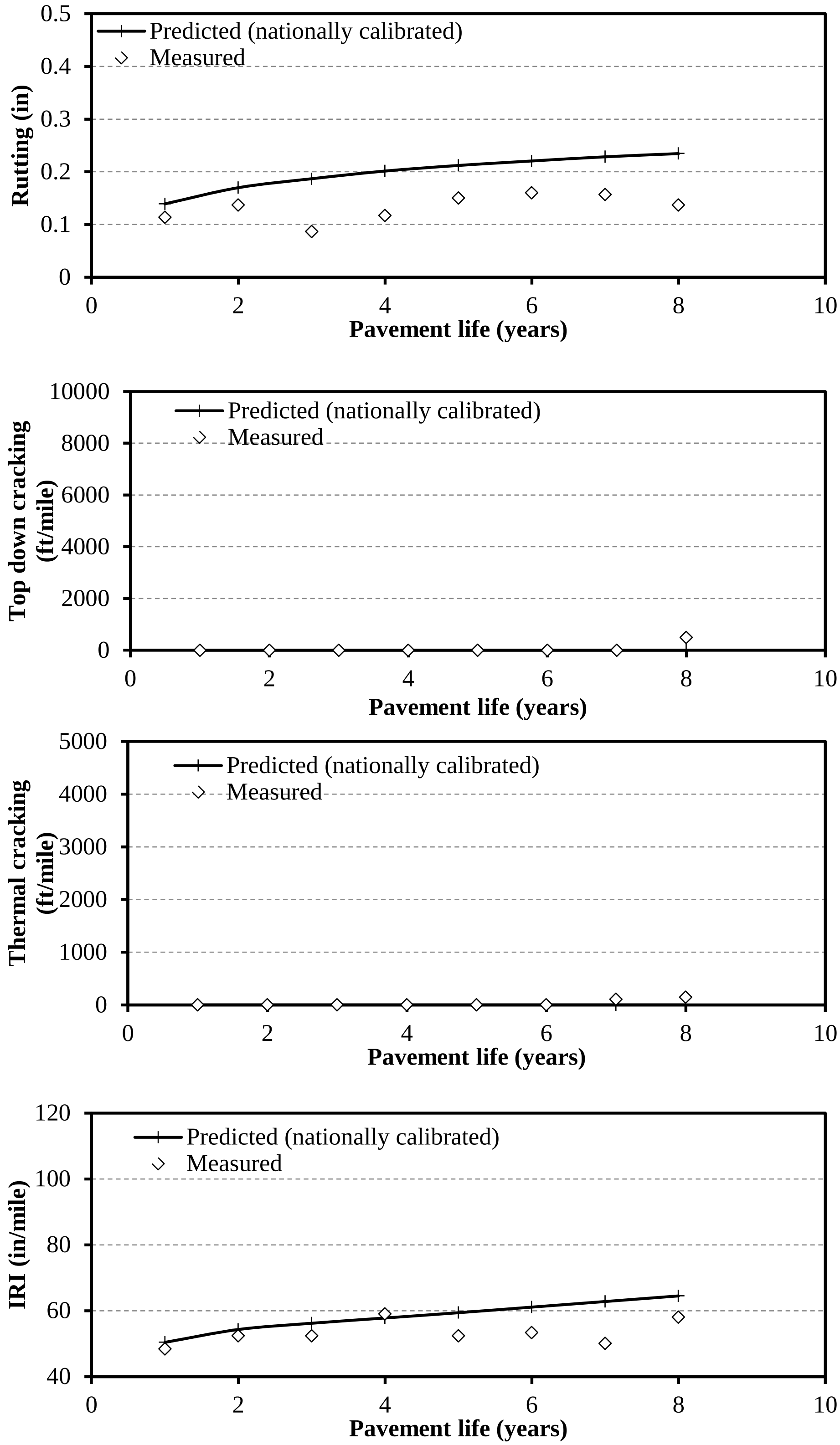

Figure C.20: Measured and Predicted Performance Data by the Nationally Calibrated MEPDG for Project 065U0005600-EB

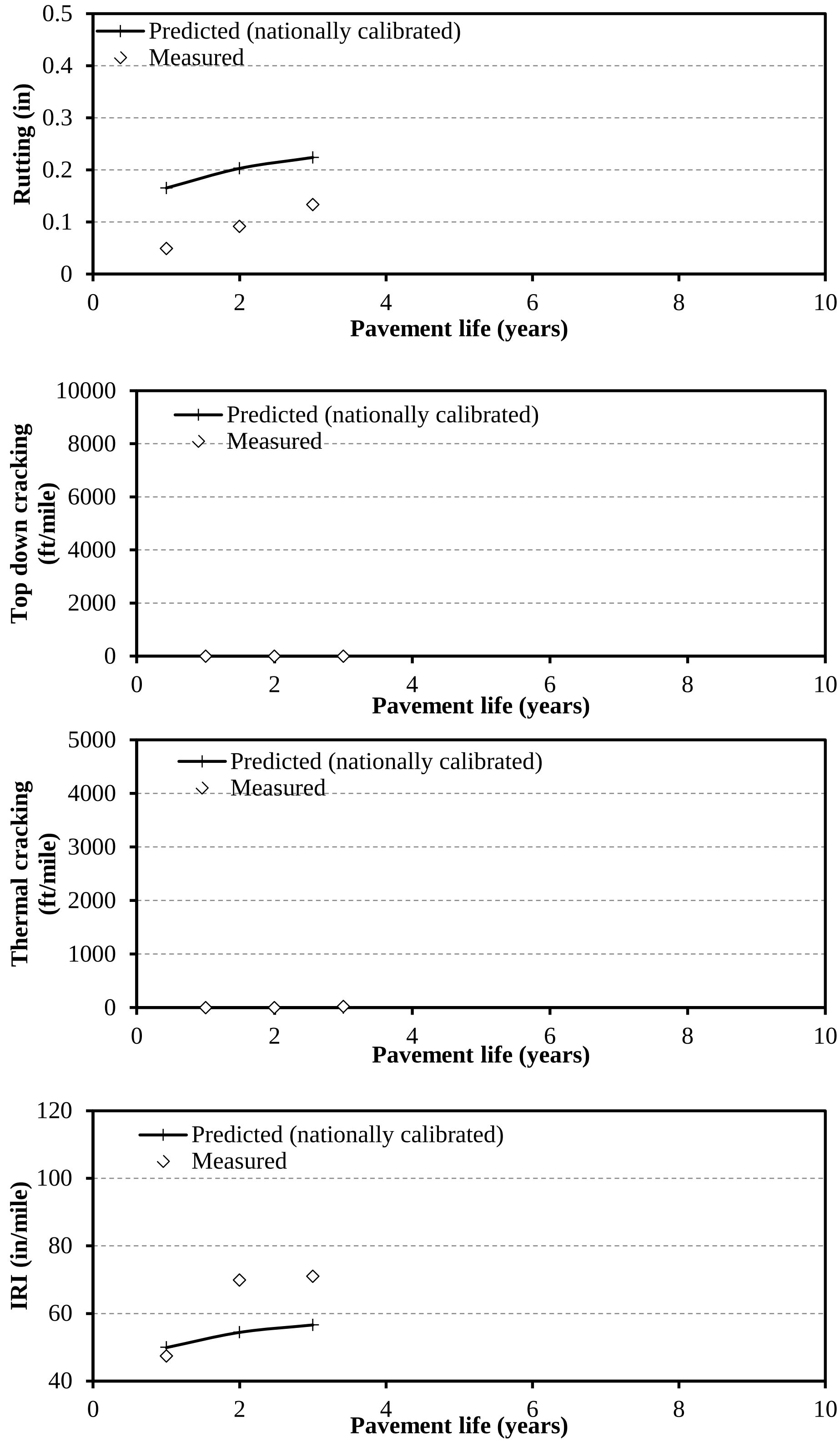

Figure C.21: Measured and Predicted Performance Data by the Nationally Calibrated MEPDG for Project 069U0028300-NB

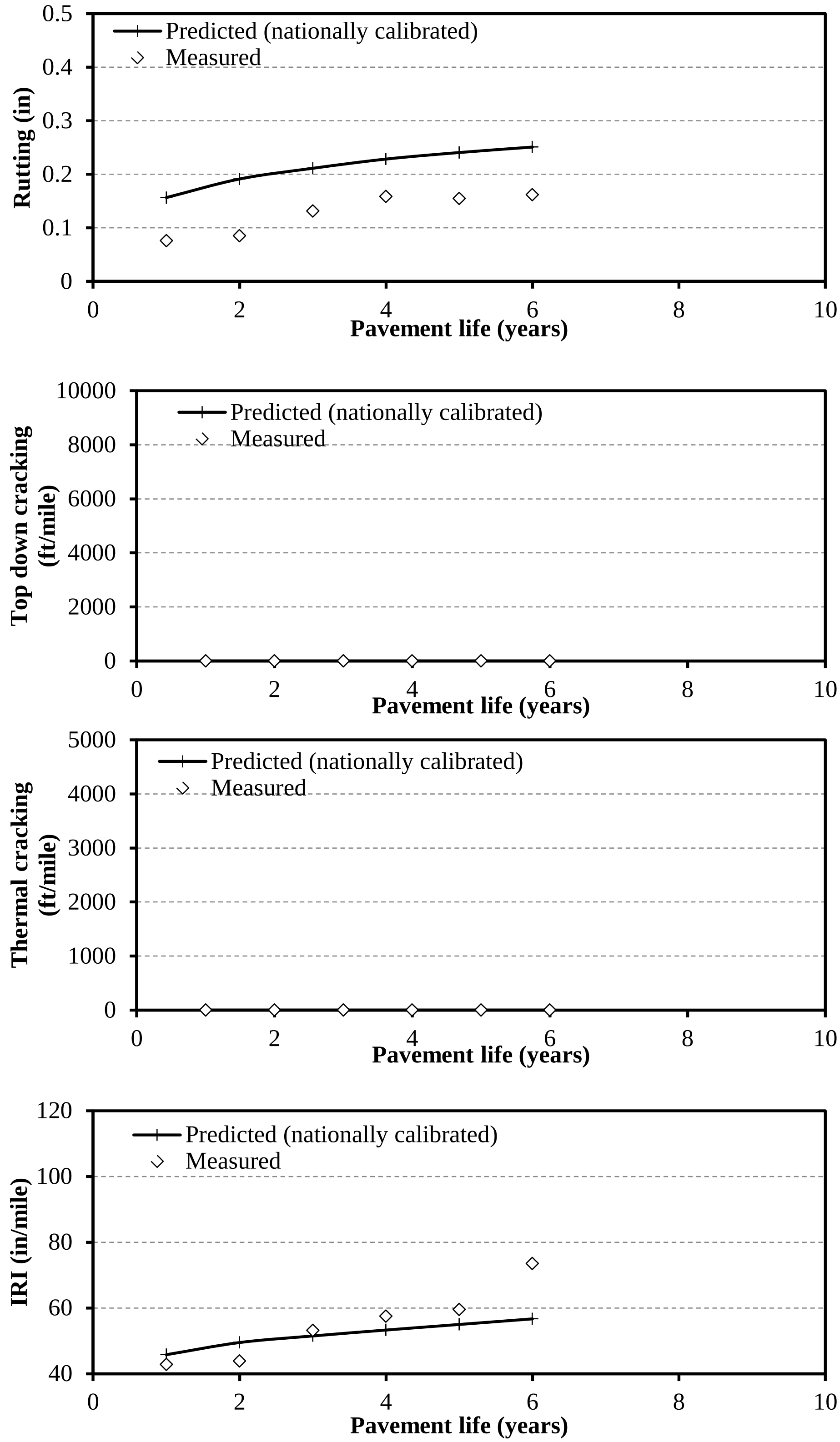

Figure C.22: Measured and Predicted Performance Data by the Nationally Calibrated MEPDG for Project 082U0018300-NB

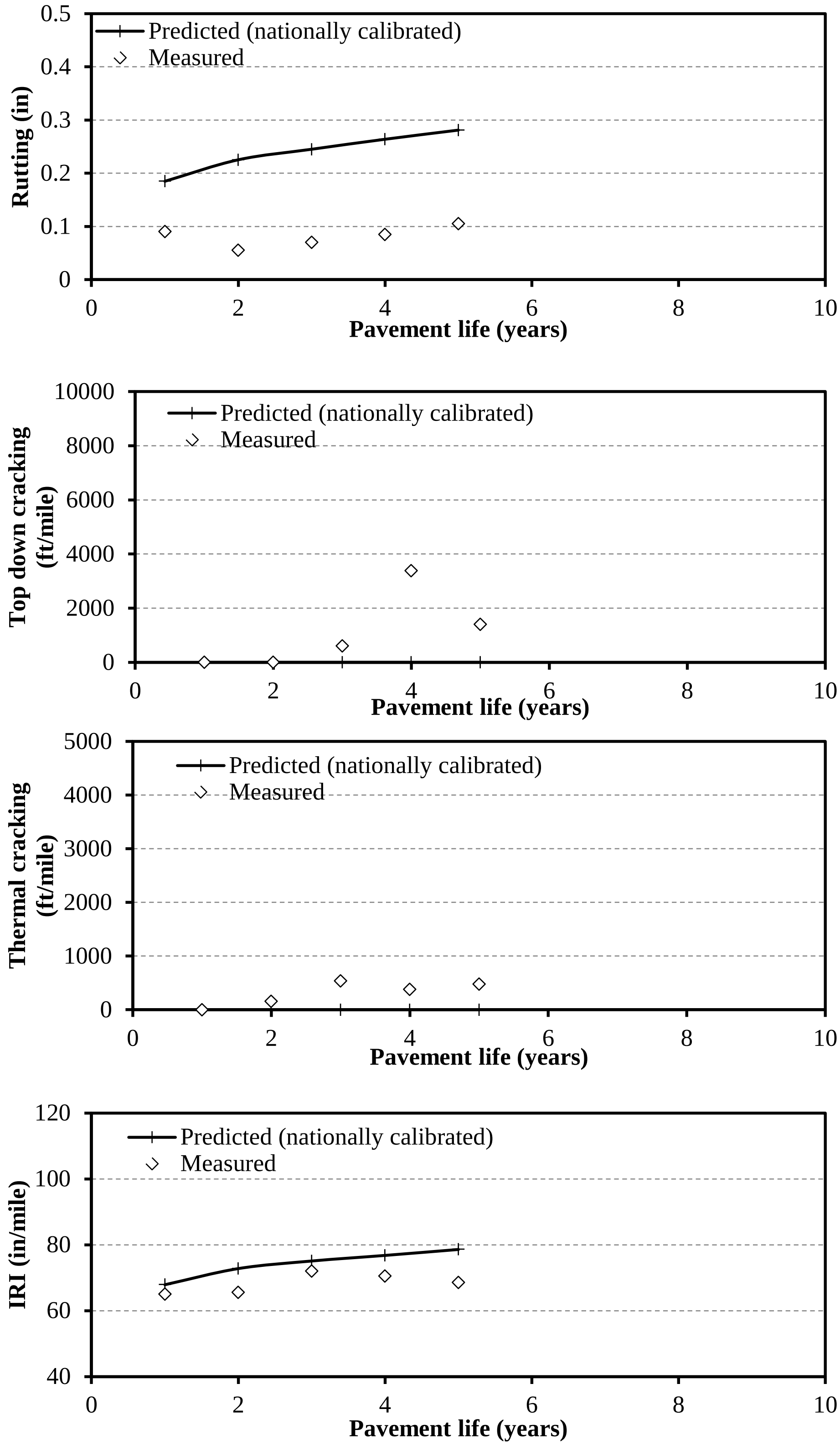

Figure C.23: Measured and Predicted Performance Data by the Nationally Calibrated MEPDG for Project 084U0028100-NB

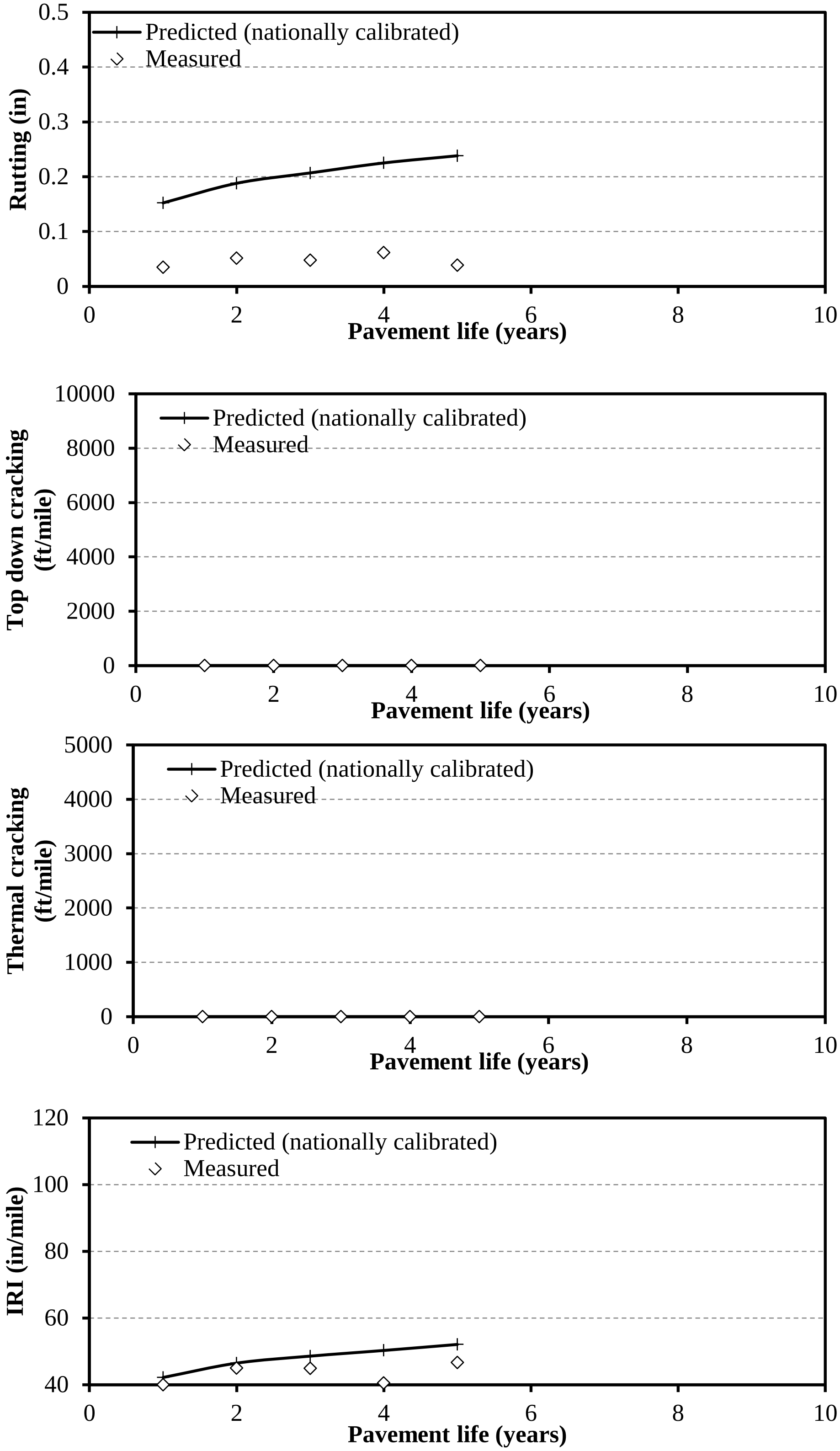

Figure C.24: Measured and Predicted Performance Data by the Nationally Calibrated MEPDG for Project 088U0005400-WB

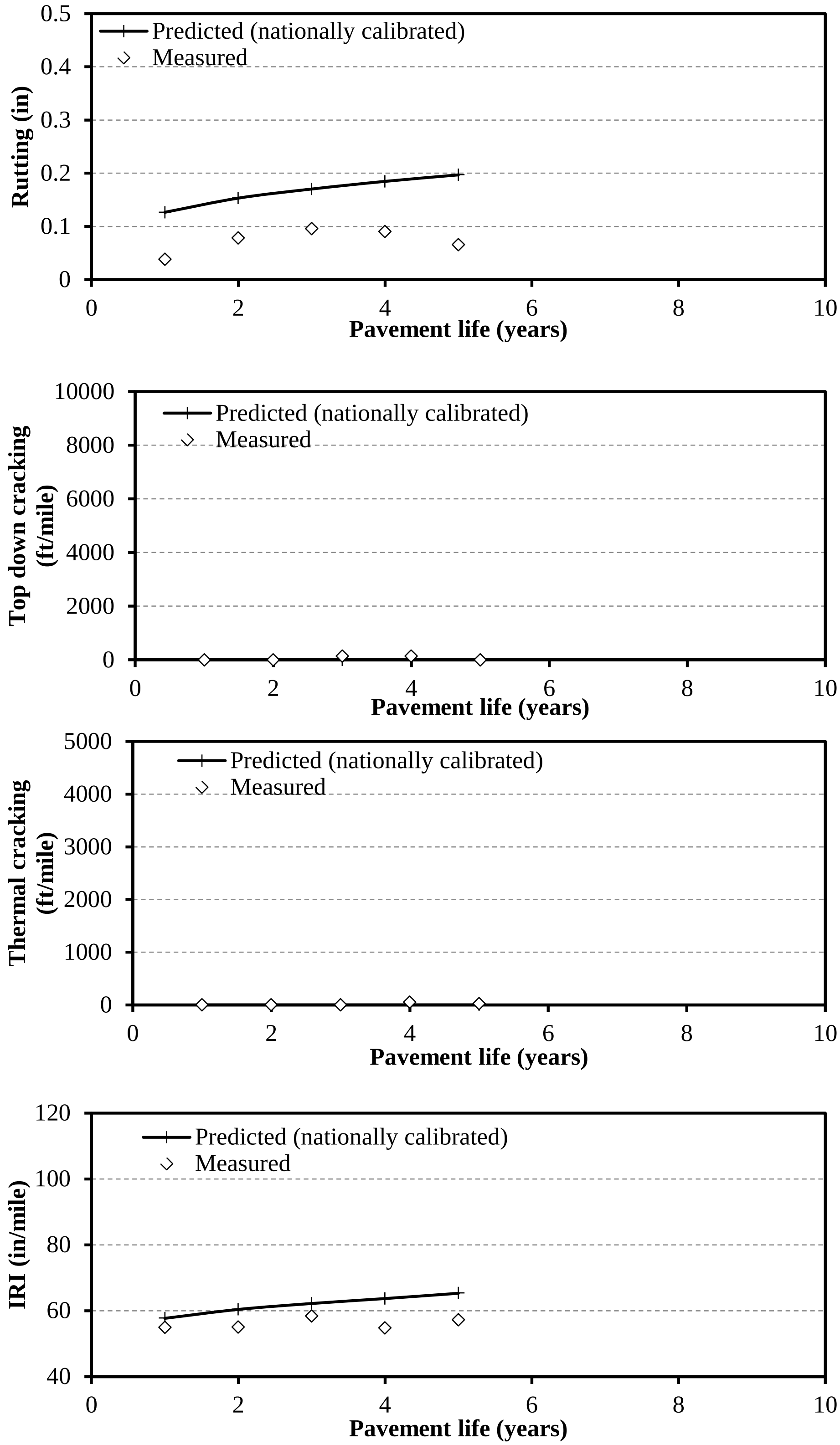

Figure C.25: Measured and Predicted Performance Data by the Nationally Calibrated MEPDG for Project 091K0002700-NB

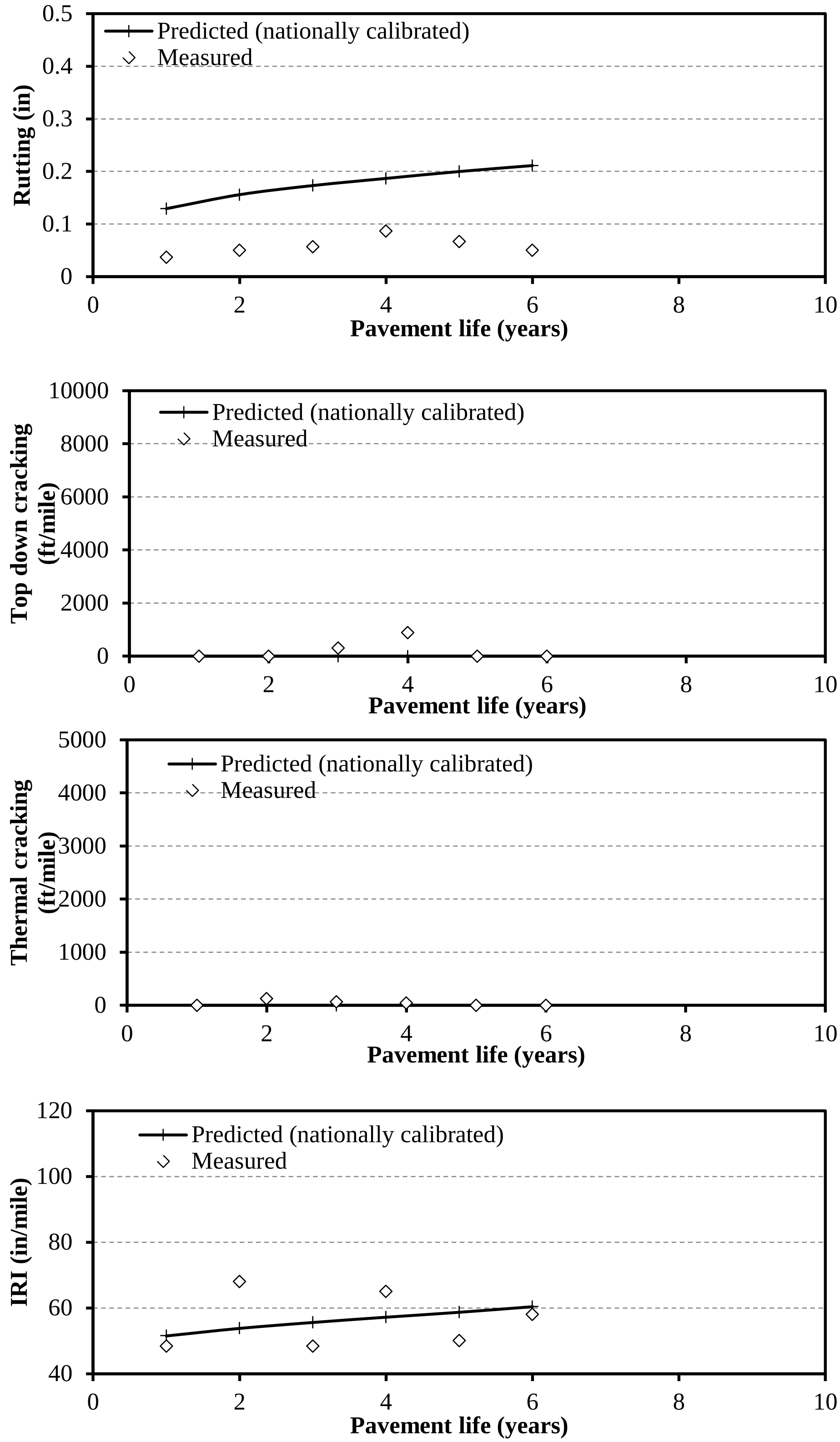

Figure C.26: Measured and Predicted Performance Data by the Nationally Calibrated MEPDG for Project 095U0005600-EB

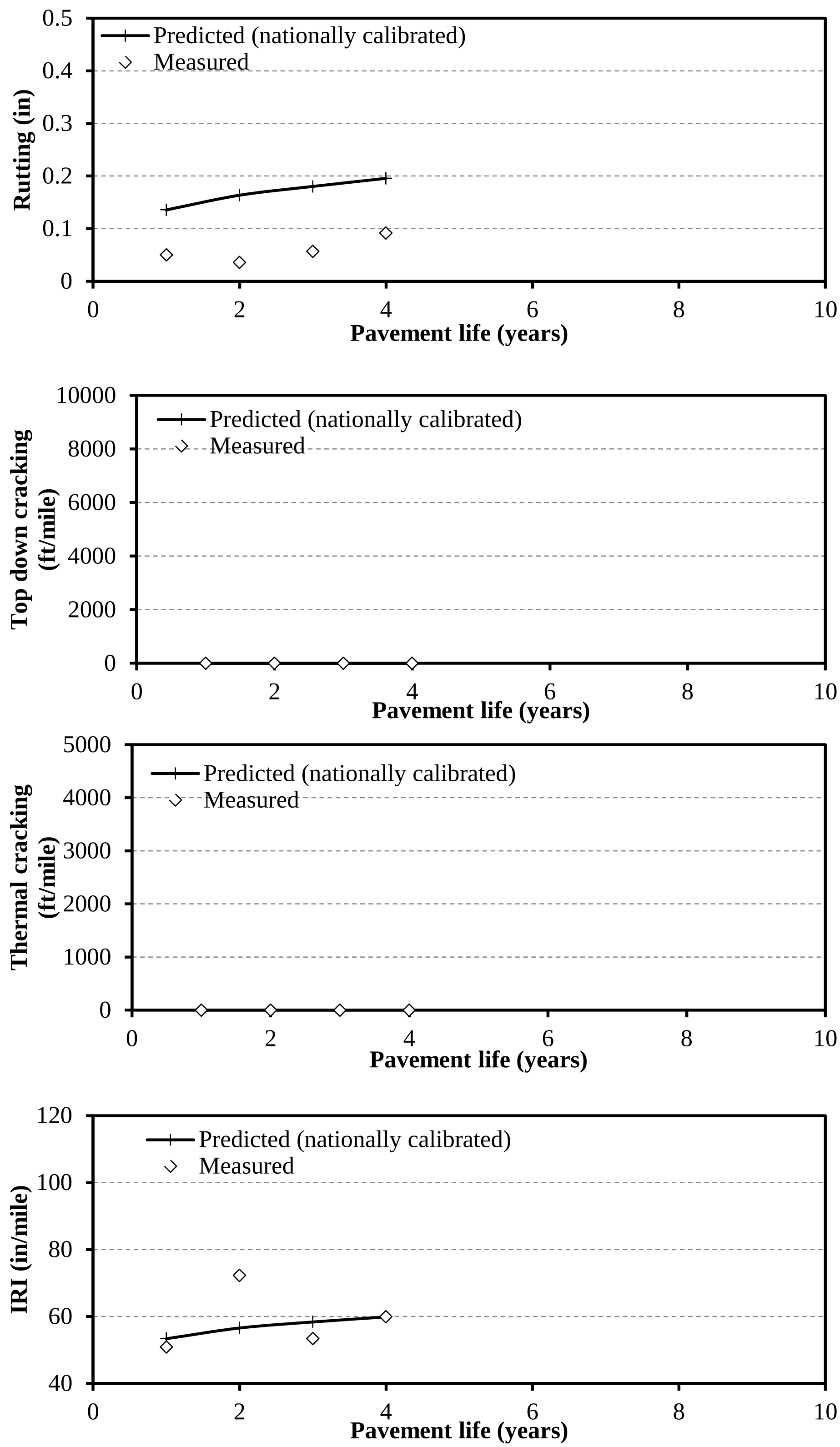

Figure C.27: Measured and Predicted Performance Data by the Nationally Calibrated MEPDG for Project 098U0028300-NB

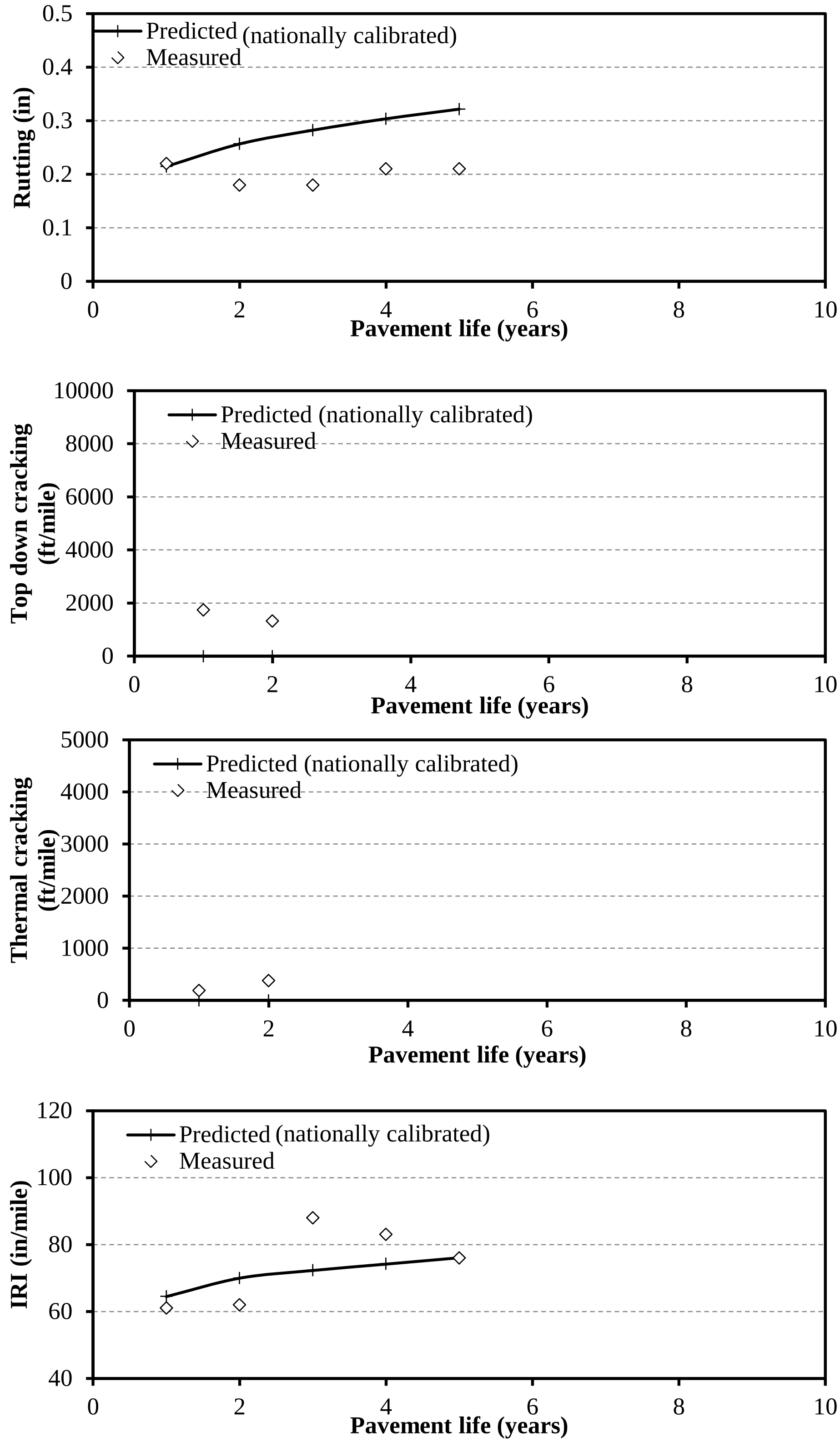

Figure C.28: Measured and Predicted Performance Data by the Nationally Calibrated MEPDG for Project 103K0003900-NB

Appendix D: Measured and Predicted Performance Data for New Rigid Pavements (Nationally Calibrated)

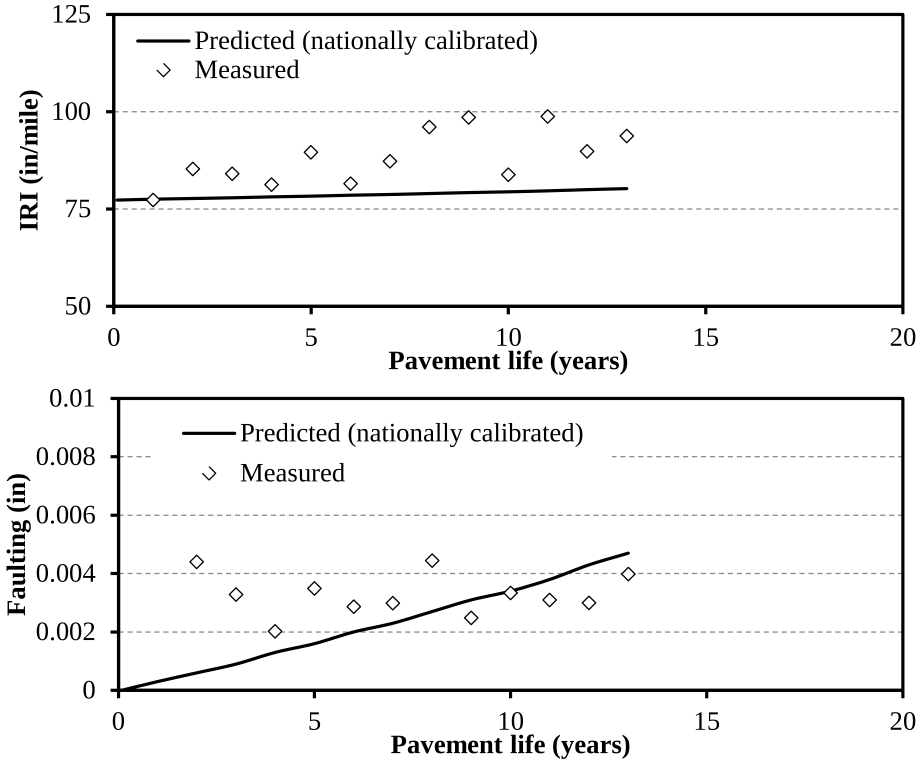

Figure D.1: Measured and Predicted Data by the Nationally Calibrated MEPDG for Project 018U0007700-NB

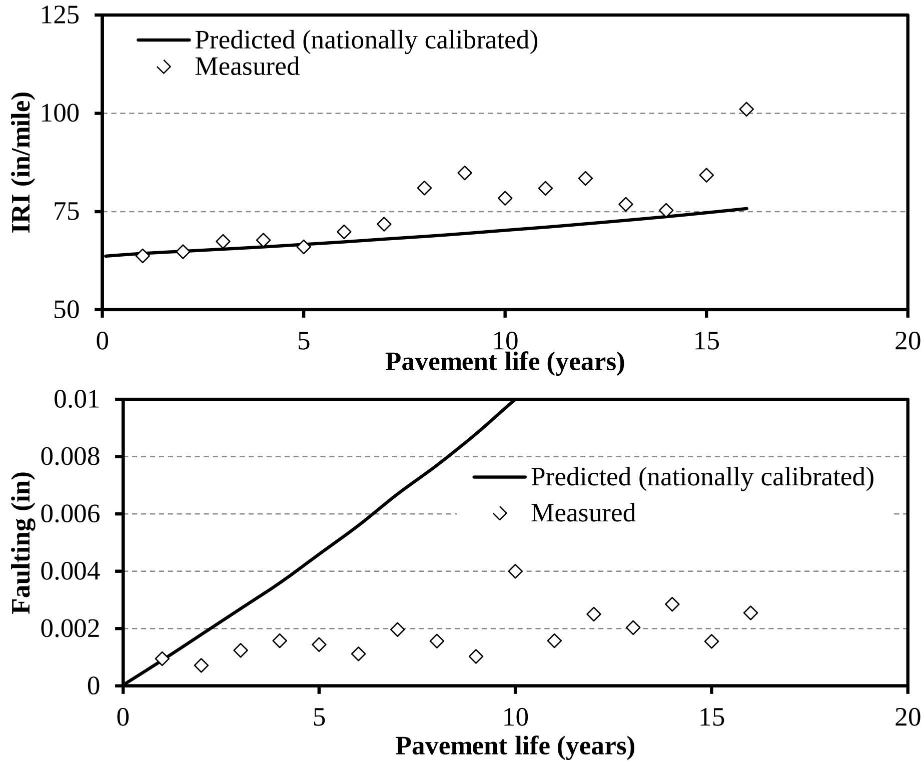

Figure D.2: Measured and Predicted Data by the Nationally Calibrated MEPDG for Project 043U0007500-NB-2

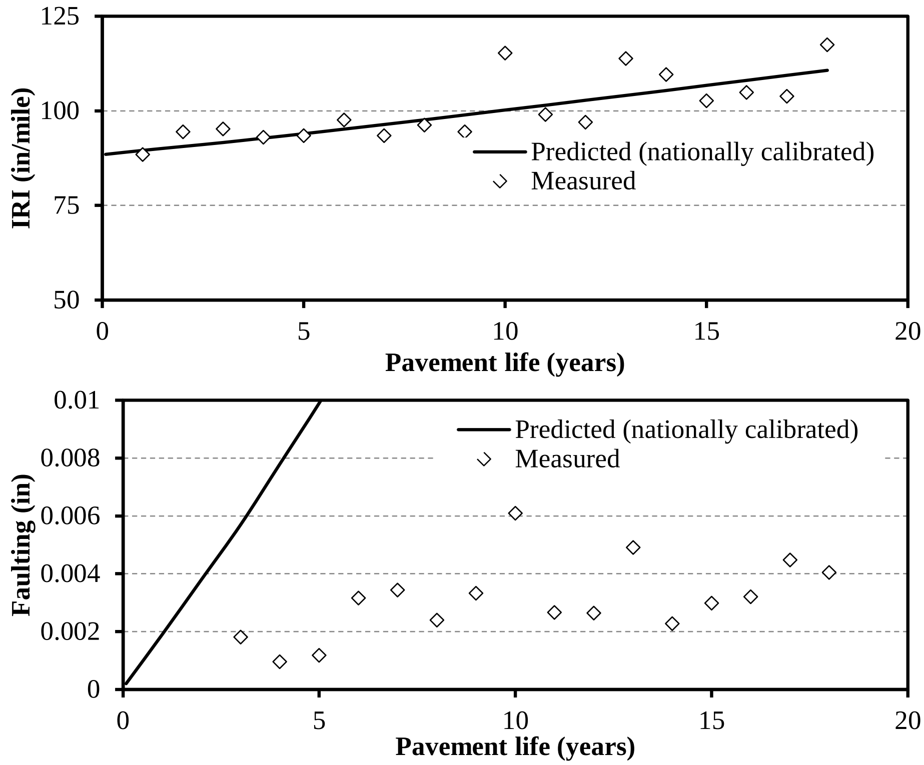

Figure D.3: Measured and Predicted Data by the Nationally Calibrated MEPDG for Project 056I0003500-SB

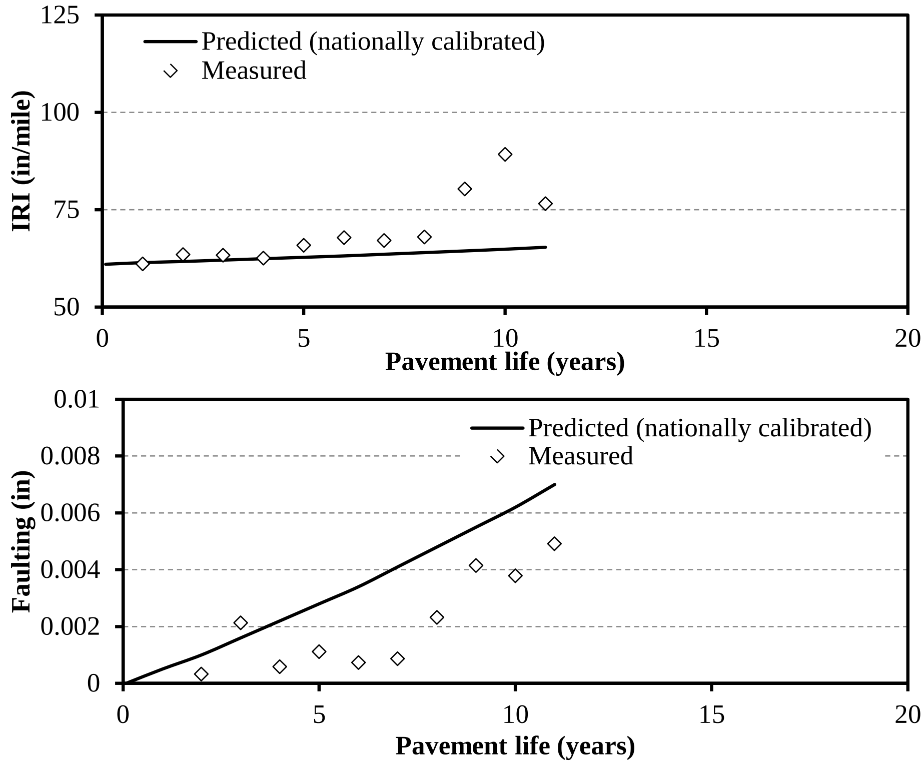

Figure D.4: Measured and Predicted Data by the Nationally Calibrated MEPDG for Project 063U0040000-EB

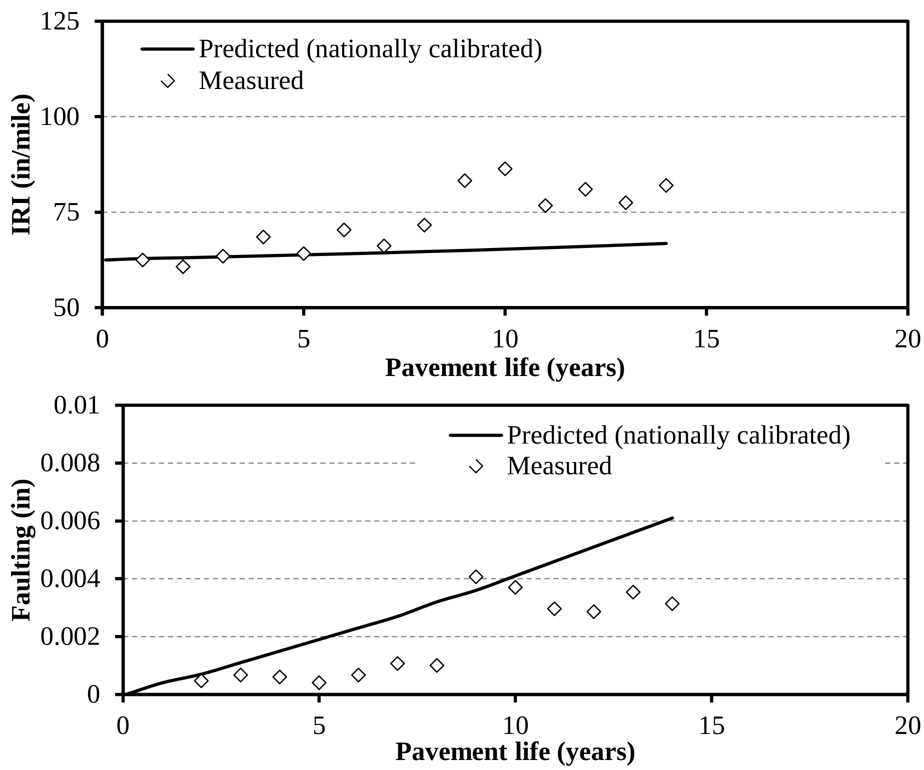

Figure D.5: Measured and Predicted Data by the Nationally Calibrated MEPDG for Project 103U0040000-EB

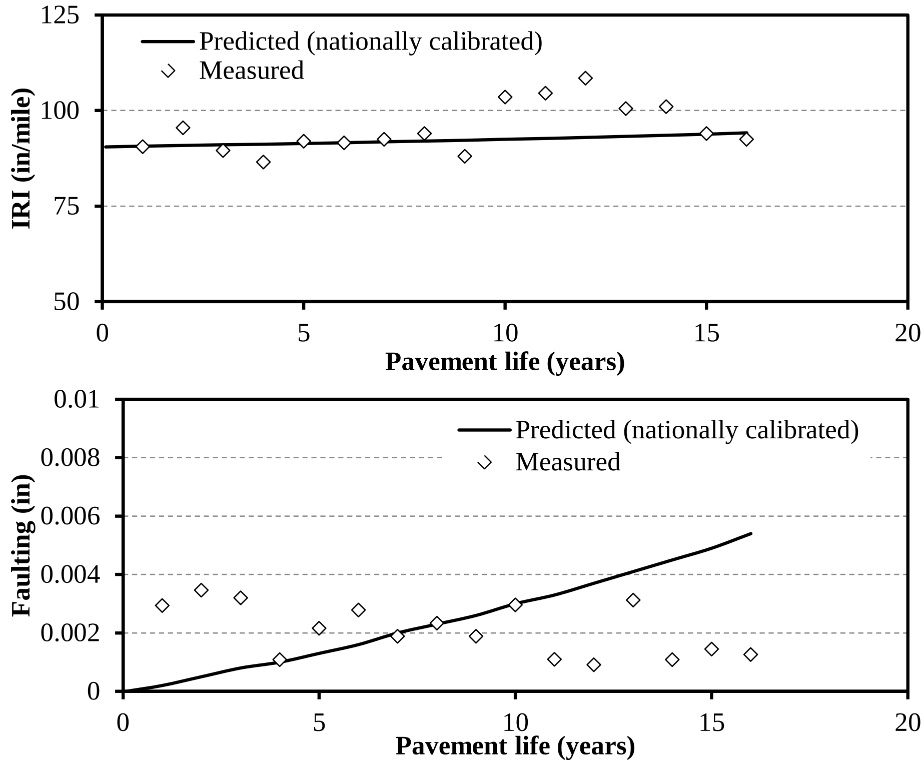

Figure D.6: Measured and Predicted Data by the Nationally Calibrated MEPDG for Project 018K0036000-EB

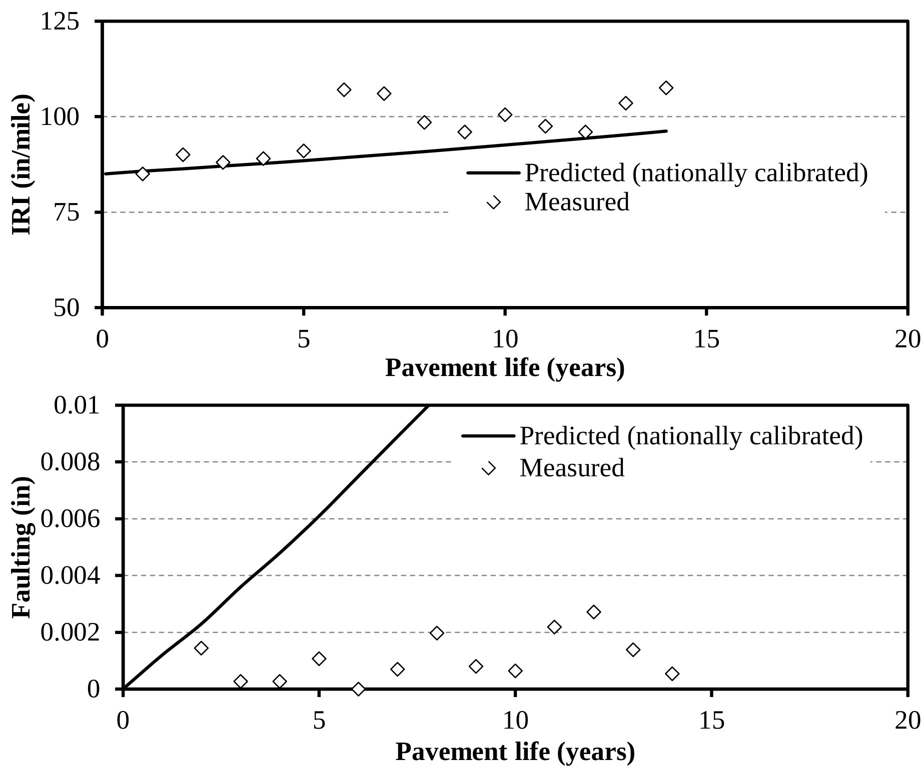

Figure D.7: Measured and Predicted Data by the Nationally Calibrated MEPDG for Project 031I0007000-EB

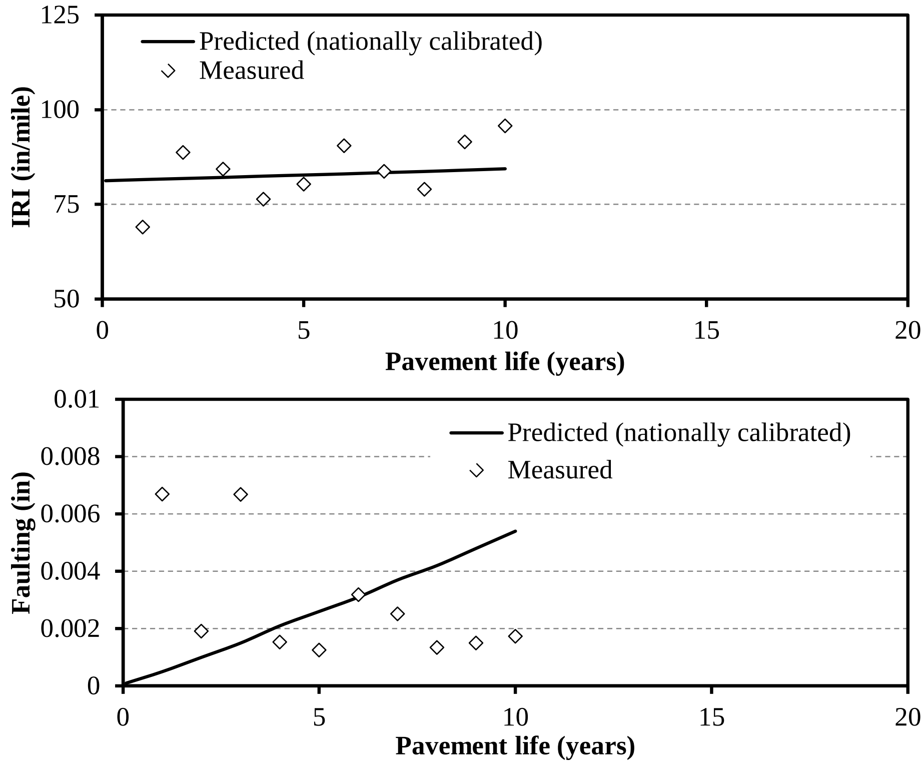

Figure D.8: Measured and Predicted Data by the Nationally Calibrated MEPDG for Project 040I0013500-NB-1

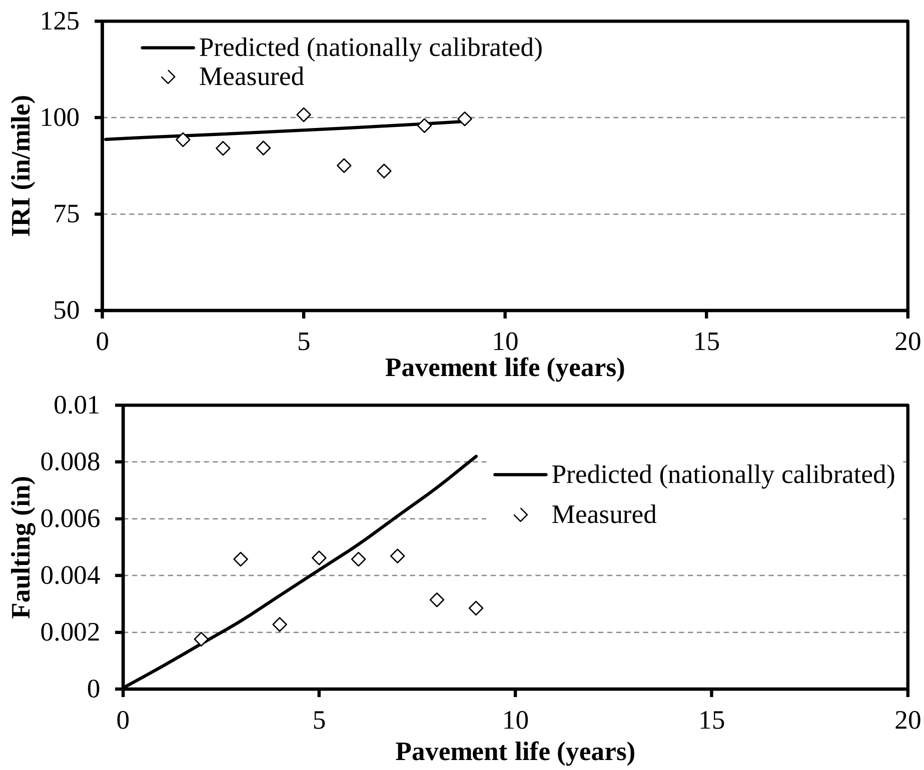

Figure D.9: Measured and Predicted Data by the Nationally Calibrated MEPDG for Project 040I0013500-NB-2

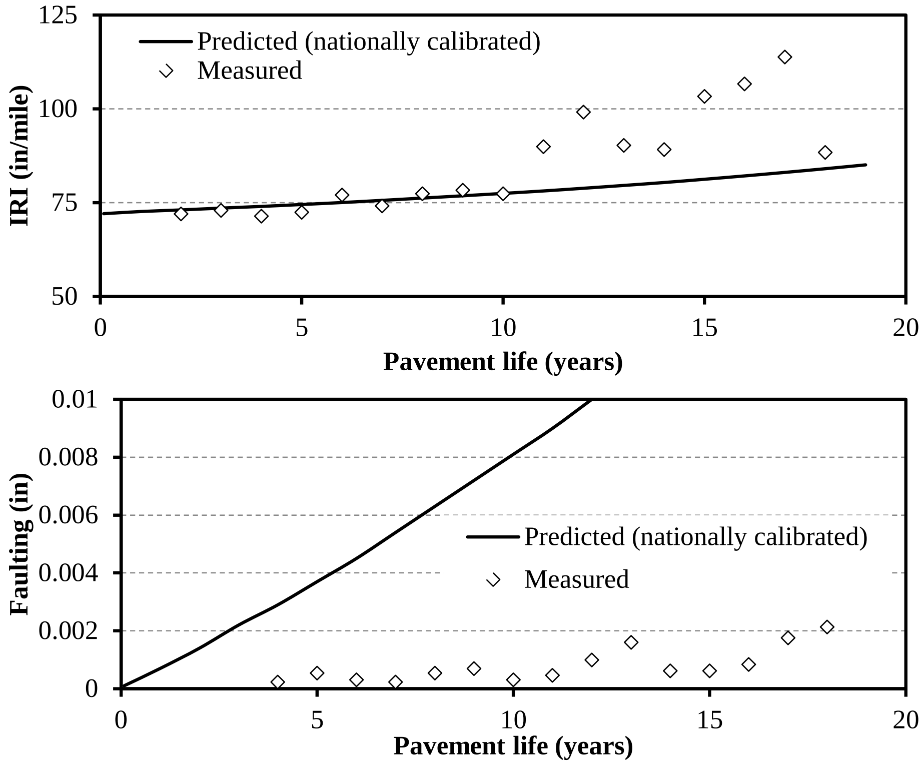

Figure D.10: Measured and Predicted Data by the Nationally Calibrated MEPDG for Project 043U0007500-NB

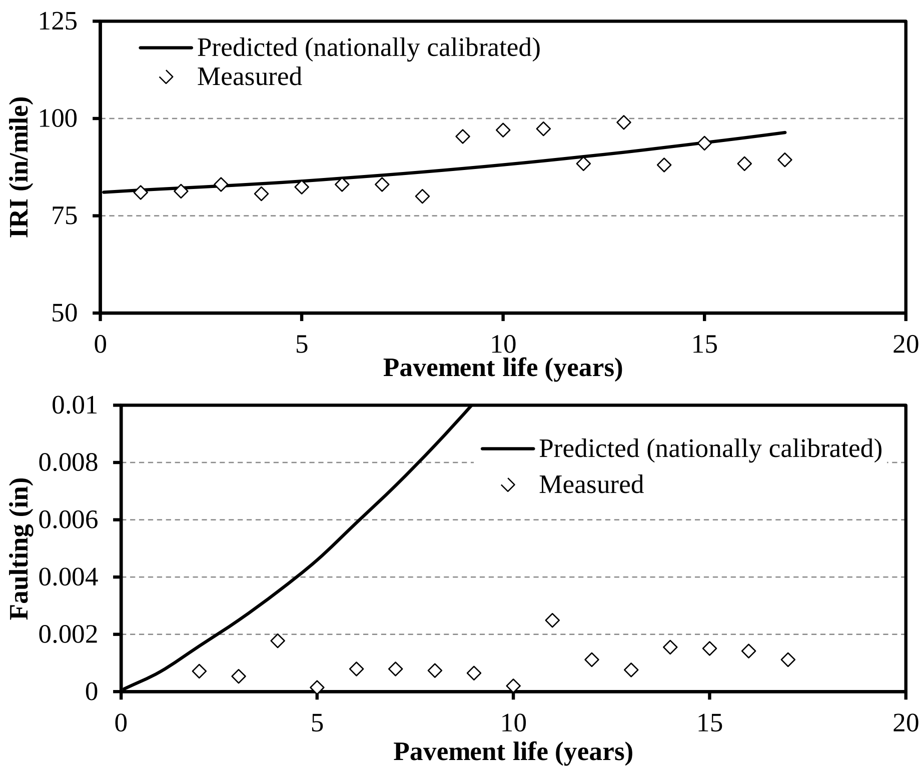

Figure D.11: Measured and Predicted Data by the Nationally Calibrated MEPDG for Project 046K0000700-SB

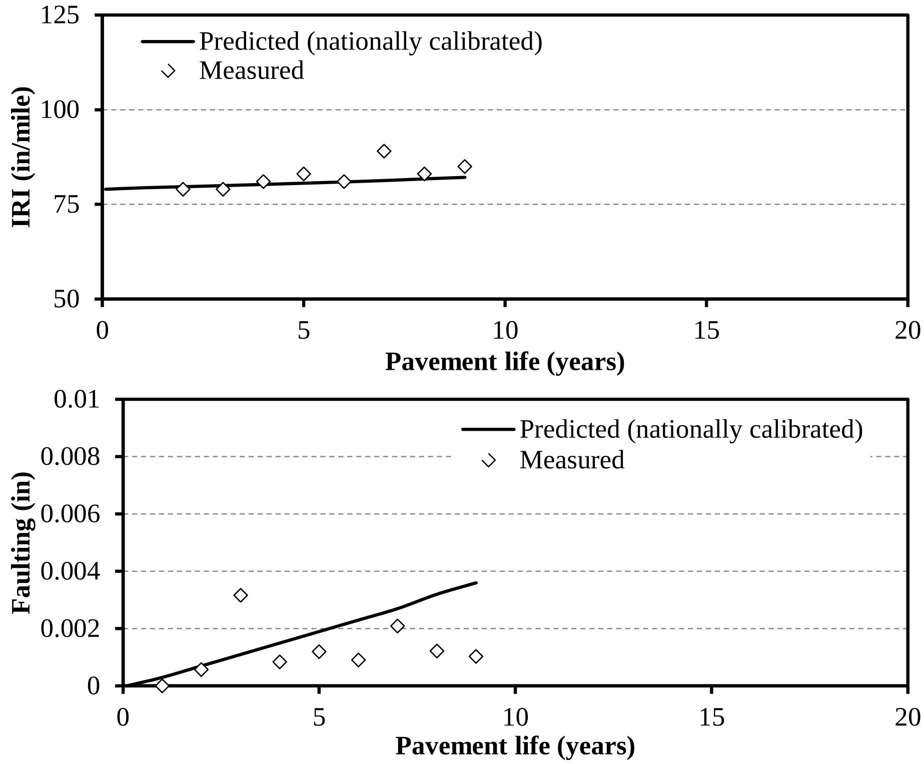

Figure D.12: Measured and Predicted Data by the Nationally Calibrated MEPDG for Project 055U0004000-EB

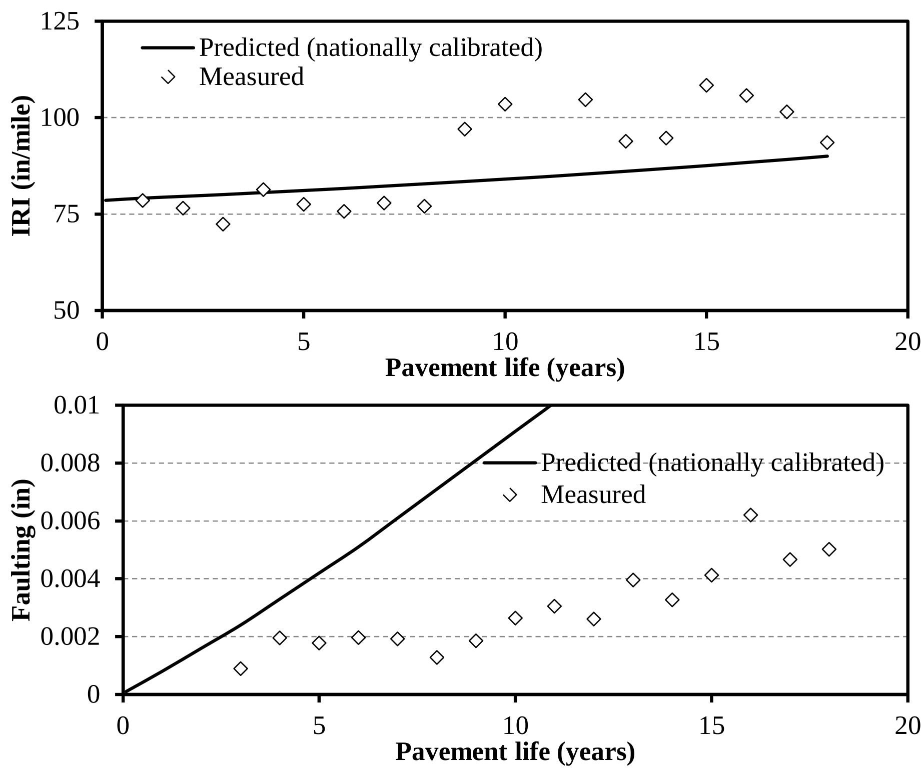

Figure D.13: Measured and Predicted Data by the Nationally Calibrated MEPDG for Project 056U0005000-EB

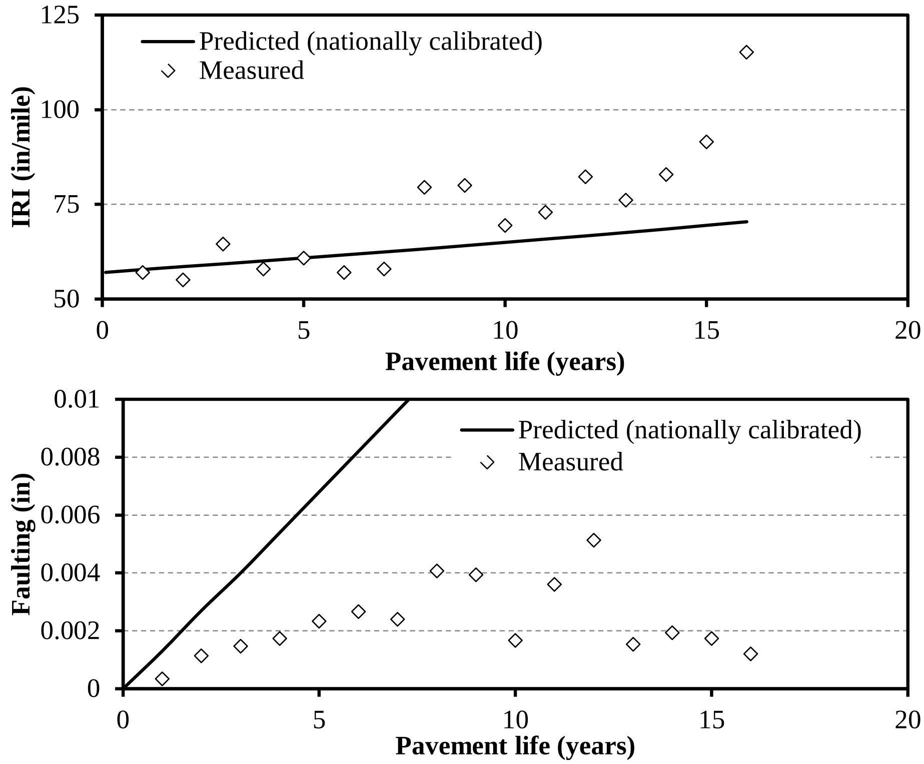

Figure D.14: Measured and Predicted Data by the Nationally Calibrated MEPDG for Project 059I0013500-NB

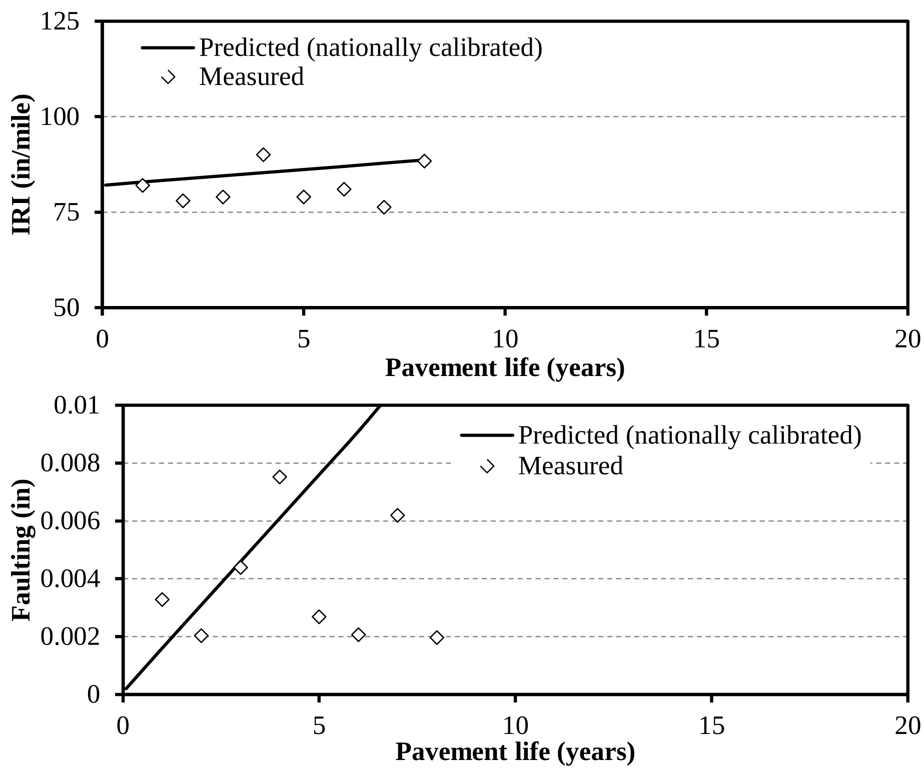

Figure D.15: Measured and Predicted Data by the Nationally Calibrated MEPDG for Project 061I0003500-NB

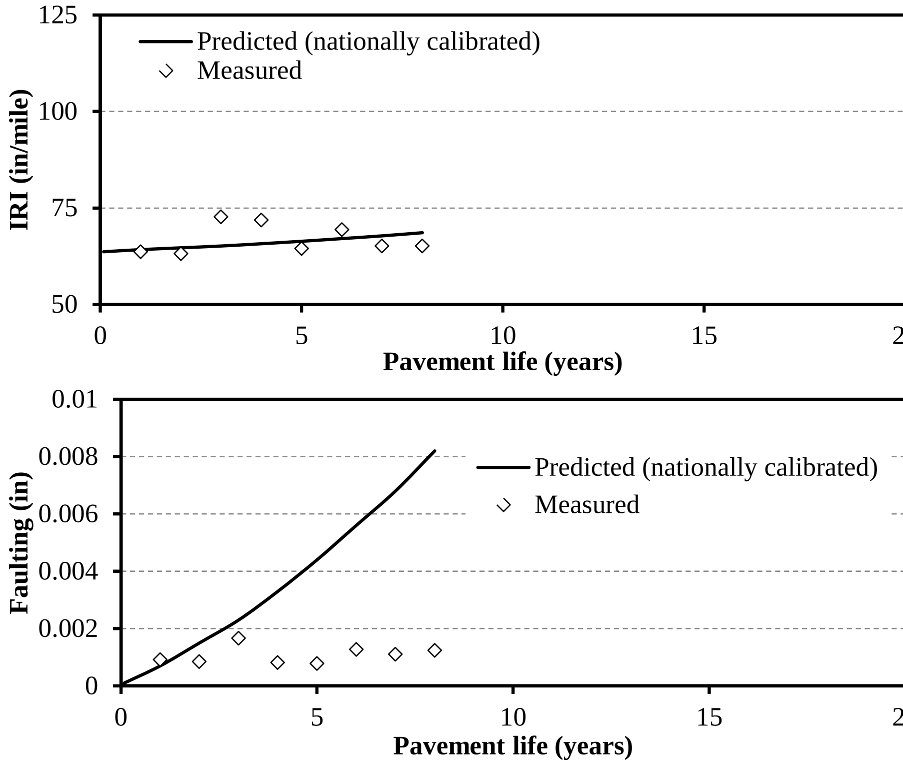

Figure D.16: Measured and Predicted Data by the Nationally Calibrated MEPDG for Project 067U0016900-NB

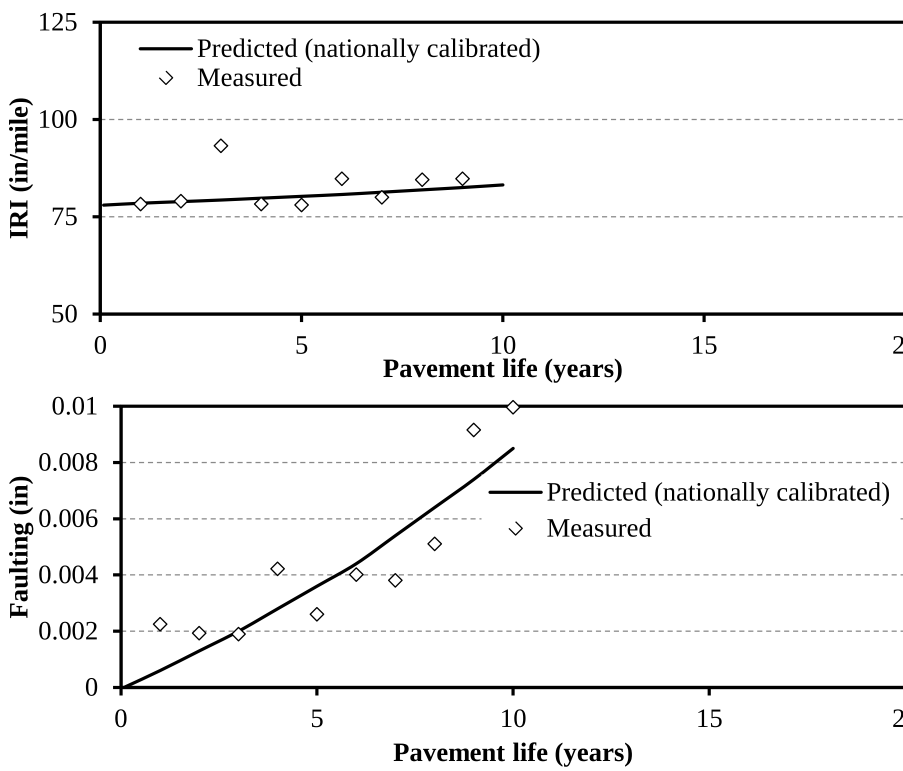

Figure D.17: Measured and Predicted Data by the Nationally Calibrated MEPDG for Project 079U0008100-NB

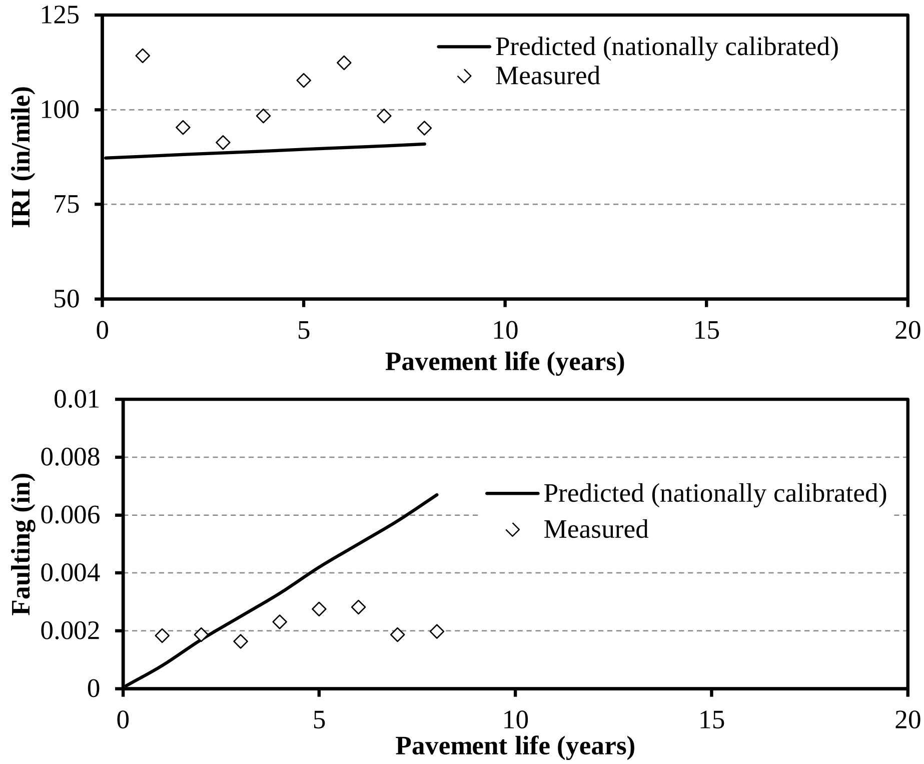

Figure D.18: Measured and Predicted Data by the Nationally Calibrated MEPDG for Project 085I0007000-EB

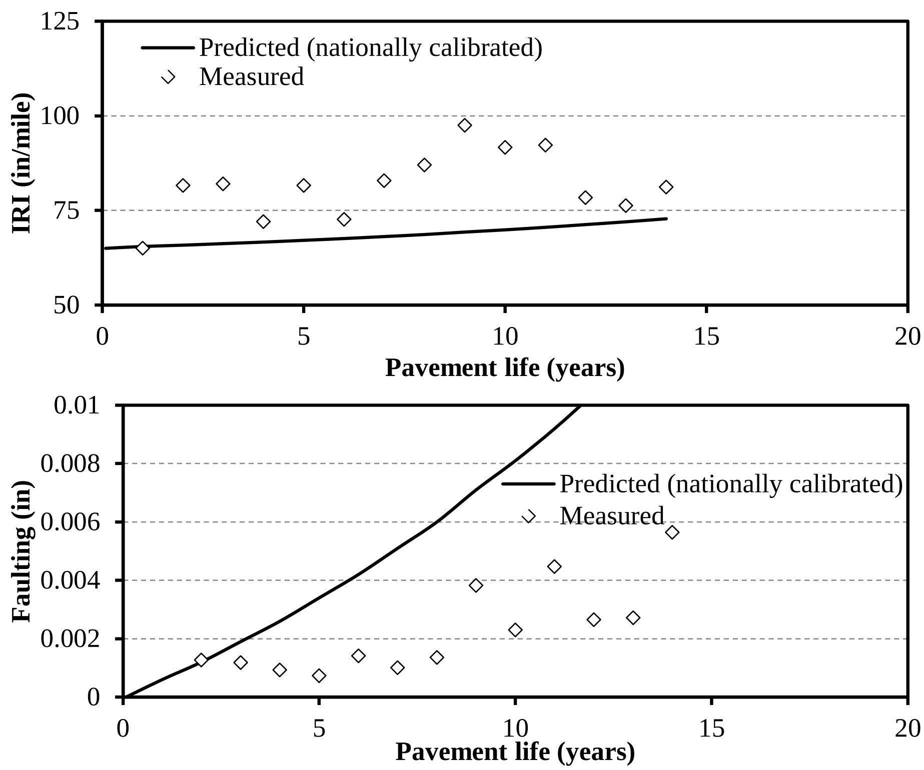

Figure D.19: Measured and Predicted Data by the Nationally Calibrated MEPDG for Project 019U0006900-NB

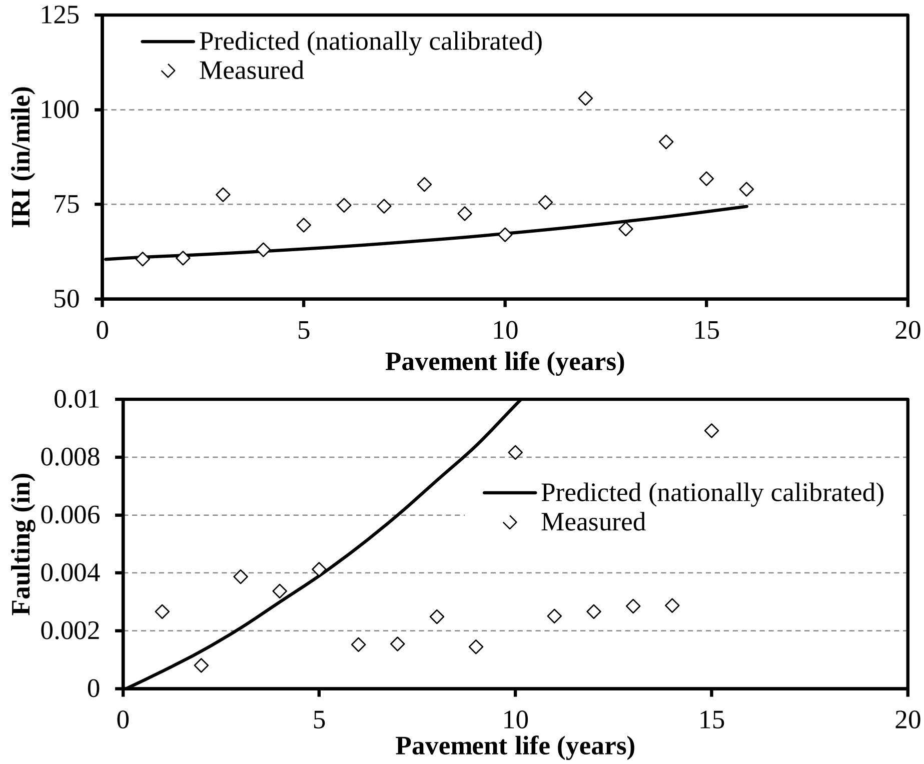

Figure D.20: Measured and Predicted Data by the Nationally Calibrated MEPDG for Project 029U0005600-EB

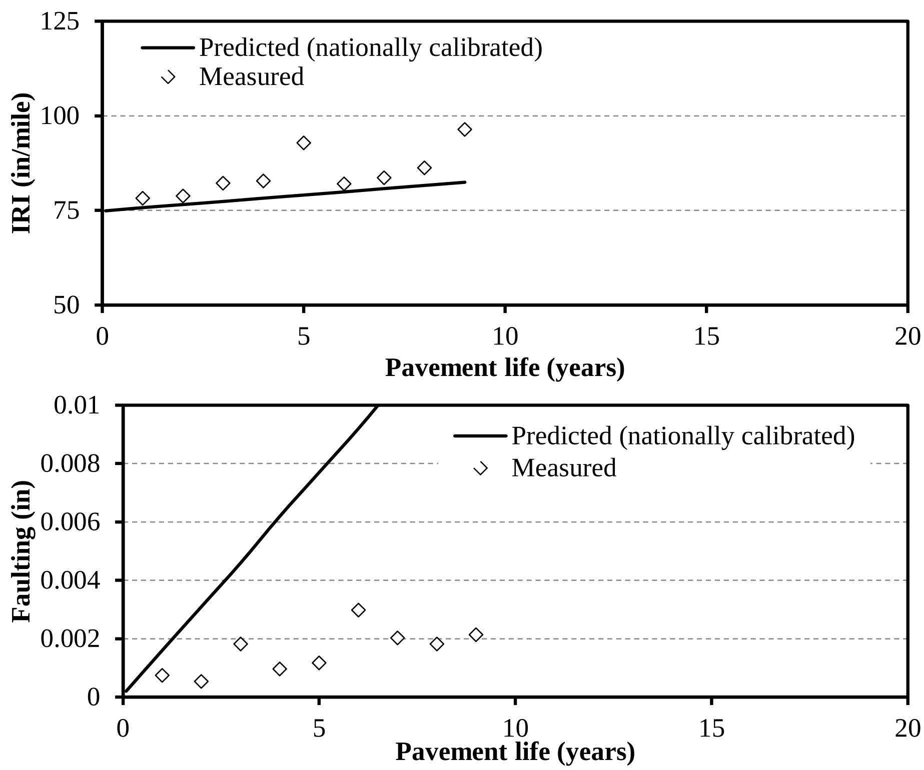

Figure D.21: Measured and Predicted Data by the Nationally Calibrated MEPDG for Project 030I0003500-2

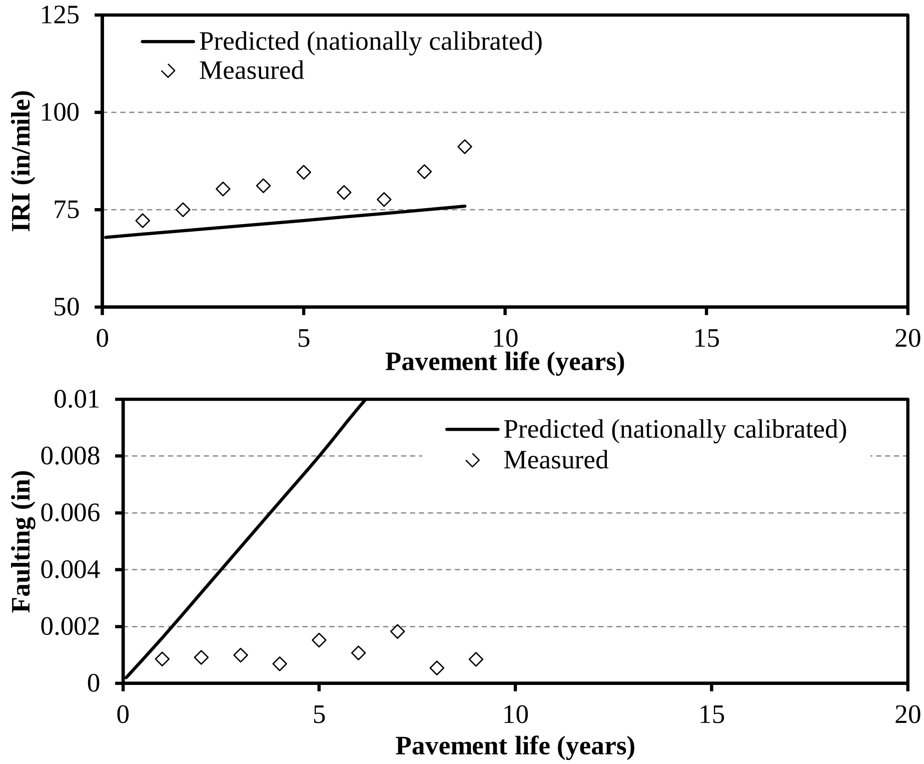

Figure D.22: Measured and Predicted Data by the Nationally Calibrated MEPDG for Project 030I0003500-3

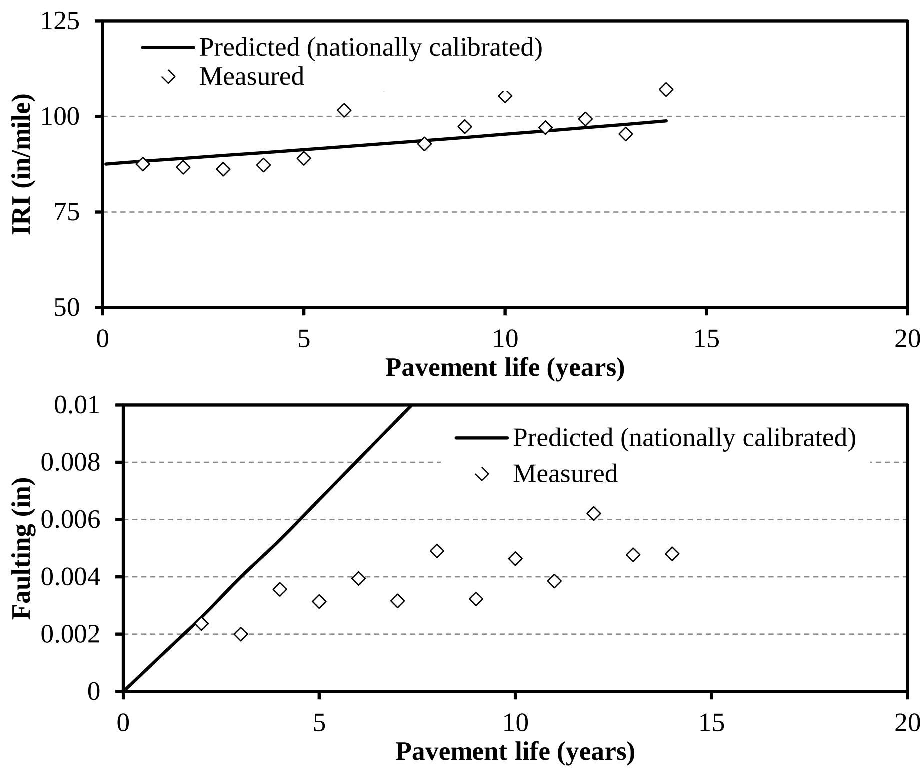

Figure D.23: Measured and Predicted Data by the Nationally Calibrated MEPDG for Project 031I0007000-2

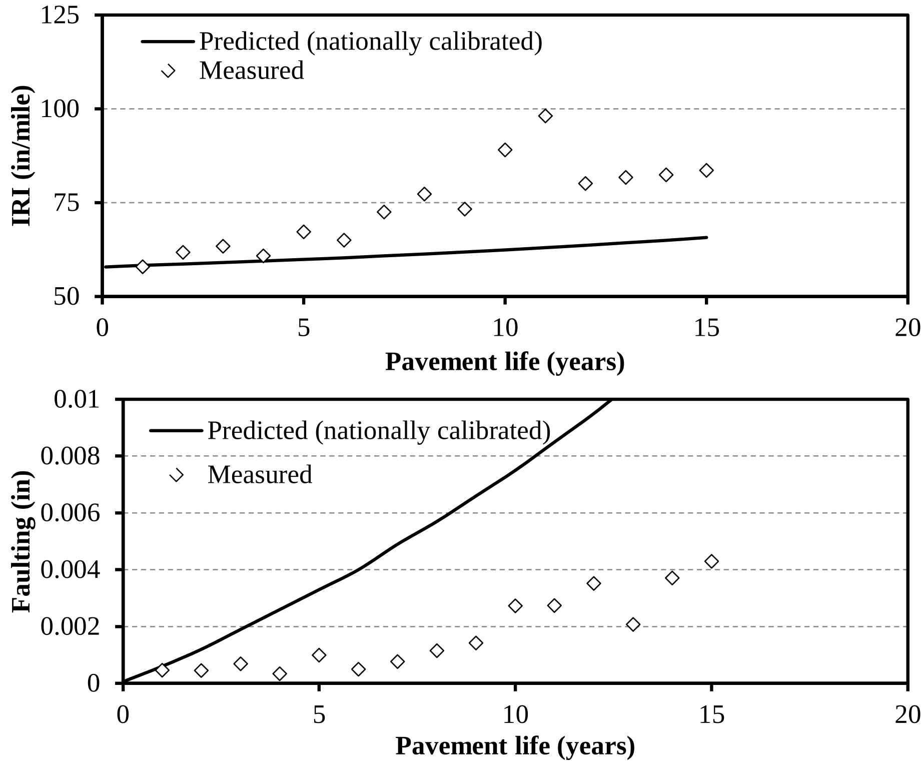

Figure D.24: Measured and Predicted Data by the Nationally Calibrated MEPDG for Project 037U0040000-EB

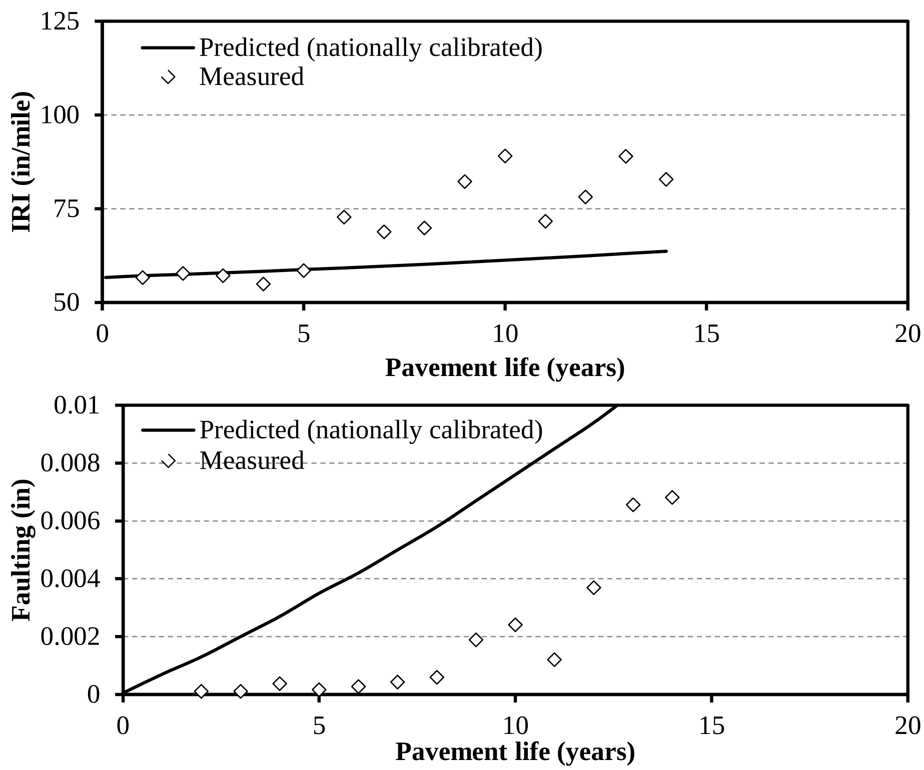

Figure D.25: Measured and Predicted Data by the Nationally Calibrated MEPDG for Project 037U0040000-EB-2

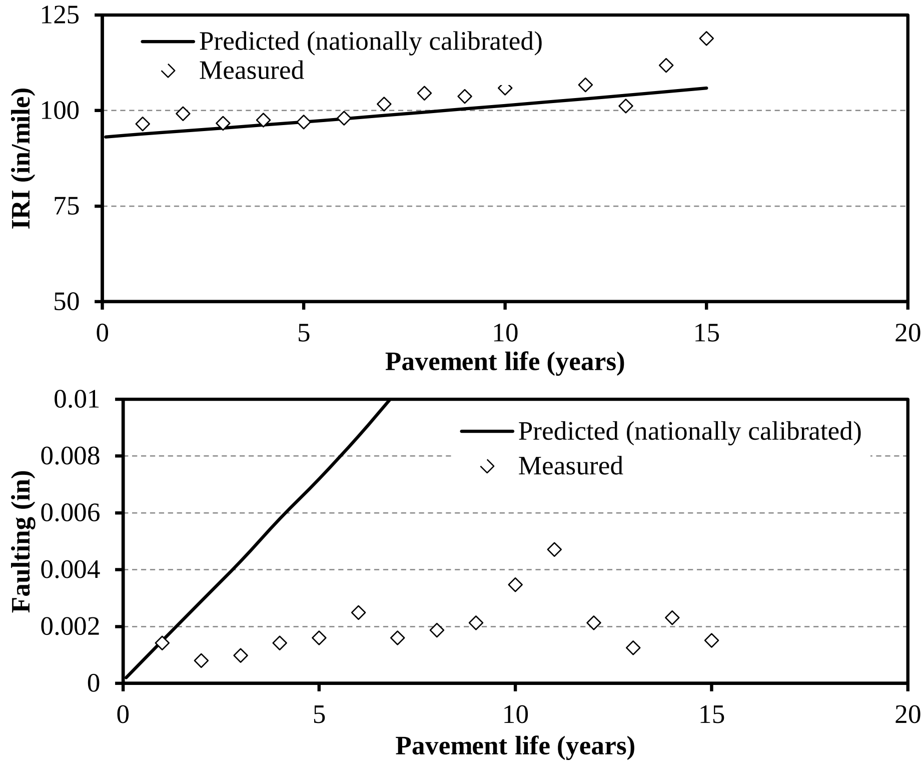

Figure D.26: Measured and Predicted Data by the Nationally Calibrated MEPDG for Project 030I0003500-1

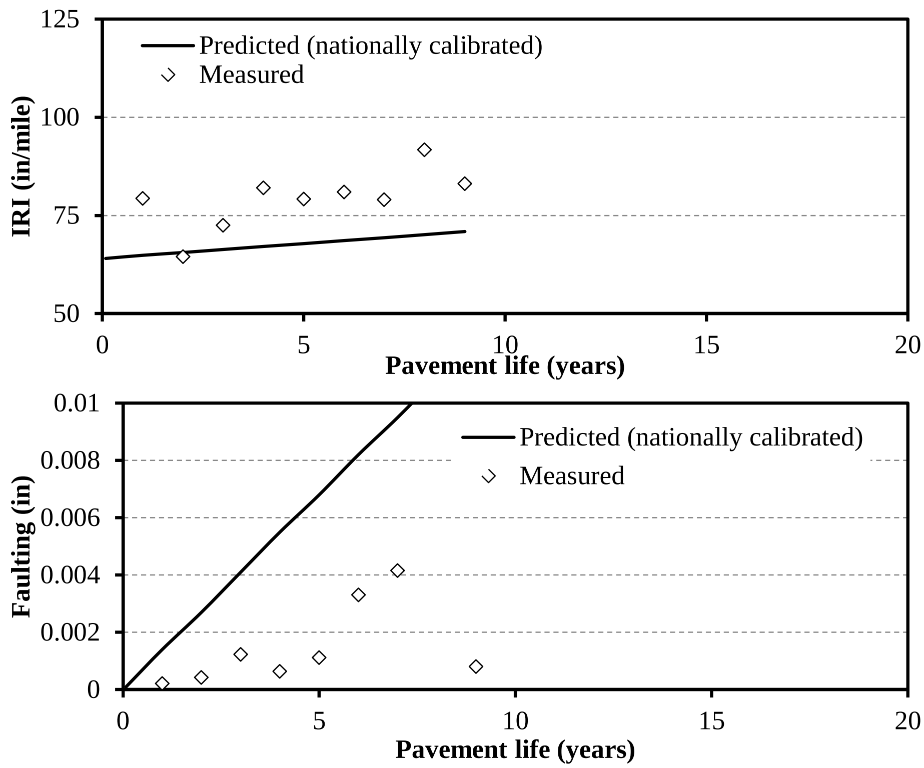

Figure D.27: Measured and Predicted Data by the Nationally Calibrated MEPDG for Project 056I0003500-SB-2

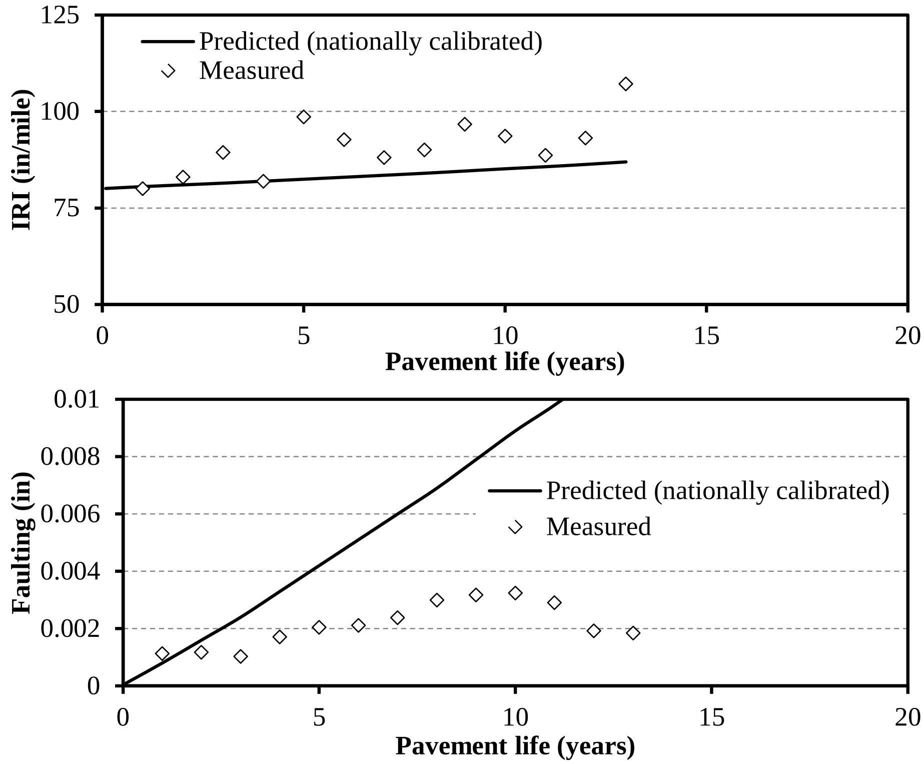

Figure D.28: Measured and Predicted Data by the Nationally Calibrated MEPDG for Project 085I0013501

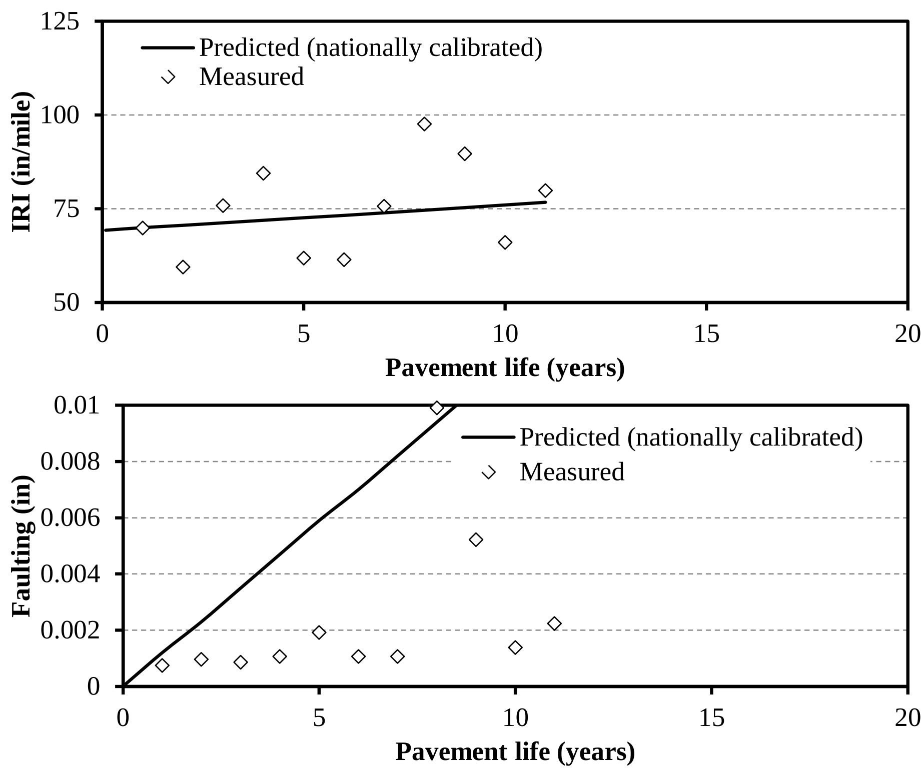

Figure D.29: Measured and Predicted Data by the Nationally Calibrated MEPDG for Project 099I0007000-EB-1

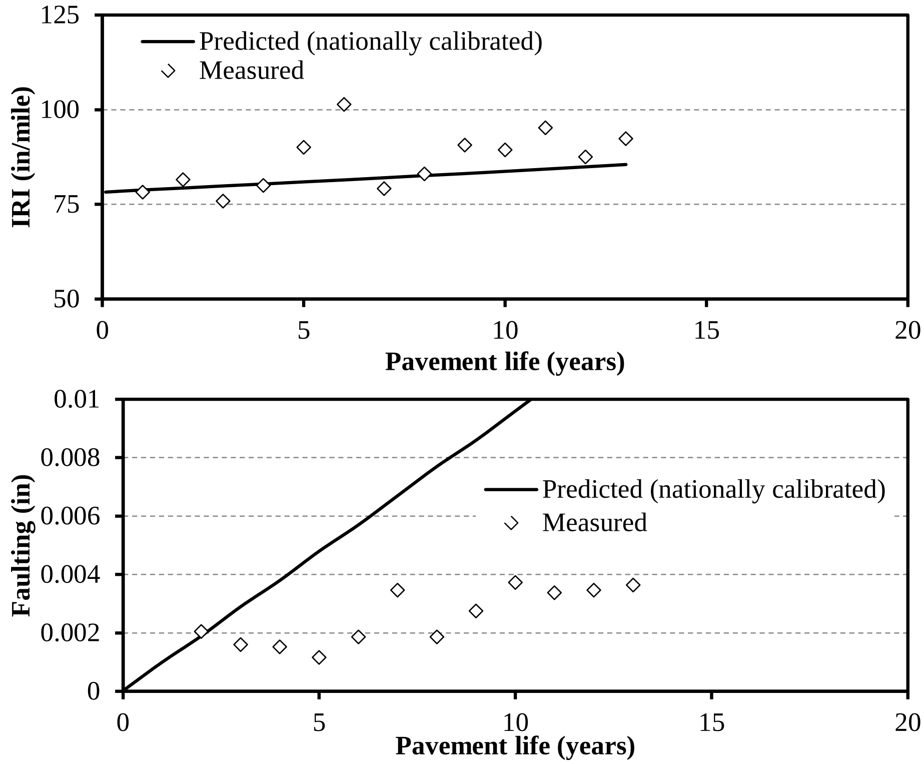

Figure D.30: Measured and Predicted Data by the Nationally Calibrated MEPDG for Project 099I0007000-EB-2

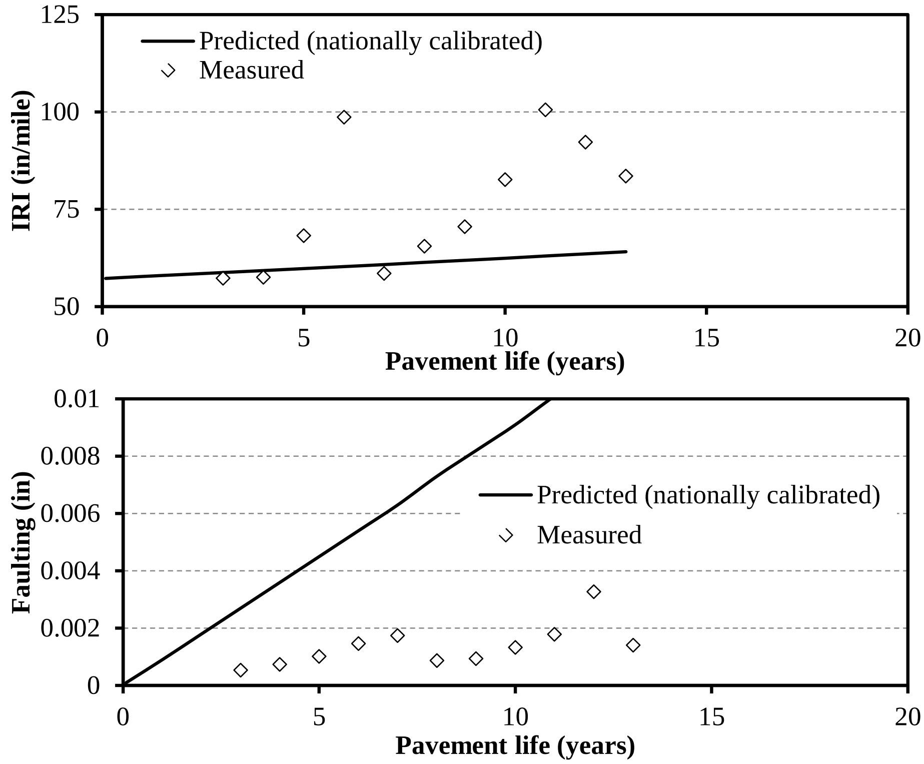

Figure D.31: Measured and Predicted Data by the Nationally Calibrated MEPDG for Project 099I0007000-EB-3

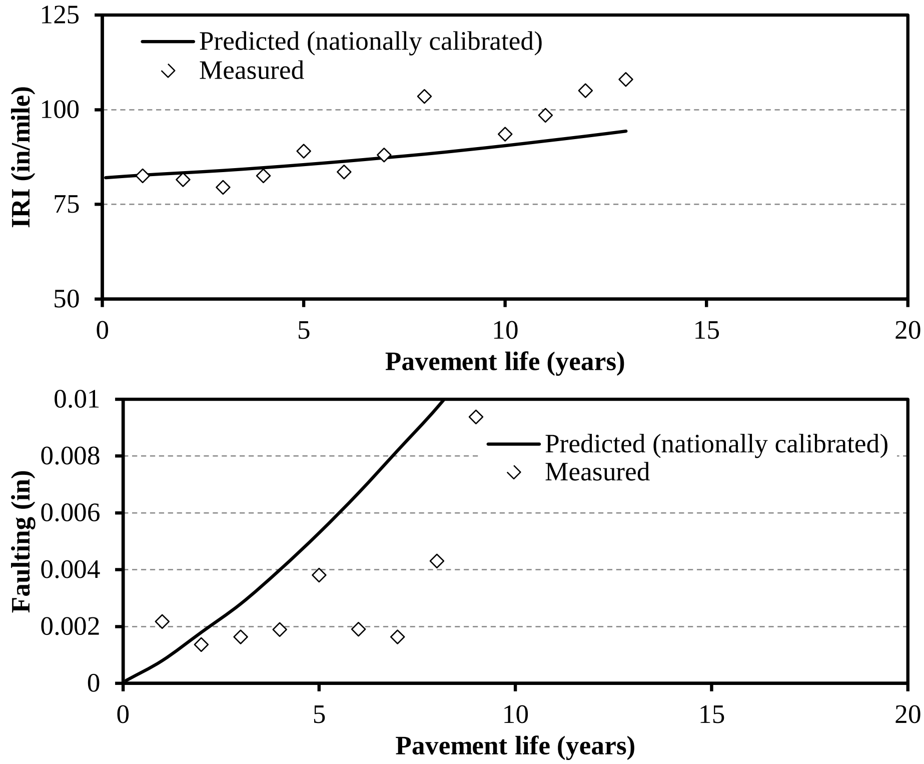

Figure D.32: Measured and Predicted Data by the Nationally Calibrated MEPDG for Project 103U0007500-SB

Appendix E: Measured and Predicted Performance Data for New Flexible Pavements (Locally Calibrated)

This page intentionally left blank.

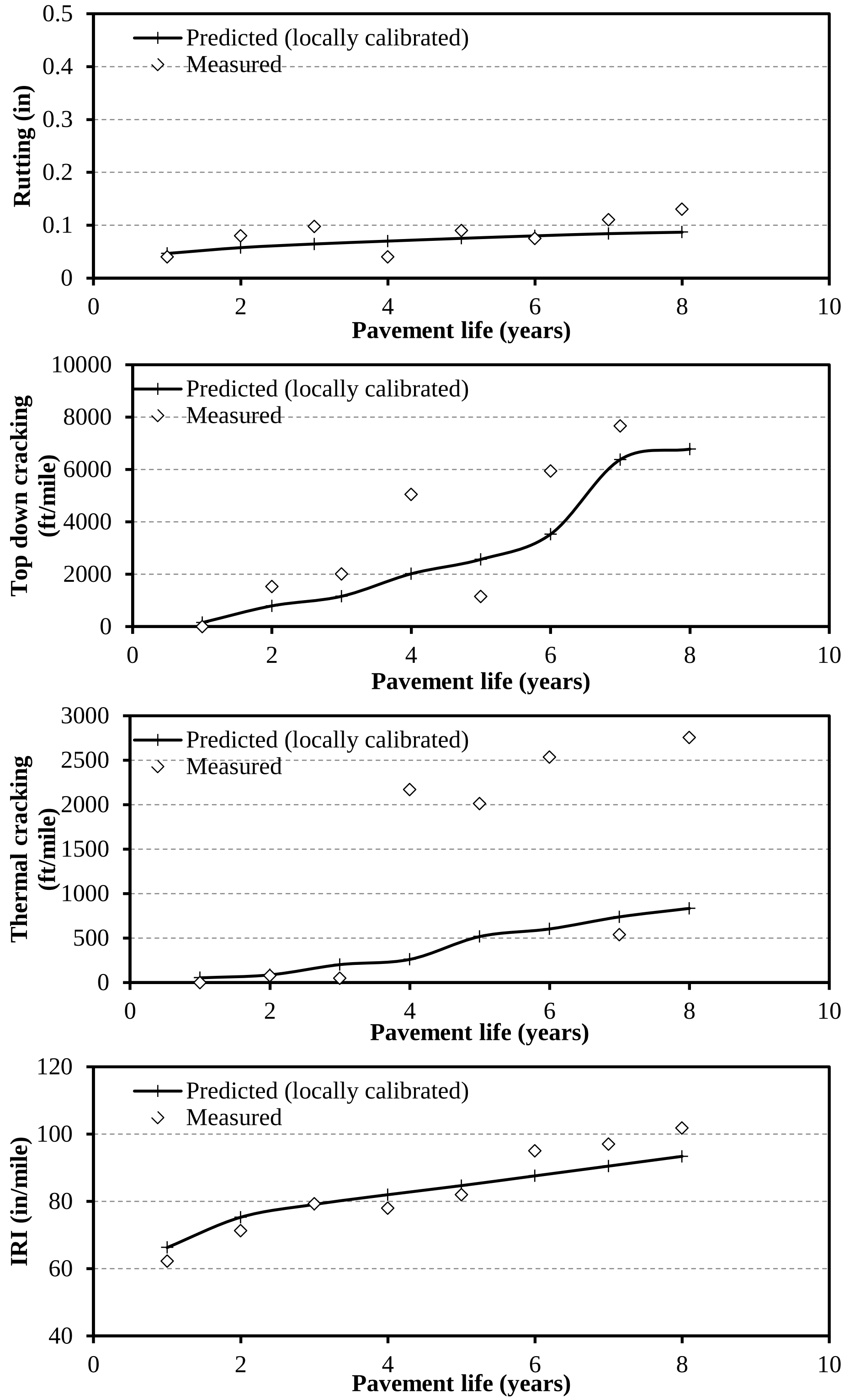

Figure E.1: Measured and Predicted Performance Data by the Locally Calibrated MEPDG for Project 003U0007300-NB

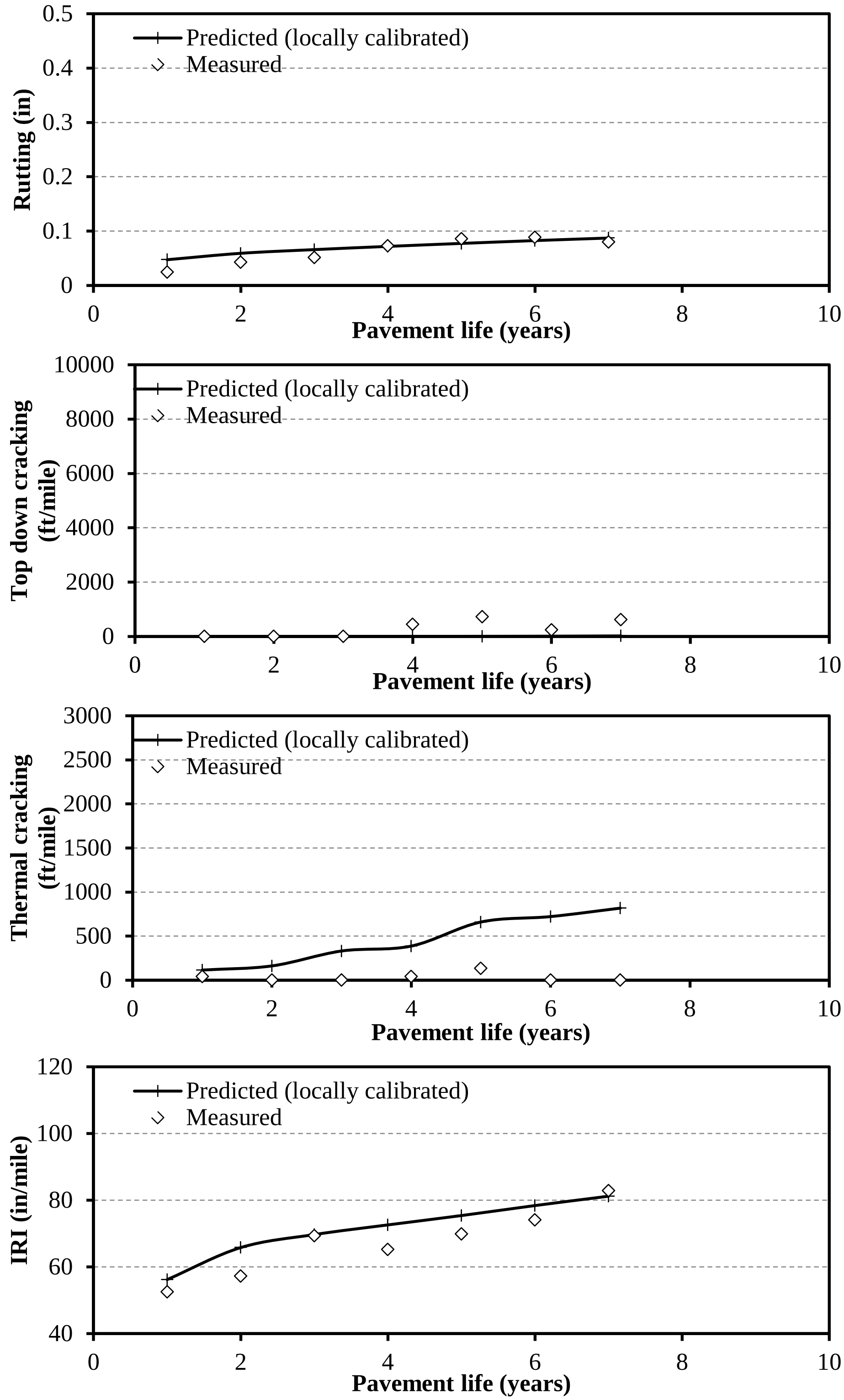

Figure E.2: Measured and Predicted Performance Data by the Locally Calibrated MEPDG for Project 007U0007500-NB

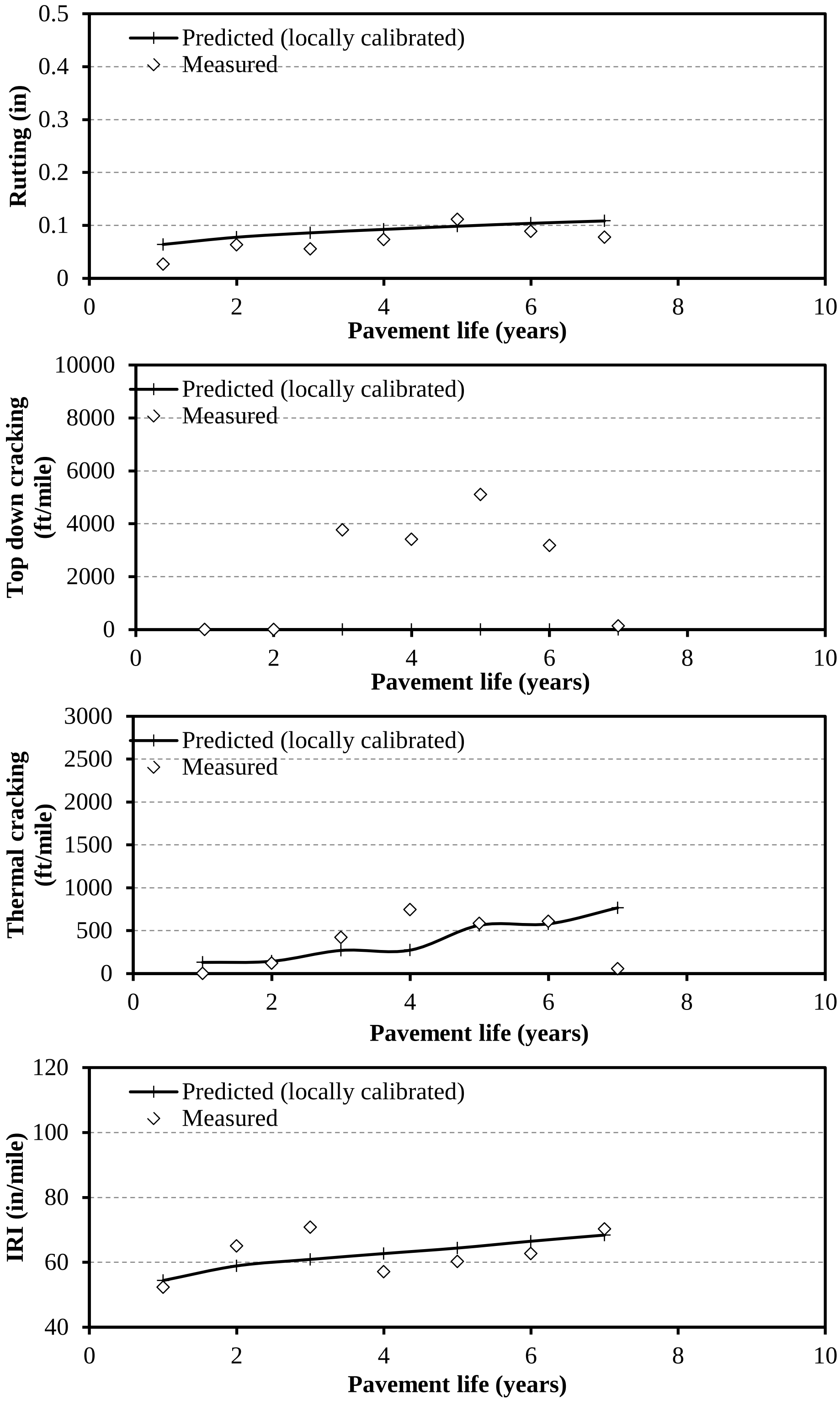

Figure E.3: Measured and Predicted Performance Data by the Locally Calibrated MEPDG for Project 008U0005400-EB

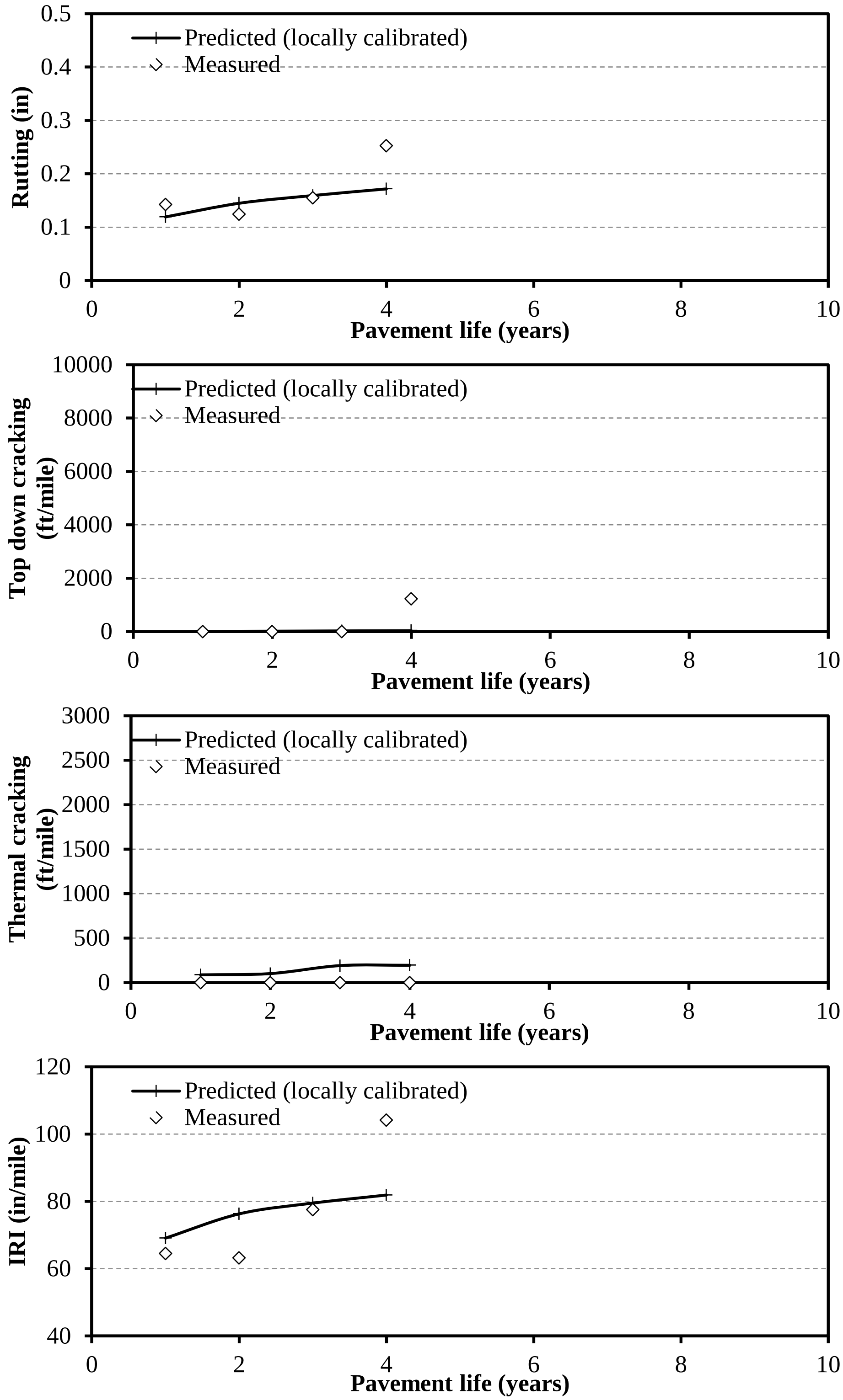

Figure E.4: Measured and Predicted Performance Data by the Locally Calibrated MEPDG for Project 008U0007700-NB-1

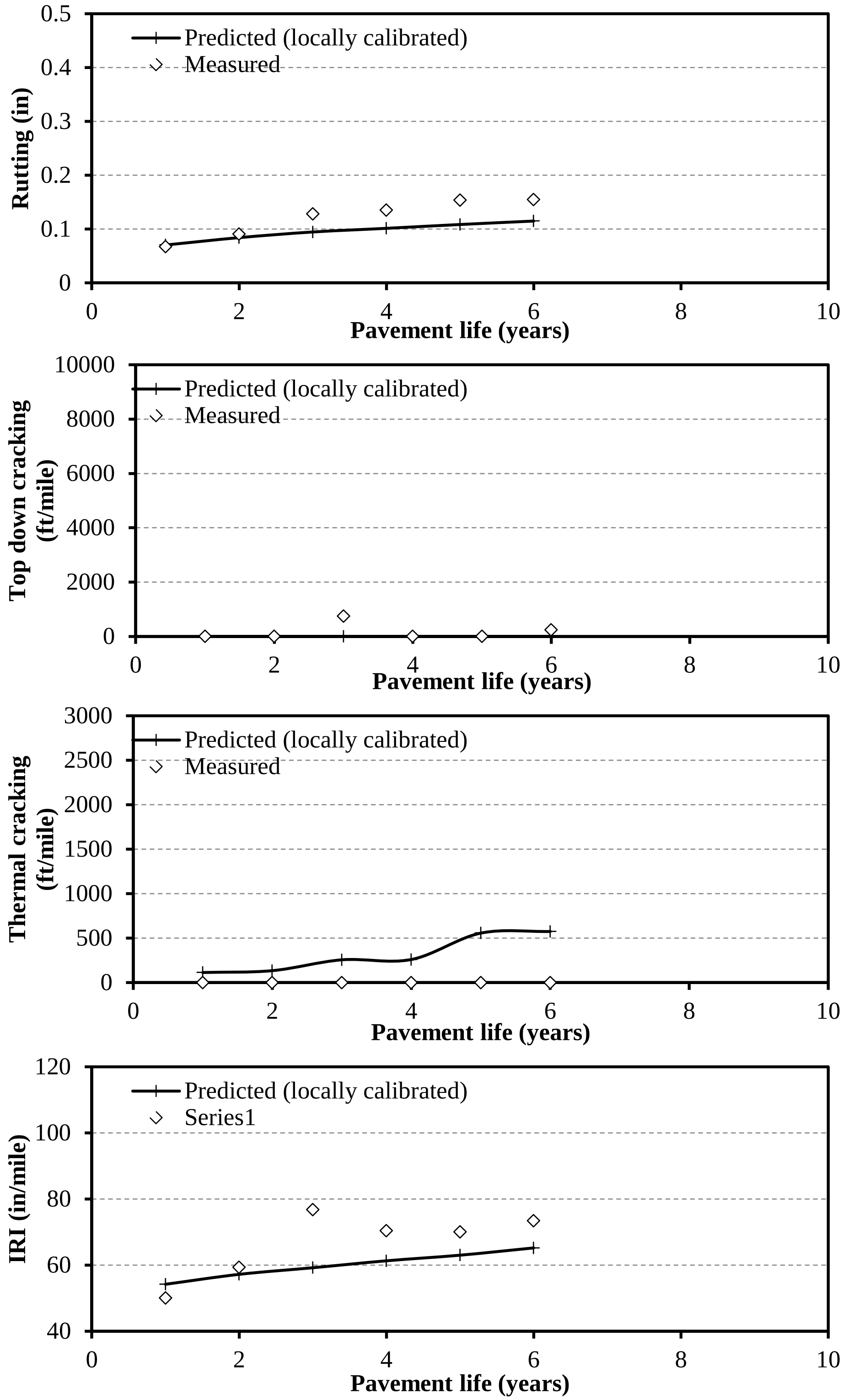

Figure E.5: Measured and Predicted Performance Data by the Locally Calibrated MEPDG for Project 008U0007700-NB-2

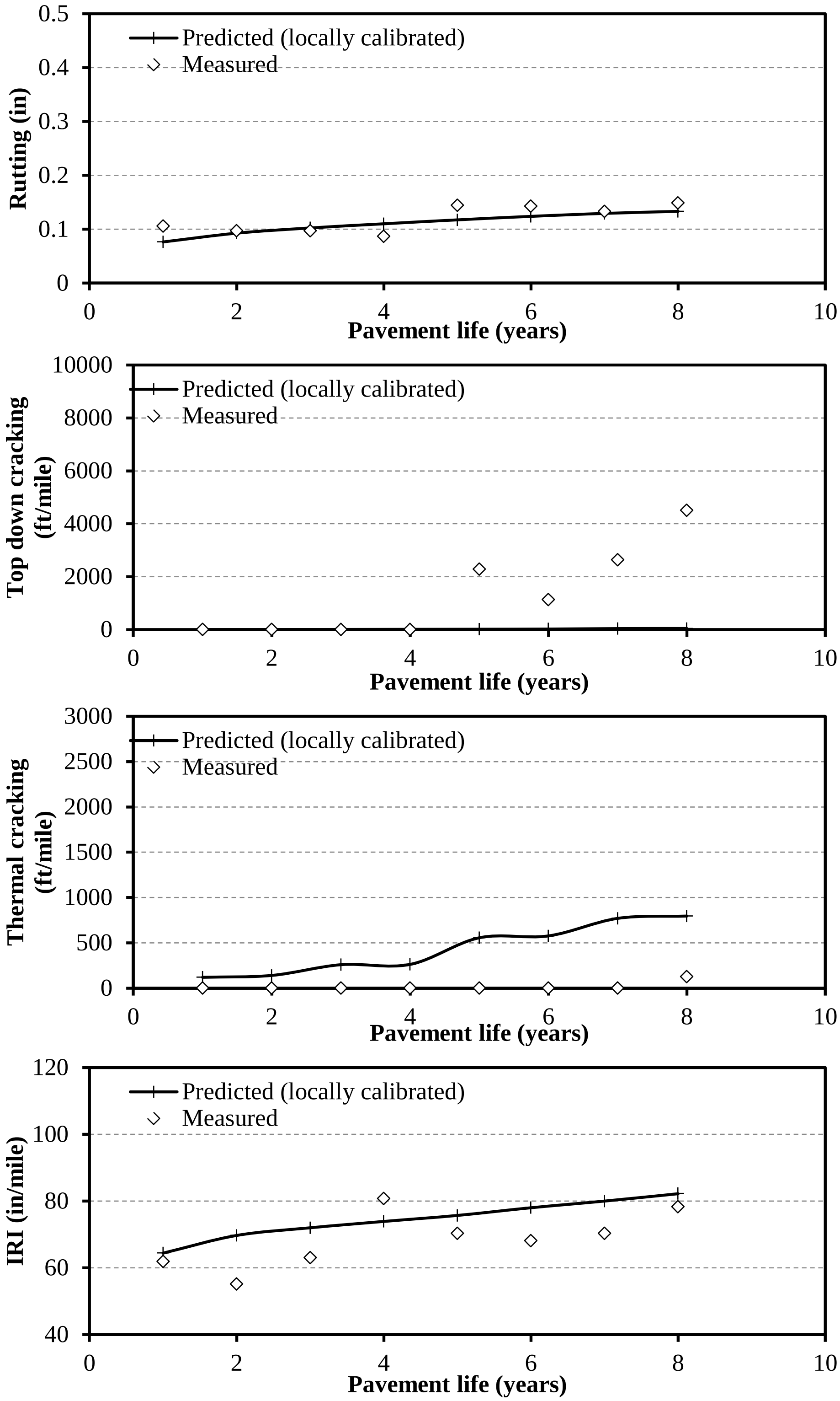

Figure E.6: Measured and Predicted Performance Data by the Locally Calibrated MEPDG for Project 008U0007700-NB-3

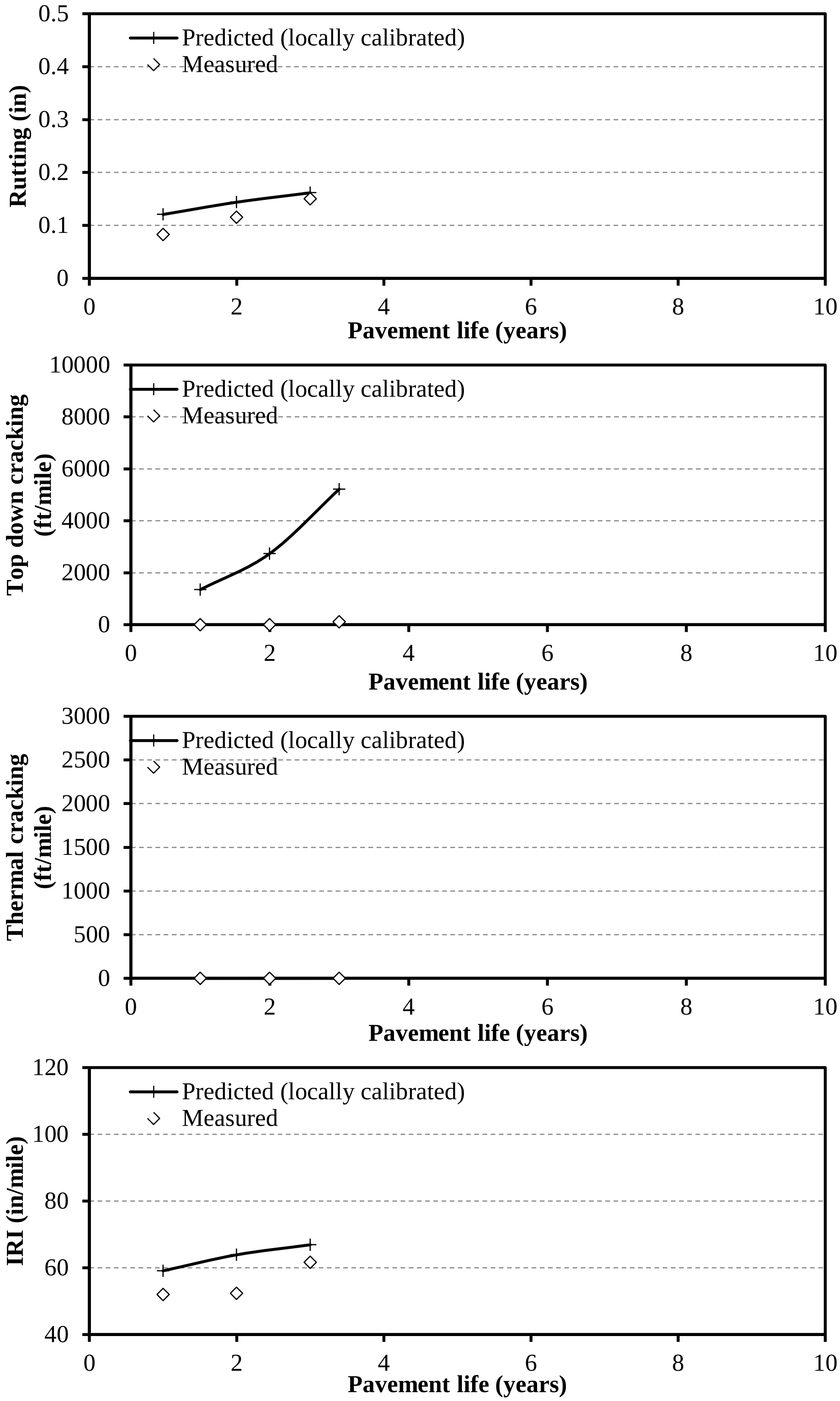

Figure E.7: Measured and Predicted Performance Data by the Locally Calibrated MEPDG for Project 011U0006900-NB

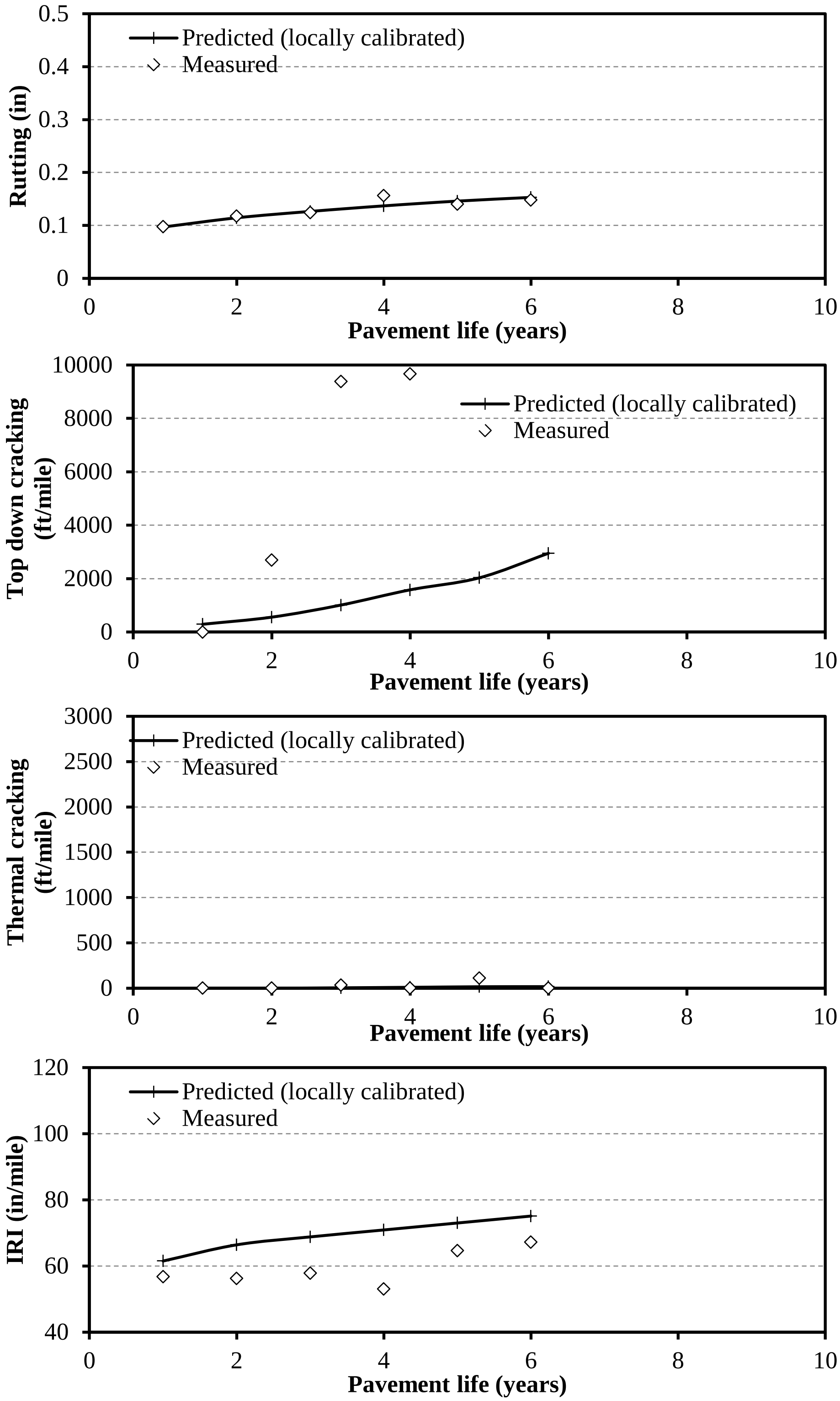

Figure E.8: Measured and Predicted Performance Data by the Locally Calibrated MEPDG for Project 019K0000700-NB-1

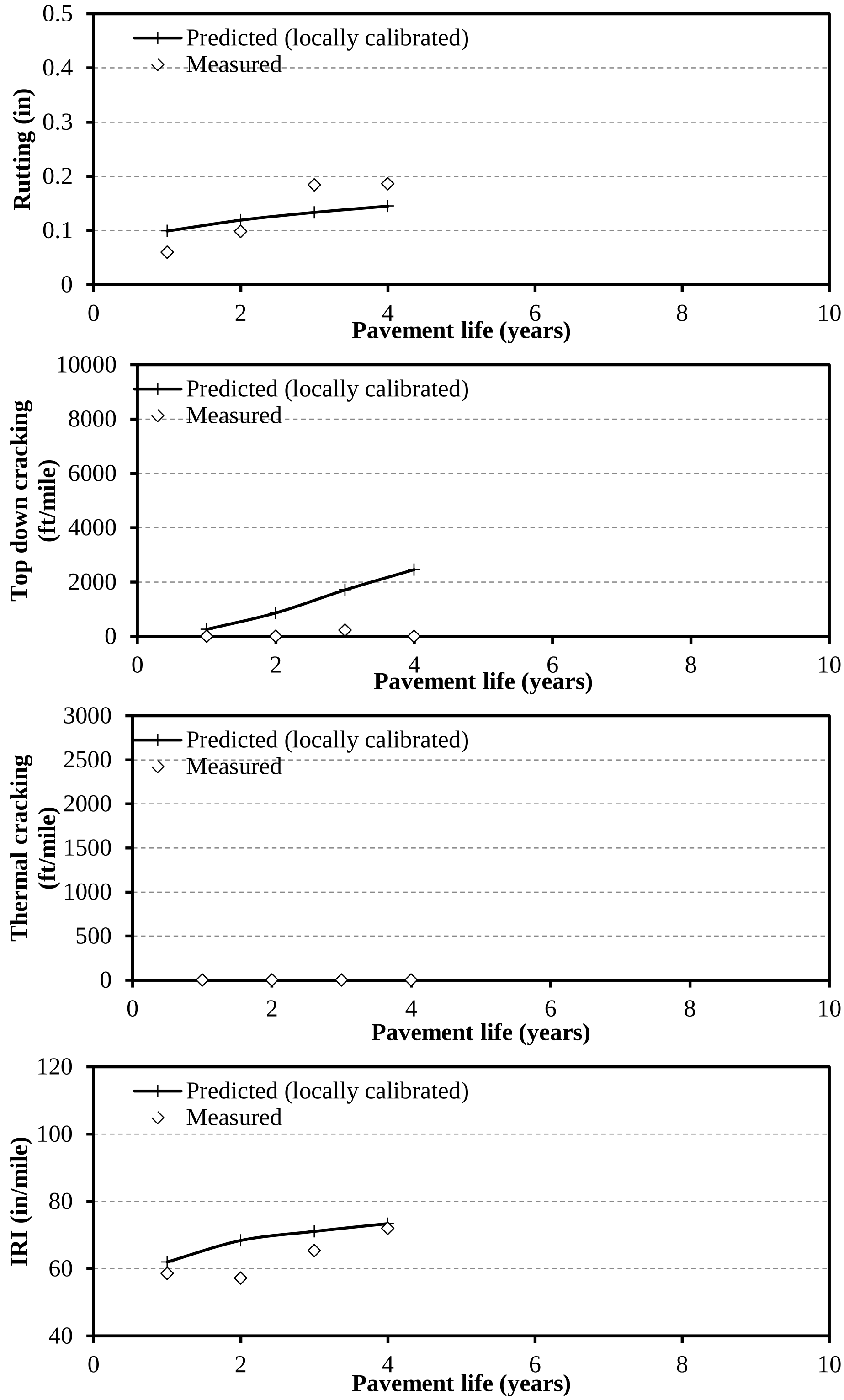

Figure E.9: Measured and Predicted Performance Data by the Locally Calibrated MEPDG for Project 019K0000700-NB-2

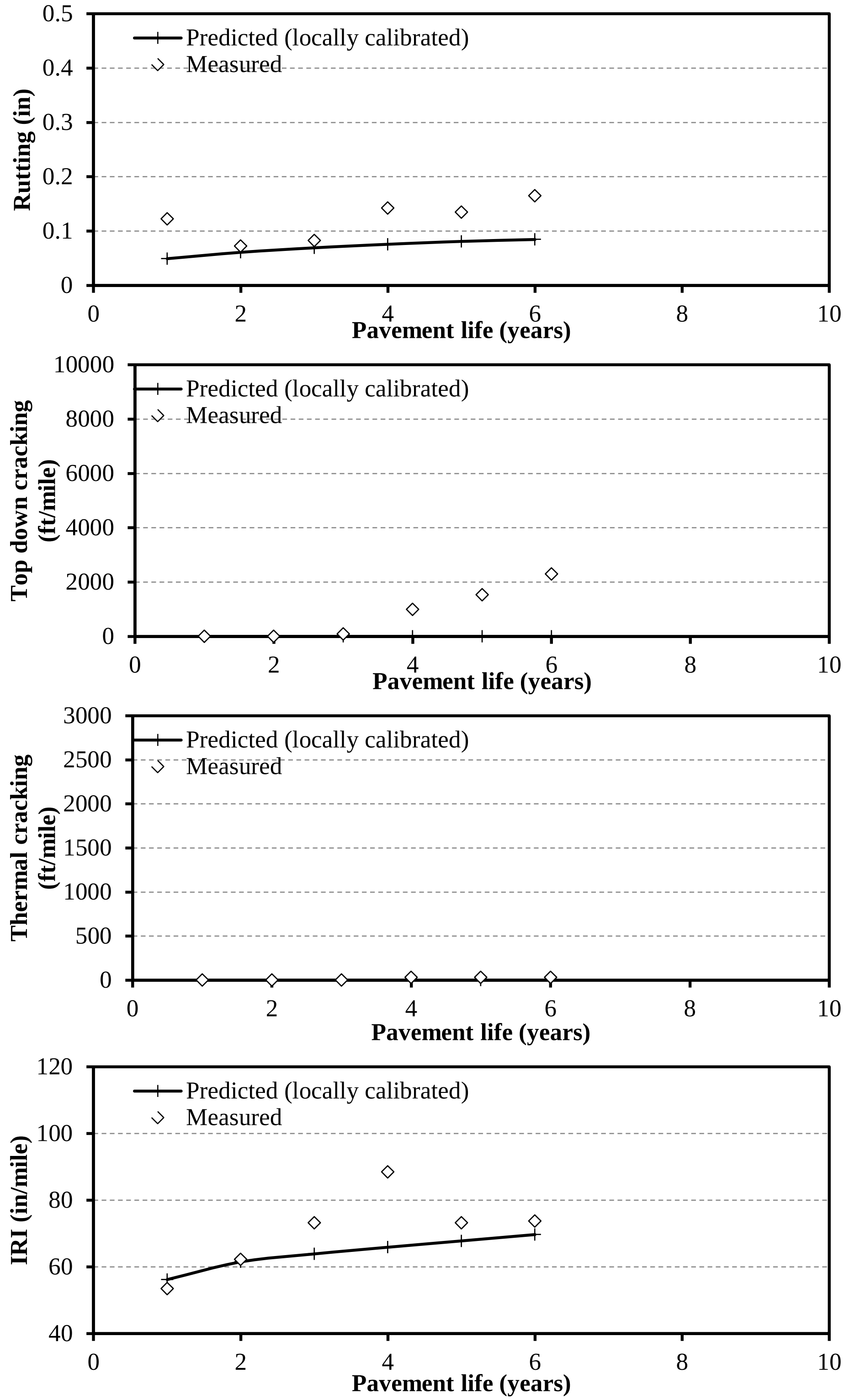

Figure E.10: Measured and Predicted Performance Data by the Locally Calibrated MEPDG for Project 019U0016000-EB

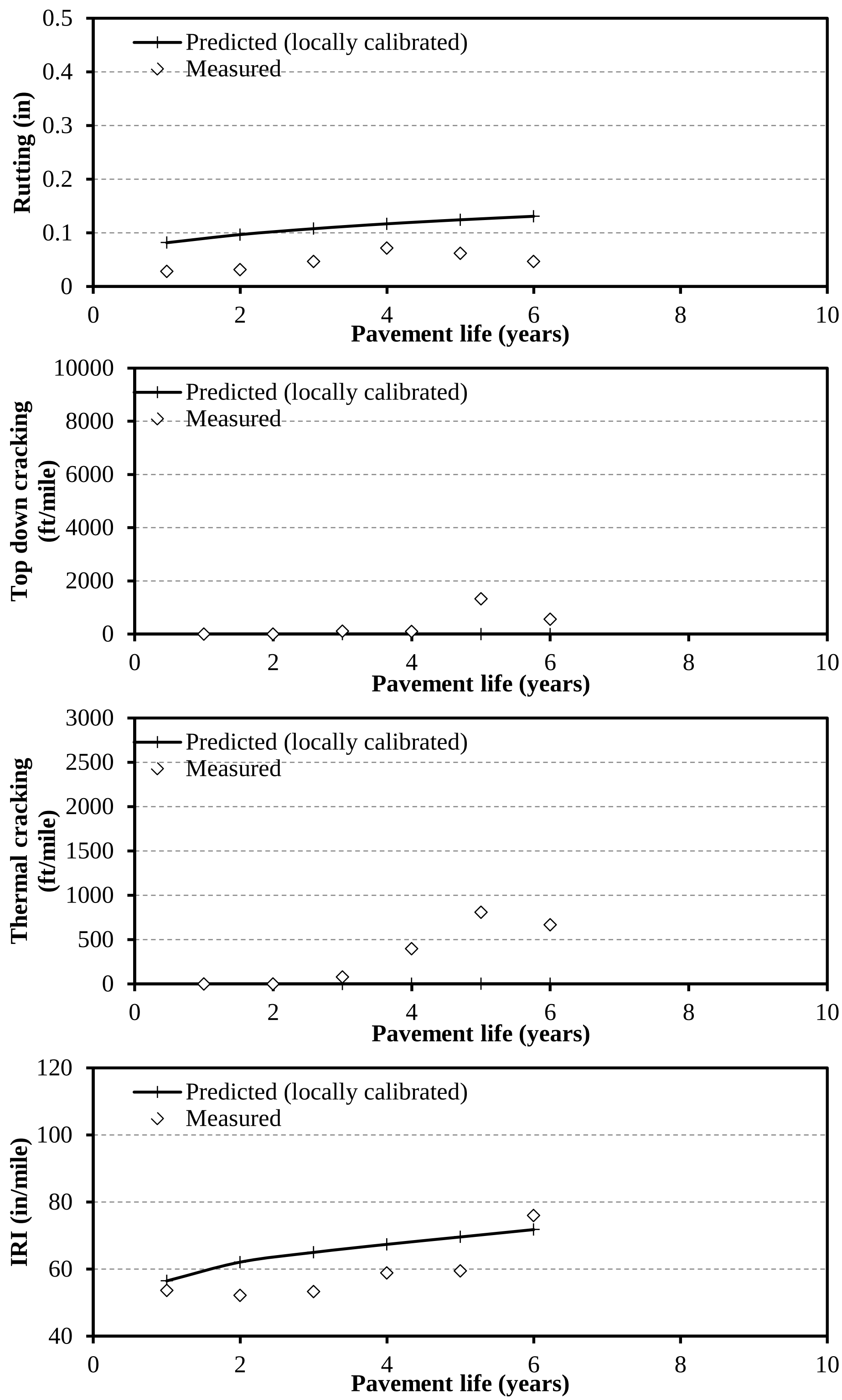

Figure E.11: Measured and Predicted Performance Data by the Locally Calibrated MEPDG for Project 022K0000700-NB

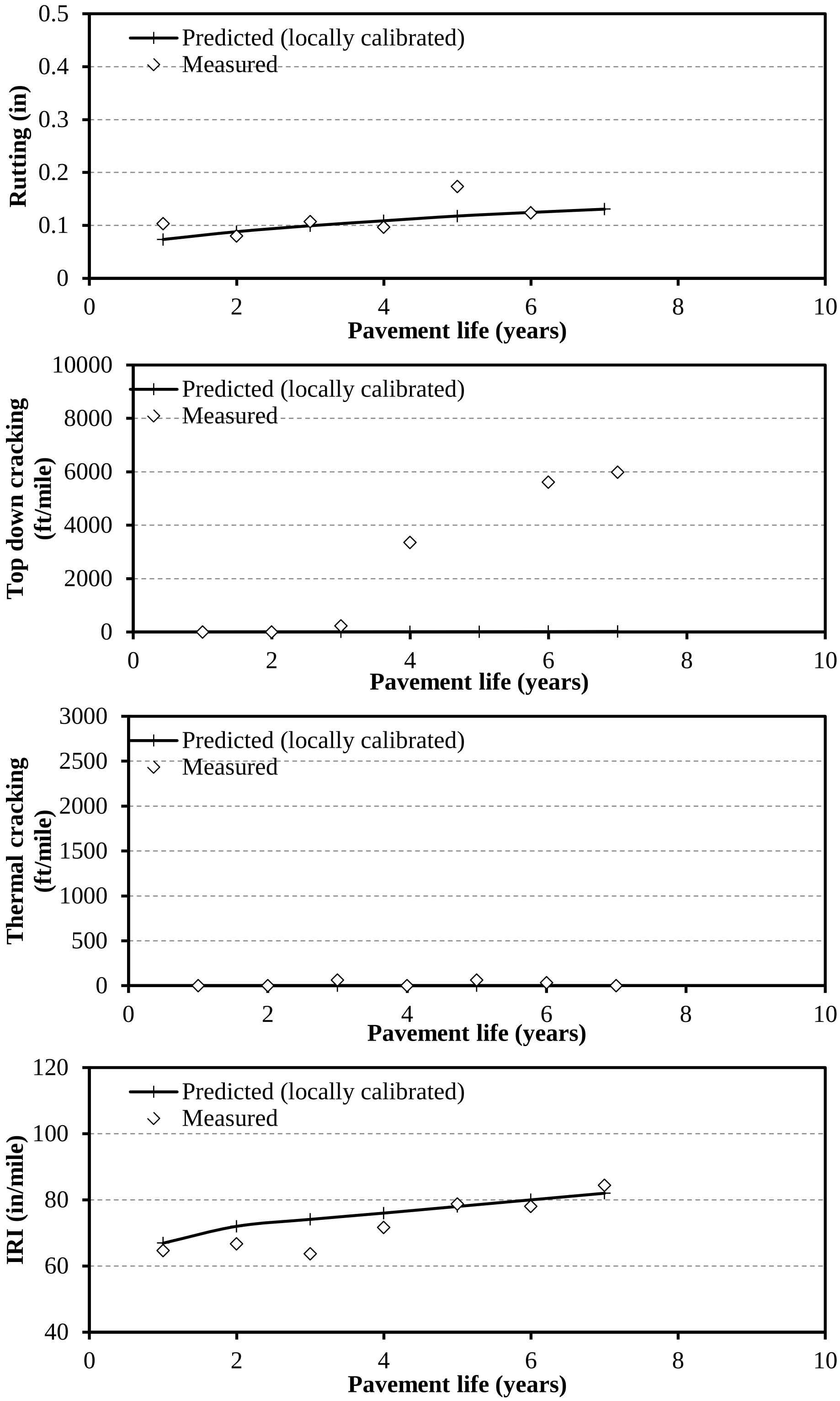

Figure E.12: Measured and Predicted Performance Data by the Locally Calibrated MEPDG for Project 023U0004000-EB

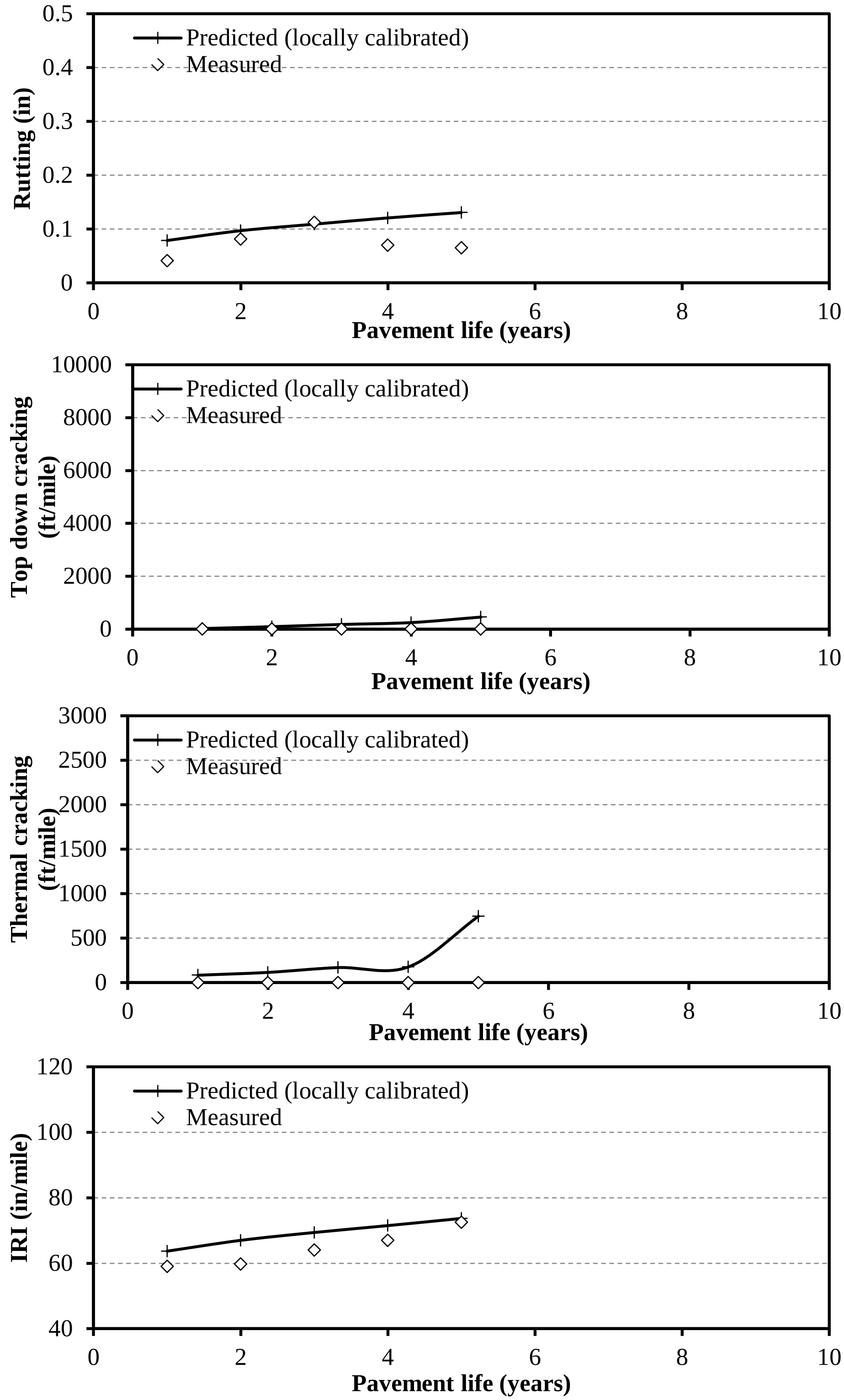

Figure E.13: Measured and Predicted Performance Data by the Locally Calibrated MEPDG for Project 025K0009900-NB

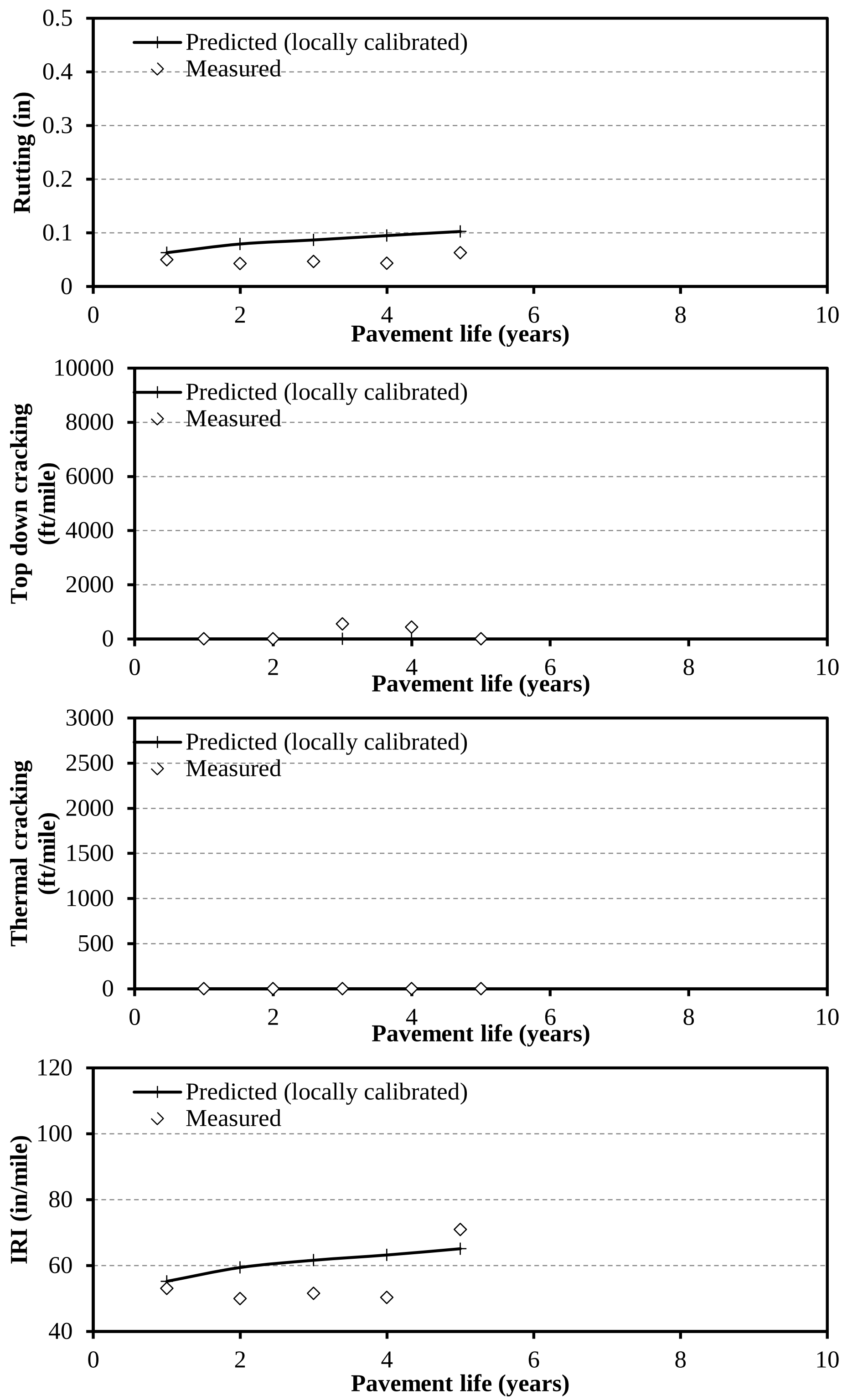

Figure E.14: Measured and Predicted Performance Data by the Locally Calibrated MEPDG for Project 027K0015600-EB

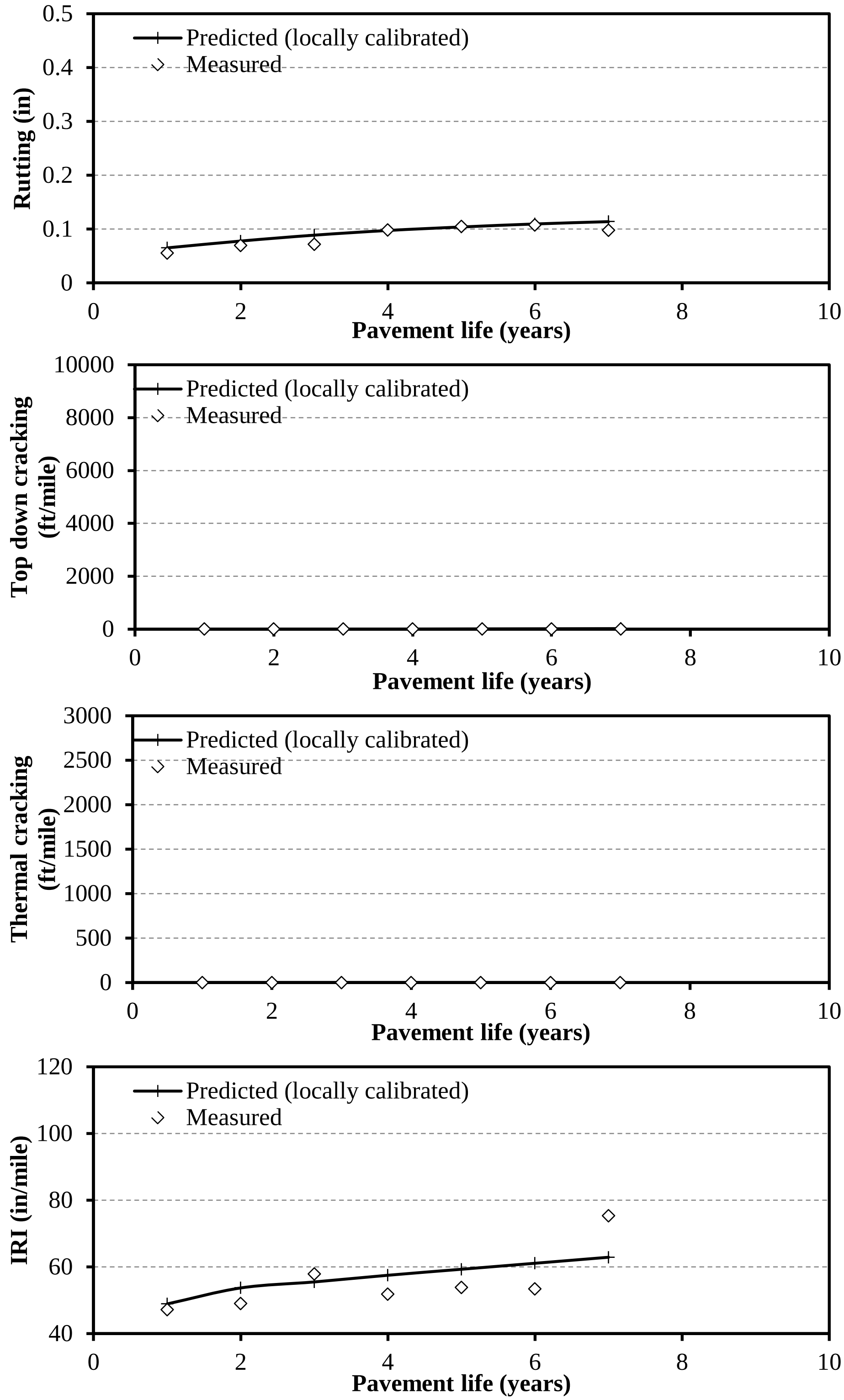

Figure E.15: Measured and Predicted Performance Data by the Locally Calibrated MEPDG for Project 028U0005000-EB

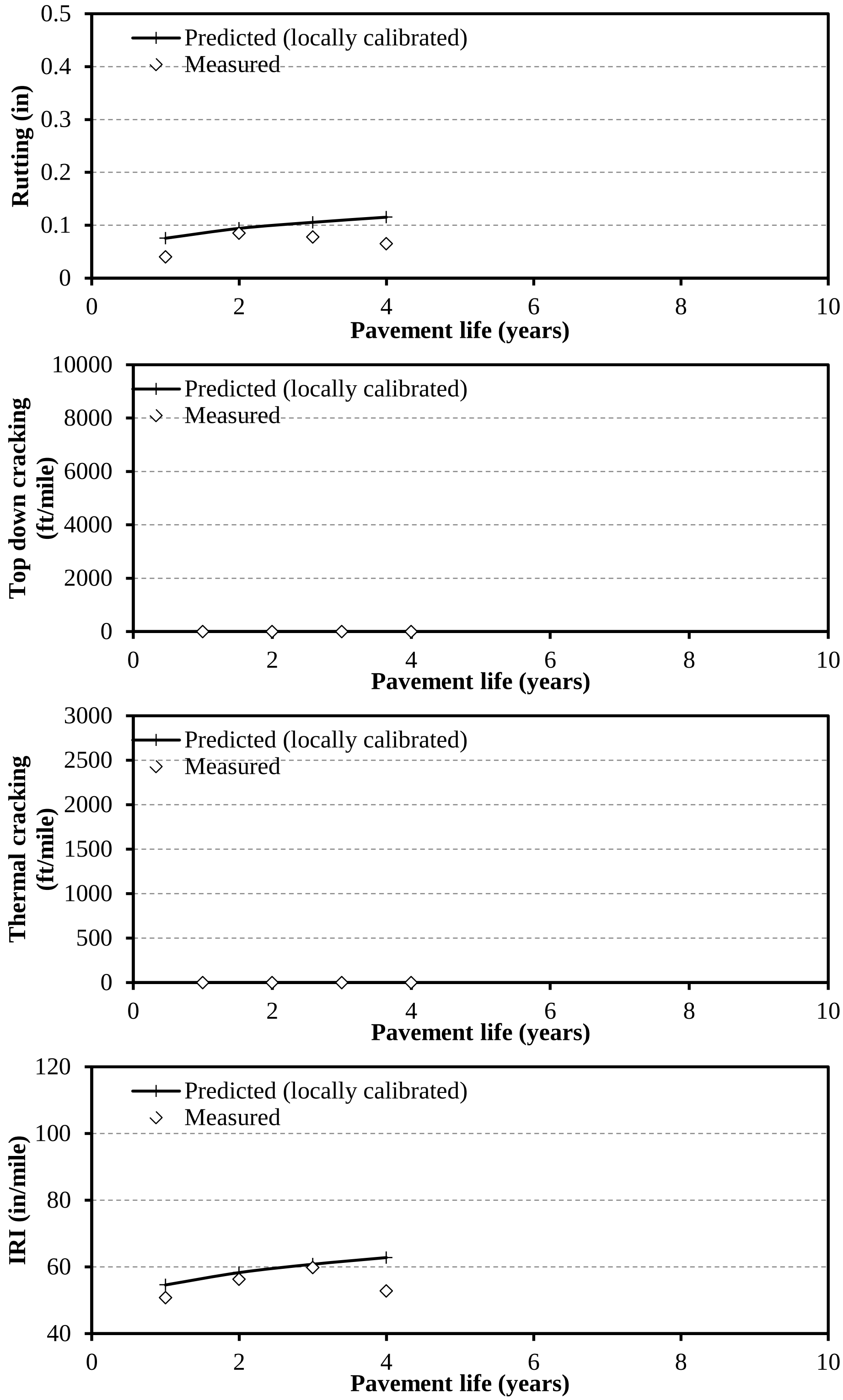

Figure E.16: Measured and Predicted Performance Data by the Locally Calibrated MEPDG for Project 031K0001800-WB

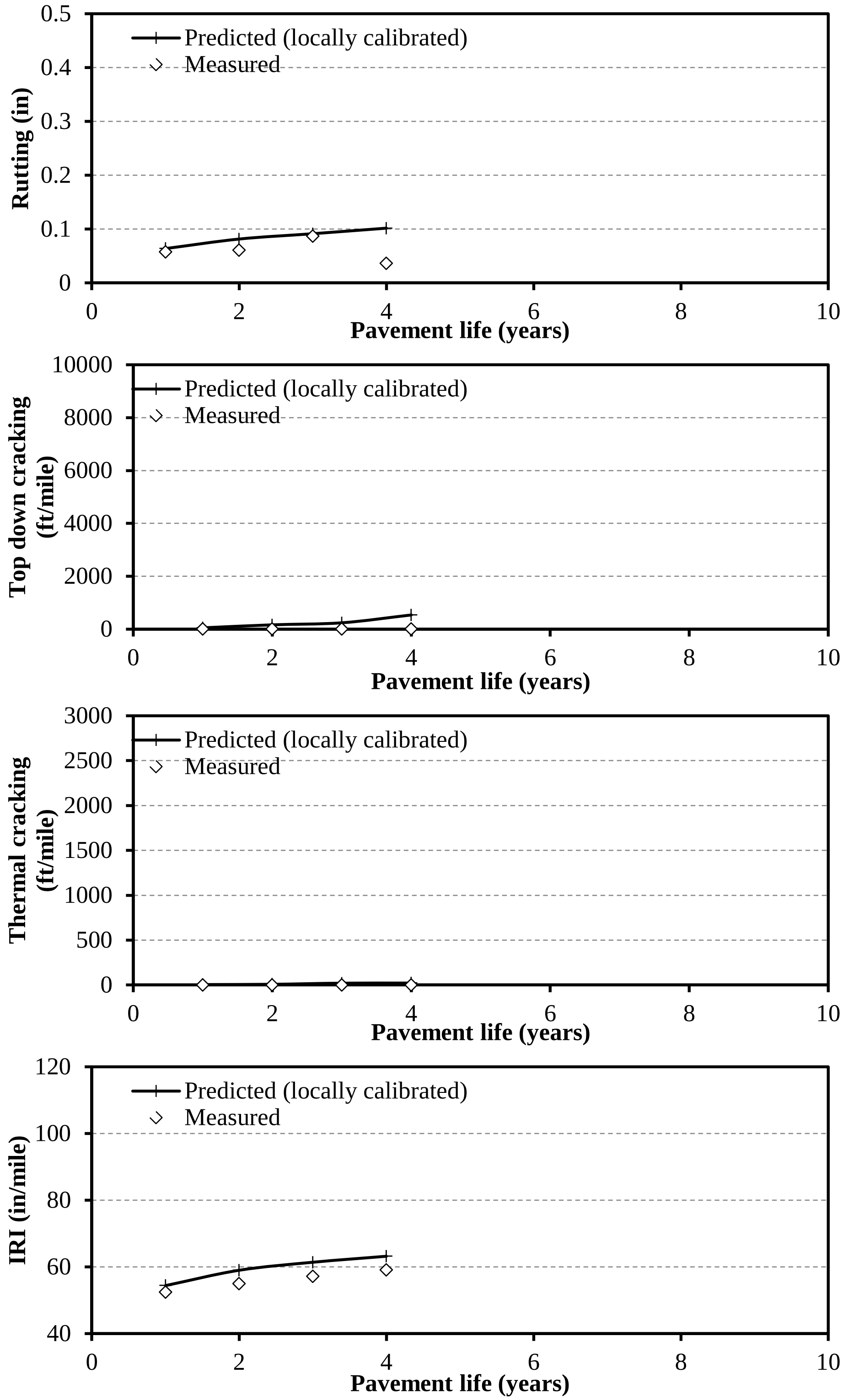

Figure E.17: Measured and Predicted Performance Data by the Locally Calibrated MEPDG for Project 033U0028300-NB

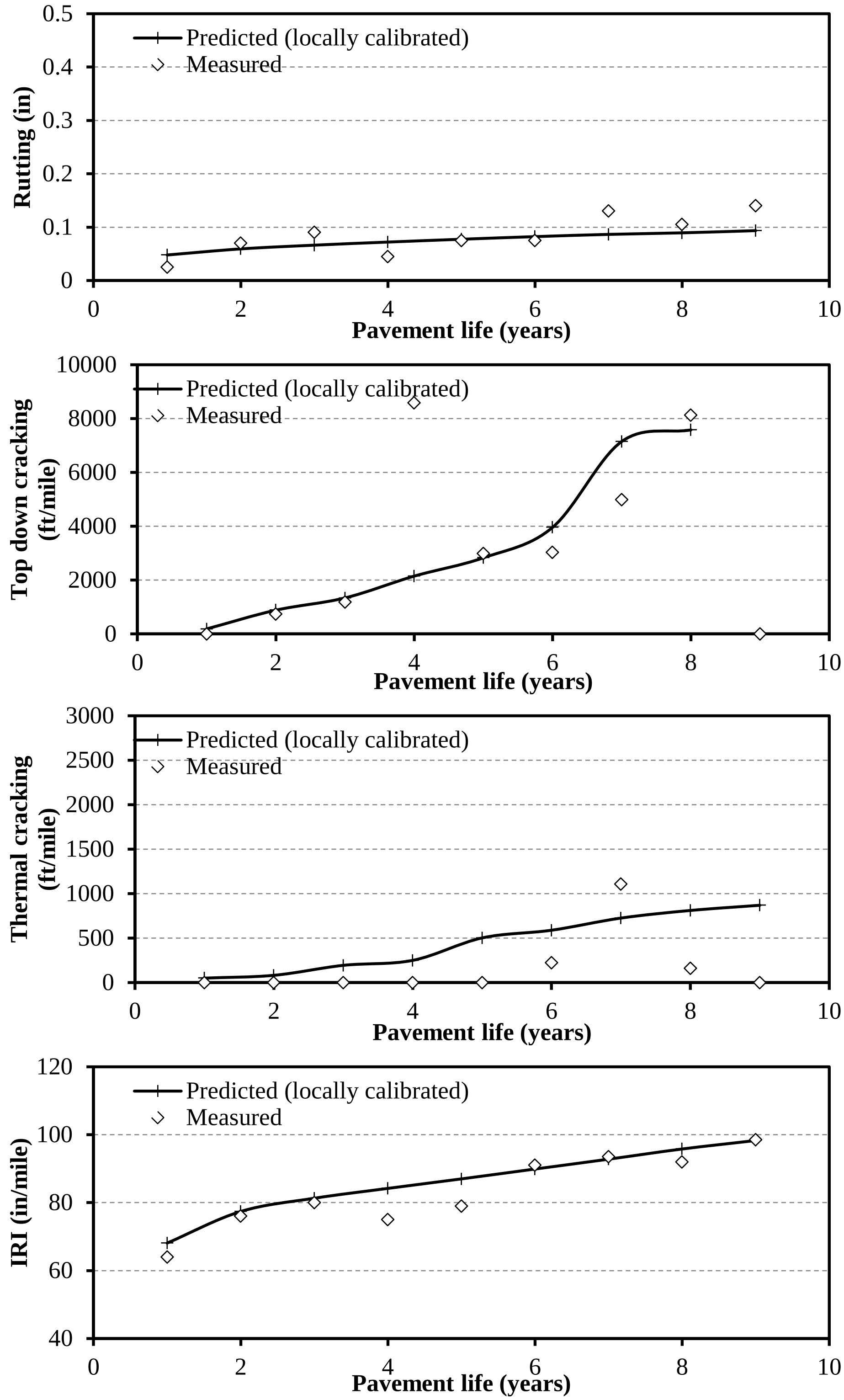

Figure E.18: Measured and Predicted Performance Data by the Locally Calibrated MEPDG for Project 052U0007300-NB

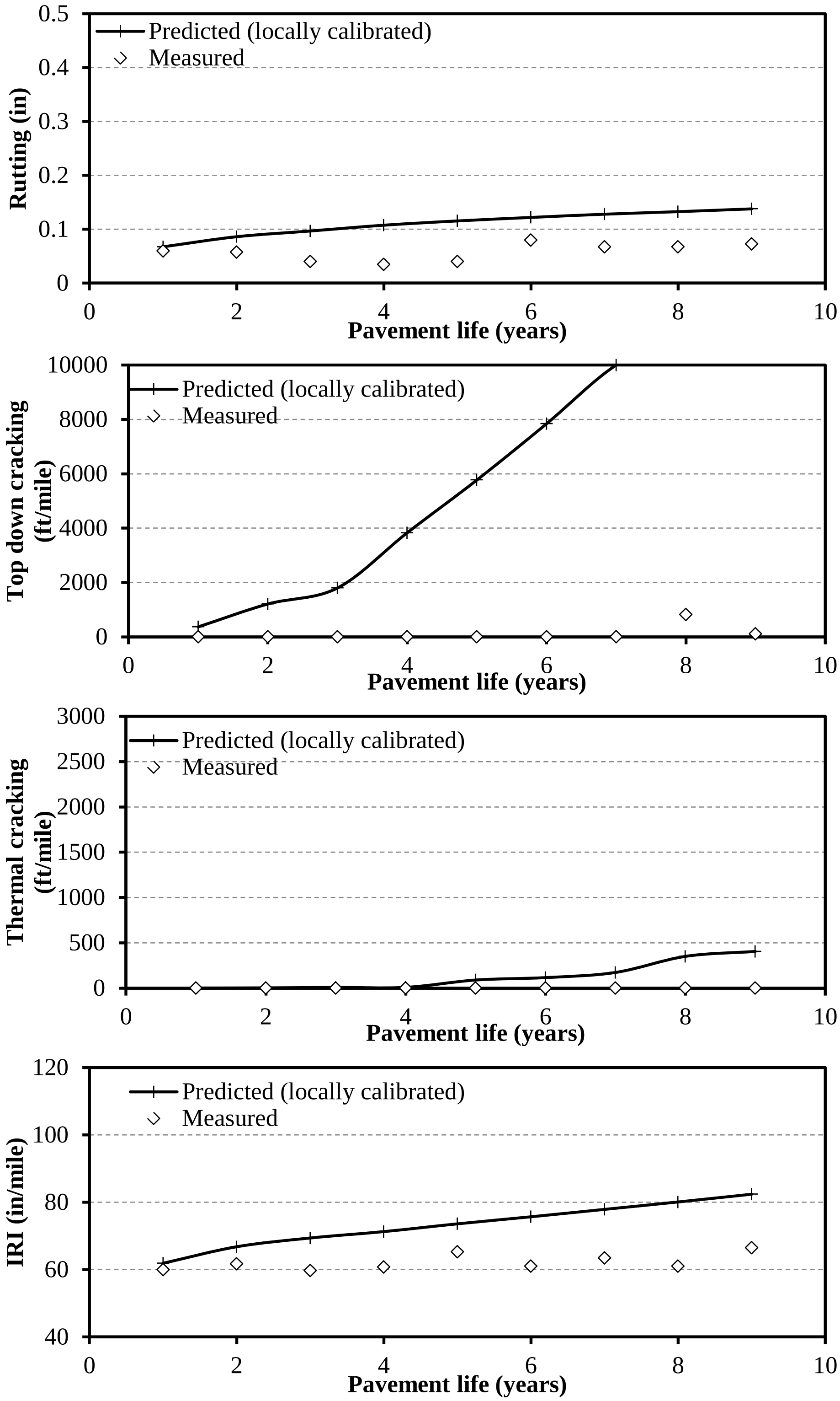

Figure E.19: Measured and Predicted Performance Data by the Locally Calibrated MEPDG for Project 065K0002700-NB

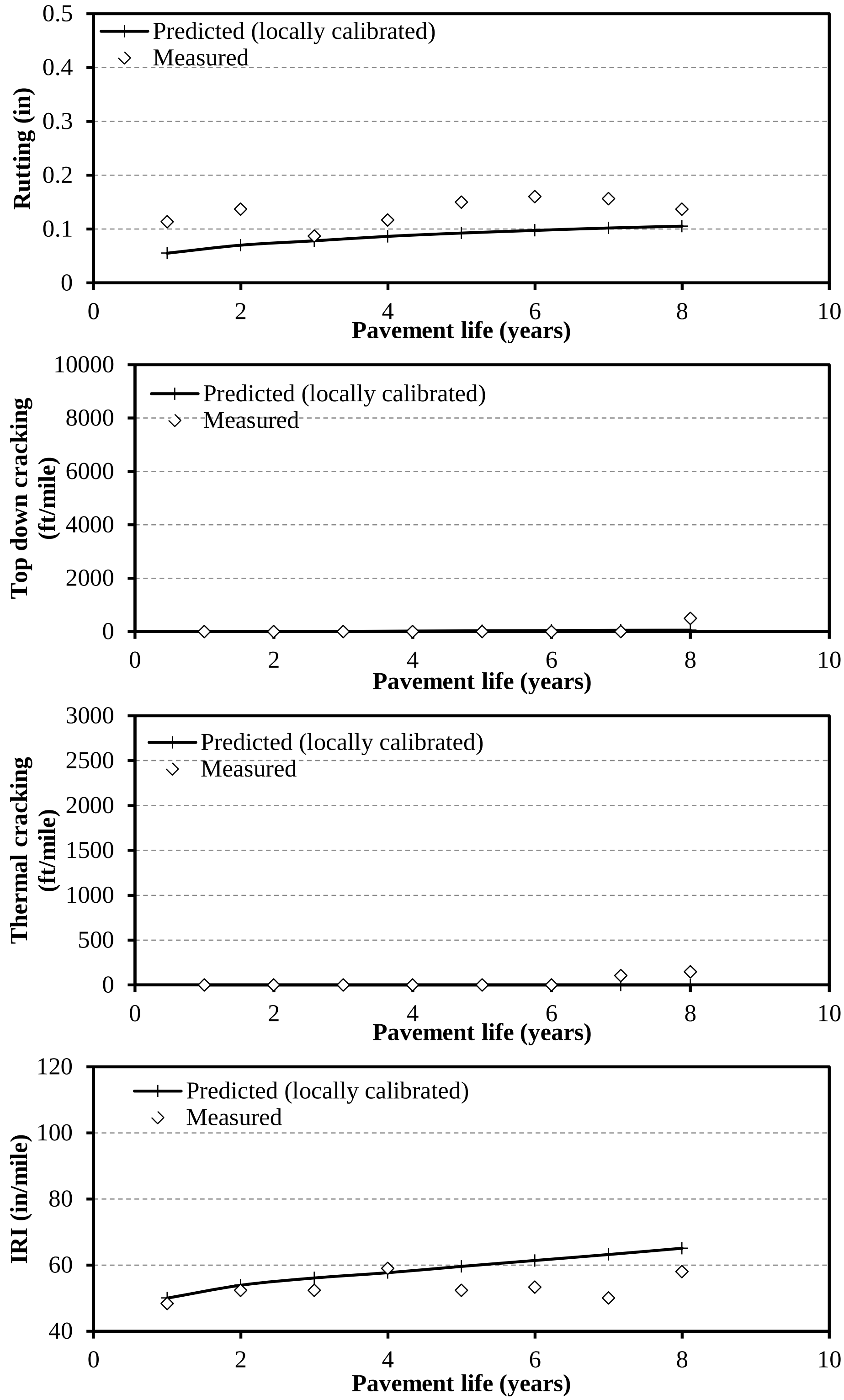

Figure E.20: Measured and Predicted Performance Data by the Locally Calibrated MEPDG for Project 065U0005600-EB

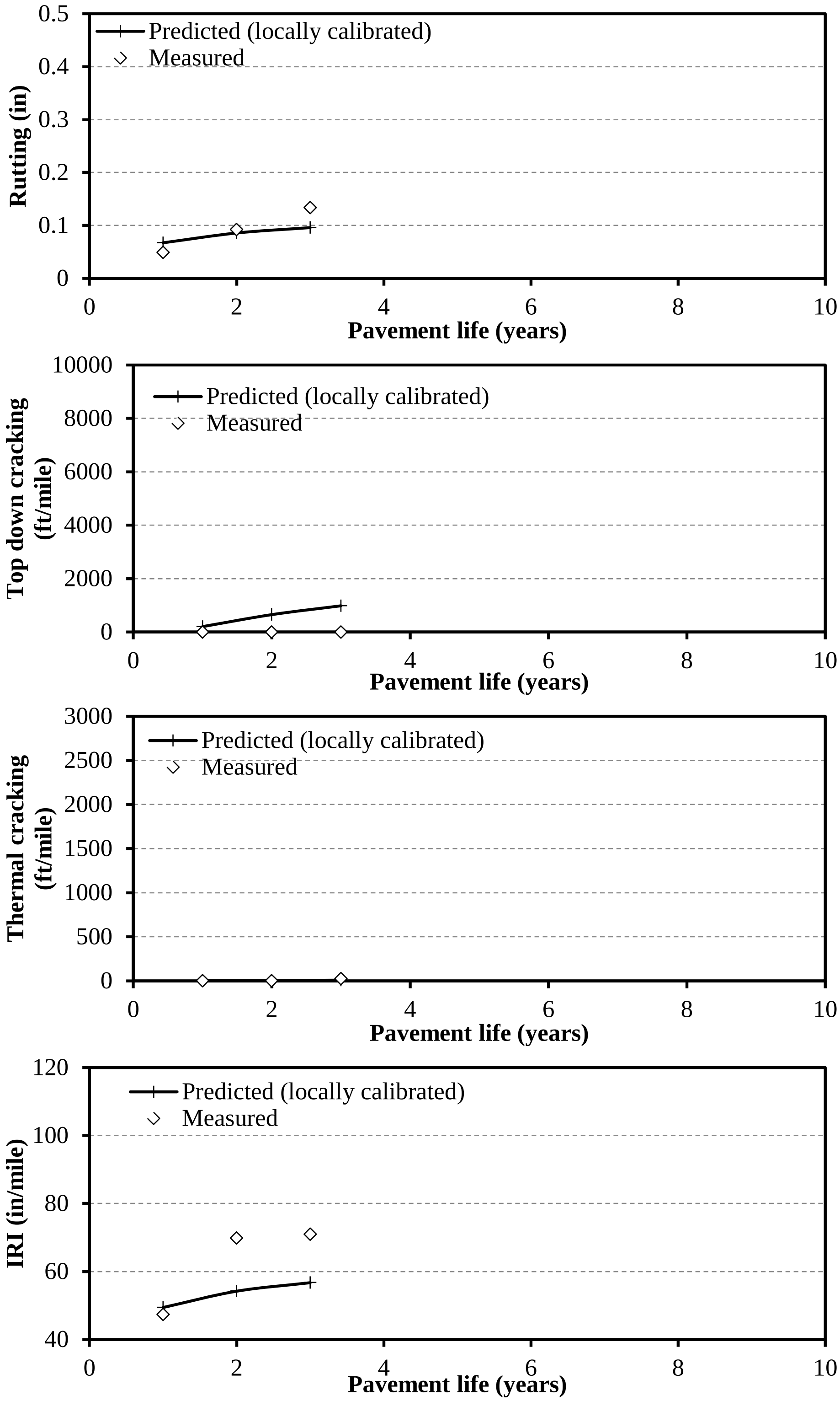

Figure E.21: Measured and Predicted Performance Data by the Locally Calibrated MEPDG for Project 069U0028300-NB

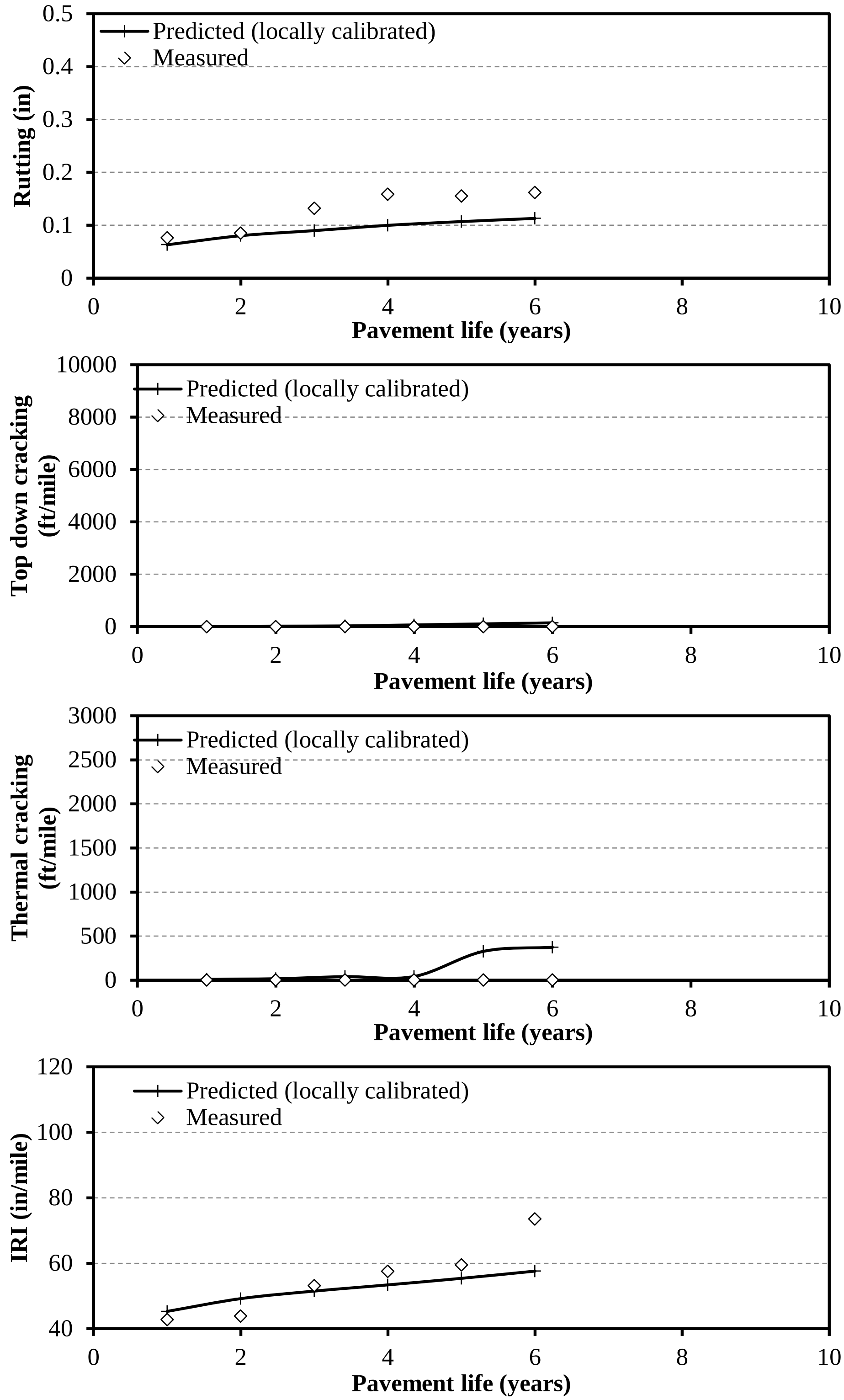

Figure E.22: Measured and Predicted Performance Data by the Locally Calibrated MEPDG for Project 082U0018300-NB

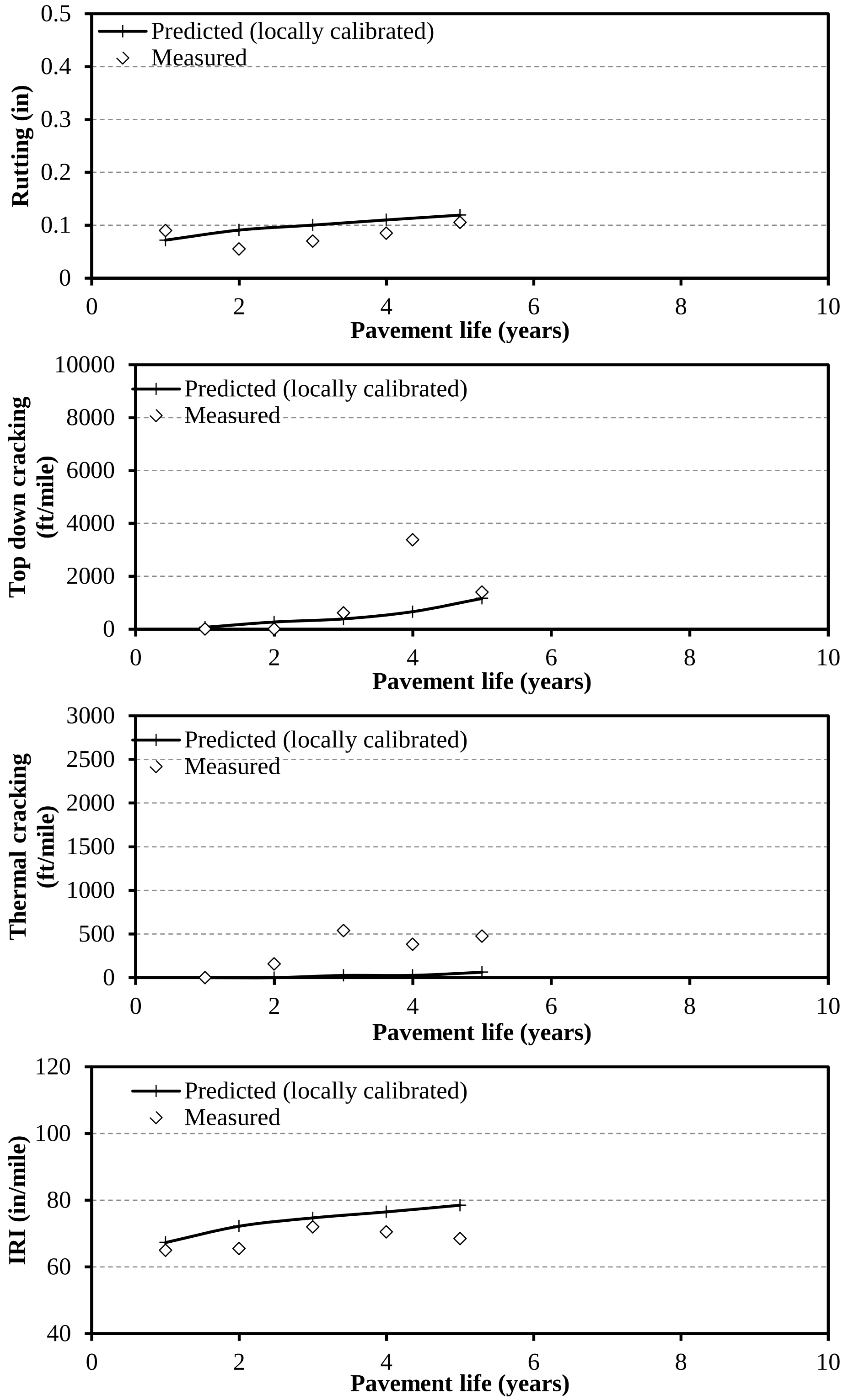

Figure E.23: Measured and Predicted Performance Data by the Locally Calibrated MEPDG for Project 084U0028100-NB

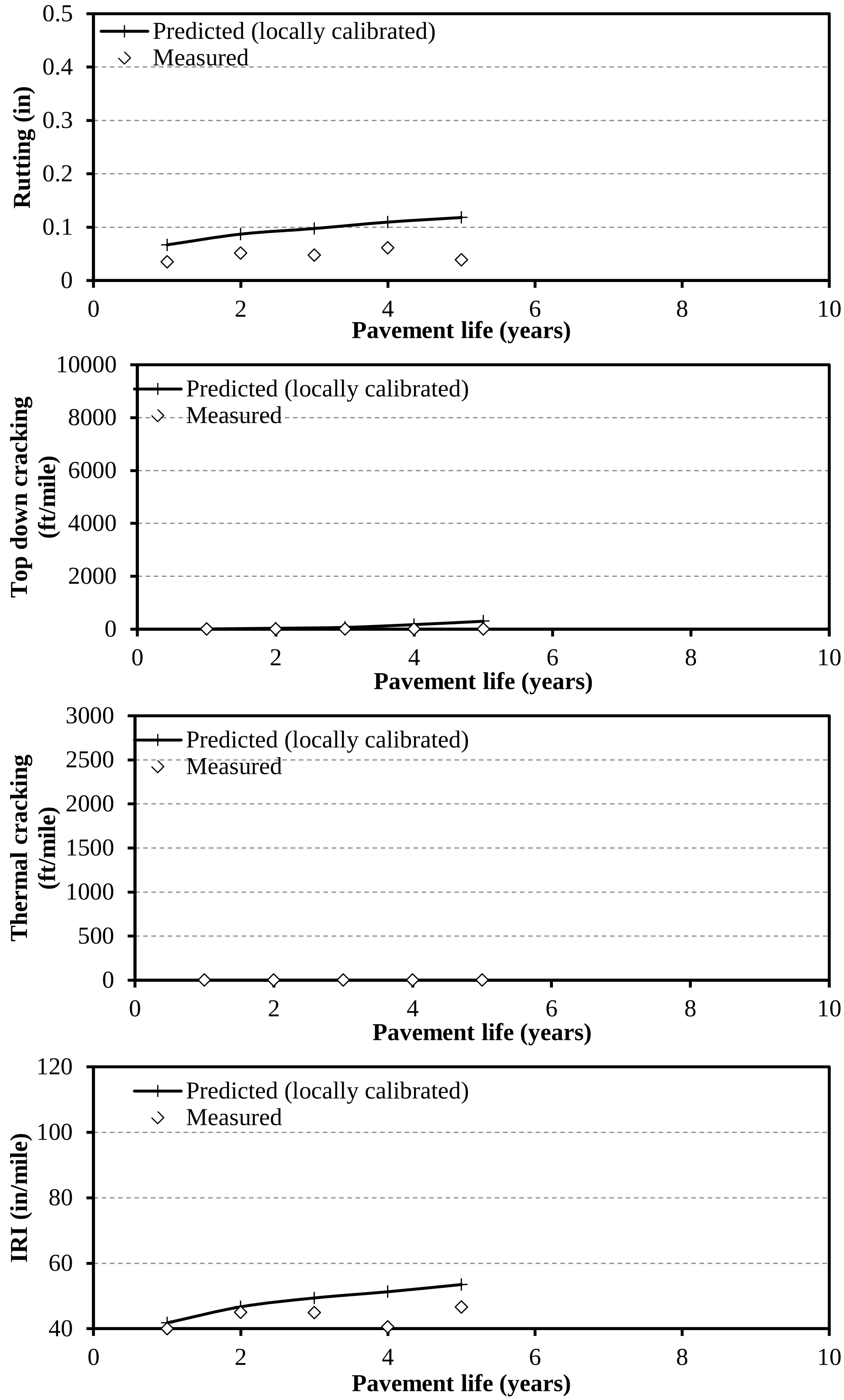

Figure E.24: Measured and Predicted Performance Data by the Locally Calibrated MEPDG for Project 088U0005400-WB

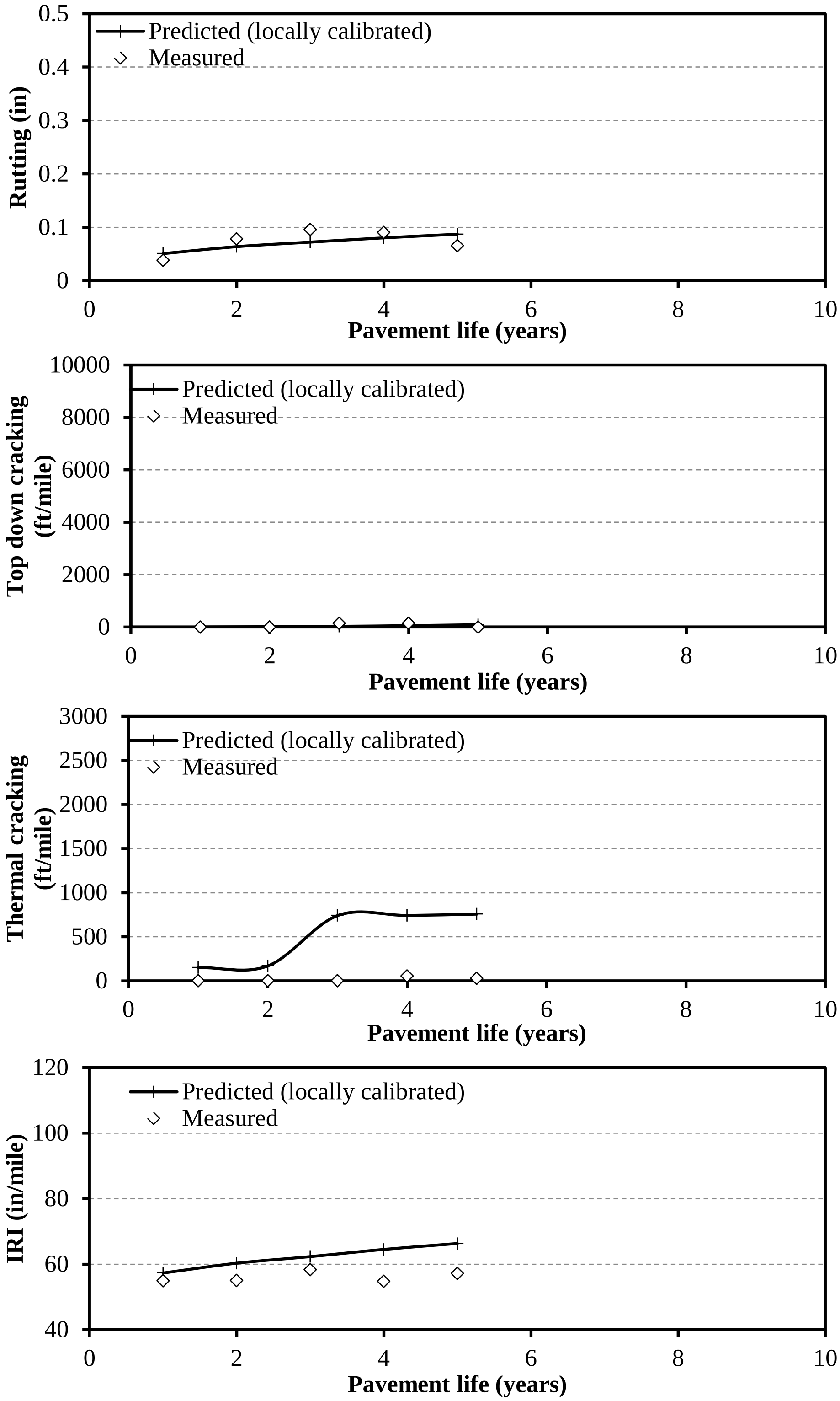

Figure E.25: Measured and Predicted Performance Data by the Locally Calibrated MEPDG for Project 091K0002700-NB

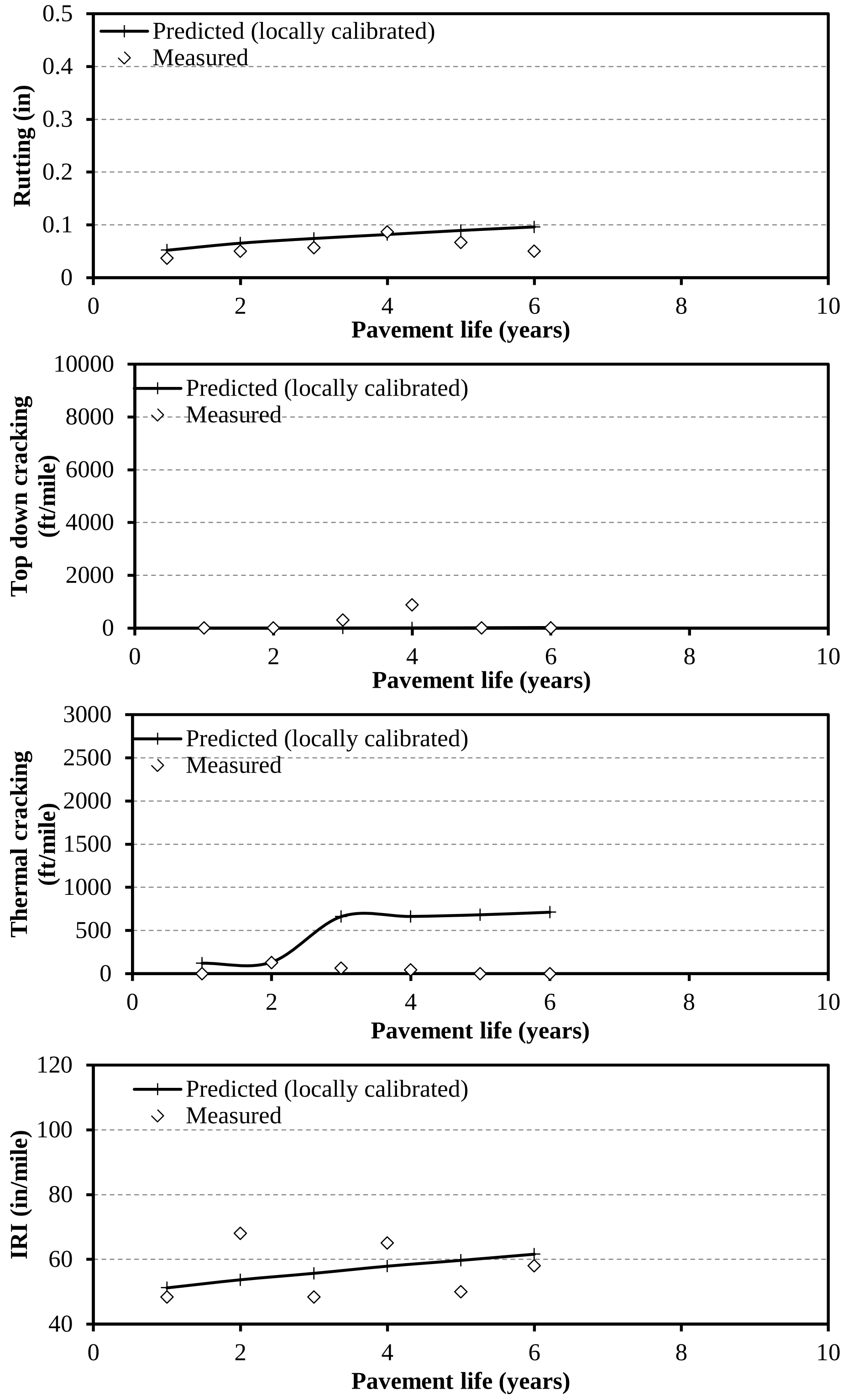

Figure E.26: Measured and Predicted Performance Data by the Locally Calibrated MEPDG for Project 095U0005600-EB

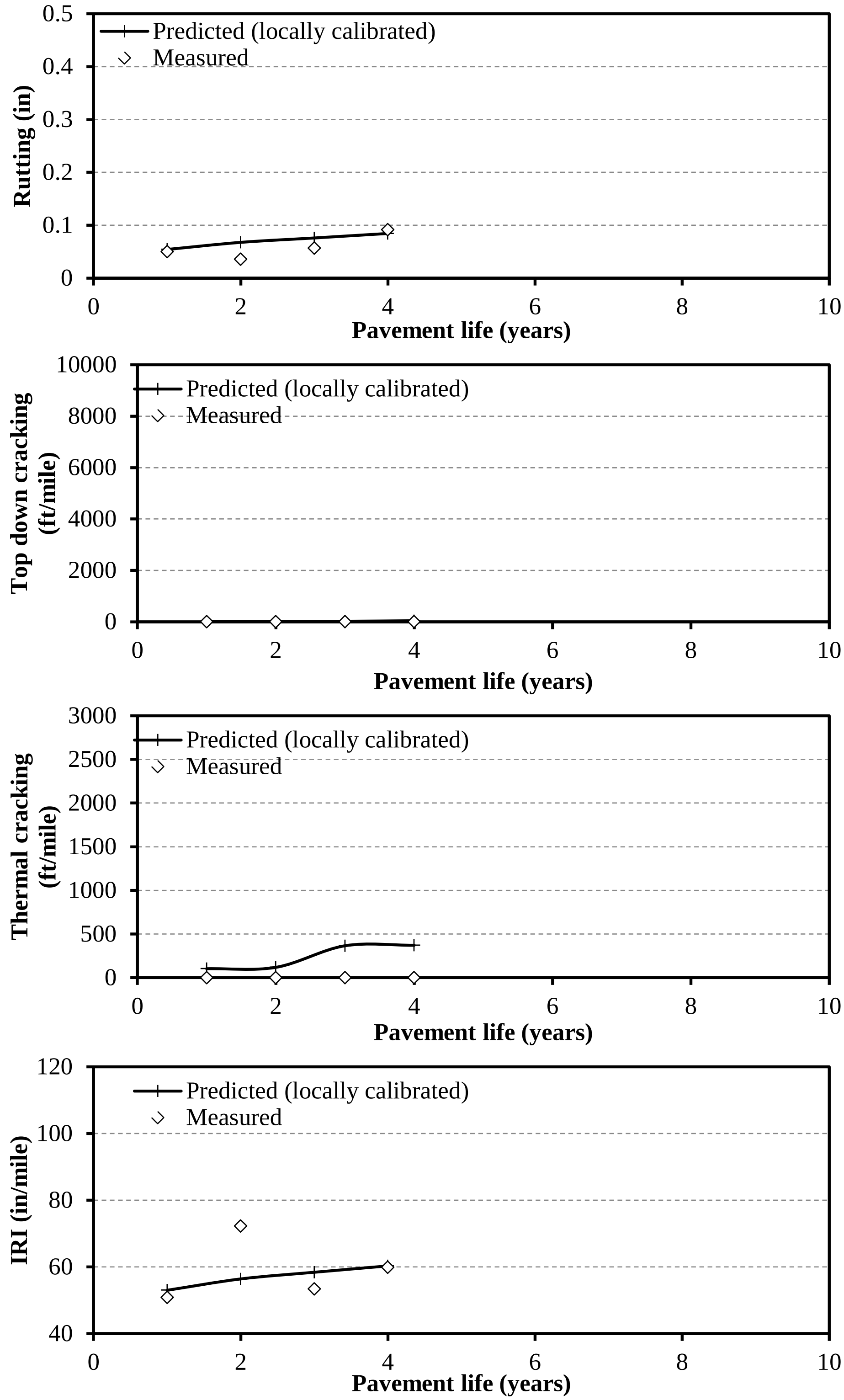

Figure E.27: Measured and Predicted Performance Data by the Locally Calibrated MEPDG for Project 098U0028300-NB

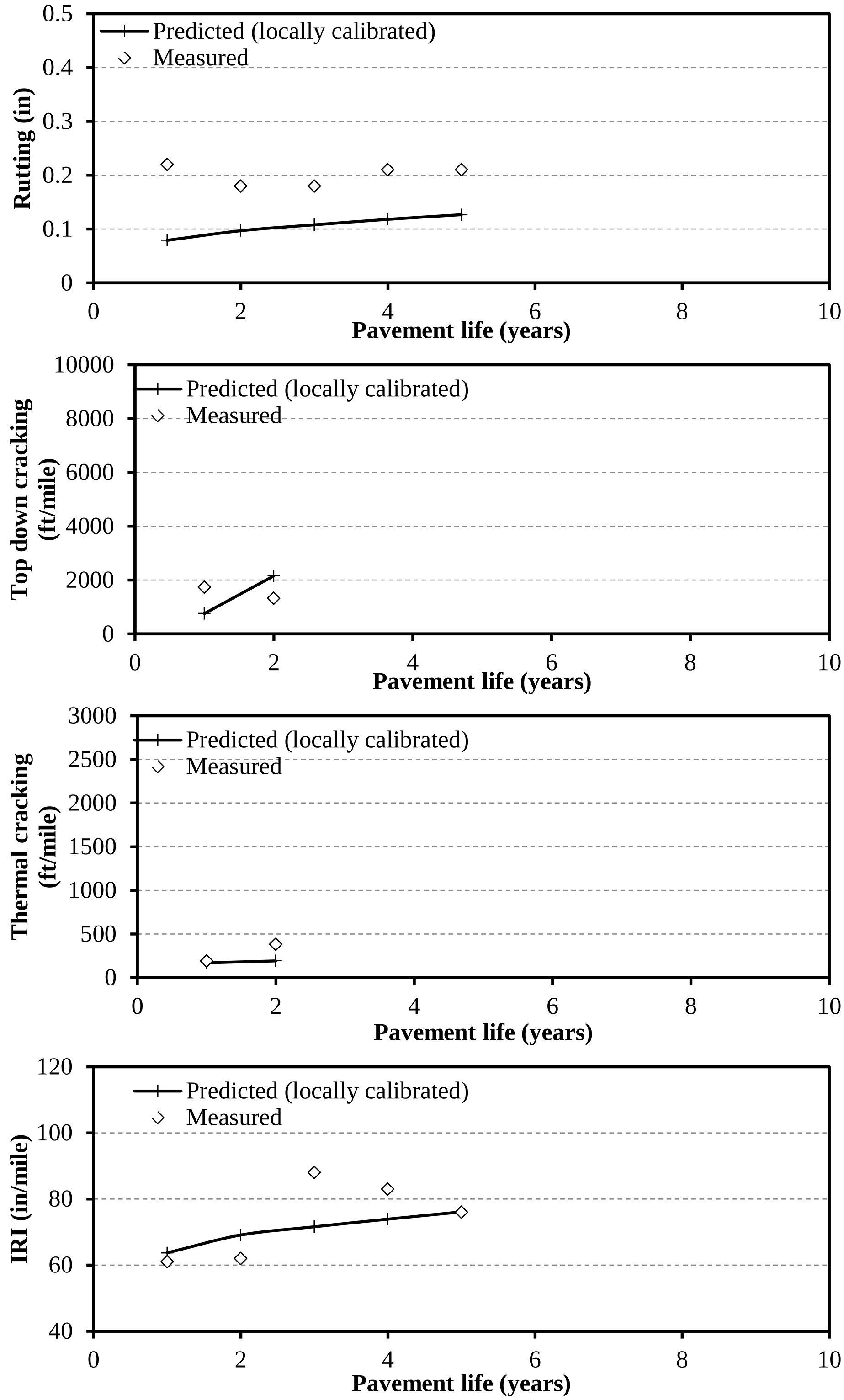

Figure E.28: Measured and Predicted Performance Data by the Locally Calibrated MEPDG for Project 103K0003900-NB

Appendix F: Measured and Predicted Performance Data for New Rigid Pavements (Locally Calibrated)

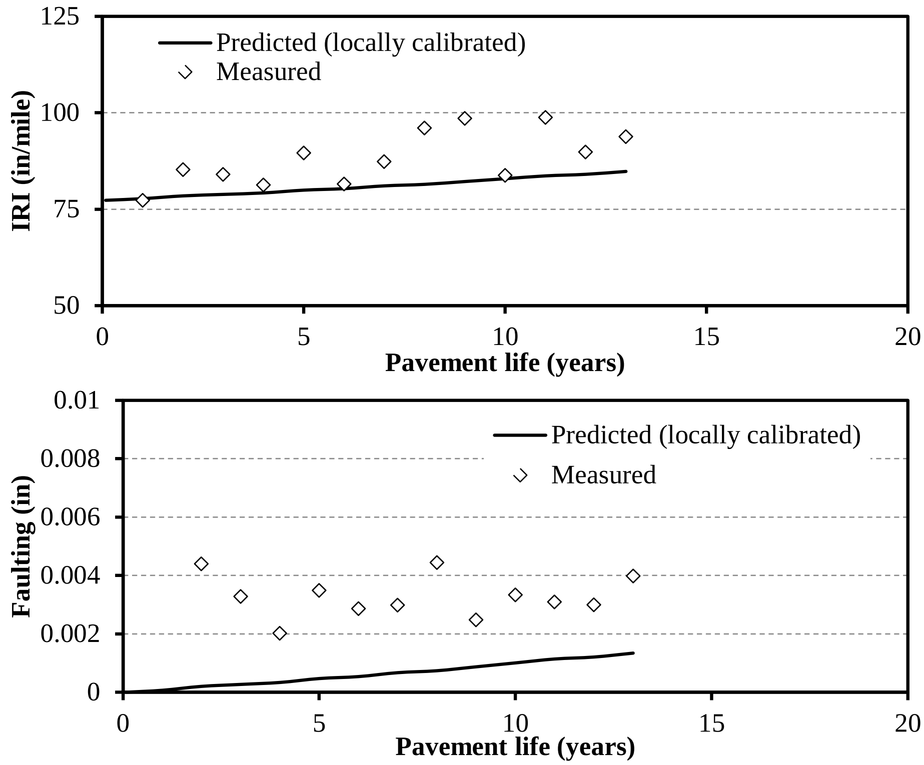

Figure F.1: Measured and Predicted Data by the Locally Calibrated MEPDG for Project 018U0007700-NB

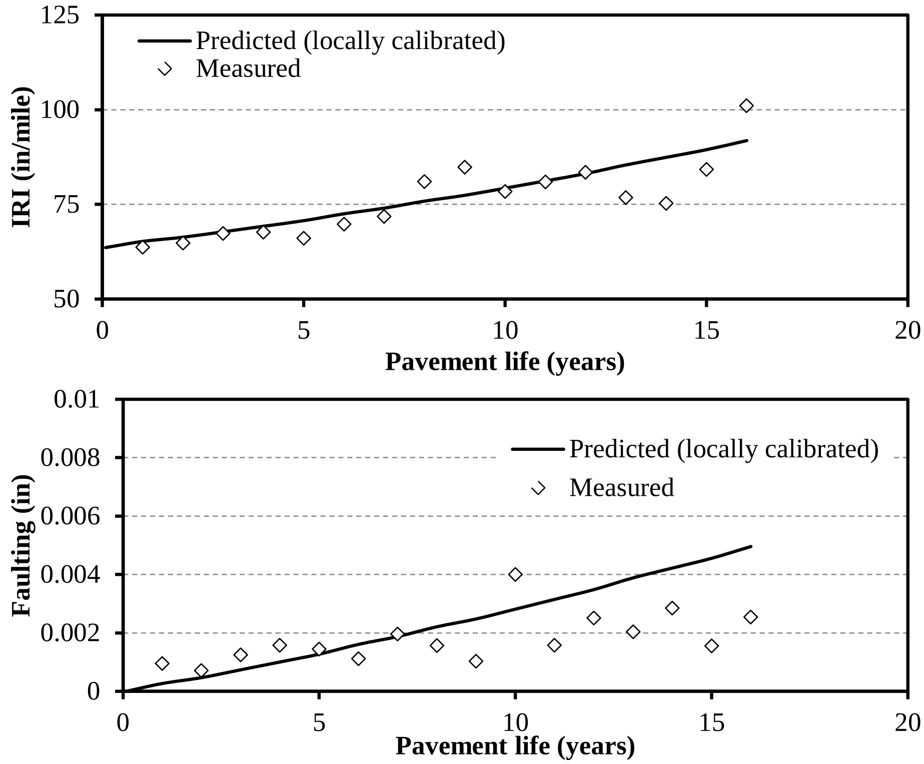

Figure F.2: Measured and Predicted Data by the Locally Calibrated MEPDG for Project 043U0007500-NB-2

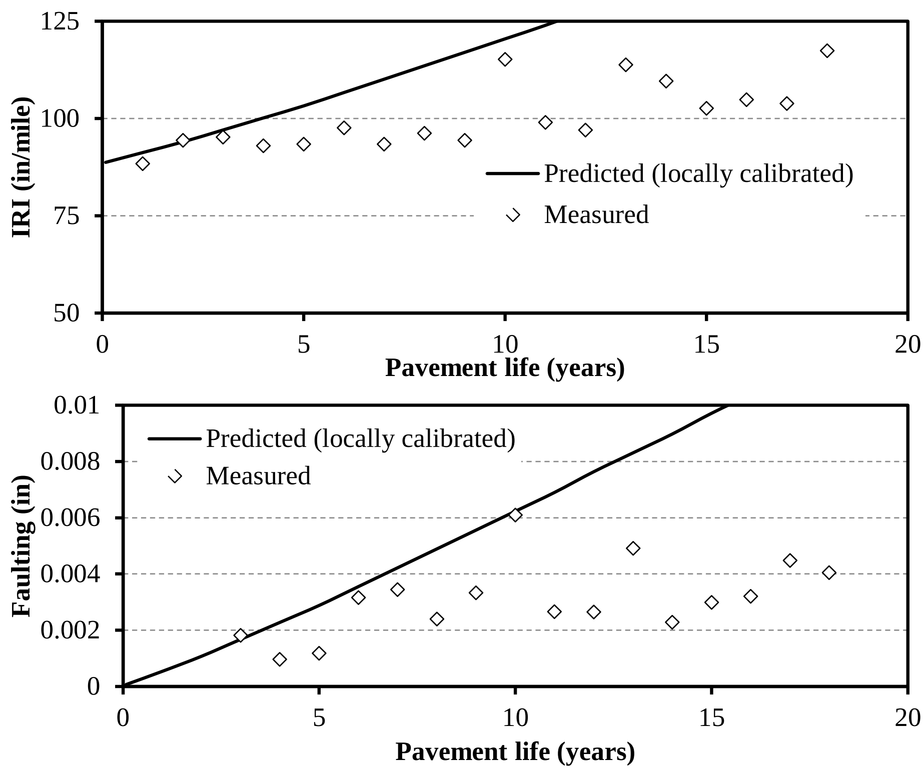

Figure F.3: Measured and Predicted Data by the Locally Calibrated MEPDG for Project 056I0003500-SB

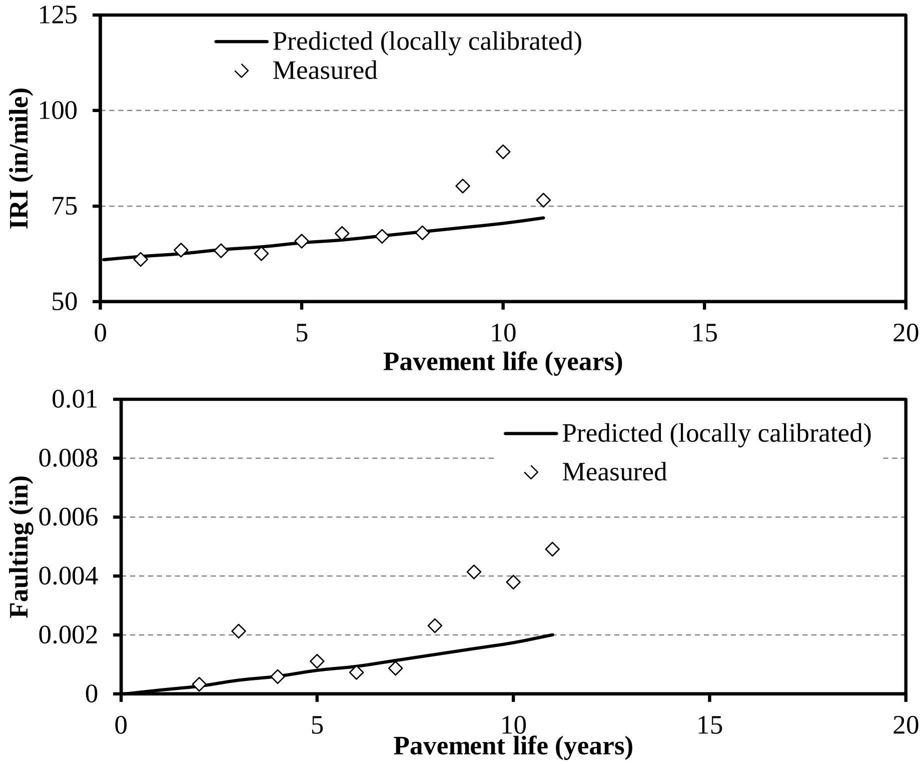

Figure F.4: Measured and Predicted Data by the Locally Calibrated MEPDG for Project 063U0040000-EB

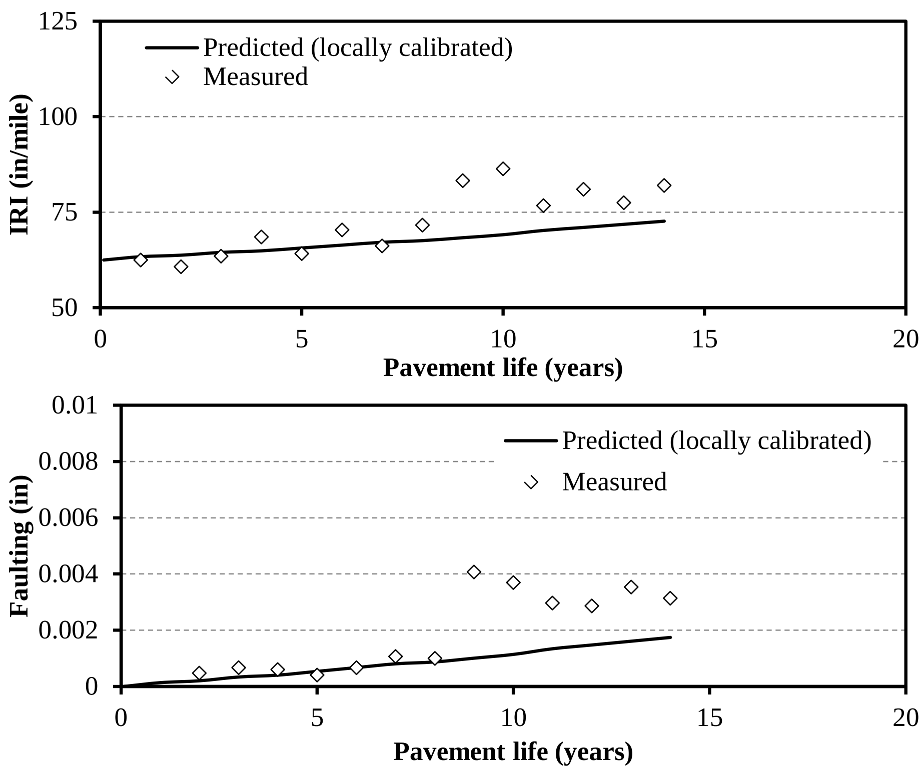

Figure F.5: Measured and Predicted Data by the Locally Calibrated MEPDG for Project 103U0040000-EB

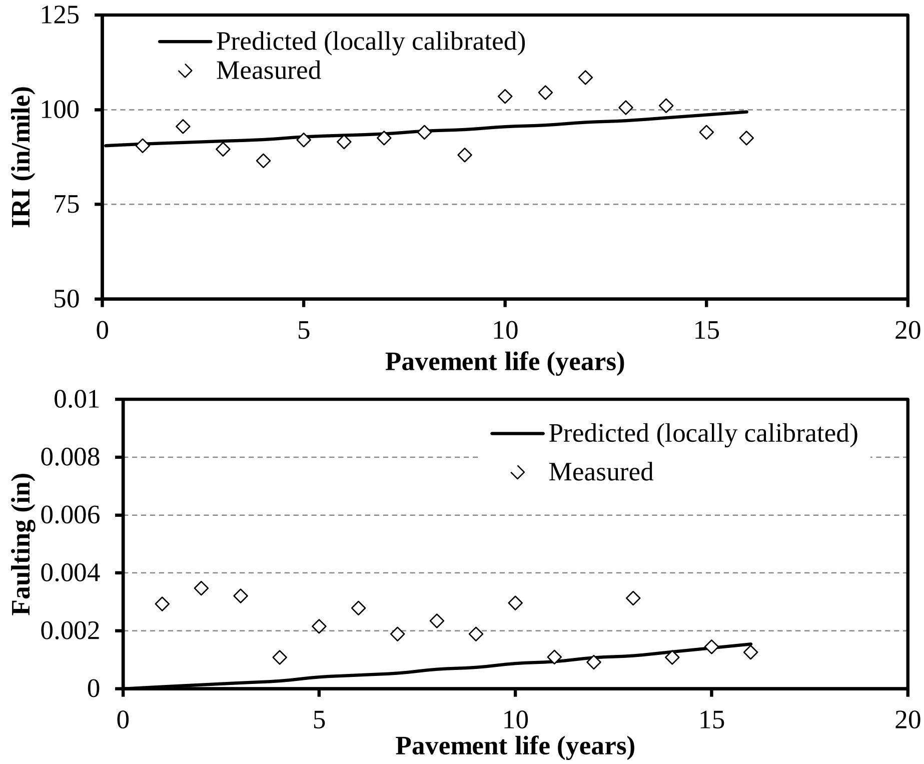

Figure F.6: Measured and Predicted Data by the Locally Calibrated MEPDG for Project 018K0036000-EB

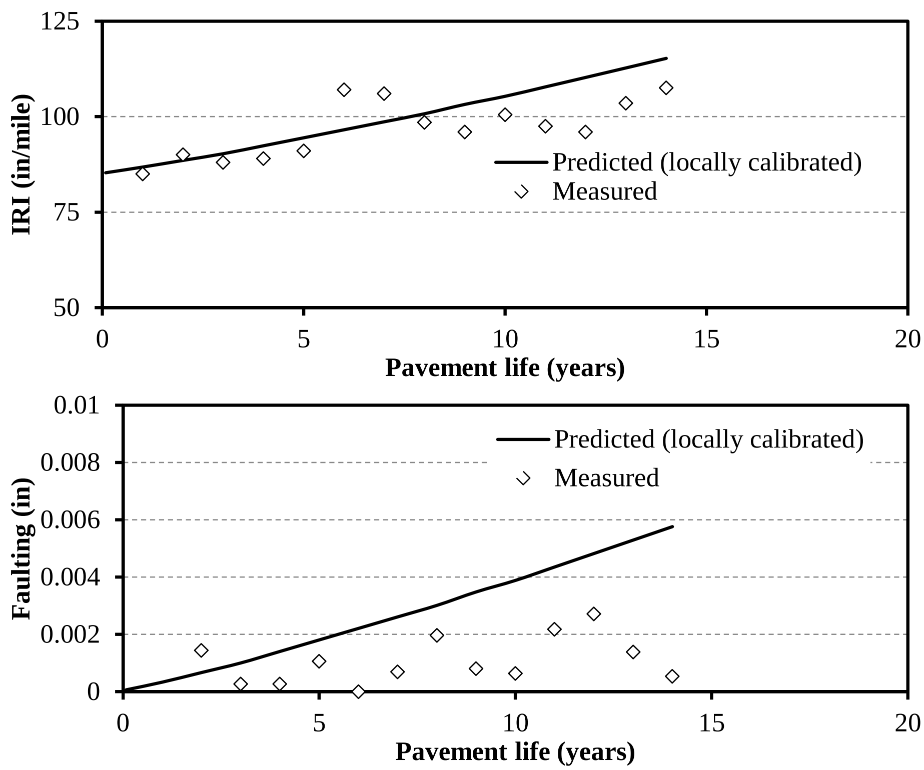

Figure F.7: Measured and Predicted Data by the Locally Calibrated MEPDG for Project 031I0007000-EB

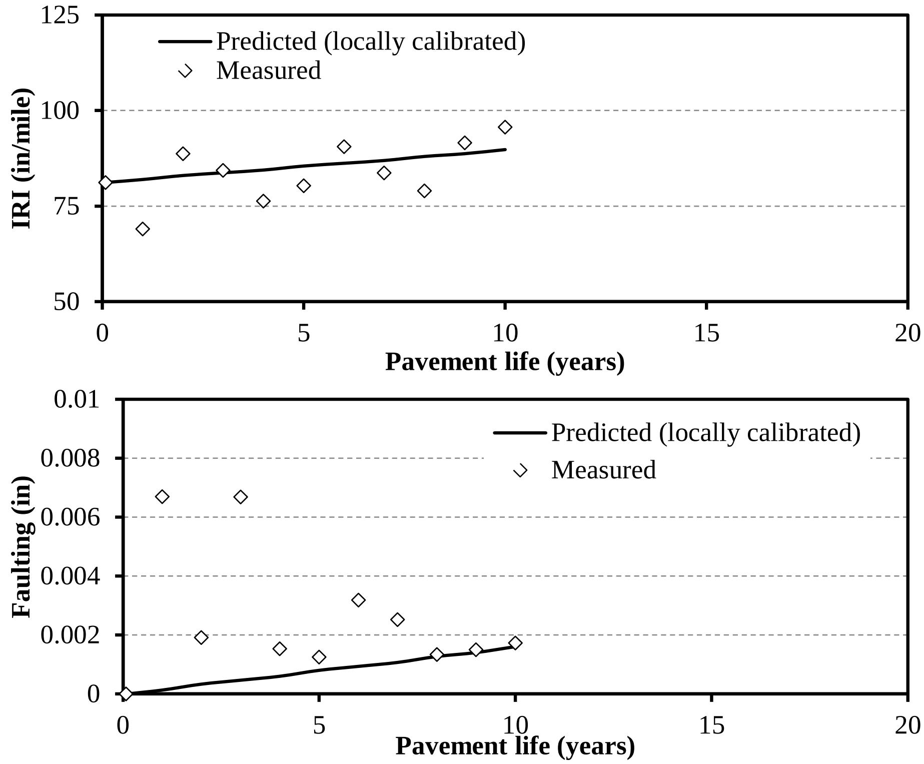

Figure F.8: Measured and Predicted Data by the Locally Calibrated MEPDG for Project 040I0013500-NB-1

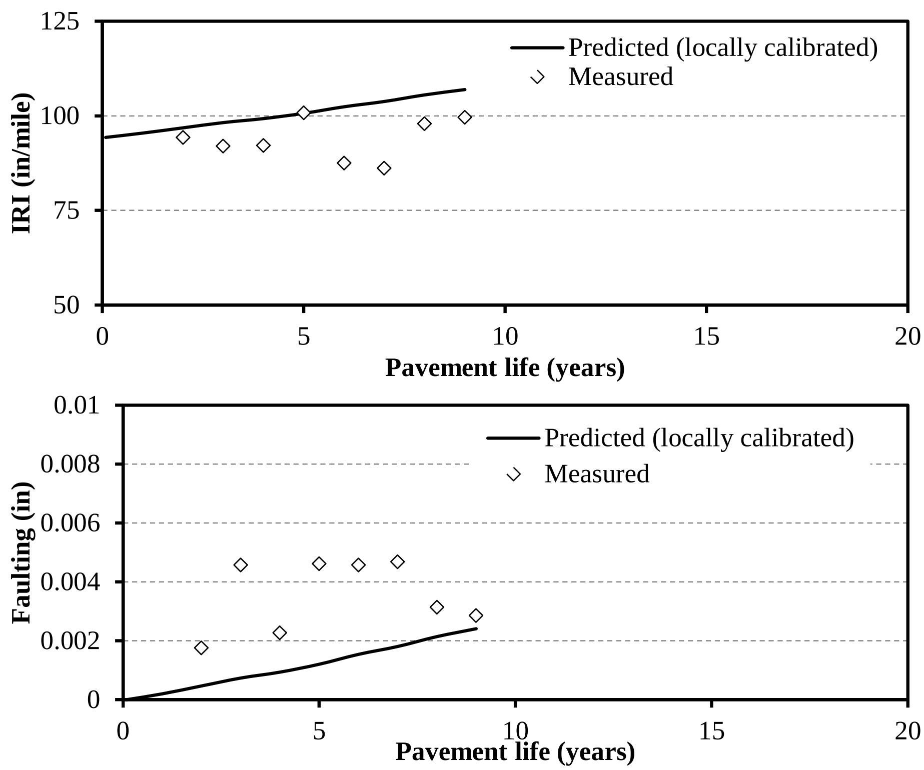

Figure F.9: Measured and Predicted Data by the Locally Calibrated MEPDG for Project 040I0013500-NB-2

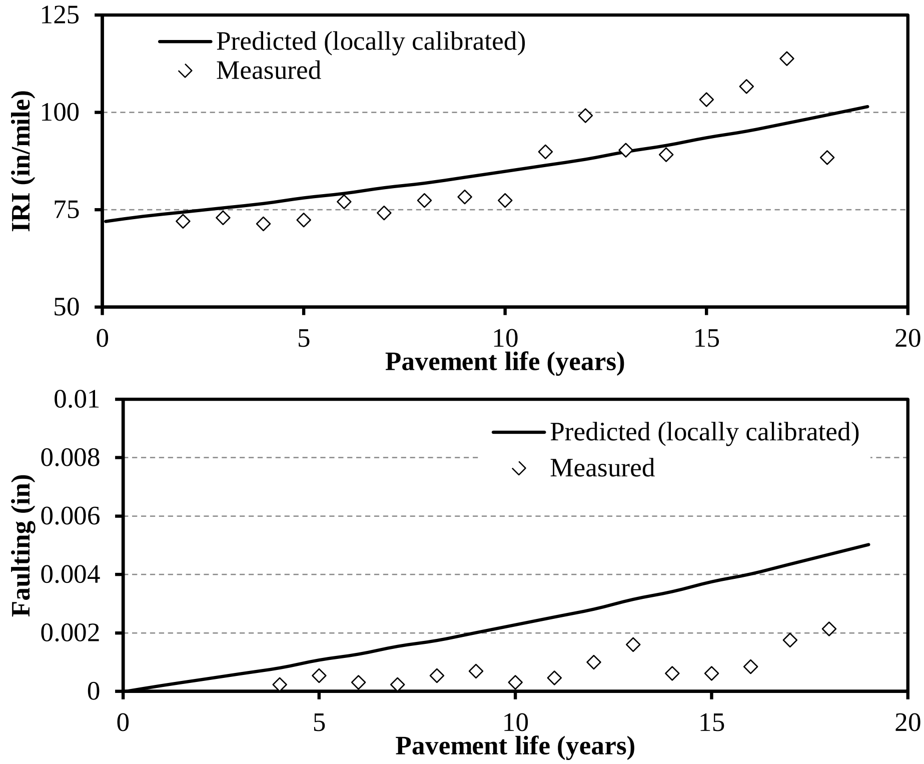

Figure F.10: Measured and Predicted Data by the Locally Calibrated MEPDG for Project 043U0007500-NB

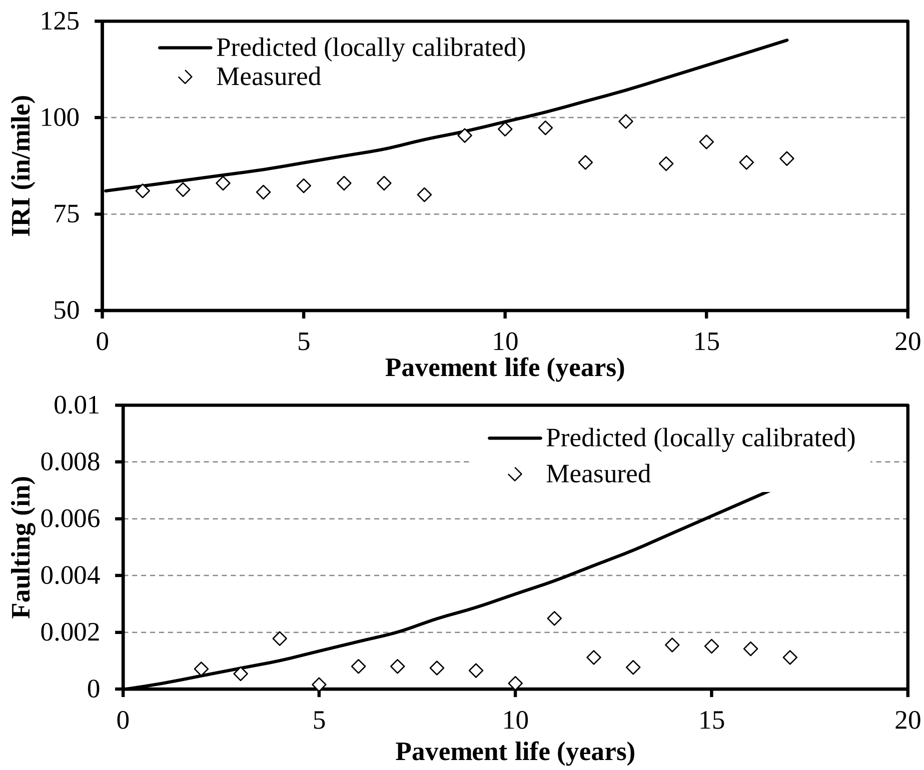

Figure F.11: Measured and Predicted Data by the Locally Calibrated MEPDG for Project 046K0000700-SB

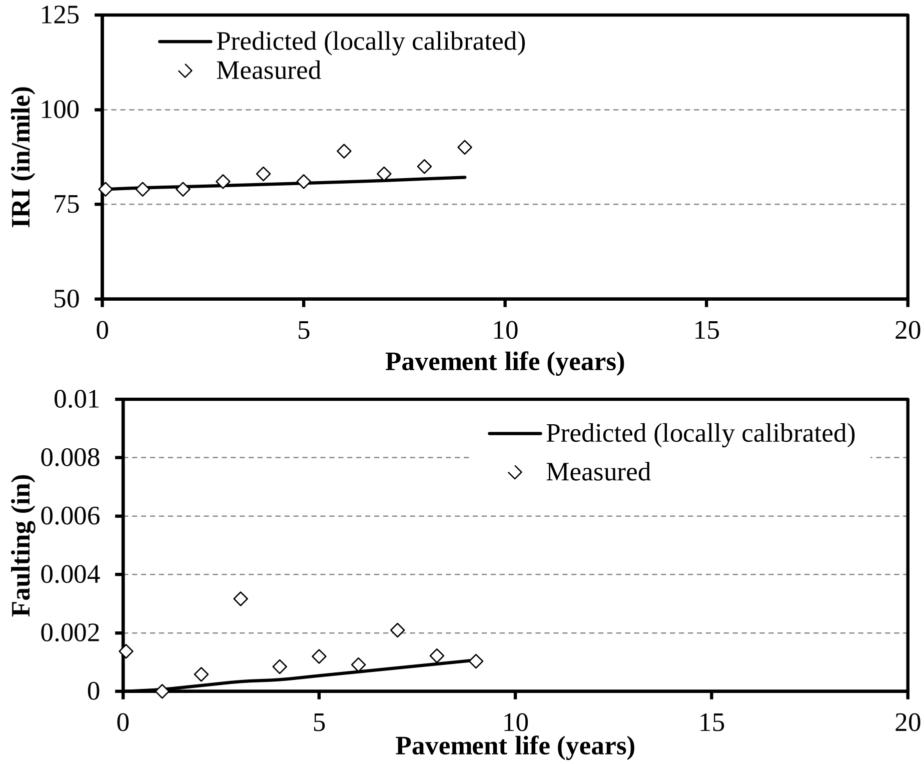

Figure F.12: Measured and Predicted Data by the Locally Calibrated MEPDG for Project 055U0004000-EB

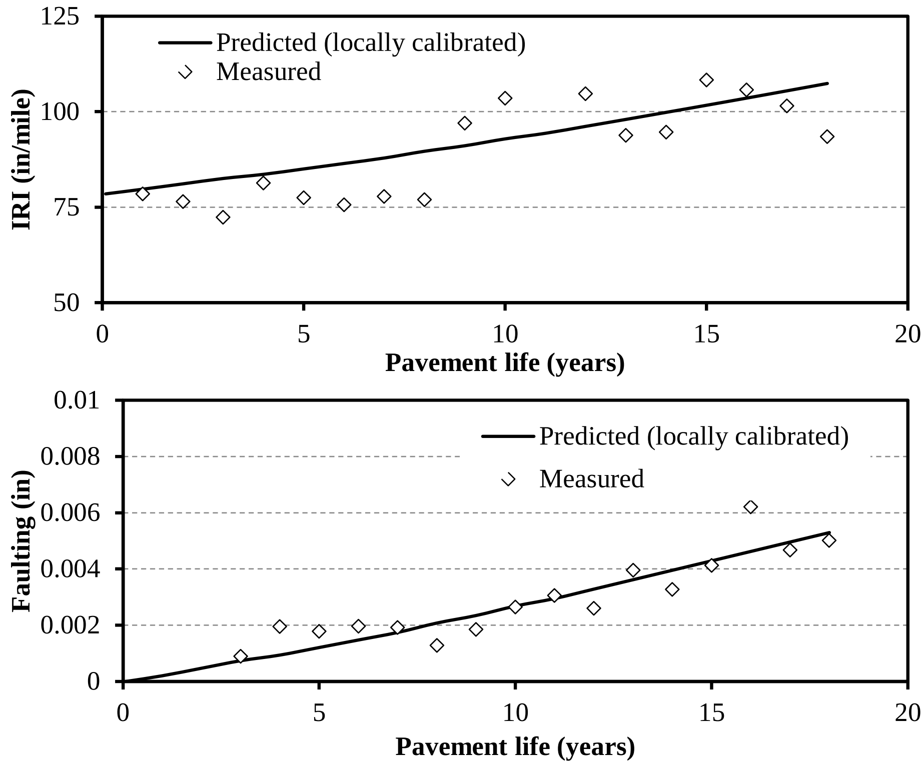

Figure F.13: Measured and Predicted Data for by the Locally Calibrated MEPDG Project 056U0005000-EB

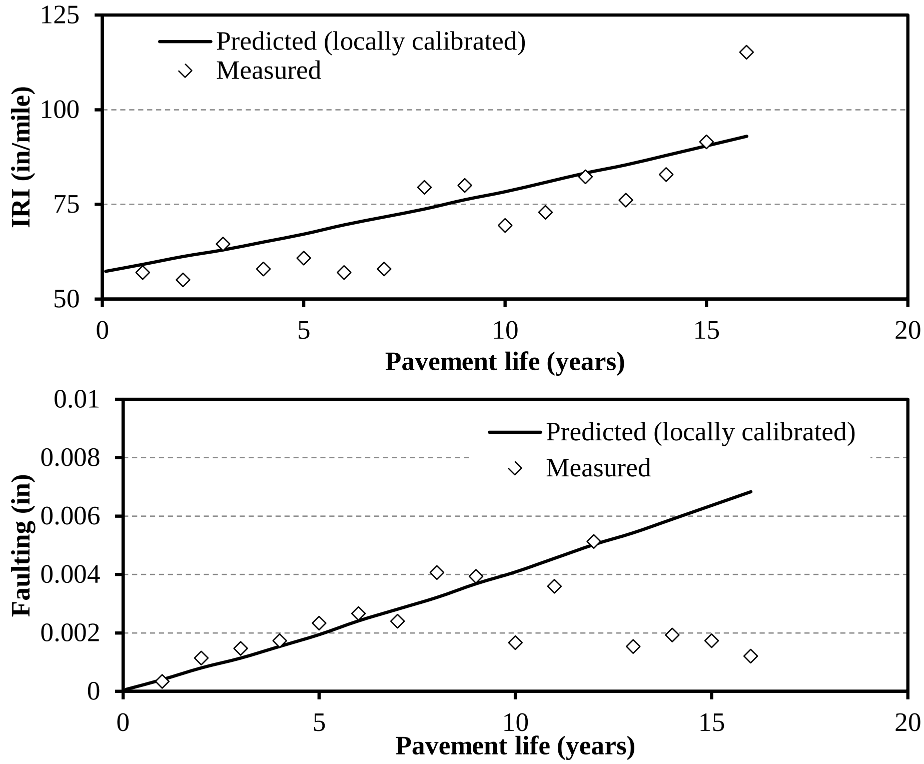

Figure F.14: Measured and Predicted Data for by the Locally Calibrated MEPDG Project 059I0013500-NB

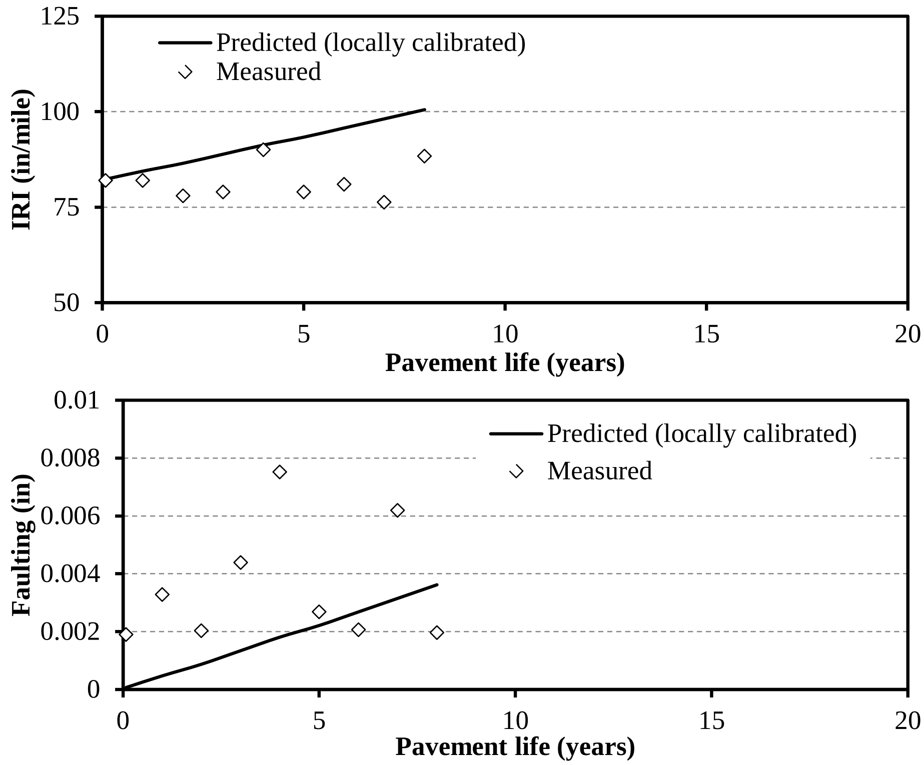

Figure F.15: Measured and Predicted Data by the Locally Calibrated MEPDG for Project 061I0003500-NB

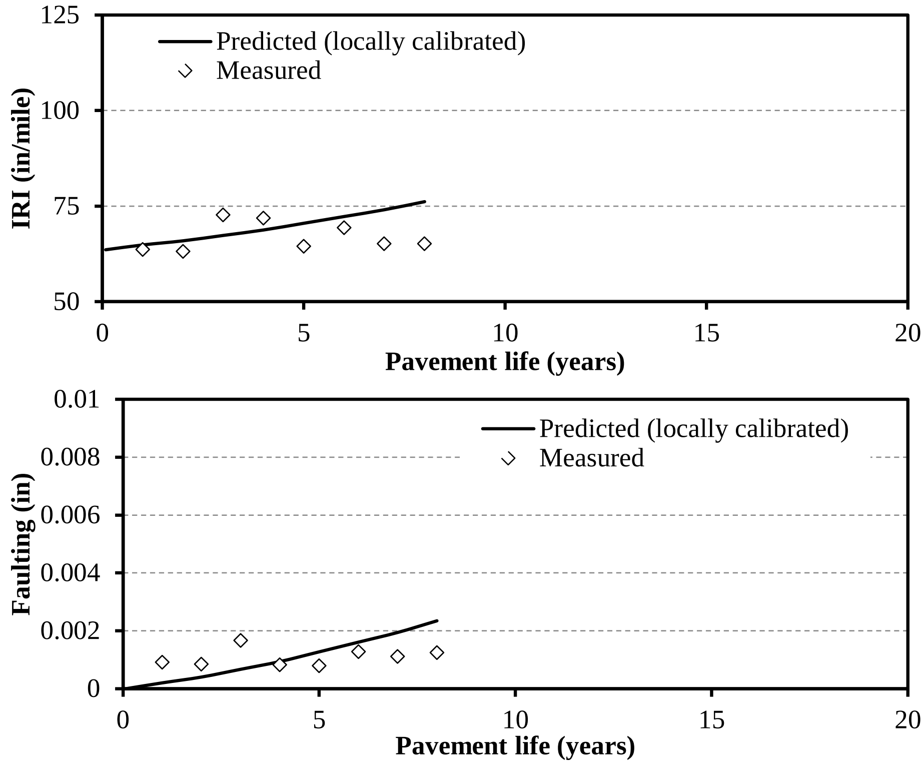

Figure F.16: Measured and Predicted Data by the Locally Calibrated MEPDG for Project 067U0016900-NB

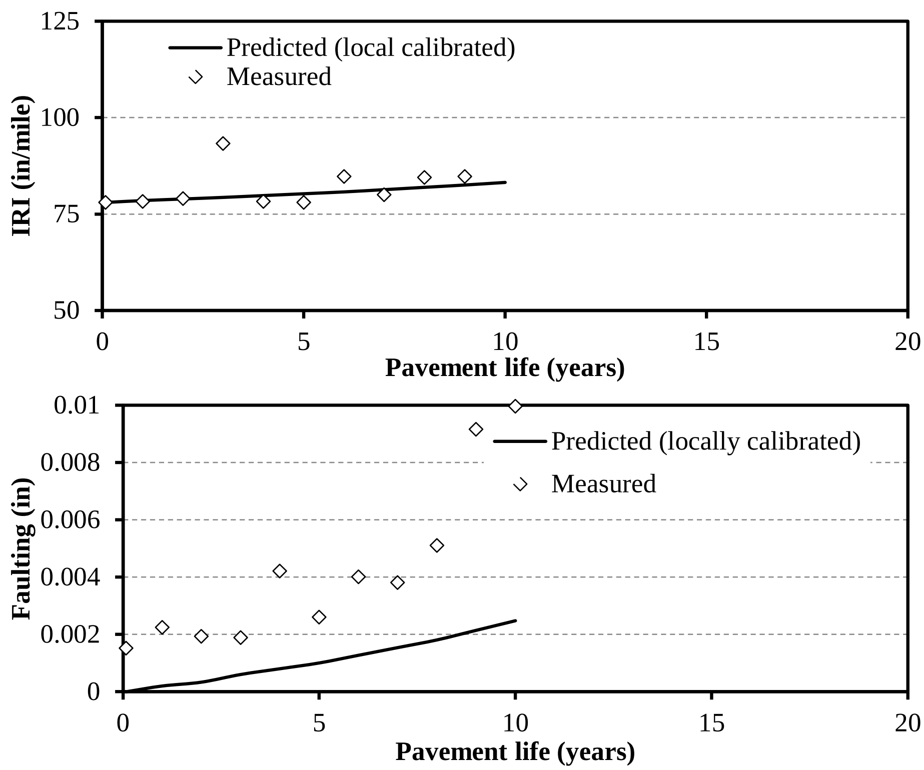

Figure F.17: Measured and Predicted Data by the Locally Calibrated MEPDG for Project 079U0008100-NB

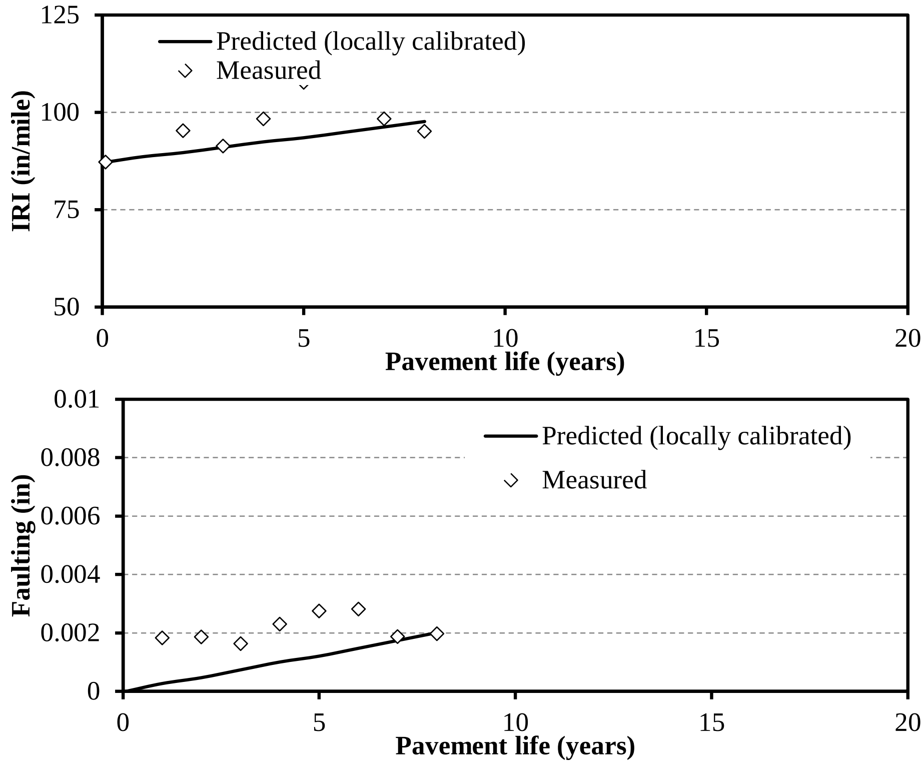

Figure F.18: Measured and Predicted Data by the Locally Calibrated MEPDG for Project 085I0007000-EB

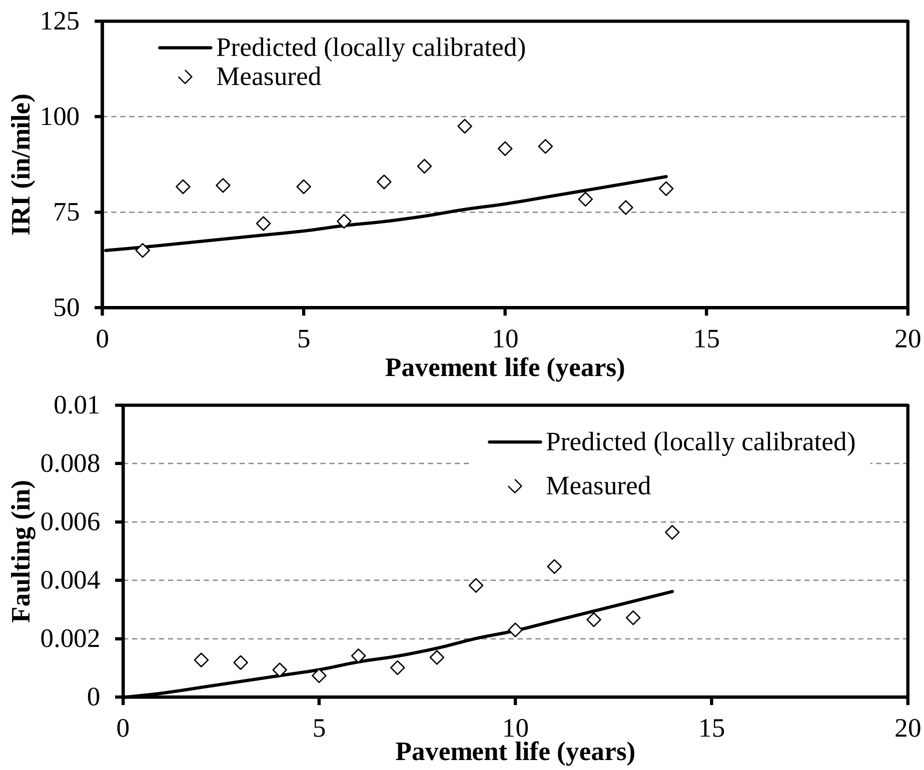

Figure F.19: Measured and Predicted Data by the Locally Calibrated MEPDG for Project 019U0006900-NB

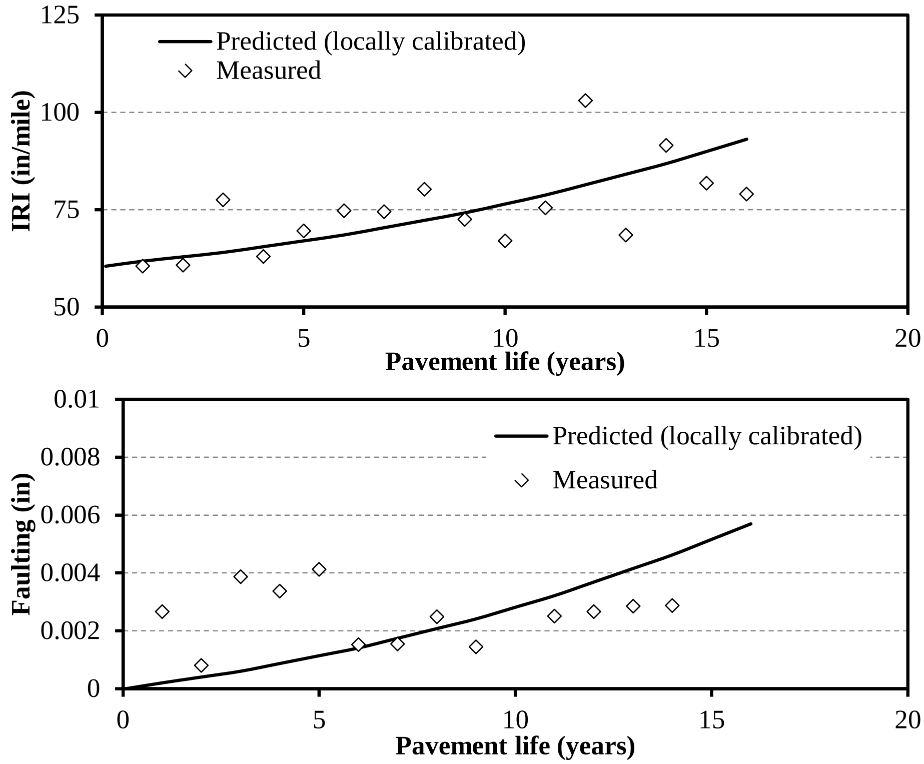

Figure F.20: Measured and Predicted Data by the Locally Calibrated MEPDG for Project 029U0005600-EB

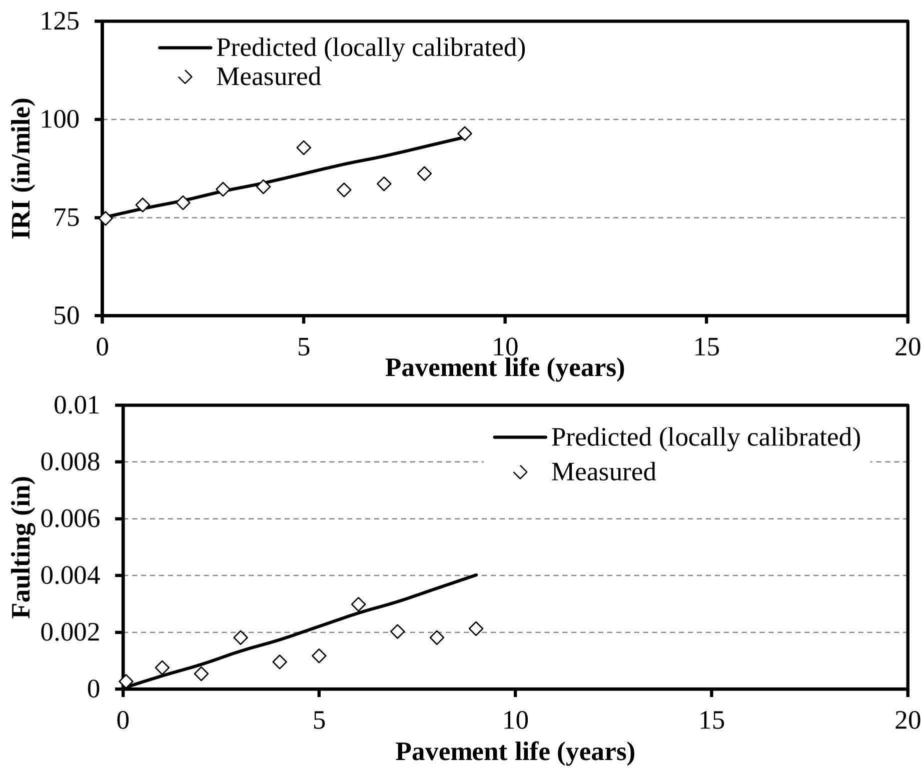

Figure F.21: Measured and Predicted Data by the Locally Calibrated MEPDG for Project 030I0003500-2

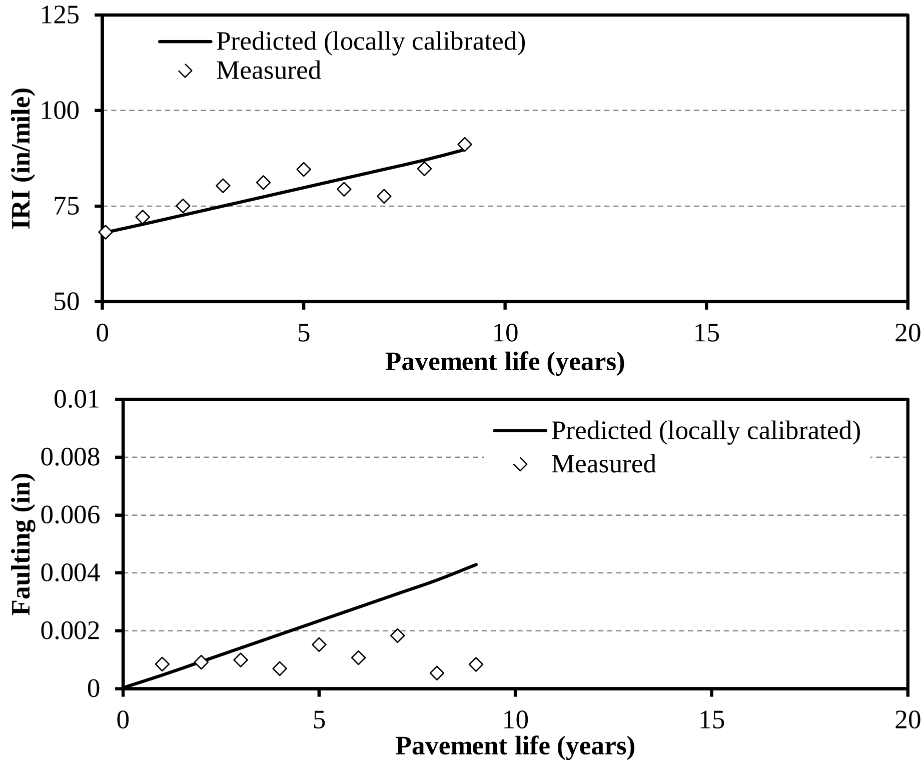

Figure F.22: Measured and Predicted Data by the Locally Calibrated MEPDG for Project 030I0003500-3

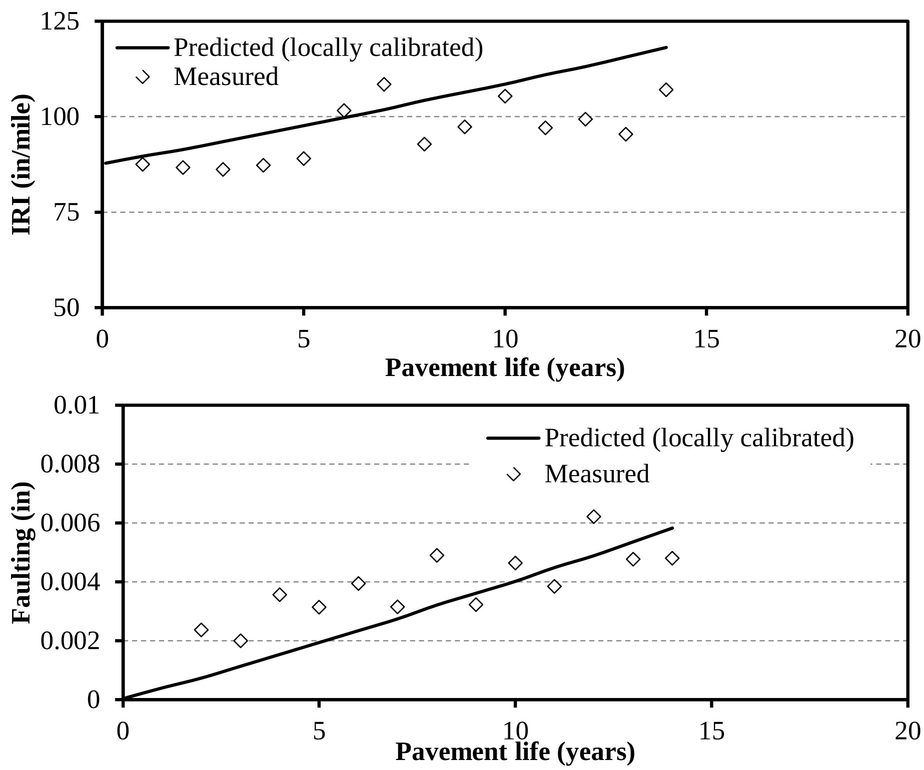

Figure F.23: Measured and Predicted Data by the Locally Calibrated MEPDG for Project 031I0007000-2

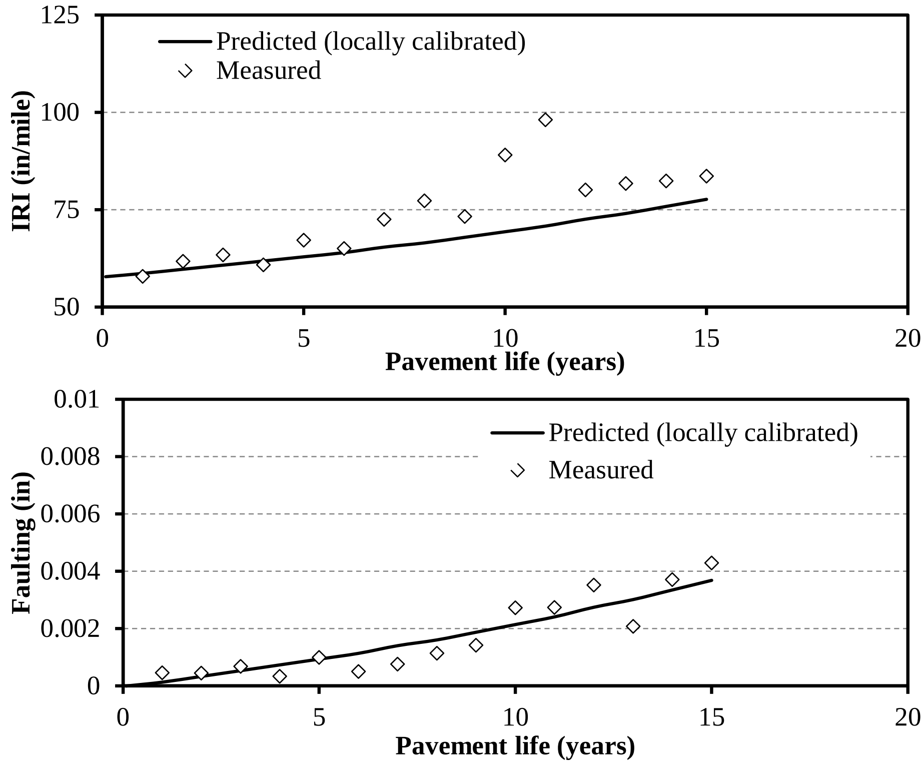

Figure F.24: Measured and Predicted Data by the Locally Calibrated MEPDG for Project 037U0040000-EB

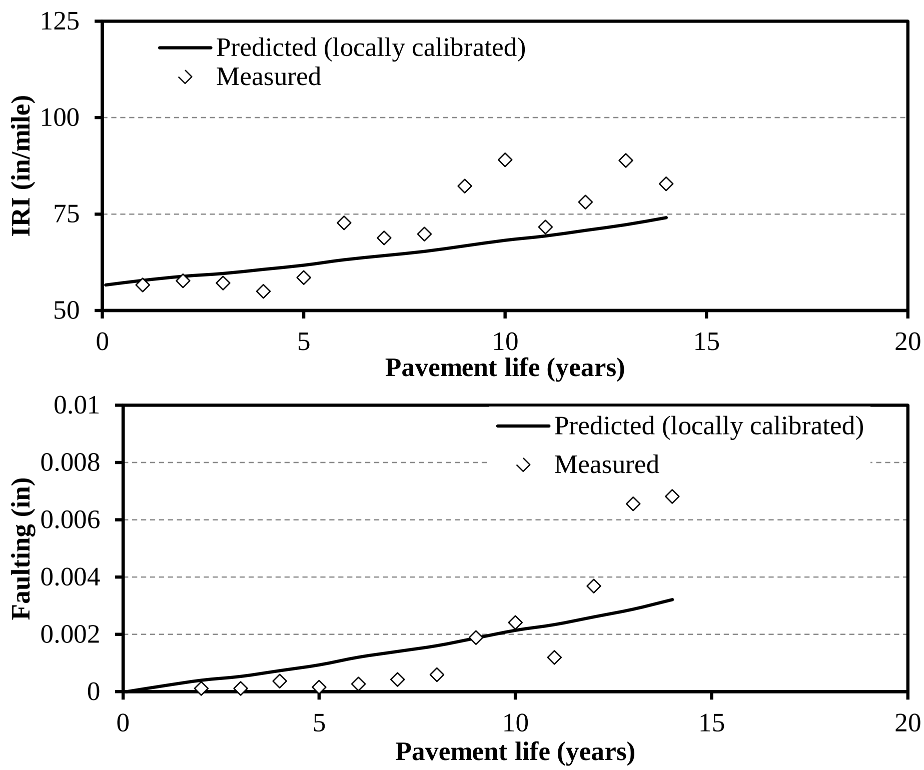

Figure F.25: Measured and Predicted Data by the Locally Calibrated MEPDG for Project 037U0040000-EB-2

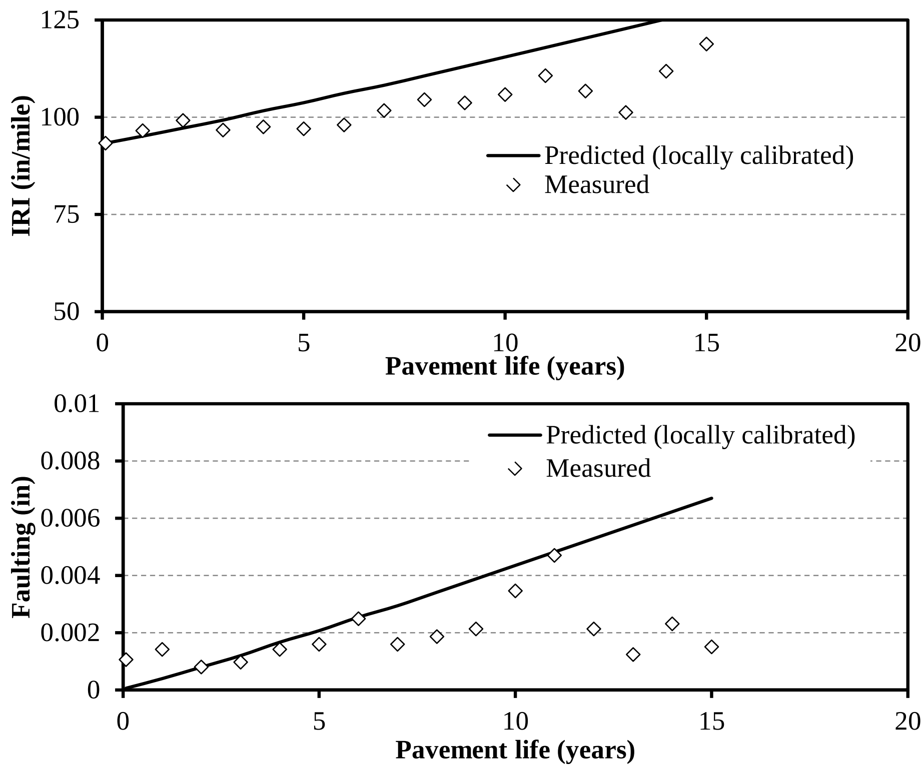

Figure F.26: Measured and Predicted Data by the Locally Calibrated MEPDG for Project 030I0003500-1

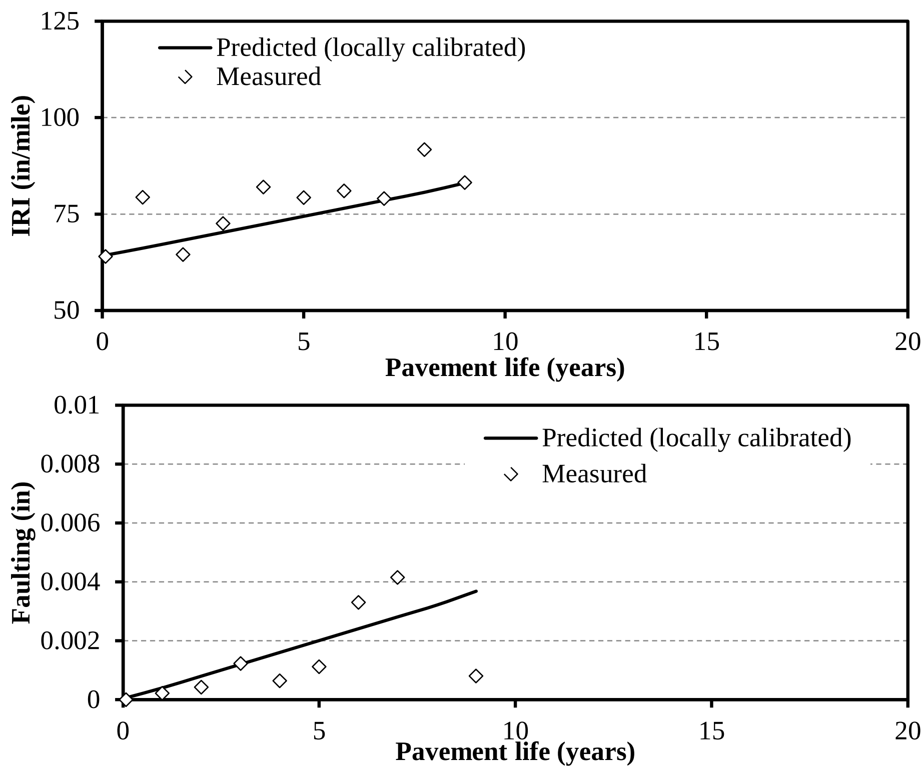

Figure F.27: Measured and Predicted Data by the Locally Calibrated MEPDG for Project 056I0003500-SB-2

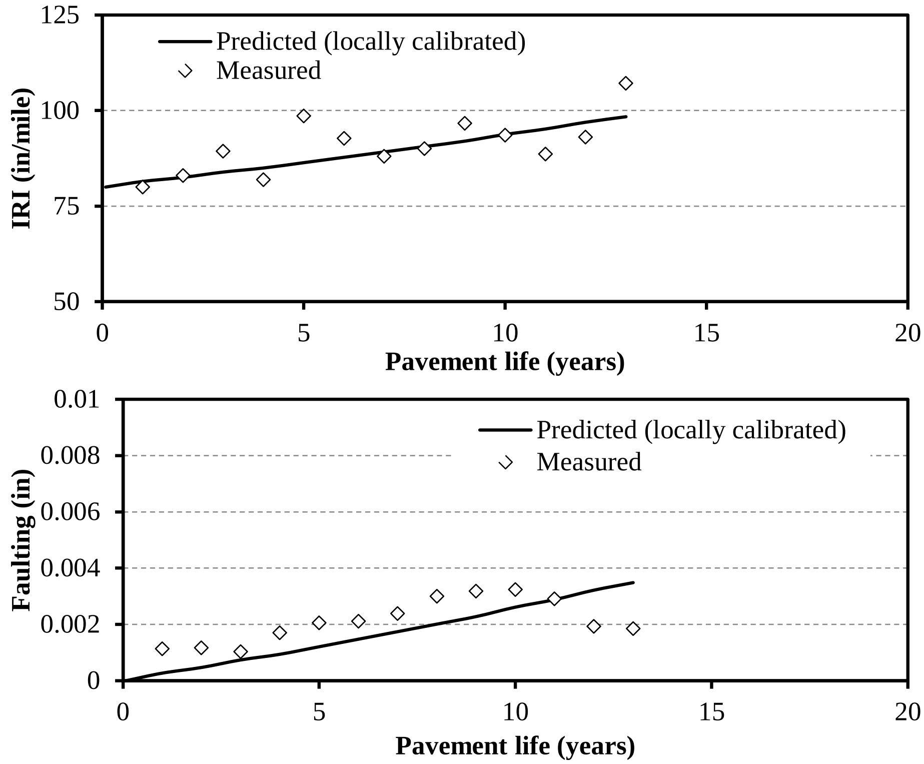

Figure F.28: Measured and Predicted Data by the Locally Calibrated MEPDG for Project 085I0013501

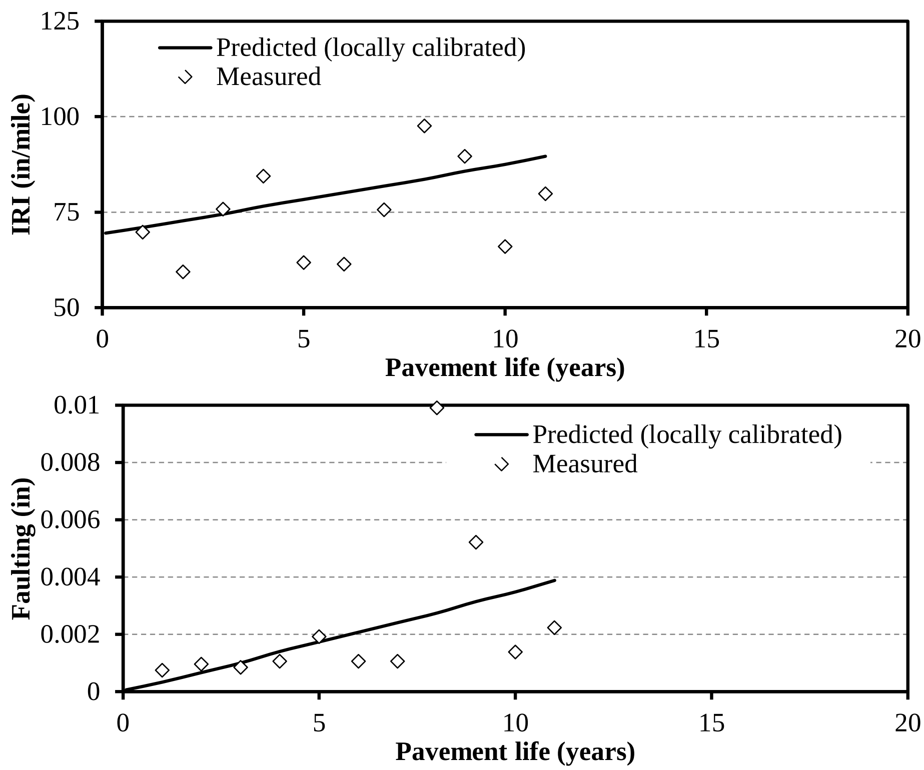

Figure F.29: Measured and Predicted Data by the Locally Calibrated MEPDG for Project 099I0007000-EB-1

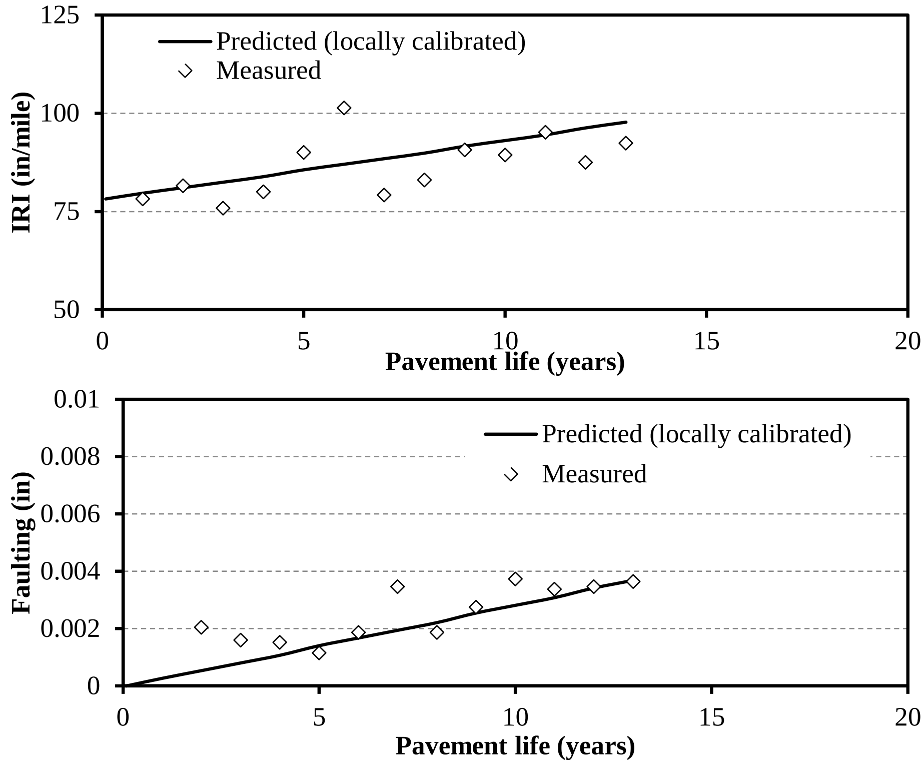

Figure F.30: Measured and Predicted Data by the Locally Calibrated MEPDG for Project 099I0007000-EB-2

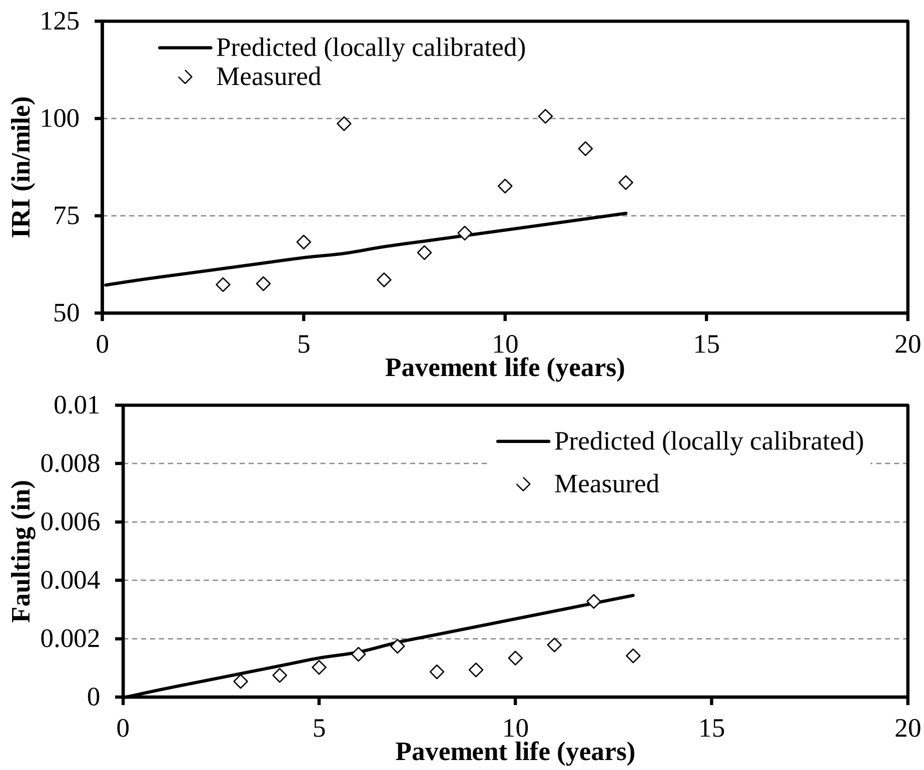

Figure F.31: Measured and Predicted Data by the Locally Calibrated MEPDG for Project 099I0007000-EB-3

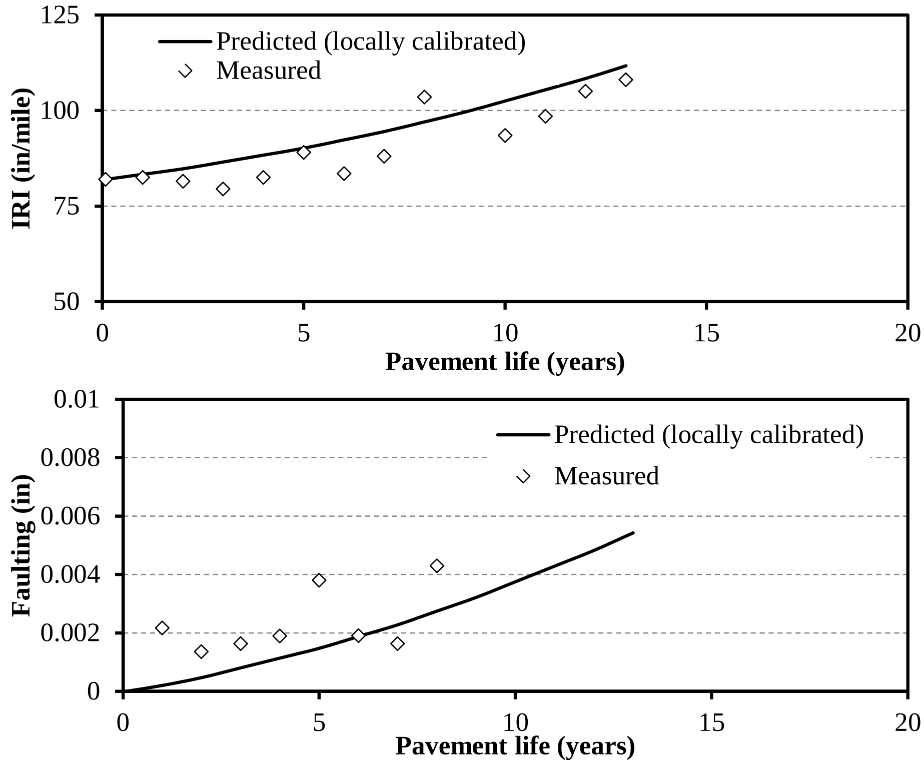

Figure F.32: Measured and Predicted Data by the Locally Calibrated MEPDG for Project 103U0007500-SB


AD ASTRA PER ASPERA
Kansas
Department of Transportation